BuMines OFR 135-83

A mining research contract report
JANUARY 1983

PB83238394

CRITICAL PARAMETERS FOR TAILINGS EMBANKMENTS

Contract J0215028

Baecher, Marr and Associates
Concord, MA

Bureau of Mines Open File Report 135-83

BUREAU OF MINES
UNITED STATES DEPARTMENT OF THE INTERIOR

The views and conclusions contained in this document are those of the authors and should not be interpreted as necessarily representing the official policies or recommendations of the Interior Department's Bureau of Mines or of the U.S. Government.

50272-101

REPORT DOCUMENTATION PAGE	1. REPORT NO. BuMines OFR 135-83	2.	3. Recipient's Accession No. PB83 238394
4. Title and Subtitle: Critical Parameters for Tailings Embankments			5. Report Date: January 1983
			6.
7. Author(s): Gregory B. Baecher, W. Allen Marr, J. -S. Lin, and John A. Consla			8. Performing Organization Rept. No.
9. Performing Organization Name and Address: Baecher, Marr and Associates, 342 Sudbury Rd., Concord, MA 01742			10. Project/Task/Work Unit No.
			11. Contract(C) or Grant(G) No. (C) J0215028 (G)
12. Sponsoring Organization Name and Address: Office of Assistant Director--Mining Research, Bureau of Mines, U.S. Department of the Interior, Washington, DC 20241			13. Type of Report & Period Covered: Contract research, 8/12/81--7/11/82
			14.

15. Supplementary Notes

Approved for release June 13, 1983.

16. Abstract (Limit: 200 words)

Geotechnical data on copper, uranium, and phosphate tailings from 41 mines were collected and analyzed to empirically establish the variability in strength properties for tailings embankments. These data were analyzed both from geotechnical and statistical perspectives to infer typical strength parameters for slope stability analysis. The results indicate large variability of strength properties both within and among tailings embankments. However, this variability in most cases appears statistically regular and tends toward normal distributions when spatial trends are removed. The implication is that probabilistic techniques can be used to assess the importance of strength property variability for embankment stability and that the assumption of common distributional forms for input to such modeling is appropriate.

17. Document Analysis a. Descriptors

Mining
Cone penetration tests
Failure
Shear strength
Tailings dams
Safety factor
Pore pressures
Slope stability
Statistical analysis
Design
In situ tests

b. Identifiers/Open-Ended Terms

Probabilistic modeling
Spatial variation
Autocorrelation functions
Measurement noise
Variance
Statistical distributions

c. COSATI Field/Group 08I

18. Availability Statement	19. Security Class (This Report)	21. No. of Pages
Release unlimited by NTIS.	Unclassified	282
	20. Security Class (This Page) Unclassified	22. Price

(See ANSI-Z39.18) See Instructions on Reverse OPTIONAL FORM 272 (4-77) (Formerly NTIS-35) Department of Commerce

FOREWARD

This report was prepared by Baecher, Marr and Associates of Concord, MA under USBM Contract number J0215028. The contract was initiated under the Minerals, Health and Safety Technology Program. It was administered under the technical direction of the Spokane Research Center with Mr. Douglass Tesarik acting as Technical Project Officer. Mr. Larry J. Anderson was the contract administrator for the Bureau of Mines. This report is a summary of the work recently completed as a part of this contract during the period August 1981 to August 1982. This report was submitted by the authors on January 1983.

The work reported here has benefitted greatly from the advice, suggestions, and discussions of a great many people, who willingly gave their time to help the effort. Mr. Douglass Tesarik of the Bureau of Mines had a strong and beneficial influence on the work, both due to his technical suggestions and to his coordination of the work with other USBM projects. Many geotechnical engineering firms and individuals generously contributed data from their files. The work reported herein would not have been possible without this assistance. We are especially grateful to the following individuals and firms for their help:

AMAX Phosphate Inc., Palmetto, FL
Loren Anderson, Utah State University
Ardaman and Associates, Orlando, FL
ARMAC, Tampa, FL
Borden Chemical Co., Lakeland, FL
David S. Bowles, Law Engineering Co., Inglewood, CO
Bromwell Engineering, Lakeland, FL
Geotechnical Engineers Inc., Winchester, MA
Francois Heuze, Lawrence Livermore Laboratories, CA
T. William Lambe, Inc., East Perrerell, MA
Law Engineering Co., Tampa, FL
Nchanga Consolidated Copper Mined Ltd., Rokana, Zambia
John Nelson, Colorado State University
OYO Corporation, Tokyo, Japan
Roan Consolidated Mines Ltd., Kalulushi, Zambia
Steffan, Robertson, and Kirsten, Denver, CO
Watermeyer, Legge, Piesold and Uhlmann, Kent, UK

We are also grateful to many others who prefer to remain anonymous. Many people have kindly assisted with the completion of this work, but the conclusions and errors remain the responsibility of the authors.

EXECUTIVE SUMMARY

Geotechnical data on copper, uranium, and phosphate tailings from 41 mines, as shown in the table below were collected and analyzed to empirically establish the variability in strength properties for tailings embankments. These data were analyzed both from a geotechnical perspective and from a statistical perspective to infer typical strength parameters for slope stability analysis. This work is part of a larger USBM program of research on the safety of tailings embankments, which intends to provide improved empirical information for both traditional and probabilistic analysis of tailings materials.

Geotechnical Data Summary

COMMODITY	Number of mines with specific data			Total number
	SPT	Cone penetration	Lab tests	of mines
Copper	10	15	12	16
Uranium	3	1	14	15
Phosphate (Gypsum)	4	1	10	10
				41

The results of these analyses indicate large variability of strength properties both within and among tailings embankments. However, this variability in most cases appears statistically regular and tends toward normal distributions when spatial trends are removed. The implication of this finding is that probablistic techniques can be used to assess the importance of strength property variability for embankment stability, and that the assumption of common distributional forms for input to such modeling is appropriate.

Strength data determined from in situ tests show erratic spatial variability; data fluctuate significantly over short horizontal and vertical distances. From a probablistic modeling view, this erratic variability manifests as short autocovariance distances.

The strength data consist of in situ measurements by the cone penetration test, and laboratory measurements of various types, principally direct shear and triaxial compression.

Collateral data were collected where available on strength index properties (water content, Atterberg limits, grain size distribution) and on pore pressures within embankments. Many of these data were kindly provided by a large number of individuals and firms from their own files, most of whom have requested confidentiality.

The data analysis proceeded in seven (7) stages. In Stage 1 data from each site were reviewed to form a concept of the tailings materials and the structure of the embankments into which they were formed. In Stage 2 individual soundings and borings were studied to identify zonation in the embankments. In Stage 3 individual records were reviewed to identify outlying data and to establish whether weak features were continued between borings. In Stage 4 data were digitized and stored in computer readable format. In Stage 5 quality indices were assigned to reflect geotechnical and strength considerations. In Stage 6 statistical analyses were performed to establish trends, statistical moments, best fitting distributional forms, autocorrelation structures and cross correlation. In Stage 7 all results were reviewed for consistency and accuracy.

The interpretation of in situ test data, primarily SPT blow counts and cone penetration resistances, involved considerable effort, as the implications of such data are more complex than routine interpretations suggest. Many tailings materials are partially drained during testing and thus neither drained ($c,\bar{\phi}$) nor undrained (s_u) interpretation yields correct strength parameters. An unsettling conclusion of the present work is that many, and possibly even most, in situ strength data for tailings are useless for estimating strength parameters, since drainage conditions during testing are unknown.

Data Quality Indices were assigned to all data to avoid mixing meaningful data with data that were difficult to interpret. A single attribute index was developed for Laboratory data, reflecting test procedures and specimen quality. A more involved, two attribute index was developed for in situ data to reflect (1) the procedure used in testing, and (2) whether sufficient information was provided on pore pressures and other conditions to allow unambiguous interpretation of test results. These indices were directed at the clarity with which data could be interpreted in the present project and not the "quality" of the data per se- thus they do not reflect the care with which tests were performed or the competence of the individuals or organizations performing the tests.

Statistical Analyses were performed both within and among sites principally to establish (1) means and variances of data scatter (i.e., statistical moments), (2) empirical distributional forms, and (3) the structure of spatial variability within tailings embankments. To test distributional forms the raw data were plotted on Pearson diagrams and plotted with best fitting normal, lognormal, gamma, exponential and beta cumulative distribution functions (cdf). "Best fitting" distributions were based on maximum likelihood parameters. Residual data (raw data with trends removed) were also plotted on Pearson charts and then plotted against normal and beta cdf's. Spatial structure was analyzed by estimating autocovariance functions for the residual data from in situ measurements. Too few laboratory data were available with which to estimate autocovariance functions.

Results of the data analyses to establish means and variances for the strength properties of copper, uranium and gypsum tailings are summarized below. Compared to other geotechnical materials and properties, the tailings are quite variable both within embankments and from one mine to another. This finding conforms to common wisdom about copper and uranium tailings, but not about gypsum. Both direct and indirect strength on gypsum show considerable scatter, a fact that contradicts the widely stated view within the industry that gypsum is relatively uniform in its properties. Speculative causes of this variability include variations in composition of the gypsum particles, variable effects of excess pore pressures generated during field tests, and variable effects of sampling and laboratory testing.

Average within site variability for various strength measures and commodities

COMMODITY	MEAN STRENGTH	AVERAGE COEFFICIENT OF VARIATION
Copper		
SPT	28	39%
Cone	308.4	76%
ϕ	30.4	8%
Uranium		
SPT	14	52%
ϕ	35.8	17%
Gypsum		
SPT	20	56%
Cone	161.0	52%
ϕ	41.6	14%

Raw strength data in most cases show skewed distributions which become increasingly regular and symmetric when spatial trends are removed. For many sites the residual data appear by inspection to be well modeled by normal distributions, although given the often large data sizes (e.g., n=1000) they often fail to satisfy statistical goodness-of-fit tests. For such large data sizes even minor variations from a theoretical distribution of frequencies can be significant from a statistical view. For the practical purposes of geotechnical engineering these variations are often unimportant. Beta distributions, principally due to their increased number of parameters, in many cases also provide an adequate fit.

Vertical autocovariance functions could be estimated for a number of sites, and tended to display autocovariance distances on the order of 1 to 3 meters. This is on the low end of the range typical of both man-made and naturally occuring soils on other projects and as reported in the literature.

Conclusions

The data analyses reported here support several conclusions·

1. The variability of strength parameters for tailings materials is similar across commodities. Coefficients of variation from one mine to another are about 10% for copper and gypsum, and slightly higher for uranium.

2. The variability of strength data within an embankment differs considerably with type of measurement. For laboratory tests coefficients of variation of 10-20% are typical. For in situ measurements, such as SPT and cone penetration, 50-100% are typical.

3. No one distributional form appears appropriate as a general model of tailings strength variability. However, individual data sets appear to follow regular distributions.

4. The amount of measurement noise (or small scale variability) in in situ measurements can be large, often on the order of 50% of the data scatter, and differs significantly with measurement procedure. SPT data display considerably more noise than do cone penentration data.

5. The spatial variability of tailings properties is erratic, leading to autocorrelation functions which decay rapidly in both the horizontal and vertical directions. Vertical autocovariance distances on the order of 1 to 3 meters are typical· horizontal autocovariance distances may be about ten times the vertical.

Our results show that at any specific site an appropriate distributional form to serve as input for reliability modeling must be verified against site specific data. No universally best distribution was found to exist. However, once spatial trends are removed, most of the data sets studied displayed unimodal distribution which were more or less symmetric. Highly skewed distribtions were infrequent.

Two non-statistical conclusions are also supported by the data analyses. For practical purposes these are as important as the statistical conclusions which were the goal of the study. The first is that many of the in situ data collected in tailings materials are nearly impossible to interpret because drainage conditions during testing are not known. Therefore, the results can neither be interpreted to infer undrained strength parameters, nor to infer effective strength parameters. The piezocone may improve this situation.

The second conclusion is that equilibrium pore pressures in tailings embankments for which data are available range from one half hydrostatic for inactive ponds to twice hydrostatic for active ponds. The uncertainty in pore pressure may be the most important of all the uncertainties about geotechnical parameters.

Recommendations

From this work we offer the following recommendations for future activities that would improve methods for safety analysis of tailings dams.

1. Extend the analysis reported herein to other commodities.

2. Evaluate the use of piezocones to assess in situ strength of tailings.

3. Undertake an analytical and field study of uncertainty in pore water pressure in tailings dams and the effect of that uncertainty on a safety evaluation.

4. Conduct a comprehensive risk analysis for an existing tailings dam to define the analytical tools necessary for such a study, to isolate the principal uncertainties in the safety of tailings dams and to illustrate the use and benefits of reliability analysis to the mining industry. This analysis should include systematic uncertainties as well as spatial variation, multiple modes of failure, subjective opinion, and economic aspects of construction, instrumentation and failures. Earlier work by Anderson et. al., 1982, sponsored by the USBM, could serve as a starting point.

CONTENTS

CONTENTS (CONTINUED)

ILLUSTRATIONS

ILLUSTRATIONS (CONTINUED)

ILLUSTRATIONS (CONTINUED)

ILLUSTRATIONS (CONTINUED)

ILLUSTRATIONS (CONTINUED)

ILLUSTRATIONS (CONTINUED)

ILLUSTRATIONS (CONTINUED)

ILLUSTRATIONS (CONTINUED)

TABLES

TABLES (CONTINUED)

1. INTRODUCTION

The engineering design of tailings embankments and storage ponds, like most of geotechnical engineering, is now performed on a deterministic basis. 'Safety' of these facilities is sought by designing to sufficiently large factors of safety such that probabilities of failure are reduced to small, although unspecified levels. Recent interest has developed in both mining and geotechnical engineering in the use of risk-based design, in which uncertainties and probabilities are explicitly considered in assessing safety and making decisions. Among other factors, this trend is being supported by increased mining costs, the introduction of more data intensive site characterization (e.g., through the use of continuous in situ profiling devices), and improved statistical and probabilistic procedures.

In response to this trend, the U.S. Bureau of Mines sponsored research at Utah State University under Contraact J0295029 to review current reliability models applicable to tailings embankments, and to apply such models to a test site. This work was reported in January 1982. One result of this work identified the need for better information on the variability of tailings properties, characterized in ways useful for reliabiltiy analysis. The present report is a direct result of that perceived need.

This report summarizes work conducted under, Contract J0215028 entitled, "Critical Parameters for Tailings Embankments." This work identified a number of sites for which extensive field or laboratory data had been collected on geotechnical properties of tailings, statistically analyzedthose data, and drew conclusions on appropriate distributional forms for use in reliability modeling of geotechnical parameters. In addition, sufficient data were available at several sites to allow inferences of the spatial structure of data ariability, and for these data sets attempts were made to determine spatial trends, infer autocorrelation functons, and establish levels of measurement error (noise). the contract was limited to tailings from copper, uranium and phosphate mining.

This report is organized in three parts. The first part, comprising Chapters 2, 3, and 4, presents background information on geotechnical and statistical issues. The second part, Chapters 5, 6 and 7, summarizes the sites and the problems of measuring geotechnical properties. The third part, Chapters 8, 9, and 10, presents results and conclusions. Detailed site descriptions and descriptions of computer codes are presented in the Appendices.

2. TAILINGS DAM CONSTRUCTION

Introduction

Most tailings are highly variable in their physical characteristics. Differences in ore, milling processes and storage facilities produce these variations. A good understanding of the processes that produce tailings seems essential for one to examine the variability in properties of tailings. Therefore this section reviews the processes, facilities and techniques by which tailings are produced and stored.

Tailings

Mining and milling metal ores and phosphates produces from several tons to several thousands of tons of waste material per day at a given mill. Milling is accomplished primarily by crushing and then grinding, with details of the procedure depending on the properties of mineral and gangue. The most important of these properties are mineral type, specific gravity, hardness, particle size and mineral dissemination. Following crushing, each ore fraction is ground to free the metal. The wastes of this milling consist of the ground remains of the host rock minus the extracted minerals plus large quantities of water. The wastes commonly known as tailings, are deposited in settling basins. Several millions of tons of tailings can accumulate during the life of an individual mine. In order to avoid the spoilage of large land areas, to circumvent the physical and chemical pollution of surface and or underground water, and to minimize disposal costs, tailings are most commonly confined by embankments constructed of the coarser fraction of the host rock (see Figure 2.1).

Most copper is obtained from one or more copper sulfide minerals, although native copper and copper oxides are also mined. About 80% of copper mining is done by open pit. Uranium mining, principally of oxides, uses similar techniques.

Phosphate mining for agricultural chemicals produces these tailings: sand, slimes and gypsum. Most United States phosphate is mined as a gravel sized pellet of apatite in a matrix of sand, silts and clay. The phosphate rock is separated from the matrix mechanically, then ground and mixed with sulfuric acid to produce phosphoric acid and a by-product of gypsum. These gypsum tailings mixed in water are pumped to ponds for disposal. Separation of phosphate from the matrix produces two other waste products,

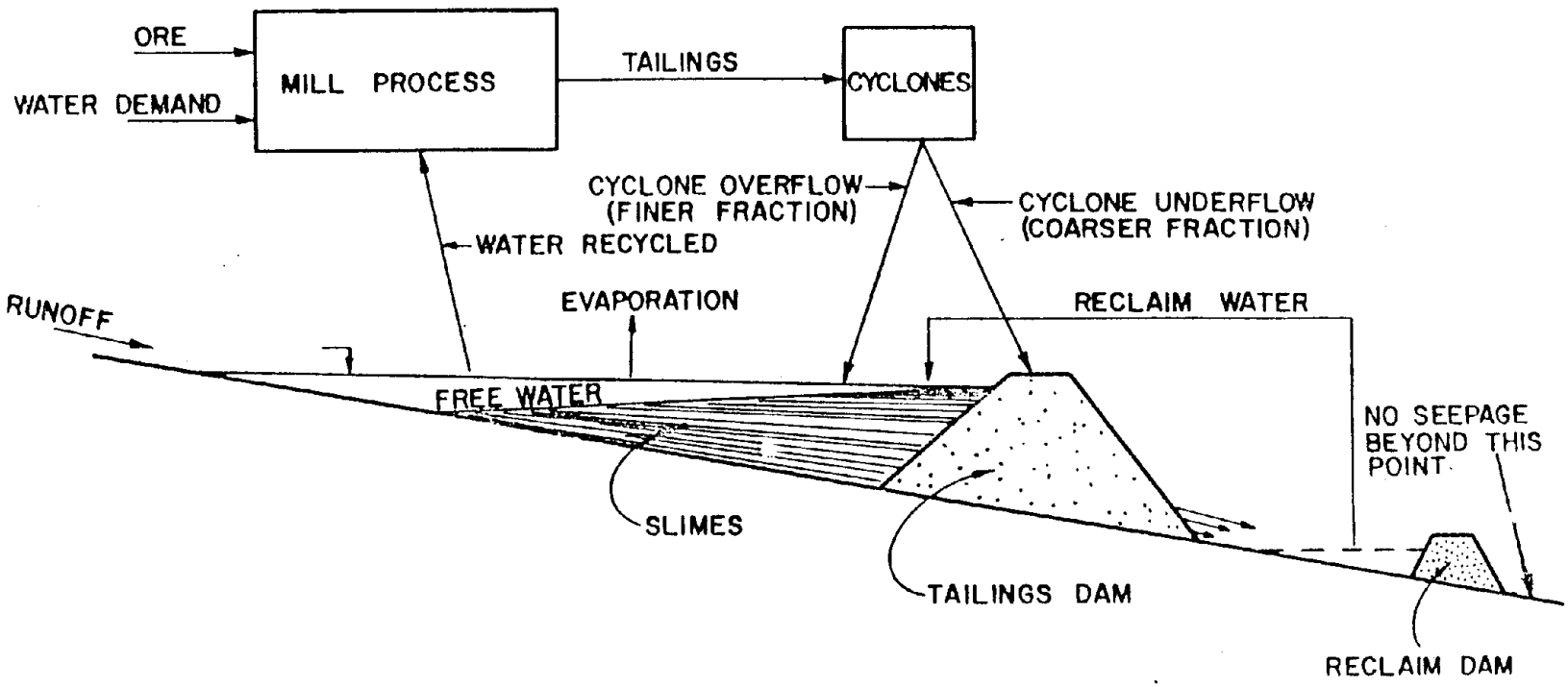

FIGURE 2.1 MILL-TAILINGS POND FLOW SHEET
(AFTER KLOHN, 1972)

coarse sized sand particles and fine grained silts and clays. The fine grained components, slurried in water (slimes), are discarded into a pond. The coarse sized particles are typically used to construct retention embankments for holding the slimes. Thus the waste products found in a complete phosphate operation are waste gypsum sand tailings and slimes.

Tailings Dams v. Traditional Dams

There are several important differences between tailings dams and conventional earthen water retention structures. First, the material stored is not water, but soft, loose and relatively impermeable sedimented tailings. Depending upon the grain size, the time elapsed since deposition, and the location of the phreatic surface, the consistency of the tailings may range from a solid to a semi-fluid. Due to their method of deposition, most tailings are candidates for liquefaction in the event of severe seismic shock. Liquefied tailings become a fluid of high unit weight and zero shear strength. A second major difference results from the method of construction. Many tailings dams use the coarser fraction of the tailings for the tailings dam, as opposed to borrow and overburden used in conventional dams. The tailings are placed without compaction and zonation. Thirdly, tailings dam construction is carried out by the mining operators as part of the mill waste disposal process, with the dam's height increased as needed to provide waste storage. Conventional water storage dams, on the other hand, are generally completed before filling. Finally tailings dams are of no economic value to the owner. The owner wishes to dispose of the tailings in the least expensive, acceptable way.

Initial Design Parameters

Little if any engineering went into tailings dam construction until recent years. Several spectacular failures (El Cobre and Aberfam) and regulatory actions have brought change. Careful engineering is now done on most new large tailings dams, particularly for uranium tailings. Engineers responsible for waste storage now become involved in long term planning of storage facilities, plant water balance, transportation of wastes, location of waste storage facilities and environmental controls, in addition to geotechnical design of the waste retention facility.

Dam Size

Dam size is initially estimated based upon the volume of waste a particular mill produces over a given time. The engineer must determine the availability of embankment construction materials (overburden and borrow fill as well as coarse tailings), the range in quantity of tailings which will need to be disposed, and the rate at which the tailings will be produced as mining operations proceed in space and time. Some tailings dams reach heights of 500 feet or more. Typical of these larger tailings dams is one in the southwestern United States accepting 23,000 tons/day of Copper tailings into a storage area of two square miles. The present height of the dam is 260 feet, and has a projected service life of an additional 26 years. Pond area may be dictated by the required evaporation rate. Height may be controlled by available storage area, foundation conditions and pumping costs.

Dam Location

With an estimate of pond area and required height one can proceed to identify possible storage areas. The location decision must balance tailings and fill transportation costs with potential environmental risks, topography and competing uses of the land. Examination of topography of a site is facilitated by on-site inspection, topographic maps and aerial photographs. The latter are particularly useful for identifying dangerous geomorphic features such as old landslide fault scarps and other features hidden by their scale. Both maps and photographs are useful in identifying flood or floodplain features. For copper and uranium extraction, milling uses toxic chemicals and leaves toxic elements in slurry which must be stored (e.g. arsenic, selenium, molybdenum and radioactive elements. Thus it may be desirable to site the dam as remote from people as possible. To reduce air pollution one may locate the dam in areas most sheltered from wind. The processing of unrefined copper and uranium ores also produces quantities of toxic liquid in addition to tailings solids and these must be stored or treated for release. Pollution control regulations may require control of the amount of water leaving the tailings pond area either through the embankment or through the pond foundation. For uranium, current Nuclear Regulatory Commission (NRC) guidelines control the minimum distance between a dike and a permanent flowing water course, allowable foundation and embankment materials and treatments, dam freeboard level, dike and pond seepage control methods, means of protecting slope and pond surfaces against environmental release, and

other engineering factors.

Tailings Transport

The classic method of transporting tailings from mill to pond is by slurry in either pipes or open flumes. Topography often dictates the most economical route. Alternatively the tailings can be moved in "dry" form by belt-conveyor or truck. Clearly the form of transport and even operational details can have significant influence on the construction and engineering properties of tailings dams. Among these influences are the density and water content of placement, separation or gradation by grain size, zonation and heterogeneity of the dam, and degree of consolidation. Each of these factors effects strength behavior.

Dam Foundation

Given a site for tailings impoundment and a means of transport from mill to pond, a geotechnical assessment is made of foundation conditions as well as of materials proposed for embankment construction. The foundation investigation is typically carried out with borings and sampling. This ascertains the location, thickness, and areal extent of subsoil types. A combination of in-situ and laboratory tests are used to determine shear strength, stress-strain properties, grain size distribution, permeability and moisture-density compaction-related properties for the foundation and fill. These properties may be improved by compaction. Compaction of cohesionless sands, sand-gravel mixtures or fine rock mixtures is achieved by using vibrating drum rollers or pneumatic-tired rollers. For cohesive materials compaction is normally achieved using grid rollers or sheep's foot rollers. For most cohesionless materials water content may range a few percentage points above or below optimum and still yield satisfactory compaction.

Stability and Flow

A stability analysis for the dam design can be easily done using any one of several methods (e.g. ordinary method of slices, simplified Bishop's method of slices, method of wedges, etc.). Iterative computer solutions (ICES-LEASE, SSTAB, SLOPE) are available to search for the potential failure surface with the lowest factor of safety. These analyses require strength parameters and pore pressures for the embankment and foundation.

Undrained analyses are necessary to predict pore pressures for stability analysis, to design against flow related failures, and to predict the path and quantity of seepage leaving the pond. Such analyses may show the need for artificial drainage within the dam or foundation.

Drainage facilities, for example blanket drains or weep tubes, can be used to control the height of the phreatic surface within the embankment and to prevent seepage breakout on the downstream face. Preventing seepage breakout reduces the possibility of internal erosion, piping, low effective stress and downstream failure. If a drain is used, a filter is often required between the embankment fill and drainage zone to avoid erosion of the fill into the drain.

The embankment and foundation for most tailings dams is sufficiently complex that a hand drawn flow net using a simplified section can give misleading results for quantity of seepage and magnitude of pore pressures. One should make conservative use of the results of these simplified analyses or seek more complete solutions of flow through the dam and its foundation. All of the flow and stability design considerations discussed in the literature for water retention dams apply to tailings dams.

Tailings Dam Construction

Construction Materials

Construction materials for a tailings dam may consist of a combination of overburden, waste rock from the mining pit, the solid fraction of the tailings slurry as well as material from borrow pits close to the structure. The economics of tailings disposal dictates that the tailings themselves are usually the major material forming the embankment. The low grade ores produce tailings which have a grain size distribution significantly finer than those of older, richer millings. Grain size data for the copper, uranium and gypsum tailings analyzed in this study are shown in Table 2.1. Generally the gypsum tailings were found to be uniformly fine. The copper and uranium tailings while also fine, tended toward well graded soils.

Table 2.1: TYPICAL GRAIN SIZE DATA

Material	Tailings Dam	% Passing #200 Sieve
Copper	Chino	22
	Magna	91-100
	Mindola	75-99
	Brenda	55-97
	Japan Mine A	25-93
	Japan Mine B	25-90
	Japan Mine D	20-100
	Japan Mine E	10-98
	Japan Mine F	15-100
	Japan Mine J	12-92
Gypsum	Texas	78-93
	Lousiana1	90-100
	Florida1	60-80
	Vick Article	83-98
	Florida4	100
	Lousiana2	80
	Florida2	50-100
	North Carolina	70-95
	Florida3	80-100
	Piney Point	59-82
Uranium	Colorado	19-67
	Shiprock	22
	Grand Junction	12-62
	Ambrosia Lake	28-42
	Durango	5-7
	Falls City	22-32
	Green River	15-29
	Maybell	12-15
	Monument Valley	9
	New Rifle	11-37
	Old Rifle	8-29
	Riverton	35-48
	Slick Rock	21
	Spook	11-19
	Tuba City	20-41

Dam Geometry

Several embankment configurations are typical for slurry ponds as dam geometry largely depends on local topography. It is common to construct a tailings dam around a hill thus using the hill as part of the containment (Figure 2.2). Rectangular or ring dam geometries are used in flat areas and are usually located close to the mining pit. Given this greater flexibility in siting, the dikes can be located to be less susceptible to erosion or flood. Additional storage is developed by building side dikes out from existing berms.

Construction Techniques

Regardless of the geometry an embankment is begun by the constructing a 10-20 feet high starter dike. The starter dike is usually constructed from borrow at the dam location. When the initial pond is nearly filled, the dike is raised by borrowing materials from the dried surface of previously deposited tailings or by hydraulically depositing coarse tailings onto the crest. Successive stages follow one of several schemes in raising the dam.

The Upstream Method

Tailings disposal adds to the cost of production, therefore one would prefer to keep tailings operation as inexpensive as possible. The "upstream method", less common today than in earlier times, is the least expensive method of constructing tailings dams. In common practice tailings dams are raised progressively as needed for additional storage over a period of years. Raising the dam by the upstream method involves shifting the centerline of the crest of the embankment toward the tailings pond as the height of the berm is increased (Figure 2.3). The downstream toe of each succeeding phase of dam building is supported by the top of the previous stage. Thus the majority of each dike cross-section is supported on tailings that have been placed adjacent to the upstream face of the previous stage and are thus weaker than the embankment materials themselves. Dams built this way were rarely engineered or designed.

The coarser tailngs or sedimented tailings are used as construction material for raising the dam. Two methods are commonly used to separate the coarser solids from the slurry piped to the pond. The more traditional technique (spigoting) involves piping the slurry onto the surface of

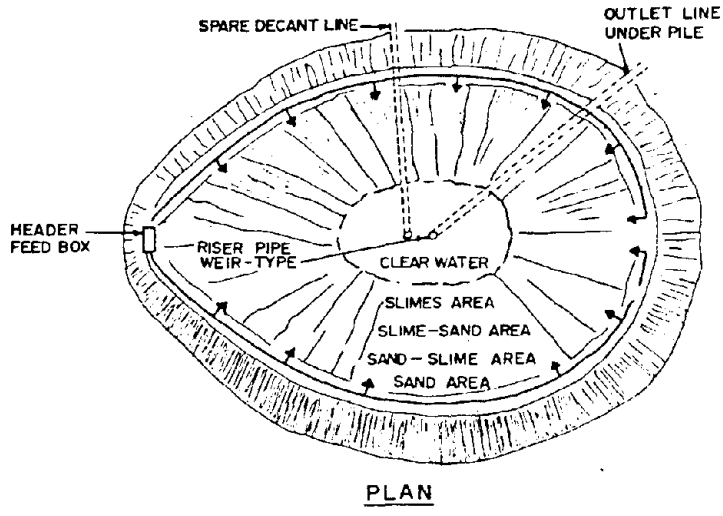

FLAT AREA DESIGN

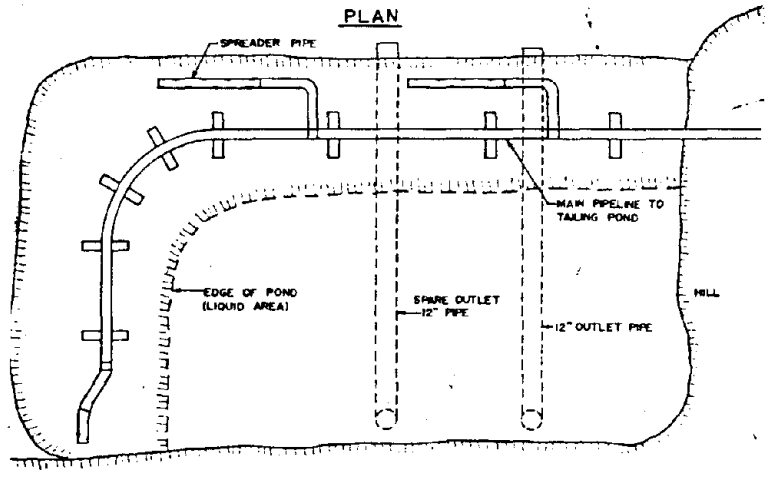

HILL ELBOW DESIGN

FIGURE 2.2 TAILINGS DAM GEOMETRY
(After Phukan, 1971)

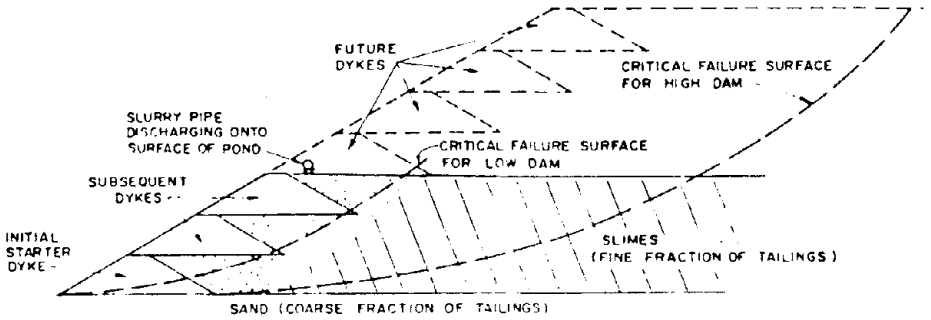

(a) UPSTREAM METHOD

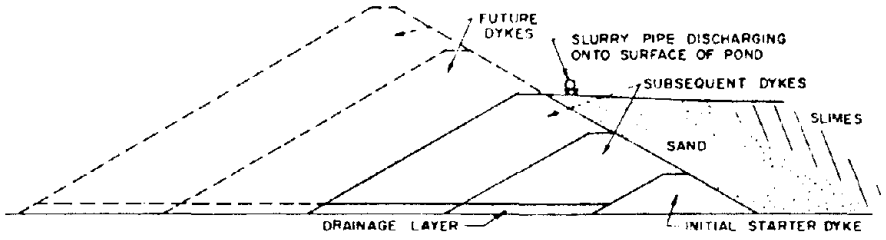

(b) DOWNSTREAM METHOD

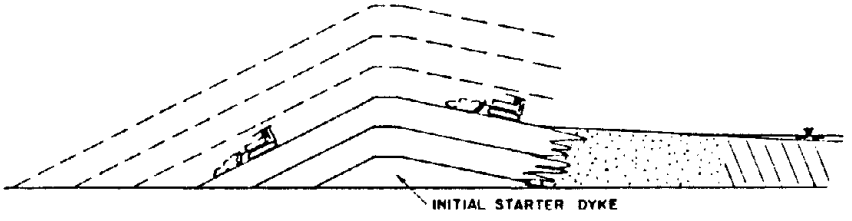

(c) CENTERLINE METHOD

FIGURE 2.3 METHODS OF DAM CONSTRUCTION
(AFTER PHUKAN, 1971)

the tailings pond at a location adjacent to the upstream face of the embankment, resulting in the formation of a gently sloping beach. The coarsest tailing fraction is deposited nearest the spigot discharge point while the finer fraction (slimes) flows toward the center of the pond away from the spigot. The density, permeablility and shear strength of the settled solids decrease with increasing distance from the dike (spigot).

If the grain sizes of the tailings are fine, adequate separation of coarse and fine fractions may not occur by releasing the slurry on a beach. The settled tailings remain loose with low shear strength. Thus cycloning is often used to separate tailings solids into coarse and fine components. The coarse conmponent is placed at the embankment, and the fine component is discharged into the pond. For example, at a coppermine in Arizona, four-inch plug valves are spaced at 26 feet intervals along the dike, and feed through manifolds into 366 twelve-inch cyclones. Each cyclone has a 60 foot, four-inch discharge pipe to take the slimes fraction away from the dike. Deposition is altered between the north and south sections of the dam. One end is allowed dormant while the other end is fully operational.

The upstream construction method involves a great deal of manual labor to maintain and continually relocate piping and equipmemt. Also, the safety of a structure built by the upstream method is hampered by thin layers of slimes that tend to develop within the embankment. Potential stability failure surfaces with the upstream method are located progressively further away from the downstream face as the dam increases in height. A larger proportion of the critical failure surface passes through the lower strength slimes, and thus the outer stronger sandy shell contributes progressively less and less to dam stability as the dam is raised. Shear failure becomes more likely as height increases. Also the settlement of the slurry portion into sedimented layers adds to the probability of embankment failure by liquefaction in the event of seismic shock. Thus use of the upstream method for high tailings dams, particularly in areas of seismic activity, has become less common.

Gypsum dikes are typically constructed using the upstream method. Sedimented gypsum is cast by dragline to raise the perimeter of the dike. The cast gypsum is then shaped and compacted with a bulldozer. The dragline used for gypsum stack raising commonly has a working reach of 60 feet with 2-3 cubic yard buckets. Gypsum stacks in the phosphate industry are generally built as steep as possible to maximize storage capacity, often at the angle of repose

of the material.

The Downstream Method

In contrast to the upstream method, in the "downstream method" the embankment is shifted downstream as the elevation of the crest of the dam is raised (Figure 2.3). Thus each subsequent phase of dike is built directly on the crest and downstream slope of the previous stage. Underdrainage systems are installed as required while the dam is built. Underdrainage permits control of the phreatic surface and increases dam stability. A further advantage of the downstream method is that it allows the materials to be compacted as they are placed within the embankment section, and thus enables design and construction to engineering standards. The major disadvantage of the downstream method is cost; a larger volume of placed fill is required to raise the dam. In the early stages of mill operation it may not be possible to produce sufficient volumes of suitable fill to maintain adequate freeboard between dam crest and rising pond levels. In this case borrow fill is needed to augment the available tailings, thus raising construction costs.

The Centerline Method

The third principal construction technique is the "centerline method" (Figure 2.3), basically a variation on the downstream method. Instead of the dam crest moving downstream as the dam is built, it is raised vertically. Thus the dam is raised by placing additional fill on the crest as well as on the upstream and downstream shoulders. When tailings are used in construction they must be coarse-grained so they consolidate rapidly and are thus able to support construction equipment.

Unlike the upstream method, both the downstream and centerline methods can be used in seismic areas. For liquefaction to occur, sands must be in a loose state and must be saturated. Therefore the best protections against liquefaction are drainage and densification. Well-compacted, unsaturated fills generally do not liquefy and rarely suffer appreciable deformation during earthquake. For dense sands liquefaction is unlikely regardless of saturation. However in areas of low seismicity, it is more economical to design for full drainage rather than maximum density. For areas of high seismicity it is currently thought best to be conservative by requiring both high density and maximum drainage. The centerline method requires less material than the downstream method does to

raise the crest a given height. Thus a dam can be raised quickly and can easily stay ahead of tailings pond growth during early construction phases. One caution to be exercised with centerline construction is to avoid unstable upstream slopes which can initiate breach failures.

Pond Construction

Aside from the embankment, pond construction itself has become routine. Heavy earth moving equipment is used to clear plant growth and loose debris in the area below the final pond level. Usually a basin is scooped out to a surrounding slope at 1 on 3 or less. Rocks and roots are removed before the pond base is compacted. Leak drains or other protective devices are installed deep enough to be undamaged by equipment used to compact the base or install liners. A protective layer of screened earth or sand is usually rolled in place before pond sealing operations are begun.

The choice of pond sealer or liner is important and must consider: (1)type of pollutants in the waste water; (2)soil characteristics (e.g. permeability, clay fraction, sealer shrinkage or swell resistance); (3)geographic location and climatic features (e.g. precipitation, evaporation, wind velocity, temperature ranges, and permafrost); (4)geological structure underlying the site; (5)prevailing restrictions on seepage rates set by government agencies; and (6)characteristics of the sealant (e.g. type, performance effectiveness, durability and resistance to decay and deterioration).

Pond Sealants

Pond sealants fall into nine general categories. The most common is the compacted earth sealant. Compaction of earth at the base of the pond results in reduced porosity. This implies a reduced strength, stability and resistance to erosion. Although minimum permeabilities are asociated with maximum compaction several factors must be considered when using an earth sealer: (1) permeability changes with time; (2) minimum permeability with maximum compaction of a particular soil may still be too high to meet government standards; (3)pond seepage is often greater than pond evaporation; (4)wastewaters may be beneficial or harmful to a given sealer (e.g. alkaline wastes such as sodium carbonates reduce soil permeability while acidic wastes destroy expansive soil characteristics); and (5)physical factors (e.g. freezing, thawing, drying and wetting) may crack the liner, and linings should be kept moist to

maintain stable conditions. Gravelly and sandy clays with plasticity indices (PI) from 12-24 are best suited for thick compact earth linings; clays with PI>24 are sticky and hard to handle while clays with low PI are susceptible to frost damage. Choice of thickness also depends on the depth of the tailings to be stored, but should not be less than 8 inches.

A second common type of pond sealant is the clay sealant. The ability of a soil to seal is proportional to its silt and clay content. An increase of the quantity of clay in a soil proportionately decreases its permeability. Bentonite is widely used as a soil supplement to control seepage due to its high swelling capacity caused by water adsorption. Bentonite adsorbs five times its weight in water and swells to 12-15 times its dry volume when fully saturated. Clays with high ratios of sodium to calcium absorb more water and swell more than low sodium clays. Bentonite with 10% sodium saturation and high colloidal content is often placed as a one-half inch layer on a compacted base and covered with at least six inches of soil to inhibit ion exchange with Ca++ or Mg++.

A third common sealant is the chemical sealant. Sodium bearing chemicals (Na_2CO_3 and $NaSiO_3$) are common. They function as sealers by filling the interstices of the soil or by reacting with soil constituents to form impermeable precipitates or gels. Chemical sealants require retreatment every 2-3 years. Other common chemicals sealers are waxes, resins and various other polymers. One must consider the effects on permeability of reactions between chemical sealants and the permeating fluid.

A variety of other sealants are used in tailings ponds. Among these are waste tailings slimes, asphalt membranes, asphaltic concrete, soil cement, Portland cement, shotcrete, stones and brick. Waste tailings (industrial slimes) are colloids produced by the mining and milling process. Obviously, the ore tailings themselves increasingly seal the pond bottom as they accumulate in the pond. Asphalt membranes are resistant to low temperatures, and are tough and durable. Soil sterilants are used to prevent the growth of vegetation on the subgrade which could puncture the asphaltic liner. Asphaltic concrete is useful for large ponds where heavy equipment must be supported during installation, cleaning and repairs. A six-inch thick layer gives consistently good results. Soil cement satisfies the same needs as asphaltic cement. Portland cement, shotcrete, stones and brick perform poorly when exposed to freeze-thaw cycles and also perform poorly in high sulfate soils as they decompose.

An increasingly common pond sealer is the synthetic membrane liner. One popular product, the polyvinyl chloride liner, ranges from 10-60 mils in thickness with a life expectancy of up to 20 years. It has the qualities of good resistance to inorganic substances excellent seepage control, and low installation cost. Unfortunately PVC is subject to attack by some organic substances to deterioration caused by sunlight and to tears and puncture.

Design of a pond sealer depends upon a balance between economics and the demands of a particular tailings pond site.

Instead of a sealer or liner, pollution control may be achieved by using a combination of injection and pumping wells. Clean water is supplied to the injection wells while contaminated groundwater is extracted through the pumping wells. Provided the piezometric water elevation along the line of the injection wells is maintained higher than along the line of pumping wells, a hydraulic barrier will be maintained which precludes the loss of pond seepage downstream.

Tailings Management Systems

Continuing operations once an embankment and pond are in place requires a construction control and managememt system. Much more than with water retention structures, the conditions of operation of a tailings dam can change significantly during its operating life. Hydrological conditions often differ from those assumed. The mill water balance sometimes changes, resulting in either more or less water being added to the pond and changing the phreatic surface. Changes in mill grind may result in either more or less sand being available for tailings dam construction. Unforseen cycloning problems caused by a clay mineral content in the ore may drastically reduce the recoverability of suitable embankment sand and thus may require two-stage cycloning. Unexpected or prolonged mill shutdown causing a halt to dam building with pond levels continuing to rise could threaten dam safety by overtopping. Climatic conditions may combine an unusually long winter season (which in turn shortens the dam construction period) with an unusually heavy runoff endangering freeboard required to store a flood discharge. These departures from assumptions in design may lead to serious failures if the dam is not properly managed.

Many activities during construction and operation may violate assumptions made in the design. For example, the ponding of water from cyclone underflow should not be

permitted on the dam fill. This ponding results in the deposition of lenses of fine relatively impervious tailings which creates perched water due to interference with flow. This may result in exit of water on the downstream face rather than through the underdrain. Another common problem is in the use of water to place tailings on the dike. Water and sand should be added in any one area for short periods only. This avoids saturation of large masses of sand starting from the crest and reaching to the base of the dam and avoids possible instability. In general it is best to work along the entire line of the dam when raising the crest. This procedure reduces seepage flow and sloughing along the downstream toe. It should be noted that fill should be placed in uniform lifts--usually 8-12 inches. Thicker lifts are possible for cohesionless granular materials. The rate of dam construction must be adequate to maintain a safe freeboard with respect to a continually rising tailings pond. It is advisable to periodically recompute the rate of dam building, the rate of pond rise, runoff volumes, evaporation rates and reclaimed water volumes. The original design must be flexible and capable of change. Dam operators must keep adequate records to facilitate ongoing design changes responsive to changing design variables. To this end the site should be sufficiently instrumented. Well-placed piezometers give information to predict flow and stability conditions by monitoring water pressures and phreatic surfaces in the embankment. Settlement gauges should be used on dams built on compressible foundations. Time settlement data gained from them can indicate average rates of pore pressure dissipation within the foundation. Ideally all relevant geotechnical data (permeability, dry unit weights, pore pressure, shear strength) should be measured periodically for comparison with values used in the original design.

A flexible design allows the control of aspects of several critical factors of dam maintenance. First, the volume and location of the fines or slimes can be controlled by the manner of distribution and segregation of the tailings solids within the impoundment. Second the amount of tailings kept underwater is a direct control on potential air pollution problems. Third, within limits, the density, compressibility, permeability and shear strength of the tailings in various zones of the pond can be affected by the manner in which the tailings are distributed. Fourth, the control of the amount of water stored in the pond during the operating period affects seepage, head, and the probability of failure. It also represents the total amount of fluid that can be lost in the event of a failure. Surface erosion by waves and rain can endanger dam stability. If gullying does occur it is best to use coarser, erosion-resistant rock, gravel or even sand bags for stabilization. Generally

if the tailings contain iron pyrites in excess of about 0.7% by weight, a relatively hard erosion-resistant crust often develops. Cement or lime slurries or vegetation (grass, sod) are frequently used to stabilize embankments and thereby also control erosion. A final crucial control variable is regulation of maximum freeboard variability to prevent overtopping.

Overtopping of the dam could result in a breach, water and ground contamination, loss of property and possibly loss of life. Since earthfill structures generally can't withstand overtopping, decant systems are used to keep the water surface safely below the embankment crest. A decant system must have a capacity great enough to maintain the water surface in the tailings pond below crest level and to be able to handle the maximum expected inflow into the tailings pond from surface runoff, precipitation, and the tailings slurry. Generally there are three basic types of decant systems decant towers, syphon systems, and pump systems mounted on floating barges. A decant tower is a vertical structure complete with stop logs or decant holes. Pond water level is controlled by placing stop logs or plugging decant holes. These openings in the decant tower function as a weir over which the tailings water flows, drops to the tower bottom and exits via a decant pipe through the base of the embankment. One advantage of a decant tower is that since it operates by gravity forces it is not vulnerable to the breakdown of mechanical equipment. However there are disadvantages to the tower system. For large dams the decant tower requires a large capital investment. Further, tower walls must be designed to withstand the maximum horizontal force exerted by tailings. In seismic areas it may be assumed that adjacent tailings may liquefy producing hydrostatic pressures. Stop logs and plugs must be fail-safe as they are difficult to repair at great depths. Design loads for the tower and its footings should also consider tower weight. negative skin friction loads from consolidation and settlement of the tailings, wind forces and hydrostatic uplift forces on the base. The tower and decant pipe must be immovably supported on foundations to guard against line distortions and differential settlement between tower and pipe. Rupture of pipe-tower joints can initiate internal erosion in the embankment, leading to piping and dam instability.

Unlike decant towers, syphon decant systems are used to move tailings effluent water over the dam crest and to the downstream toe of the dam. Such a system can be installed inexpensively. However, it must be maintained close to the upstream face of the embankment with the attendant possibility of wave erosion on the upstream face. Most syphon systems require daily inspection.

Pumps mounted on floating barges permit pond water to be maintained at a considerable distance from the embankment. They are easily moved, allowing reclamation of the clearest tailings effluent water. The disadvantage of the pump-barge system is the possibility of mechanical breakdown and the requirement of periodic maintenance.

A final issue to be addressed by an adequate tailings management system is cold weather operations. Winter construction is undesirable during severe freezing conditions. The operation of cyclones, sluiceways and spigots becomes difficult and often results in an unsuitable embankment. Snow and ice from cycloning or sluices become buried in the dam. When warmer temperatures arrive these melt leaving holes or causing sloughing or sliding in the slopes. Voids can thus be created which concentrate seepage flows and lead to possible piping failures. In winter cold the compaction of cycloned sands and other materials can not be achieved, and can result in an extremely loose fill. The best practice during cold months is to discharge unclassified tailings directly into the pond by end-spilling at convenient locations.

3. STRUCTURAL STABILITY OF TAILINGS EMBANKMENTS

Engineering Behavior

The principal design criteria in the engineering of tailings embankments is that (1) they retain tailings materials, and that (2) they control seepage. In certain cases minimizing fluid loss is a principal design criterion, as fluid wastes may by harmful to water supplies or to plant and wildlife. These criteria may be violated through a variety of geotechnical failures, the commonest of which are (1) strength instability (i.e., slope or bearing capacity failures), (2) excessive or differential settlement, and (3) high permeability. The present report deals only with the first of these failure modes, and specifically with the question of estimating tailings strength parameters from which to analyze structural stability.

This section considers the engineering analysis of embankment stability, the role of strength parameters in those analyses, and recent moves toward reliability-based design.

Embankment Stability

Stability analyses determine whether the strength of soils in an embankment is sufficient to resist shearing stresses developed by gravity and other applied forces. Most methods of stability analysis define factor of safety as the ratio of the resisting moment along the most critical potential failure surface through the embankment;

$$FS = \frac{\sum \text{strength x area x moment arm}}{\sum \text{shear stress x area x moment arm}}$$

Figure 3.1 illustrates the key variables for calculating factor of safety. In any stability analysis three things must be determined to obtain the minimum factor of safety:

(1) the strength acting along a trial failure surface

(2) the shear stress mobilized along that trial failure surface

(3) the trial failure surface with a minimum factor of safety

The critical surface is found by analysing many trial failure surfaces until the minimum acceptable failure surface is located. The mobilized shear stress is found by using equations of static equilibrium applied to the potential sliding mass to find the shear stress required to maintain equilibrium. Mobilized shear stress depends on slope geometry, unit weight of soil, seepage forces, and other applied forces.

By far the most difficult factor to assess is soil strength. Most stability analyses model strength by the Mohr-Coulomb failure criterion,

$$S = c + \bar{\sigma}_{N_f} \cdot \tan \phi \qquad (3.2)$$

where:

S =shear strength

σ_{N_f}=the stress normal to the failure plane at

$$F.S. = \frac{\text{Resisting Moment}}{\text{Driving Moment}} = \frac{S \cdot R}{W \cdot a}$$

W = total weight of sliding mass
S = strength times area of failure surface
R = radius of circular failure surface
a = distance from center of circle to center of sliding mass

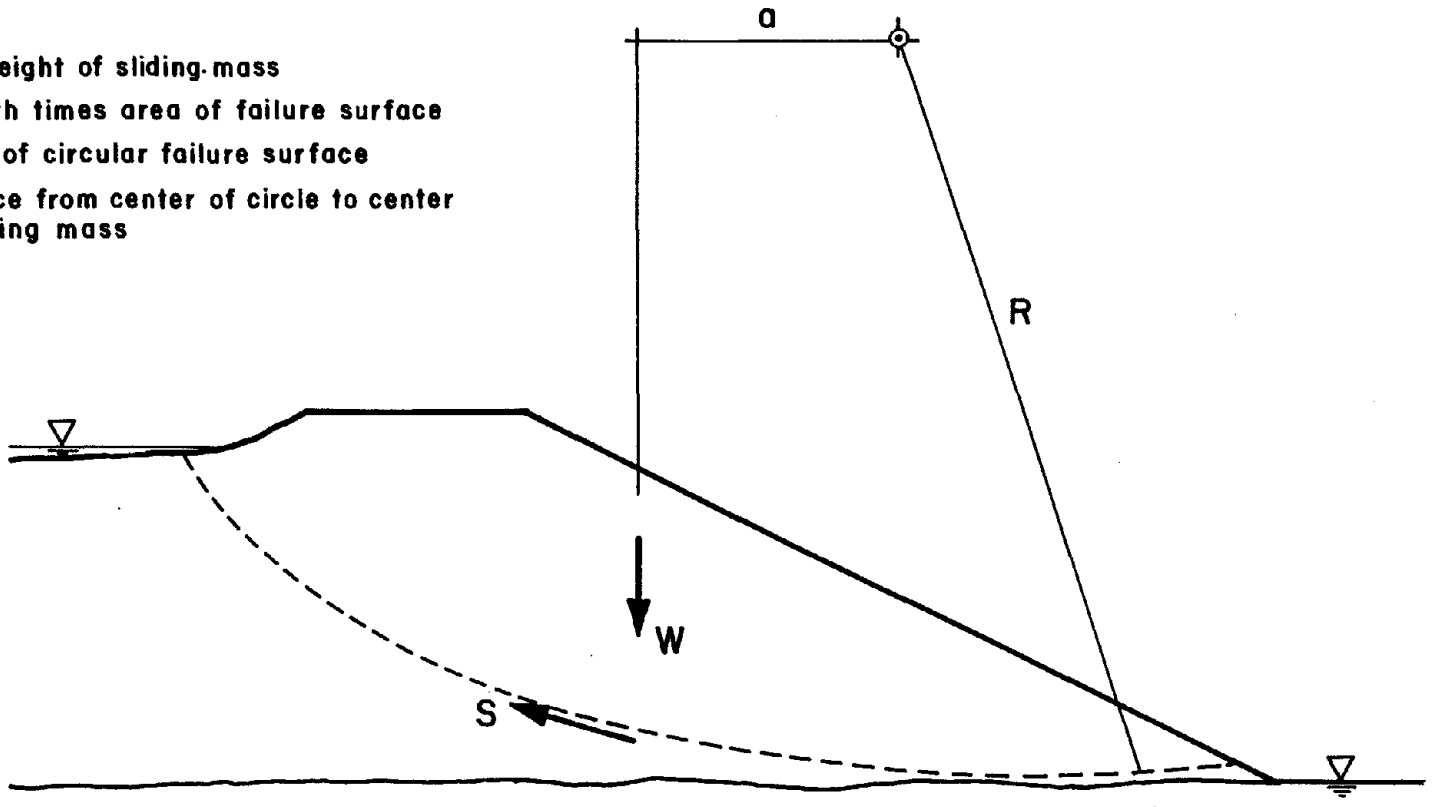

FIGURE 3.1 FACTOR OF SAFETY AGAINST STABILITY FAILURE

failure for the point under consideration

c =the cohesion intercept of the soil or strength at σ_{N_f} of zero

ϕ =the friction angle of the soil, tan ϕ equals the coefficient of friction of the soil.

u =pore water pressure

Two measures of stress are commonly used for soils effective and total stresses and confusion often develops over whether σ_{Nf} in Equation 3.2 should be effective stress or total stress. Fundamentally, the strength of soil is related to the effective stresses (see e.g., Lambe and Marr, 1979). Thus Equation 3.2 is correctly written as

$$S = c + \bar{\sigma}_{N_f} \cdot \tan \phi \qquad (3.3)$$

where the bar signifies effective stress. Making use of the relation between effective and total stress, $\bar{\sigma} = \sigma - u$, Equation 3.3 can also be written

$$S = c + (\sigma_{N_f} - u_f) \cdot \tan \phi \qquad (3.4)$$

where u_f is the pore pressure at failure.

To determine c and ϕ, tests must be performed in which strength at different values of $\bar{\sigma}_{N_f}$ is measured (Figure 3.2). Values of $\bar{c}$ and $\bar{\phi}$ with the bar indicate that they have been determined from tests with known values of . Equations 3.3 and 3.4 become

$$S = \bar{c} + \bar{\sigma}_{N_f} \cdot \tan \bar{\phi} = \bar{c} + (\sigma_{N_f} - u_f) \cdot \tan \bar{\phi} \qquad (3.5)$$

and

$$S = \bar{c} + \bar{\sigma}_{N_f} - u_f \qquad (3.6)$$

σ_{Nf} and u_f along the sliding surface are required to complete a determination of strength. In all common methods of stability analysis, a simplification is used: σ_{N_f} is assumed equal to σ_N determined from static equilibrium under existing conditions. If the sliding mass is at failure with a factor of safety of 1, σ_{N_f} equals σ_N. One can not determine σ_{N_f} easily for conditions other than failure.

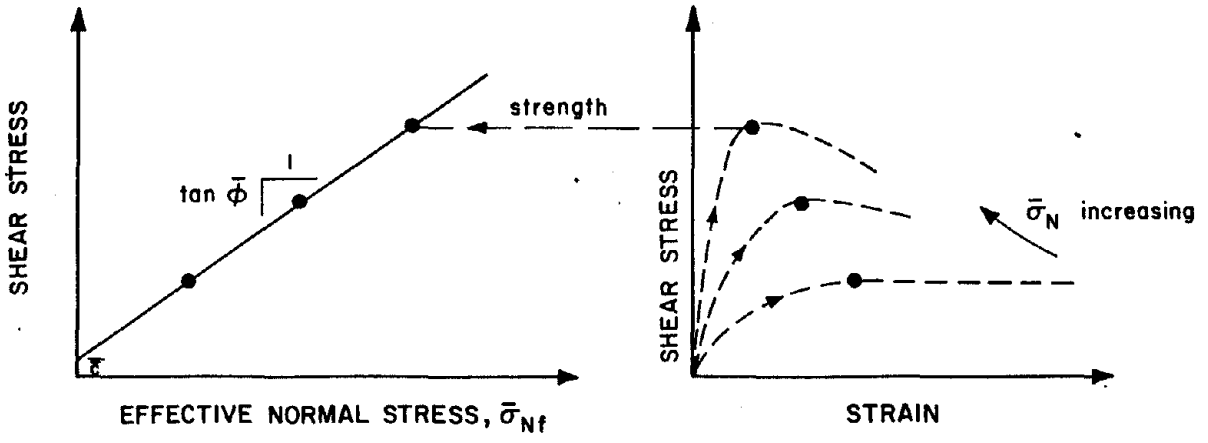

FIGURE 3.2 EFFECTIVE STRESS STRENGTH

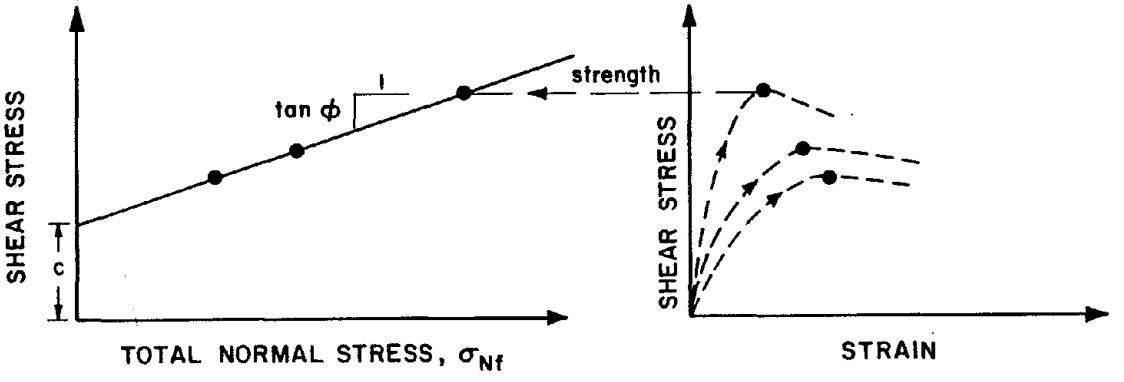

FIGURE 3.3 TOTAL STRESS STRENGTH

Similarly we may know pore pressure for existing conditions or from field measurements or analysis of flow may be known, but these may not equal pore pressures at failure. If failure results from some increase in shear stress along the critical surface and that increased shear stress induces changes in pore pressure which can not rapidly dissipate, u_f no longer equals the steady state pore pressure.

Two approaches are used to handle this question. One approach considers $u_f = u_s$. The stability is then made by determining $\bar{c}$ and $\bar{\phi}$ from tests, determining u_s from flow analyses or field measurements and calculating σ_N and shear stress from the equations of static equilibrium. This procedure, called "the effective stress approach", finds widespread use in stability problems where changes in shear stress are slow enough to allow complete drainage of shear induced pore pressure. The second approach seeks to circumvent the difficulty of predicting u_f by interpreting strength in terms of total stresses. Strengths measured at different values of σ_{Nf} are used to determine c and ϕ, as shown in Figure 3.3. As in the effective stress approach, most analyses of this type employ a simplification that σ_{Nf} equals σ_N determined from considering equilibrium with existing conditions. With this simplification, one can determine c and ϕ from tests and calculate σ_N and shear stress from the equations of equilibrium. This procedure is commonly called "the total stress approach." It appears simpler to use than the effective stress approach because it does not need to consider u_f . However there is a drawback. This approach works only when the soil samples used for strength testing are consolidated to the same effective stresses prior to shear as exist in the field and when shear in the test and in the field occur with no change in volume of the soil. The second requirement is met when changes in shear stress occur so rapidly that no drainage of shear induced pore pressures can occur, the so-called undrained condition. The first requirement is met by some but not all strength testing equipment and procedures. The total stress approach finds widespread use in stability problems where changes in shear stress are rapid enough to preserve undrained conditions and one can recover undisturbed samples for the strength tests. Other assumptions on the distribution of forces within the sliding mass enter when developing the equations of static equilibrium. However these assumptions are relatively unimportant to determining the minimum factor of safety when using and considering common methods of analysis. Lambe and Whitman (1969) and Wright (1969) review the importance of these assumptions. One common error in stability analysis results from using total stress strength parameters, c and ϕ, in an effective stress analysis. This error can produce serious

consequences including unexpected failure.

Summarizing, the Mohr-Coulomb strength criterion with the equations of static equilibrium are commonly used to determine factor of safety along a potential sliding mass. Factor of safety is defined either as the ratio of strength times area to mobilized shear stress times area or as the ratio of associated moments. In the commonly used effective stress analyses the following simplifications and assumptions are made

(1) $\bar{c}$ and $\bar{\phi}$ define strength in terms of effective stress using σ_{N_f}

(2) $\bar{\sigma}_{Nf}$ equals $\bar{\sigma}_N$ (the effective normal stress for existing conditions)

(3) u_f equals u_s (the steady state pore pressure)

In the commonly used total stress analyses the following simplifications and assumptions are made·

(1) c and ϕ define strength in terms of total stress using

(2) σ_{Nf} equals σ_N (the total normal stress for existing conditions)

(3) strength parameters are determined from tests consolidated to the field effective stresses and sheared with no volume change

(4) shearing in the field occurs with no volume change.

Next we consider ways of determining drained and undrained strength parameters.

Reliability Analysis of Embankments

The extension of geotechnical analysis to include reliability assessments, particularly in embankment stability calculations, requires information on engineering properties that heretofore has seldom been systematically gathered. Specifically, reliability analysis attempts to assess the uncertainty in predictions of engineering performance, and in so doing, requires a quantification of uncertaities in the geotechnical parameters used to predict stability. This section briefly summarizes reliability approaches to embankment stability analysis, focusing on the input requirements that differ from traditional practice. A more complete discussion of reliability-based design of tailings embankments is found in Anderson, et al. (1982).

Fundamentals of Reliability Analysis

Reliability analysis, as considered here, specifically addresses the influence of uncertainties in geotechnical properties, boundary and initial conditions, external loads, and other identifiable aspects of engineering modeling on predictions of facility performance. That is, it translates input uncertainties in engineering calculations to uncertainties in the results. As defined here, reliability analysis does not deal with all the uncertainties of engineering practice, nor does it seek to balance uncertainties against costs to achieve optimal designs. These latter activities, which might more accurately be described as risk analysis, involve qualitative information, subjective estimates, and value judgements. While important they are outside the scope of this report.

Schmematically, an embankment stability model can be reduced to a simple mathematical function of the form,

$$Y = g(X) \tag{3.7}$$

in which Y is a vector of performance variables to be predicted (e.g., factor of safety, deformations, pore pressures), X is a vector of parameters, and g(.) is some function based on engineering mechanics. If X is uncertain, then Y, too, must be uncertain. However, if the joint probability distribution of $X=\{x_1, \ldots, x_n\}$ is specified, the joint probability distribution of Y can be calculated as

$$f_y(Y) = f_x[g^{-1}(Y)]\ J(X,Y) \qquad (3.8)$$

in which fy(.) and fx(.) are probabiltiy density functions and J(X,Y) is the Jacobian of the transformation from X to Y. This transformation is shown schematically in Fig. 3.4 for scalar x and y.

In essence, reliability analysis reduces to specifying the joint probability function of the input variables X, and in performing the calculations leading to the probability distribution of the predicted variables Y. The results of reliability analysis are typically expressed either as a so-called probability of failure or as a so-called reliability index. The probability of failure Pf is the probabilty that the calculated performance variable y exceeds some specified limit, as for example, the probability that a calculated factor of safety, FS, of less than 1.0 obtains, Pf = Pr(FS<1.0). Clearly, this is not a probability of failure in the true sense that it might be congruent with observed frequencies of failure, because the calculation omits many factors contributing to the possibility of failure (e.g., construction procedures). Pf is more appropriately called a nominal probability. The reliability index β is a measure of the distance of the expected value of y (i.e., the best estimate) from the limiting criterion or failure value expressed in units of the standard deviation of y. For factor of safety this becomes,

$$\beta = \frac{E(FS) - 1.0}{S(FS)} \qquad (3.9)$$

β is related to Pf, but not uniquely. It is an index of safety.

The calculation of Pf requires a full probability distribution over Y. Thus, it is called "full distribution analysis." The calculation of β, on the other hand, requires only that means, variances, and covariances of the terms of X be specified, and leads only to means, variances, and covariances of the terms of Y. Therefore, first-order approximations can be used, and the result is said to be a first-order second-moment analysis.

Variance Components

As described more fully in Section 4, uncertainty in the estimation of tailings properties in an embankment can be divided into three variance components, one due to spatial variability, one due to measurement bias, and one due to

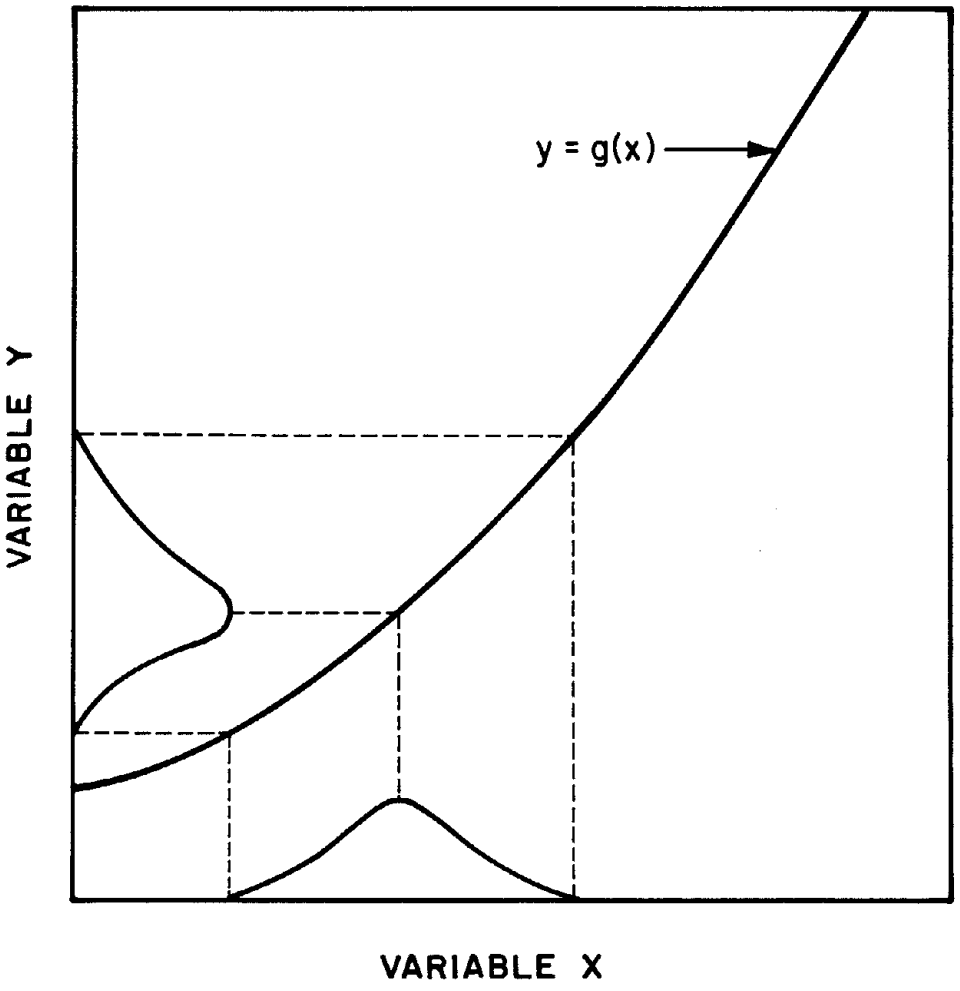

FIGURE 3.4 TRANSFORMATION FROM X TO Y

statistical estimation error. Random measurement error, as long as it can be identified, can be removed from the variance components of estimated properties because its influence is important only to statistical estimation error. Thus, two related aspects of data analysis for reliabiltiy modeling are important, establishing the magnitude and nature of spatial variability of tailings properties, and establishing the fraction of total data scatter due to measurement error. For first order second moment (FOSM) analysis these need only be specified to means, variances, and covarinaces. For full distribution analysis they must be specified in probability distribution functions.

Spatial Variation

In most geotechnical modeling the spatially varying properties of tailings in an embankment are idealized as having instead some uniform value, with "random" fluctuations about it. Clearly, the tailings properties are not in fact random--for with an infinite amount of testing they could in principle be known precisely--but since testing effort is limited it is convenient to model the spatial variability with the mathematics of random process theory. This allows interpolation errors to be predicted, and the implications of spatial variability to be studied.

An important aspect of spatial variability is that it introduces a strong scale effect, not on expected performance, but on the uncertainty of performance predictions. Under this scale effect the precision with which a stability prediction can be made depends on the size of the failure surface. Mechanisms of failure that depend on average strengths within a large volume of tailings materials are less uncertain than those within a small volume. Fluctuations about the average in an embankment ever more cancel as volume increases. Conversely, mechanisms of failure that depend on extremes within an embankment, as say piping, are more uncertain in larger volumes of materials because they depend on the worst element of soil within the embankment. The importance of such scale effects has been demonstrated by Anderson, et al. (1982) in their analyses of probable lengths of tailings embankment failures.

The most common way to characterize spatial variability for the purpose of reliability analysis is through the autocovariance function $C_x(r)$. $C_x(r)$ measures the decay of correlation of tailings propterties as a function of spatial separation. This function and its estimation are considered in Section 4.

Cross Correlations of Tailings Properties

Correlation among engineering properties is simply a measure of the degree of association among the uncertainties of those properties. When two properties vary in similar ways about their means, that is, when they tend to be simultaneously above or simultaneously below their respecti e means, they are said to be positi ely correlated. Similarly, when they tend to vary in dissimilar ways they are said to be negatively correlated. Although frequently ignored, correlations among geotechnical properties are important determinants of the reliability of earth structures. When these correlations are positive, as they usually are, the actual uncertainty in predictions can be much larger than that implied by an analysis assuming independence.

Correlations among geotechnical properties are principally introduced in three ways. They may be introduced by physical factors, as for example, dense soils are simultaneously stronger and less permeable than loose soils. They may be introduced through statistical estimation error, as for example, Mohr-Coulomb strength parameters c, phi are negatively correlated because they are regression parameters. Finally, they may result from systematic modeling errors, as for example, field measurements of strength and deformation are both inferred using elastic stress distributions which introduces similar errors in each.

In the present work correlations were analyzed when data permitted. The results are presented as correlation coefficients between pairs of properties x,y,

$$r = \frac{E[(x - m_x)(y - m_y)]}{S(X)S(Y)} \tag{3.10}$$

in which m_x, m_y are the means of x and y.

4. STATISTICAL DESCRIPTION AND INFERENCE

Concepts of Statistical Descriptions

Due to limited numbers of samples, testing errors and spatial variability, estimations of engineering profiles for tailings materials are always subject to some error. The magnitude of these errors can be specified in a number of ways, using upper and lower bounds for example, but has an important influence on the reliability with which predictions of engineering performance of tailings embankments and ponds can be made. This section summarizes techniques for describing the amount of error in engineering profiles using simple statistical methods, and serves as a background for later parts of this report.

Statistical Description of Data Scatter

Data as collected in the field or as a result of laboratory testing invariably display some amount of scatter (Fig. 4.1). For typical tailings materials, this scatter can be many tens of percents of the data averages.

Statistical Moments

Given a time series or distance dependent set of data, the simplest way to describe data scatter is with a set of two numbers, one specifying the central magnitude of the measurements, and one specifying the dispersion of measurements about that center. While there are many candidates for these two measures, the most useful and the most common are the so-called first two moments of the data scatter, specifically the average or mean and the variance.

The mean of a set of observations,

$$X = x_1, \ldots, x_n \tag{4.1}$$

is defined as the arithmetical average,

$$m = \frac{1}{n} \sum x_i \tag{4.2}$$

From a physical point of iew the mean is analogous to the center of gravity of the data along the axis of measurement. The variance of the data is defined as the mean squared variation of the data about m, or

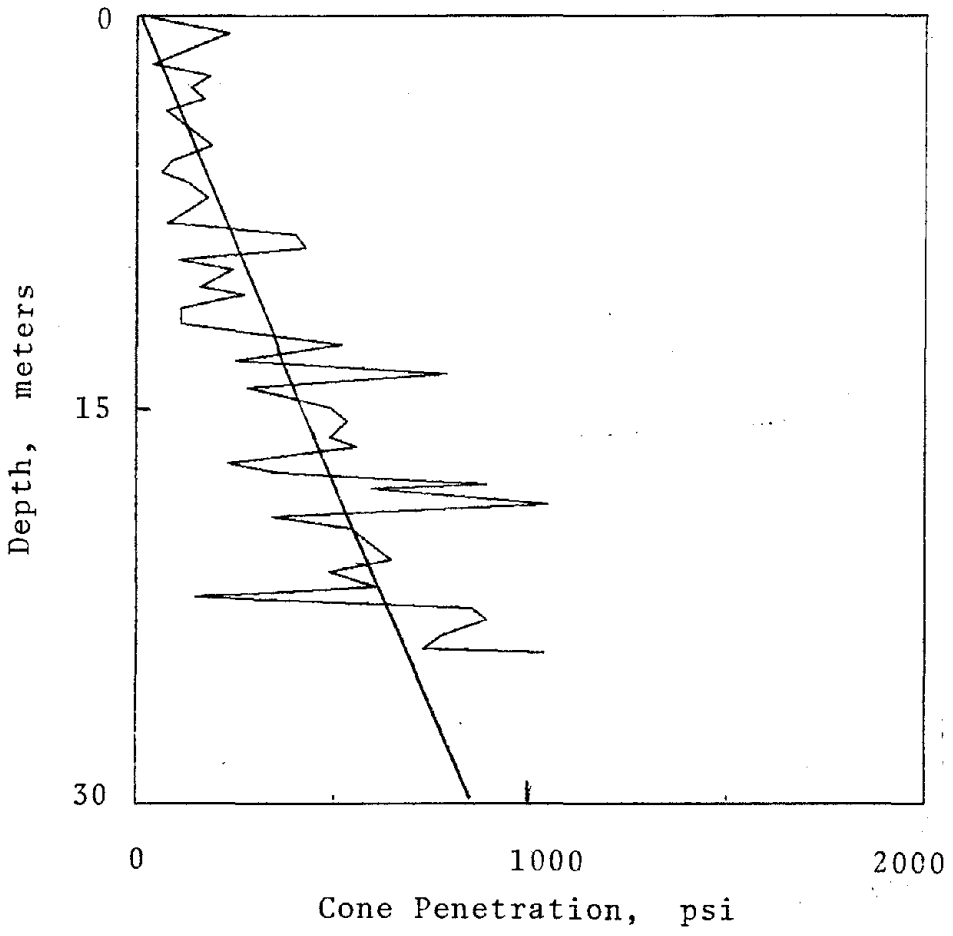

Mean trend with depth: $q_c = 11 + 28\ z$

Mean of residuals: 0.00 psi

Standard deviation of residuals: 153 psi

Number of data points: 103

Figure 4.1
Plot of cone penetration v. depth

$$V(x) = \frac{1}{n-1} \sum (x_i - m)^2 \qquad (4.3)$$

Again, from the physical point of view, this is analogous to the moment of inertia of the data about m(x). Together, the mean and variance are said to constitute a second-moment description of the data scatter.

For many purposes a convenient measure of dispersion is the square root of the variance, or rms variation, usually called the standard deviation,

$$S(x) = \sqrt{V(x)} \qquad (4.4)$$

The standard deviation is measured in the same units as the data themsel es, rather than the square of those units, and can be used to describe proportionate dispersion through the coefficient of variation,

$$Cov(x) = S(x)/m \qquad (4.5)$$

Distribution Functions

While moments of the data scatter describe the location and dispersion of the data, a complete description of the scatter is more easily obtained by the so-called distribution function. Arranging the data in order of increasing magnitude, the fraction of the observations less than some value x is summarized in the cumulati e distribution function F(x), sometimes abbreviated cdf. Cdf's (or their complements) are widely used in soil engineering to describe grain size distributions. They may be used to describe the variation of engineering properties (i.e., strength, deformation and flow) data as well. Fig. 4.2 shows the histogram of the residual data of Fig. 4.1, and Fig. 4.3 shows the cdf of these data.

The derivative of the cdf,

$$f(x) = dF(x)/dx \quad , \qquad (4.6)$$

describes the density of data along the measurement axis, and might be loosely described as a smoothed version of the data histogram. This derivative is typically called the probability density function (pdf), and has the property that its integral between two values of x gives the fraction of observations within the interval (i.e., the probability that a randomly chosen datum would lie in the interval).

Continuing the physical point of view, the moments of the data scatter are related to the pdf in the same way that

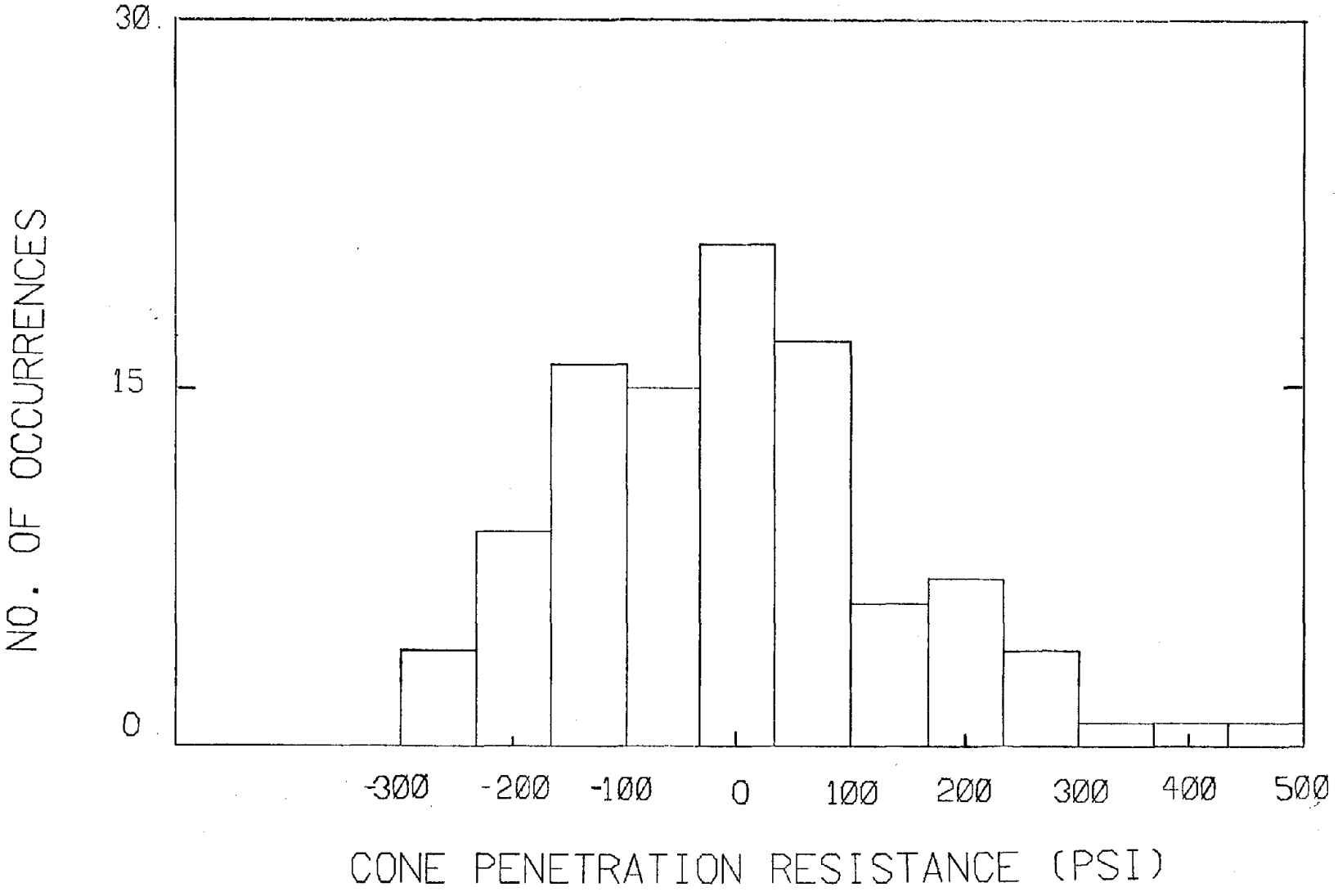

Figure 4.2 - Histogram of residual data of Figure 4.1

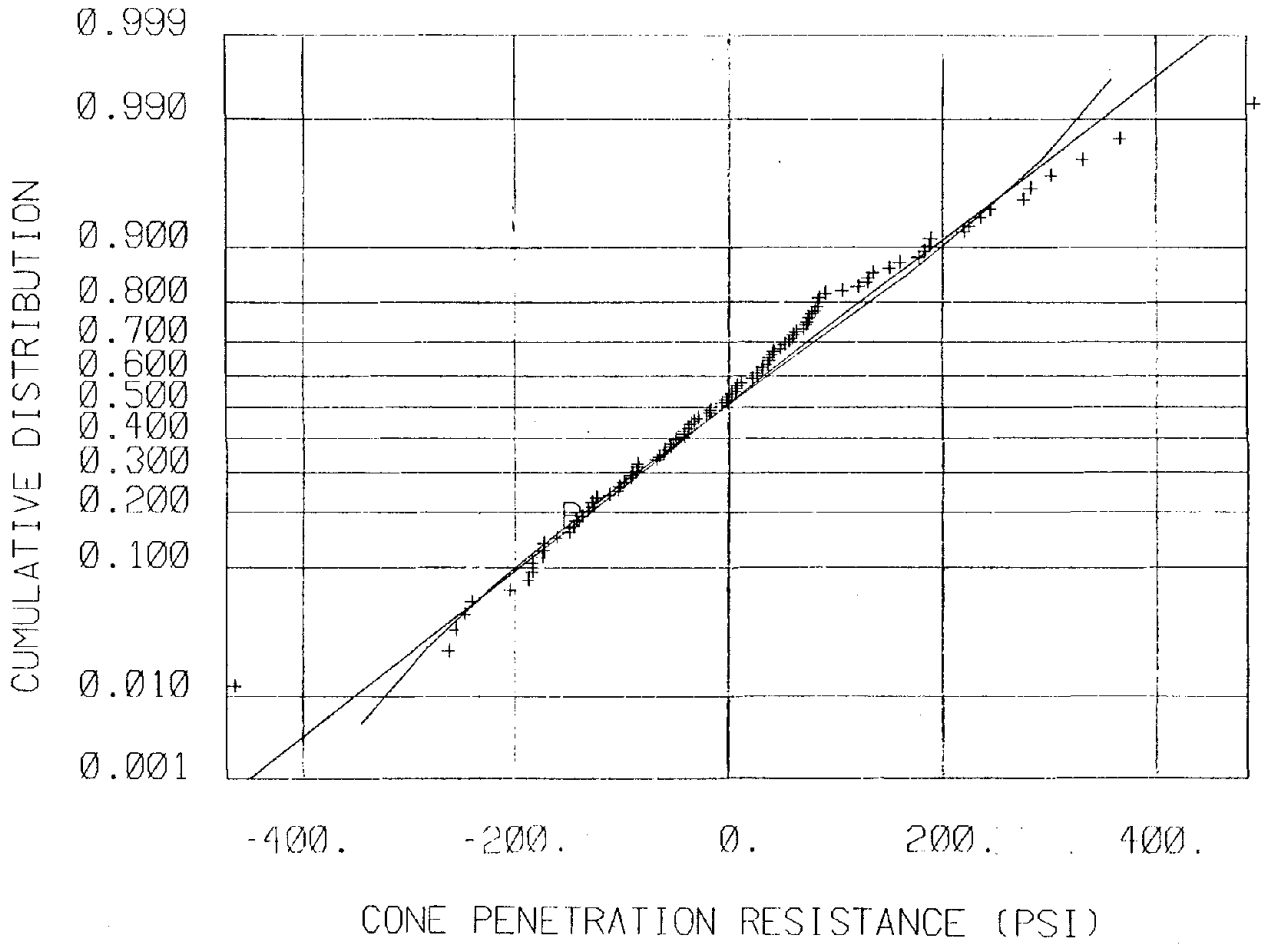

Figure 4.3 - CDF of the data of Figure 4.1

mechanical moments are related to a continuous solid,

$$m = \int x\, f(x)\, dx \tag{4.7}$$

$$V(x) = \int (x - m)^2\, f(x)\, dx \tag{4.8}$$

Distribution Theory

The preceding sections have concerned themselves with the description of observed data. The cdf's or pdf's characterizing those observations are said to be the sample distribution functions. Analytical forms, however, are also available with which to model sample distribution functions, and such models are of convenience both for statistical inference and for engineering modeling.

Certain analytical functions play a central role in statistical theory and data analysis. The more common and useful of these are described in this section.

Analytical Forms

Exponential Form

The most common analytical distribution functions are those of the general exponential form,

$$f(x) = N \exp(a + bx + cx^2)\, x^d \tag{4.9}$$

in which a,b,c, and d are constants, and N is a normalizing term to insure that the integral of f(x) over the complete measurement axis is unity. The better known distributions having this form are the normal, lognormal, exponential, and gamma.

The NORMAL DISTRIBUTION, recognized by its characteristic bell-shape (Table 4.1), is the most common of all distributions. It is observed in sample data with such frequency that Galton, in his early work on the distribution of features in human populations, coined its common name, at least for the English literature. In non English literatures the distribution is more commonly called the Gaussian, in honor of Gauss' original proof of the central limit theorem, which says that variables composed of the sum of independent perturbations

Table 4.1 -- Common Distributional Forms

Distribution	Equation	Mean	Variance
Normal	$\propto \exp[-(\frac{x-m}{s})^2]$	m	s^2
Lognormal	$\propto \exp[-(\frac{\ln x - m}{s})^2]$	$\exp(m+\frac{s^2}{2})$	$\exp(2m+s^2)$ $[\exp(s^2)-1]$
Beta	$\propto x^{r-1}(1-x)^{t-r-1}$	r/t	$r(t-r)/t^2(t+1)$
Exponential	$\propto a \exp(-bx)$	1/a	$(1/a)^2$
Gamma	$\propto x^a \exp(-bx)$	(a+1)/b	$(a+1)/b^2$

necessarily tend toward normal distributions as the number of pertubations becomes large. Thus, through the central limit theorem there exists theoretical justification for the widespread use of the normal form, and for the central position occupied by this form in statistical sampling theory.

The LOGNORMAL DISTRIBUTION is that which describes the distribution of a variable, the logarithm of which is normally distributed. Thus, the lognormal is closely related to the normal, and by an extension of the central limit theorem to show that the lognormal distribution describes a variable formed by the product of independent pertubations as the number of perturbations becomes large.

The EXPONENTIAL DISTRIBUTION, sometimes called negative exponential, is a one parameter function and is arguably the simplest of common distributions. While this distribution is often observed in geometric data, as for example the spacings among rock joint traces in outcrop, it is not commonly encountered in strength, deformation and flow data. Theoretical arguments can be made that certain types of data should be exponentially distributed, for example spacings between random events in time or space, but in the general case its use is primarily one of convenience.

The GAMMA DISTRIBUTION is positi ely skewed, as is the lognormal, and although derived from theoretical arguments pertaining to discrete measurements, its use with continuous measurements is often based on its similartiy to the lognormal and its greater convenience.

Non-Exponential Forms

Only a limited number of non-exponential forms have been proposed for use with geotechnical data. Perhaps the most publicized of these is the beta distribution, which has been advocated by some geotechnical researchers.

The BETA DISTRIBUTION is a four parameter pdf, and is thus very flexible and often appears to model empirical data quite well. A danger in this observation is that, due to the large number of parameters required to specify a beta distribution, the degrees of freedom in fitting empirical data is reduced. Thus, with limited data sets the statistical uncertainty in estimated parameters can be large. With large data sets degrees of freedom is seldom a problem, but many geotechnical data sets are not large.

The beta distribution is defined over a segment of the measurement axis rather than the entire axis. Thus, upper and

lower bounds on x must be estimated or fixed a priori. This is usually difficult to do, and presents statistical problems. It also taxes geotechnical intuition for there are often no cogent reasons for specifying bounds that a variable cannot exceed. The distribution is also mathematically difficult to use in reliability modeling--unless one resorts to simulation--and difficult for statistical inference.

Systems of Distribution Functions

Given the large number of analytical forms for distribution functions, attempts have been made to develop systems of distributions to bring order to the taxonomy of functions. The principal attempt in this direction was made by Pearson, and his chart of distributional types is used extensively in later sections of this report. Other systems are mentioned for completeness. Ord (1972) presents a more comprehensive discussion.

Pearson Family

Pearson's family of distributions comprises the solutions to the differential equation

$$\frac{f(x)}{dx} = \frac{(x-a)\ f(x)}{b_o + b_1 x + b_2 x^2} \tag{4.10}$$

in which a, b_0, b_1, and b_2 are constants. Among others, these solutions include the normal, lognormal, gamma, exponential, and beta distributons. They also include other common or useful distributions which are not extensively considered in this report, e.g., Student's.

Members of the Pearson family are usually identified by study of their low order moments, specifically those of order 1 through 4. These moments are calculated from data by extension of the discussion of section 4. The third order moment is the average of the cubes of the observed data. The fourth order moment is the average of the fourth powers of the observed data. These moments may be combined in the two statistics,

$$\beta_1 = \frac{E^2[(x_i-m)^3]}{E^3[(x_i-m)^2]} \tag{4.11}$$

$$\beta_2 = \frac{E\,[(x_i-m)^4]}{E^2[(x_i-m)^2]} \qquad (4.12)$$

which can be used to distinguish among members of the Pearson family. The simplest use of the β_1 and β_2 statistics is via the Pearson Diagram, shown as Fig. 4.4, with which distributional forms may be identified by inspection. The Pearson Diagram has been used throughout this study as a means of summarizing distributional information.

Other Families

Other systems of distributions have been studied, primarily by representing frequency functions as series expansions, or by considering the transformations of frequency functions to common shapes (e.g., to normal distributions). These are briefly listed here for reference. Discussions of these families can be found in Ord (1972) or in Kendall and Stuart (1977, v.1). The principal series expansion systems of distributions are (1) the Chebyshev-Hermite polynomials, based on polynomial multipliers of the error function integral; (2) Edgeworth's Type A series, and the (3) Gram-Charlier Type A series, each based on series of normal integrals or their derivatives; (4) the Tetrachoric function series, due to K. Pearson; and (5) Charlier's Type B series, based on derivatives of the Poisson pdf.

The principal transformation systems are (1) polynomial tranformations to normality, and (2) general (non-polynomial) transformations to normality. In each case a frequency function is catagorized by the nature of the transformation that changes it to a normal

Statistical Inference

The discussion above refers to descriptions of data sets. The present study addresses inferences of actual tailings properties from the description of limited numbers of data (i.e., finite samples) collected at a site. Since samples may vary, one from the other, inference always introduces some uncertainty. Therefore, estimates drawn from a sample must be reported with error bands, and conclusions (as e.g., on distributional shape) must be tested statistically. This section describes the techniques used in the present study to quantify estimation errors and to test conclusions on

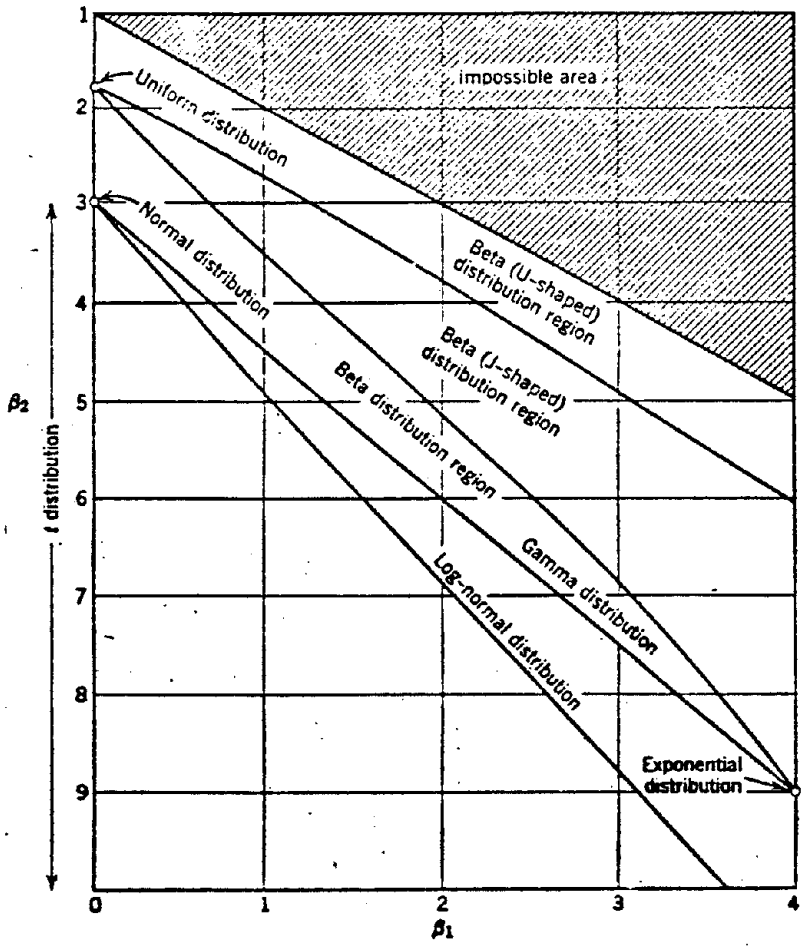

Figure 4.4 Pearson Diagram

distributional forms.

Estimates of Moments

Given a set of data $X = (x_1, \ldots, x_n)$, any mathematical function of X,

$$T(X) = fn(x_1, \ldots, x_n) \tag{4.13}$$

is said to be a statistic of the data X, or more simply a sample statistic. To estimate properties of the population from which the data came, some sample statistic, or combination of statistics, may be used to form an estimator. Here, an "estimator" is the mathematical function used to make an estimate from data, and an "estimate" is the numerical result of applying the estimator to a set of data.

For any set of data an essentially infinite number of estimators may be defined with which to make estimates of population properties. Thus, criteria must be established for choosing one estimator o er another. In traditional statistics, such criteria are based on the so-called sampling distributions of the estimators, that is, on the distribution of estimates made with a given estimator o er the possible samples that might be randomly taken from some population. Two important properties of an estimator are its mean and its variance over these possible samples. If the mean equals the parameter to be estimated, then the estimator is said to be unbiased. If the variance is the least of all alternative estimators, the estimator is said to be minimum variance (or miniumum squared error for biased estimators). The imprecision associated with an estimate is conveniently summarized by the standard deviation of the sampling distribution of the estimator, which is traditionally called the standard error.

Moment estimators use moments of the sample as estimators of the moments of the sampled population from which the sample is taken. For example, the sample mean is used as an estimate of the population mean and the sample variance is used as an estimate of the population variance. The sample mean is an unbiasesd estimator of the population mean, with sampling variance,

$$V(m) = V(x)/n \tag{4.14}$$

in which n is the number of independent measurements (i.e., sample size). The sample variance, defined as

$$S^2 = \frac{\sum (x_i - m)^2}{n-1} \tag{4.15}$$

is also an unbiased estimator, with sampling variance approximately equal to*

$$V(S^2) \doteq \frac{2\, V^2(x)}{n-1} \tag{4.16}$$

Distribution Parameters

Parameters defining a distribution may be estimated in ways similar to those for estimating moments. In certain cases, as e.g., the normal distribution, the moments are themselves the parameters defining the distribution. Two types of estimators have been used in this work, moment estimators and maximum likelihood estimators.

Moment estimators of distribution parameters use the functional relation between distribution parameters and distribution moments to estimate the parameters, essentially by back calculation. Such estimators are easily calculated, but may be far from efficient, in the sense of having small sampling variances. Maximum likelihood estimators use the conditional probability of having observed the sample X as the criterion of estimation, taking those values of the distribution parameters that maximize this probability as estimates. Such estimates are always efficient, but may be difficult to derive for certain sampling plans.

Tests of Distributional Forms

Since sample data ary from sample to sample, the shape of their frequency distribution (i.e., the sample pdf) also varies. Thus, the sample pdf may appear similar to some common analytical form when in fact the population pdf does not; or conversely, the population pdf may have some common form, but the sample data fail to reflect it. For this reason, the goodness-of-fit of an analytical form to the sample data must be tested statistically.

In the present work, chi-squared and Kolmogorov-Smirnov goodness-of-fit tests have been used on all data sets to assure statistical confidence. The chi-squared test is based on the

squared difference between observed cell frequencies in histograms and those predicted from an analytical form. It is a widely used and accepted procedure for establishing levels of confidence for distributional forms (see, e.g., Kendall and Stuart, .2, 1973). The Kolmogorov-Smirnov test is based on the maximimum deviation between observed cumulative frequencies of data and those predicted by an analytical cdf. The K-S test is also widely used and accepted, particularly as a graphical check when using probability grid.

The chi-squared test uses the test statistic

$$\chi^2 = \sum \frac{(O-P)^2}{P} \tag{4.17}$$

summed over the number of histogram intervals, in which O is the observed number of data and P is the number predicted from the analytical form for the distribution. For data actually sampled from the presumed distributional form the pdf of chi-square can be calculated. Thus, the observed chi-square can be compared with the distribution of values chi-square should have and a conclusion drawn on whether the presumed parent distribution is reasonable Fig. 4.5 shows calculated values of the chi-square statistics for the 1 and 5 percent confidence levels as a function of the degrees of freedom of the data. Observed chi-square values have only a 1 or 5 percent chance of occurring, respectively, were the actual distribution of the population that supposed. Therefore, if the observed chi-square statistic exceeds these critical values the conclusion is drawn that the supposed distribution is not supported by the data at the respective confidence levels.

In the present work the histograms were divided into 15 intervals, implying 14 degrees of freedom. For this case the 95th fractile of the theoretical distribution of chi-square is 23.685. Therefore, the observed chi-square would exceed this value with only 5% probability if the data actually came from the presumed parent pdf, so if the observed value does exceed this value the hypothesis that the presumed parent pdf is correct is also deemed unlikely, and said to be rejected at the 5% confidence level.

The K-S test uses the test statistic

$$Dm = \max_x(|F(x) - G(x)|) \tag{4.18}$$

in which F(x) is the analytical cdf and G(x) is the sample cdf. For data actually sampled from a population with cdf F(x), the

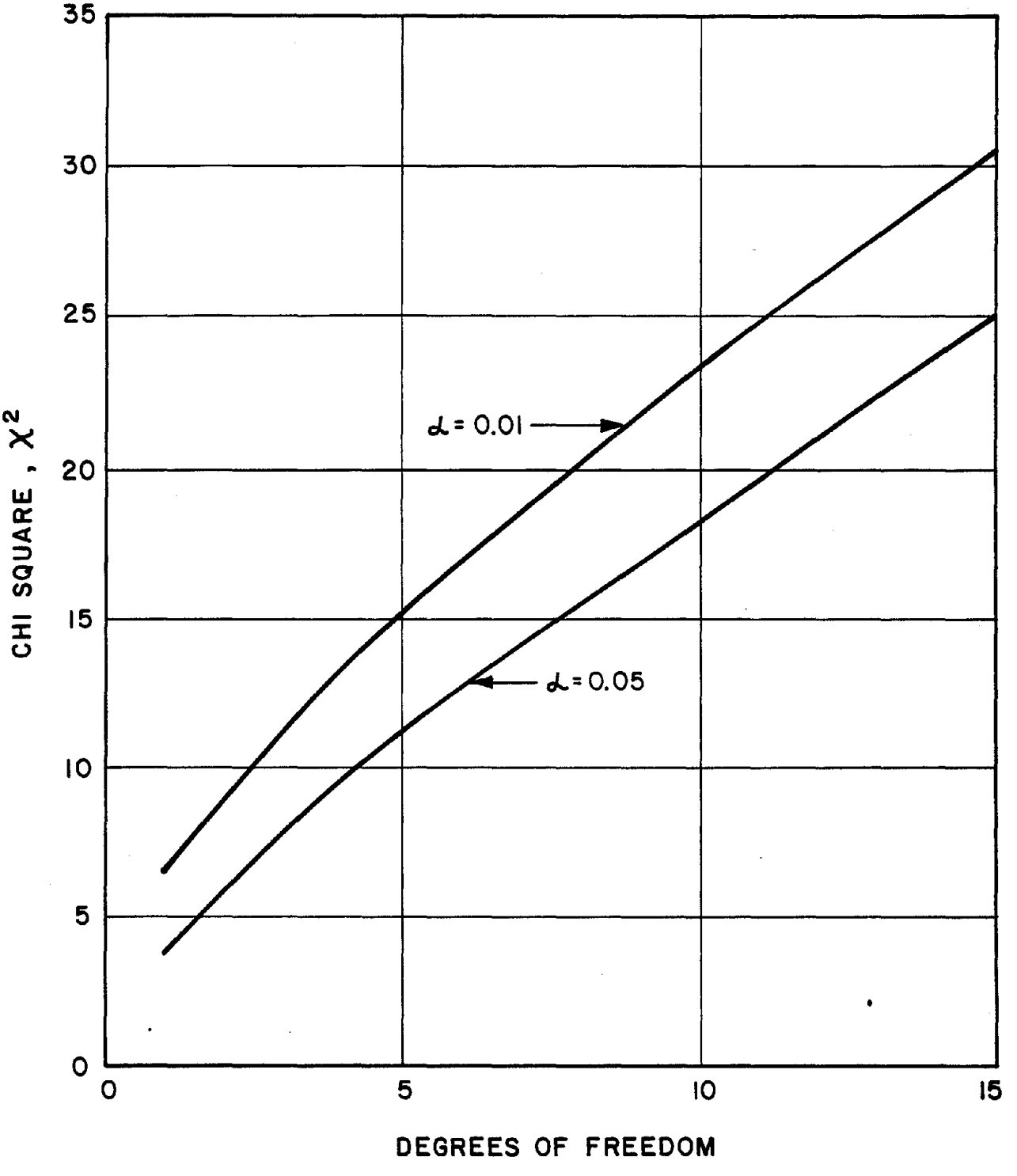

FIGURE 4.5 CRITICAL VALUES CHI-SQUARED STATISTIC AS A FUNCTION OF DEGREES OF FREEDOM 1% AND 5% CONFI DENCE LIMITS

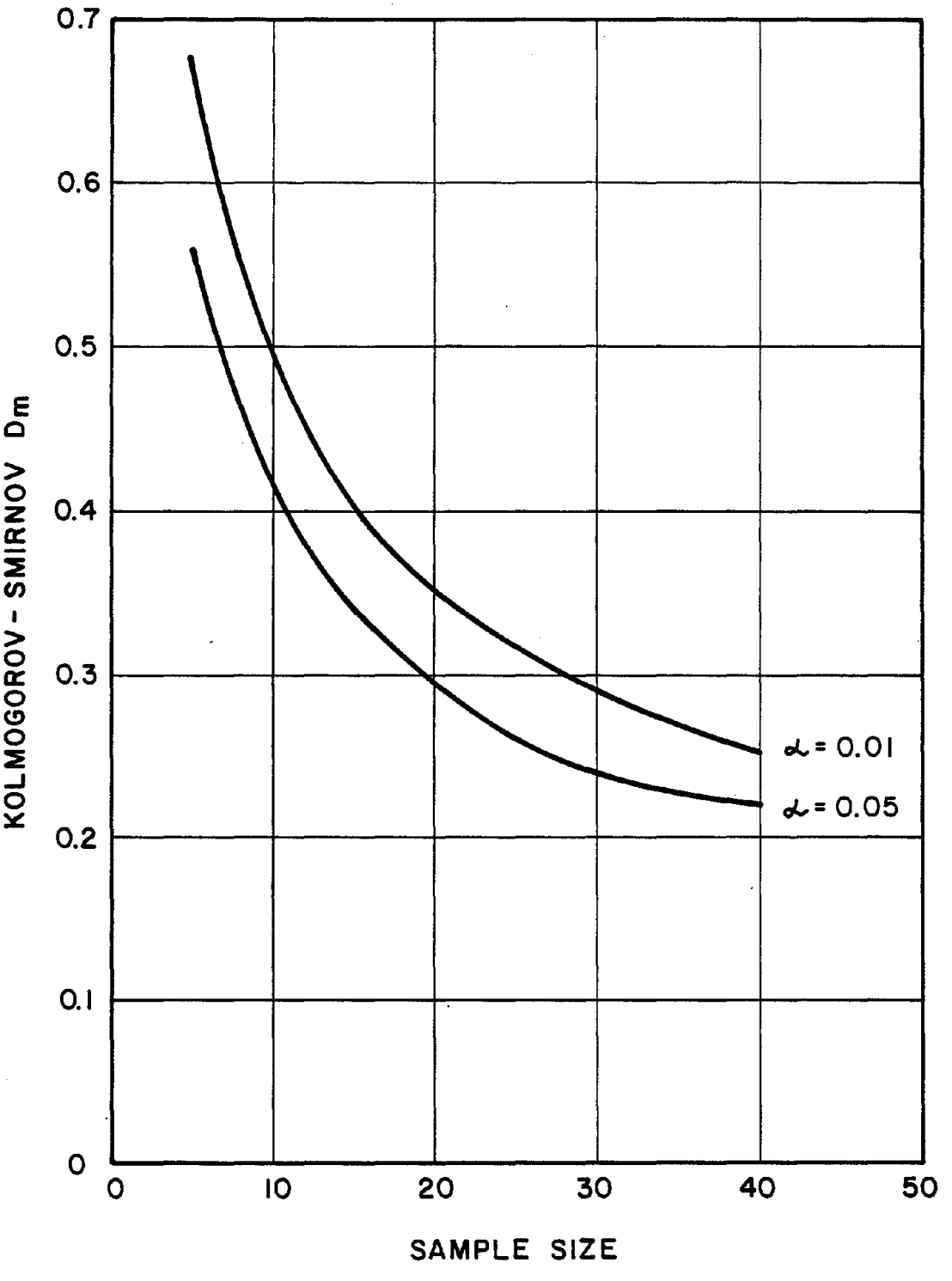

FIGURE 4.6 CRITICAL VALUES OF THE KOLMOGOROV-SMIRNOF D_m STATISTIC FOR 1% AND 5% CONFI DENCE INTERVALS

distributional form of the pdf of Dm can be calculated. This distribution depends on the sample size (i.e., the number of data), but it does not depend on the form of F(x). Thus, the observed Dm can be compared with the distribution of values Dm should have and again a conclusion drawn on whether the presumed parent distribution is reasonable. Critical values of Dm for one and five percent confidence limits are shown in Fig. 4.6.

Probability Paper

A convenient way to display data and to draw conclusions about distributional forms by inspection is through the use of probability paper. Probability paper is simply a specialized grid on which cumulative distribution funcions plot as straight lines. Such paper is widely available for normal and lognormal distributions, and can be straightforwardly generated for most other distributions. To reduce the large number of figures which would be required in the present work to plot data to four or five different grids, the data are plotted only once on normal grid and alternative theoretical cdf's are shown as continuous curves on these plots.

Profile Estimation

For engineering purposes uncertainty in tailings properties is summarized in a geotechnical design profile. This uncertainty comprises three parts: spatial variability, measurement or model bias, and statistical estimation error. Random measurement error--noise--affects profile uncertainty only to the extent that it increases statistical estimation error and possibly to the extent that it is partly confused with spatial variability.

As a first approximation data scatter in in situ measurements can be divided into two parts, a spatial or innate part, and a measurement error or noise part. Thus,

$$\text{Data scatter} = \begin{matrix}\text{Spatial variation} \\ + \\ \text{Measurement noise}\end{matrix} \qquad (4.19)$$

The spatial part is the part that the exploration program intends to characterize. The noise part is spurious. Thus, it is important to distinguish these two types of scatter.

Since spatial variability and measurement error combine to produce data scatter, they can not be directly separated. However, at least three indirect methods can be used. The first is replicate measurement on the same or similar materials, the second is multiple profiling with different instruments, and the third is through the structure of spatial variability. The last is inexpensive and often the most practical method.

The spatial structure of data scatter about a mean trend is conveniently summarized by an autocovariance function (or equivalently, a variogram). Adopting the simple, but common model,

$$z(t) = x(t) + e(t) \tag{4.20}$$

in which z(t) is the measurement at point t in the tailings, x(t) is the actual geotechnical property at t, and e(t) is a corrupting measurement noise, the autocovariance function of z(t) is

$$Cz(r) = E[(z(t)-m)(Z(t+r)-m)] \tag{4.21}$$

in which m is the mean or mean trend of z(t). Assuming stationarity (i.e., statistical homogeneity of the tailings), Cz(r) simply expresses the covariance of the observations as a function of their spatial separation. Typically, Cz(t) is anisotropic, smaller vertically than horizontally; and sometimes also anisotropic in the horizontal plane, depending on the method of placing or depositing the tailings.

Similar autocovariance funtions can be defined for x(t) and e(t), and these are related to Cz(r) by

$$Cz(r) = Cx(r) + Ce(r) \tag{4.22}$$

Cx(r) takes on the spatial variance of x at r=0 and decays to zero as r increases (Fig. 4.7a). On the other hand, e(t) is presumably independent from one measurement to another; thus, Ce(r) must be a spike of height V(e) at r=0, and zero elsewhere (Fig. 4.7b). Thus, Cz(r) should look like Fig. 4.7c. Extrapolation of the observed Cz(r) back to r=0, as in Fig. 4.7d, allows an estimate of V(e) to be made.

In addition to data scatter, which is associated with ariation about the mean trend, two systematic errors affect the estimation of the mean trend itself. First, the

Figure 4.7 Composition of data autocovariance function from spatial velocity and measurement error

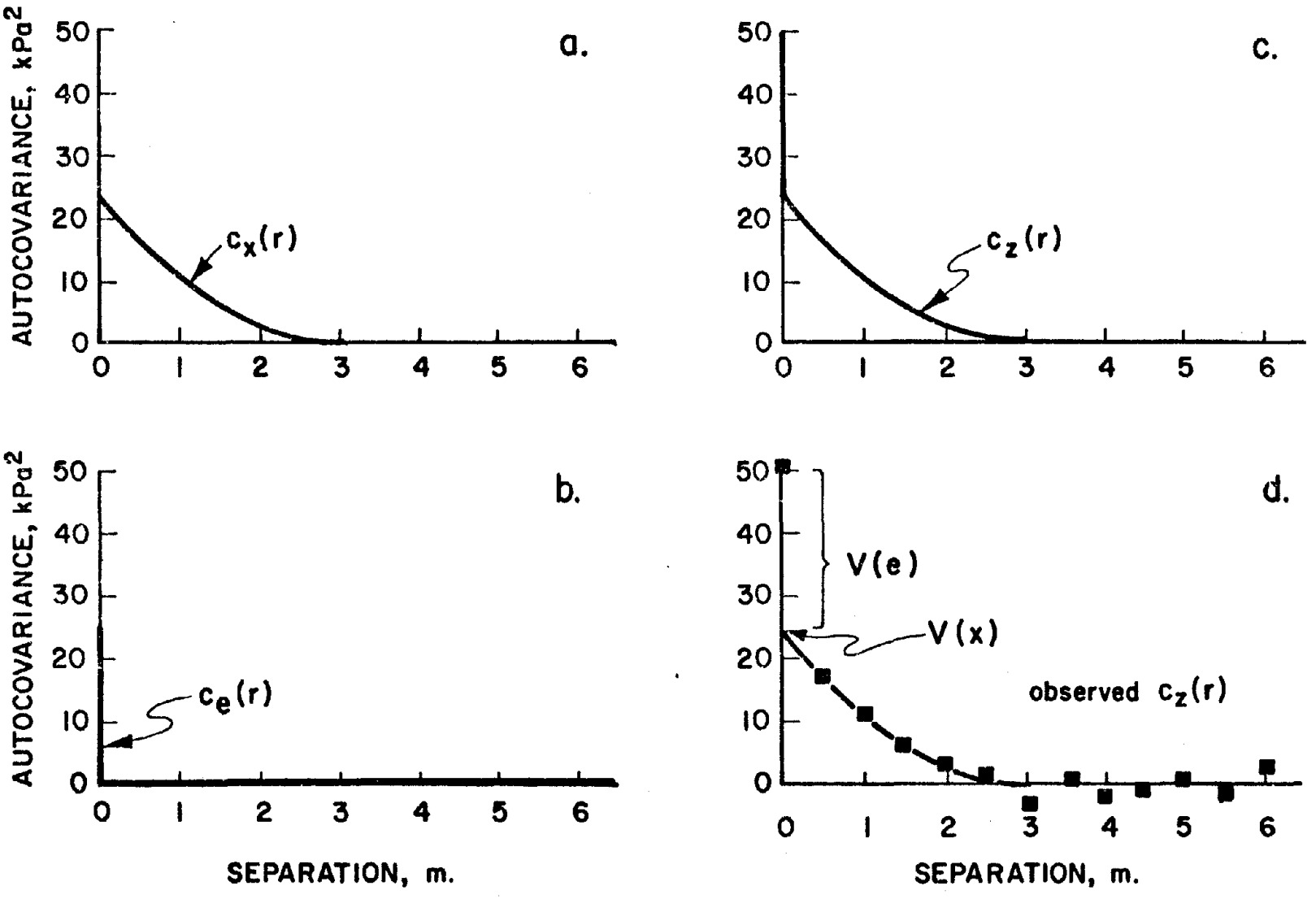

measurement procedure may introduce a systematic bias, B,

$$z(t) = B\,x(t) + e(t) \tag{4.23}$$

$$V(z(t)) = B^2\,V(x(t)) + V(e(t)) \tag{4.24}$$

Second, the total number of measurements is limited, thus statistical fluctuations introduce estimation errors. Combining, the total variance in an estimated profile becomes

$$V(\hat{x}(t)) = \begin{matrix}\text{Variance about the mean}\\ + \\ \text{Variance of the mean}\end{matrix} \tag{4.25}$$

in which the caret over x signifies an estimate. Mathematically,

$$V(\hat{x}(t)) = R\,V(x(t)) + V(B)m^2 + B^2V(m) \tag{4.26}$$

in which R is a scale factor, V(x(t)) is the spatial variance of the data, V(B) is the variance of the measurement bias, and V(m) is the statistical estimation error on the mean trend. For n widely spaced measurements,

$$V(m) = \frac{V(x(t)) + V(e(t))}{n} \tag{4.27}$$

For closely spaced measurements

$$V(m) = \frac{(\underline{1}C_x\underline{1}^t) + V(e(t))}{n} \tag{4.28}$$

in which

$$\underline{1} = \{1, \ldots, 1\}_n \tag{4.29}$$

and C is the covariance matrix of the x(t).

Based on the above development, mean profile and standard deviation envelopes are easily constructed. Note, however,

that the standard deviation envelopes, which express the uncertainy in engineering parameters for analysis, must reflect mode of behavior and scale. This dependency is summarized in the factor R. For example, circular shear instability depends on total resistance over a surface of sliding. Thus, spatial variation in part averages out. For very small instabilities R approaches 1, but for very large ones R approaches zero.

---

* This equation is based on an assumption of normality of the sampled population. For non normal populations the sampling variance is inflated by the term k4/n, in which k4 is Fisher's fourth cumulant (Cochran, 1963). This term increases the sampling variance if the population has positive kurtosis, and decreases it if the population has negative kurtosis.

5. DESCRIPTIONS OF STRENGTH TESTS ANALYZED

Three general types of strength tests were used in the cases cited in this report: Standard Penetration Testing (SPT), Dutch Cone testing, various types of drained and undrained (with pore pressure measurements) triaxial tests and direct shear (DS) tests. Only data from the triaxial tests which gave effective friction angles were considered. Table 5.1 summarizes the sites with enough information to obtain strength parameters. Many sites were evaluated but excluded from this report as having insufficient or suspect data.

Table 5.1: SUMMARY TABLE OF SOIL STRENGTH TESTS ANALYZED

MINERAL	SITE	SPT	DUTCH CONE	LAB TEST
Uranium	Colorado	26*	no	Triaxial
Uranium	Shiprock	1	no	no
Uranium	Grand Jct.	1	no	Direct Shear
Uranium	Ambrosia Lake	no	no	Direct Shear
Uranium	Durango	no	no	Direct Shear
Uranium	Falls City	no	no	Direct Shear
Uranium	Green River	no	no	Direct Shear
Uranium	Maybell	no	no	Direct Shear
Uranium	Monument Vlly.	no	no	Direct Shear
Uranium	New Rifle	no	no	Direct Shear
Uranium	Old Rifle	no	no	Direct Shear
Uranium	Riverton	no	no	Direct Shear
Uranium	Slick Rock	no	no	Direct Shear
Uranium	Spook	no	no	Direct Shear
Uranium	Tuba City	no	no	Direct Shear
Copper	Morenci	no	5	Triaxial
Copper	Chino	3	no	Triaxial
Copper	Magna	3	3	Triaxial
Copper	Mindola	no	42	Triaxial
Copper	Chingola	no	22	no
Copper	Brenda	no	1	no
Copper	Chambishi	no	30	no
Copper	Chibuluma	no	24	no
Copper	Japan Mine A	yes	1	Triaxial
Copper	Japan Mine B	yes	1	Triaxial
Copper	Japan Mine D	yes	1	Triaxial
Copper	Japan Mine E	yes	1	Triaxial
Copper	Japan Mine F	yes	1	Triaxial
Copper	Japan Mine G	yes	1	Triaxial
Copper	Japan Mine I	yes	1	Triaxial
Copper	Japan Mine J	yes	1	Triaxial
Gypsum	Texas	6	no	Triaxial
Gypsum	Louisiana1	11	no	Triaxial
Gypsum	Florida1	12	no	Triaxial
Gypsum	Vick Article	1	no	Triaxial
Gypsum	Florida4	no	no	Triaxial
Gypsum	Louisiana2	no	no	Triaxial
Gypsum	Florida2	no	no	Triaxial
Gypsum	North Carolina	no	no	Triaxial
Gypsum	Florida3	no	no	Triaxial
Gypsum	Piney Point	no	7	Triaxial

*number indicates number of borings

Gypsum Tailings Sites

For the ten gypsum sites analyzed in this study, one or more of SPT, cone resistance and triaxial testing were done. SPT testing was done using standard procedures at all sites. At Texas the SPT work was done by drilling with truck-mounted and portable drilling rigs which bored to depths ranging from 10.1 to 151.5 feet to obtain samples for laboratory testing. SPT testing was performed each time a sample core was removed from the drill hole. This was accomplished with a two inch split barrel. At Louisianal SPT testing was performed by following ASTM D 1586-67. The borings were cut to specified depths at intervals of 2.5-5 feet by a rotary drilling process which used viscous bentonite drilling mud to flush the cuttings and stabilize the hole. At the appropriate depths the drill bit was removed to allow the SPT to be done with a 2-inch sampler (O.D.=2 inches I.D.=1.4 inches) driven with "N" blows of a 140 pound hammer falling 30 inches until either 18 inches of penetration or 50 blows of the hammer resulted. Louisianal data from 1977 showed an increase of SPT N values over tests run at similar depths in 1973. The Floridal SPT data were sampled at depths ranging from 40-75 feet using a Failing 1500 rig, and with sampler dimensions similar to those used at Louisianal. In the Vick report the abandoned 80 feet high embankment was tested following ASTM specifications using equipment as described for Texas.

Triaxial testing for gypsum varied little from case to case being generally either a drained test or an undrained test with pore pressure measurements. As we were primarily interested in effective stresses, other types of undrained testing were not analyzed. Friction angles ($\bar{\phi}$) and cohesion intercepts ($\bar{c}$) were generally calculated using a least squares regression based on plotted Mohr circles or stress paths. The test specimens were prepared by trimming 1.5 inch diameter by 3-inch high samples on a soil lathe. When mounted in the triaxial cell, effluent water representative of a particular tailings pond was used for cell pressure and sample back pressure thus avoiding dissolution of the gypsum particles. Each sample was consolidated until excess pore pressure dissipated. On shearing, the rate of strain was controlled so that in the drained case, one would achieve complete pore pressure dissipation while in the undrained case one would achieve pore pressure equalization. Texas, Louisiana2, and Lousianal used only isotropically consolidated undrained tests with pore pressure measurements while North Carolina exclusively used isotropically consolidated drained tests. Florida2, Florida3 and Florida4 used both types of triaxial testing.

Uranium Tailings Sites

SPT testing at the two DOE sites (Grand Junction, Colorado and Shiprock, New Mexico) and at Colorado site was accomplished in a fashion similar to that described in the previous section. Triaxial testing was performed at Colorado while strength data at 13 DOE sites was obtained by drained direct shear (DS) testing.

Copper Tailings Sites

At Chino SPT testing was done within the upper 100 feet of the borehole. The test consisted of driving a 2-inch split spoon through 18 inches with a 140 pound hammer (recording blowcount of the last 12 inches). The blows of a diesel-powered 8000 foot-pound Becker hammer drill performing the borings were also recorded for possible correlation with the SPT blowcount. At Magna dam SPT were performed in all drill holes after every interval from which undisturbed samples were obtained. The split spoon sampler used fit ASTM specifications.

At Brenda dam the cone used had a 60 degree point with a 3.5 centimeter diameter. A fifty pound hammer dropping 30 inches drove the 1 1/4-inch diameter cone with 1-inch diameter rod. At the four Zambian tailings dams (Chingola, Chambishi, Chibuluma and Mindola) the penetrometer was a hydraulically operated Dutch Cone using an automatic recording meter and having a capacity of 2000 kilograms. At Magna dam the Dutch Cone penetrometer consisted of a hardened steel cone. The thrust required to cause a bearing capacity failure beneath the cone was measured every 6-8 inches by a hydraulic load cell, while a special friction sleeve above the cone measured side friction.

Triaxial testing was used at the eight Japanese mines, at Magna dam ($\overline{CIU}$,$\overline{CKoD}$) and at Chino dump. Due to the large grain size of the stack material at Chino dump, 6-inch diameter fabricated triaxial samples were used which were failed at a rate of about 4% strain per hour. At Magna strength data from CU tests (with pore pressure measurements) for samples from depths of 10-74 feet were analyzed. The values from these samples were thought (by Wahler and Associates) to be a bit high for a material with a dry density of 80 PCF containing over 80% fines (particles smaller than No. 200 US sieve). However, under microscope, the particles exhibited a high degree of angularity induced by ore crushing prior to flotation which influences intergranular shear strength thus perhaps explaining the higher observed strength. This trend was also reflected in

the SPT and Dutch Cone testing for this site.

Triaxial tests were performed on undisturbed samples from each of the Japanese tailing deposits. Samples were anisotropically consolidated to the estimated in situ stresses and sheared undrained.

Strength Results from Field Tests

Chapter 6 described procedures to transform results from indirect field tests to strength parameters. The predominant field test data consist of cone penetration resistance and standard penetration test resistance.

Table 6.3 assigns a Quality Index and an Interpretation Index. We have attempted to infer strength parameters from field data with a Quality Index of A or B and an Interpretation Index of I or II. However this reduces the number of cases to infer strength parameters to 15: 8 Japanese sites, Morenci, Chino, Floridal, Texas, Chingola, Louisianal and Vick.

The detailed data on static pore pressures and excess pore pressures generated by pushing the cone allow reliable interpretation of most of the Japanese data. Where measurements show no excess pore pressures during penetration we have used the approach described in an earlier section to calculate $\bar{\phi}$. Where the measurements show large excess pore pressures during penetration we have determined values of $S_u/\bar{\sigma}_v$. Parts of the Japanese cone profiles are intermediate and we have ignored these. Table 8.33 summarizes results for the Japanese data. Values of $S_u/\bar{\sigma}_v$ vary from Ø.Ø7 to Ø.3Ø. These values seem possible for such materials. Figure 8.164 shows that $S_u/\bar{\sigma}_v$ tends to decrease with increasing percent of material passing the number 2ØØ U.S. sieve. This expected trend tends to add credibility to our ability to obtain realistic strength data from the Japanese cone data. No significant trend exists between $\bar{\phi}$ from the cone data and fines content since three of the four available points have about the same fines content.

Table 8.33: Summary of Japanese Cone Data

MINE	(tsm)			% PASSING NO. 2ØØ
A	NA	NA	Ø.18	48-78
B	Ø	33.4	NA	3Ø
D	5.1	32.4	NA	21-24
E	NA	NA	Ø.Ø9	94-1ØØ
F	7.4	31.6	Ø.16	76-1ØØ
G	7.3	29.3	NA	14-37
I	NA	NA	Ø.3Ø	18
J	NA	NA	Ø.Ø7-Ø.1Ø	1ØØ

Of all the Zambian cone penetration data, only those from the Chingola mine allow inference of strength parameters. All other mines show cone data either highly variable with depth or intermediate between drained and undrained. Figure 8.29 shows the histogram of friction angles calculated from the mean trend line for each cone sounding at Chingola. The 2387 values have a mean of 518 psi and a standard deviation of 324.

Table 8.34 gives values of $\bar{\phi}$ calculated from SPT results. These were determined from the mean trend line at mid-depth of the dam, assuming static pore pressures below the ground surface and using Figure 6.5. These values generally fall within the range of values found by direct measurement; however, if we interpreted individual data points we would obtain a much larger variation in $\bar{\phi}$ than generally obtained by direct measurement.

Table 8.34: Values of $\bar{\phi}$ Calculated from SPT Results

SITE	COMMODITY	$\bar{\phi}$ FROM SPT
Morenci	copper	38
Chino	copper	44
Colorado	uranium	35
Floridal	gypsum	34
Texas	gypsum	35
Louisianal	gypsum	upper-25 lower-40
Vick	gypsum	49

Both direct and indirect strength measurements on gypsum show considerable scatter, a fact that contradicts the widely stated view within the industry that gypsum is relatively uniform in its properties. Speculative causes of this variability include variations in composition of the gypsum particles, variable effects of excess pore pressures generated during field tests, and variable effects of sampling and laboratory testing. An extreme example is the Louisianal site where N values in the lower half are much less than those in the upper half. This behavior suggests that details on pore pressures before and during the SPT may be important to interpreting the results.

All lab tests show effective friction angles greater than 35 degrees. The relatively high friction angle combined with gypsum's tendency to develop a slight cohesion

with time and its relatively high permeability may combine to make it a relatively strong tailings material.

6. STRENGTH MEASUREMENT

An earlier section described the use of the Mohr-Coulomb envelope to obtain strength for stability analysis. This section considers means of obtaining the parameters for the Mohr-Coulomb envelope, specifically c and $\overline{\phi}$ for total stress analysis and $\overline{c}$ and $\overline{\phi}$ for effective stress analysis.

Some Basic Factors Affecting Strength

Effective Stress Strength Envelope

Figure 6.1 shows a typical strength envelope determined from laboratory tests. Several points are worth noting. First the envelope may be curved. A straight line of best fit through the test data may give a substantial cohesion intercept. But this cohesion is an artifact of fitting a straight line to the curved envelope.

The parameters $\overline{c}$ and $\overline{\phi}$ in Figure 6.1 apply only to the range of effective normal stress covered by the tests. At an effective normal stress of zero the soil may have zero strength and thus zero cohesion. The important point is that the strength parameters c and may apply only to a specific range of effective stresses.

For a given soil the effective stress strength envelope depends on the density, the degree of overconsolidation, the stress level, the presence and action of cementing agents, the direction of failure through the sample, and details of the test used to measure the envelope. If one must reconstruct a sample for testing, the method of sample preparation also affects the strength envelope.

Usually the peak effective friction angle can be reliably determined to within 3 degrees (for $\overline{\phi}$) if one is testing a representative sample at a representative stress level and correctly determining the effective stresses in the test. Practical means of accomplishing this task include direct shear tests, drained triaxial tests and undrained triaxial tests with pore pressure measurements. Direct shear tests and drained triaxial tests must be sheared slowly enough to allow complete drainage at all times with the sample having free access to water. Many such tests on tailings appear to be run too rapidly. Undrained triaxial tests must be sheared slowly enough to obtain accurate readings of pore pressure and use equipment of low compressibility to measure pore pressure.

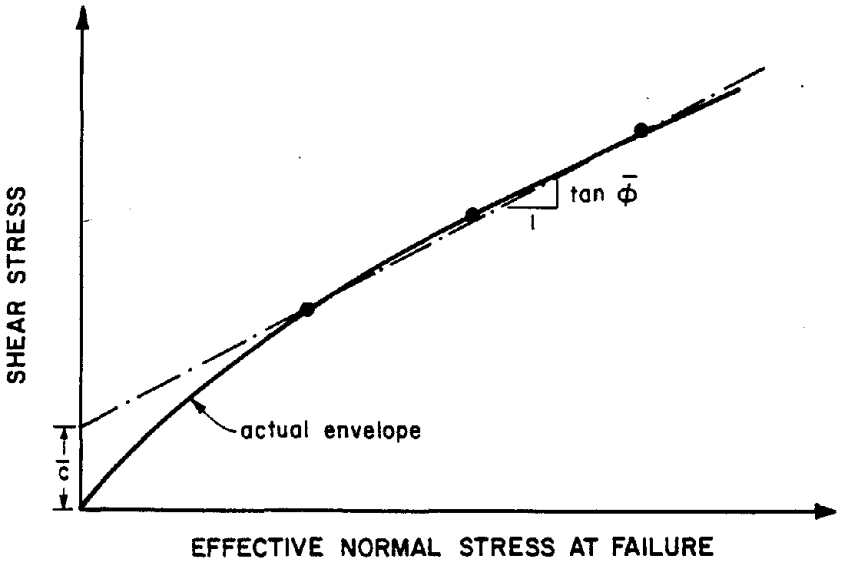

FIGURE 6.1 EFFECTIVE STRESS STRENGTH ENVELOPE

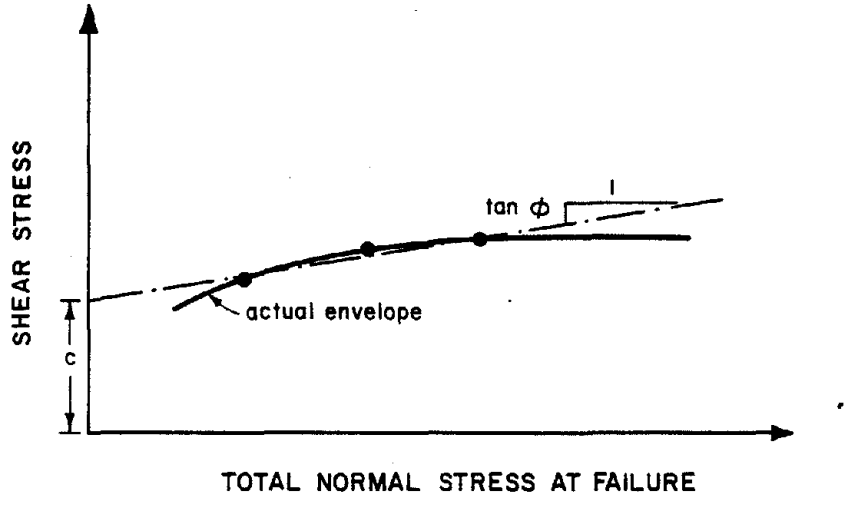

FIGURE 6.2 TOTAL STRESS STRENGTH ENVELOPE

If the above criteria are satisfied and one tests a representative sample at the representantive stress level, the resulting strength data should correlate well with in situ effective stress strength parameters.

Other means exist to measure effective stress strength parameters, including plane strain shear boxes, true triaxial tests, borehole shear devices and pressuremeters. These are rarely used on tailings and thus are not considered here.

Total Stress Strength Envelope

Figure 6.2 shows a typical total stress strength envelope determined from undrained laboratory tests on one sample of soil in its field condition. At higher total stress levels the envelope becomes horizontal, i.e. ϕ becomes zero and c equals the strength. Strength becomes independent of total normal stress. At lower levels of total normal stress, the envelope may curve downward. This curvature results from internal changes in volume of the sample during shear caused by the presence of air or gas. These conditions may exist in the field or result from sampling and testing procedures.

Unlike the effective stress envelope which can usually be uniquely determined within 3 degrees, the total stress envelope depends on many factors. Restricting our attention to fully saturated undrained conditions so that $\phi = \emptyset$ and $c = S_u$ we can examine what factors affect S_u. Ladd and Foott (1971) give a thorough summary of the important factors. These include sample disturbance, effective stress to which the sample is consolidated prior to shear, natural anisotropy in S_u of the sample, stress-induced anisotropy, stress history of the sample and rate of shear. With these many influences it is not surprising that different tests for S_u give different values. Laboratory and field tests to measure S_u, including triaxial, direct simple shear, field vane, cone penetrometer, and others, may start at different initial effective stresses, create failure on different planes and at different rates of shear. Figure 6.3 shows typical differences in undrained strength reliably determined by a variety of tests. The engineer's task is to select a type of test which will induce failure under conditions similar to those he expects in the field. The "correct" test to measure S_u will vary from one situation to another. Figure 6.4 from Ladd and Foott (1971) shows that the "correct" test to measure S_u can vary in a given situation with location along the failure surface. Unconfined compression tests should not be used to obtain strength for design. Unavoidable sample disturbance leads

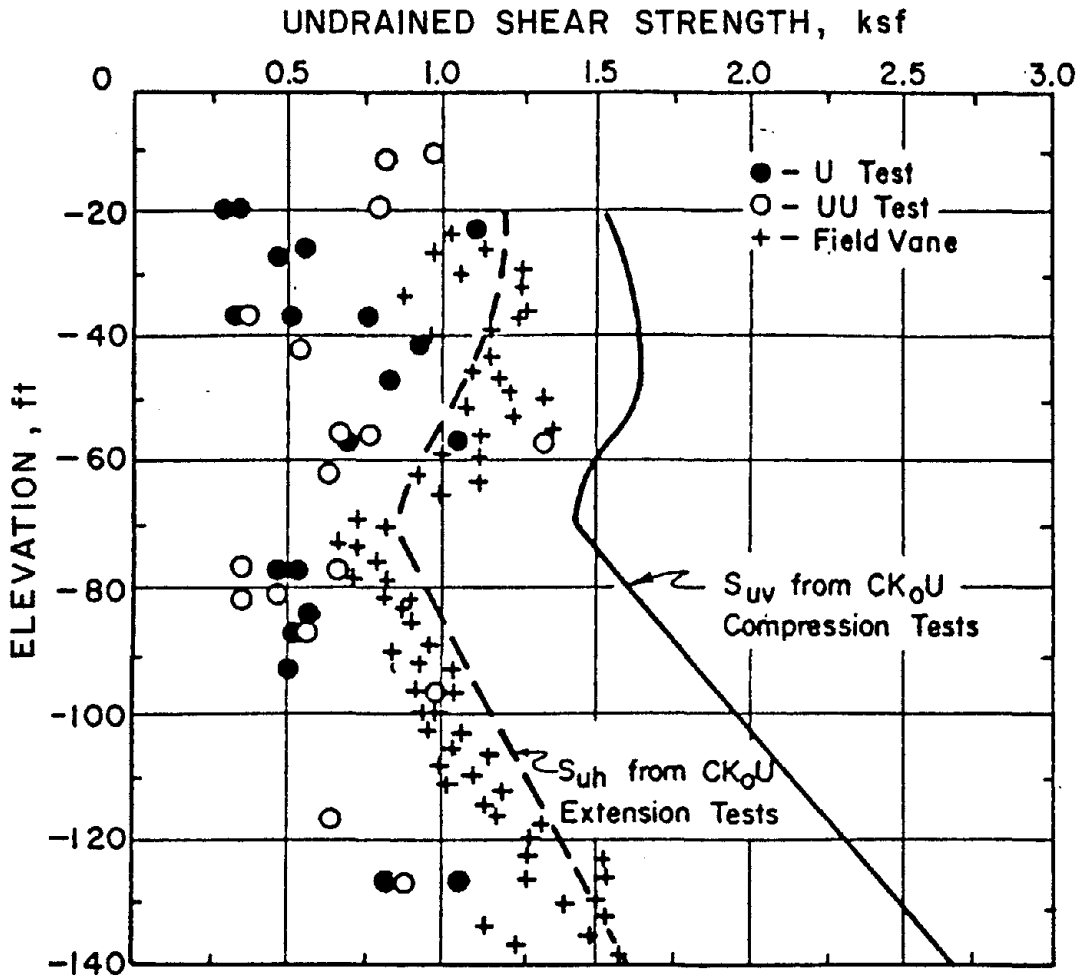

FIGURE 6.3 SUMMARY OF STRENGTH TESTS AT MIT TEST SECTION (AFTER LAMBE, 1971)

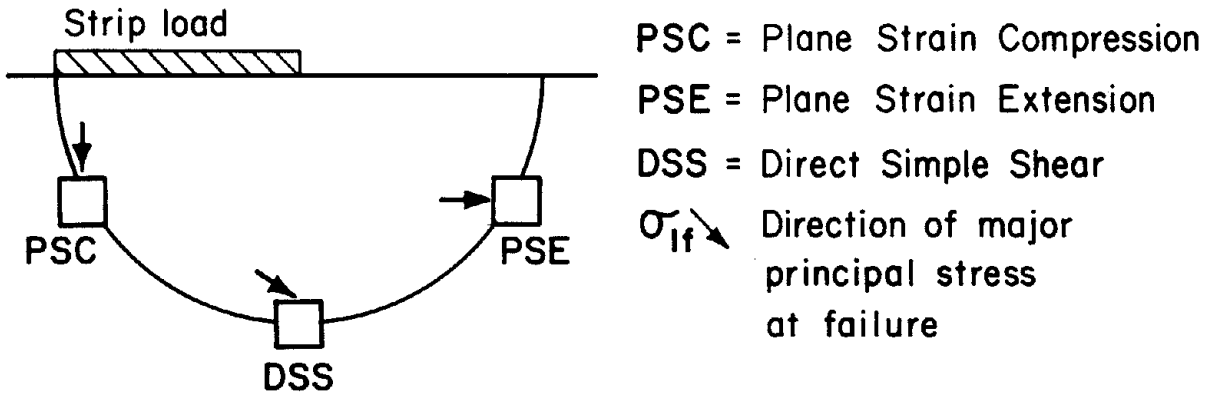

FIGURE 6.4 STRESS SYSTEMS ALONG A FAILURE SURFACE (AFTER LADD, 1978)

to measured strengths which are too low.

Triaxial compression, triaxial extension, and direct simple shear equipment all provide undrained strength data useful for tailings deposits. The engineer should determine that each test reflects the correct stress history, the sample represents in situ conditions and his interpretation of the test corresponds to conditions at failure in the field.

Strength Parameters from Standard Penetration Tests

The SPT gives a crude indication of strength. Clearly, material with a low blow count can be expected to have a low strength relative to a material with a high blow count. Figure 6.5 reproduces a relationship among effective stress, SPT, and effective friction angle developed by DeMello (1971). DeMello's chart agrees with the widely used table developed earlier by Meyerhof (1956). Figure 6.5 applies to coarse to fine sands. It does not work for silty sands, silts and clays. Therefore its usefulness in design of tailings dams is limited. Table 6.1 reproduces a crude relationship between SPT and undrained shear strength. This relation works only for clays and gives a strength comparable to that determined in an unconfined compression test.

Interpreting Strength Parameters from Cone Penetration Resistance

The cone test measures the resistance to penetration of a circular conical tip pushed into the soil at a constant rate. Penetration resistance is related to the strength of the soil. If the rate at which the soil drains excess water is fast compared to the rate of cone penetration, then the penetration resistance should relate to drained strength. Also no excess pore water pressures develop during penetration by the cone. If the rate at which the soil drains excess water is slow compared to the rate of cone penetration, then the penetration resistance should relate to undrained strength. Large excess pore pressures may develop during penetration by the cone.

Unfortunately it is not easy to determine the rate of drainage of the soil. Whether to interpret the penetration resistance as a measure of drained strength, undrained strength, or something in between becomes a difficult question.

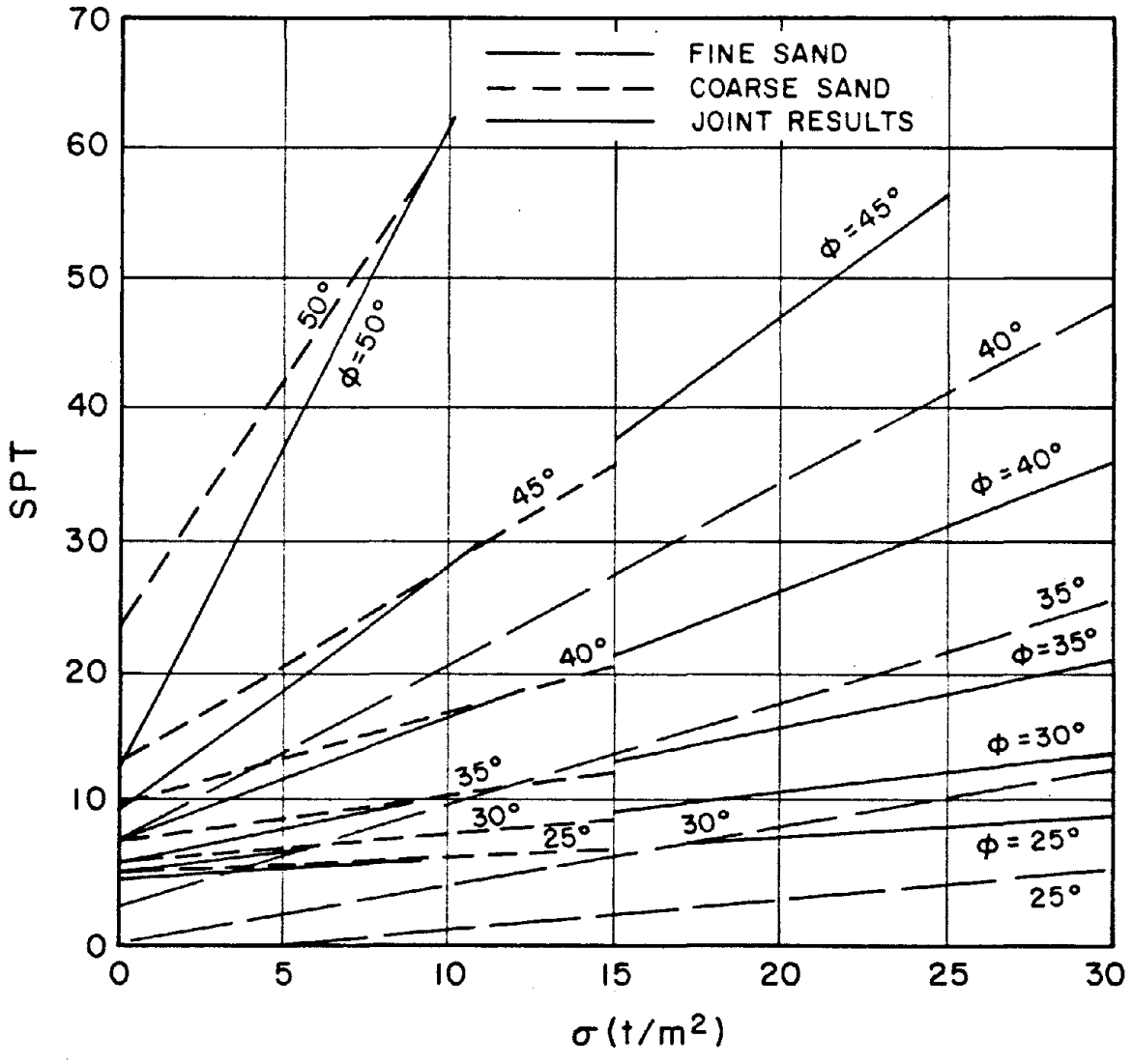

FIGURE 6.5 - FRICTION ANGLE, SPT, AND STRESS RELATIONSHIP FOR COARSE AND FINE SANDS (AFTER DEMELLO, 1970)

Consistency	Very soft		Soft	Medium	Stiff	Very stiff	
q_u, ksf	0	0.5	1.0	2.0	4.0		8.0
N, standard penetration resistance	0	2	4	8	16		32
$\gamma_{(sat)}$, pcf (kN/m^3)		100–120 (16–19)		110–130 (17–20)	120–140 (19–22)		

* These values should be used as a guide only. Local cohesive samples should be tested, and the relationship between N and the unconfined compressive strength q_u established as $q_u = KN$.

Table 6.1 SPT v. undrained strength for cohesive soils (after Bowles, 1977)

Numerous methods exist to translate penetration resistance to strength. Sangerlat (1972) contains many examples. For this work we selected an effective stress method described by Janbu and Senneset (1974) to obtain drained strength parameters and a total stress method described by Baligh, Vivatrat and Ladd (1978) to obtain undrained strength parameters. These two approaches employ current concepts of geotechnical engineering and are relatively easy to apply.

Effective Stress Interpretation

Janbu and Senneset (1974) review the theory leading to this interpretation. We summarize only the essential parts. Defining the following terms:

q_c cone penetration resistance

a attraction component of strength=c/tan

$\bar{c}$ effective stress cohesion intercept

$\bar{\phi}$ effective stress friction angle

σ_v total vertical stress

$\bar{\sigma}_v$ effective vertical stress

u_s steady state pore pressure

we can obtain the following expressions:

$$\frac{q_c - \sigma_v}{\sigma_v - u_s + a} = N_q - 1 = N_p \qquad (6.1)$$

and

$$N_q = \tan^2 \left(\frac{\pi}{4} + \frac{\bar{\phi}}{2}\right) \exp \left(0.64\,\pi + 1.8\bar{\phi}\right) \tan \bar{\phi} \qquad (6.2)$$

where π is in radians. (Note we have replaced Figure 3.2 in Janbu and Senneset's paper with the approximate equation $\beta = 0.1\pi - 0.9$ to obtain one equation relating N_q to

$\bar{\phi}$.) These expressions assume no excess pore pressures develop during cone penetration. Equation 6.1 indicates that cone resistance plotted as ($q_c - \sigma_v$) versus ($\sigma_v - u_s$) should fall on a straight line with a slope of $N_q - 1$ and intercept the ($\sigma_v - u_s$) axis at a value of "a" as illustrated in Figure 6.6.

Total Stress Interpretation

One can relate penetration resistance to undrained shear strength by the following relationship

$$q_c = N_c \cdot s_u + \sigma_{v_o} \qquad \sigma_v \tag{6.3}$$

where

N_c is a bearing capacity factor

s_u is the undrained strength of the soil

σ_v is the total vertical stress at the point of measurement

Baligh et. al. (1978) review theoretical derivations of Equation 6.3. Other sections reviewed the difficulties in selecting the appropriate value of S_u from the many methods of measurement. Thus assessing the accuracy of theoretical relations for N_c is difficult. Baligh et. al. (1978) reviewed 18 cases where actual stability failures or in-depth exhaustive studies of strength allowed determination of the field strength. They used these strengths with measured penetration resistance to determine values of N_c from equation 6.3. All cases were soft to medium clays with plasticity indices from 4-70%. Values of N_c vary from 9-23 with an average of 14. While several factors may affect N_c, including plasticity, sensitivity, overconsolidation, strain rate and strength anisotropy, a constant value for a given deposit seems to apply.

We shall use a N_c of 14 to translate the penetration data to undrained shear strength.

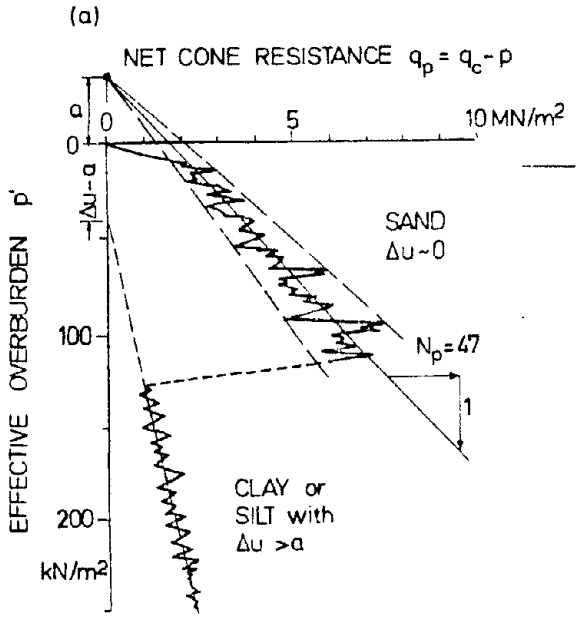

Figure 6.6 - Net cone resistance v. effective overburden (after Janbu and Senneset, 1974)

Effective Stress or Total Stress?

The standard rate of penetration of a cone, 1 to 2 cm/sec is considered to produce no excess pore pressures in sand and no drainage in clays. However with only the penetration resistance, one can not determine soil type to know how to interpret the test. Many tailings sites contain variable materials about which little is known. An engineer usually studies all available information about the site materials before choosing a method to interpret the cone data.

To extract as much useful information as possible from the large quantities of cone data available for tailings we have made some simplifying assumptions. We assume the mean trend with depth found from linear regression represents mean strength. We then convert the mean trend line to equivalent strength parameters using both an effective stress and a total stress interpretation. We then select the parameters most likely to represent strength at that location based on (1) whether the above results make engineering sense, (2) shape of the cone profile, and (3) any other available data that helps interpret the profile. This procedure should work except where distinct differences in strata exist. Such differences sometimes show up in a drastic shift in the pattern of cone resistance. We have excluded such records from this interpretation.

Quality Index

Much of the geotechnical data collected for tailings dams does not yield meaningful values of strength for assessing safety. This condition usually results from inappropriate testing equipment and procedures, tests on unrepresentative samples, or an index test which can not be uniquely interpreted. To avoid mixing high quality data with questionable data in our discussions and conclusions, we developed a rating system for laboratory tests and one for field tests.

Table 6.2 gives our criteria for rating laboratory tests to measure strength. Note that a C rating does not necessarily mean low quality testing was performed. It may mean we had insufficient information to determine if the conditions necessary for an A rating existed.

Tables 6.3 gives our criteria for rating field tests. Because most available data from field tests give only an indirect measure of strength, we use two scales. One rates the quality of test in terms of equipment and procedures. The second rates our ability to interpret the test to obtain a $\overline{\phi}$ or a S_u. For example a cone test performed using accepted procedures rates a QuaLity Index of A but if the soil is such that penetration is between drained and undrained it will have an Interpretation Index of III. It's a good cone test but we can't extract a meaningful estimate of strength. We have rated all lab and field tests with the results shown in Table 6.4.

Table 6.2: Lab Testing Quality Index

RATING	DESCRIPTION
A	accepted testing standard equipment and procedures followed and documented; acceptable undisturbed samples or samples recompacted to representative in situ conditions
B	non-standard equipment or procedures but deviations documented so one can interpret test; remoulded or disturbed samples of representative soils
C	unclear equipment or procedures for test; little or no documentation; inappropriate equipment or procedure; unknown characteristics for sample

Table 6.3a: Field Test Quality Index

RATING	DESCRIPTION
A	accepted testing equipmemt and procedures followed and documented; test intervals less than or equal to 5 feet for SPT and less than or equal to 10 cm for Dutch Cone
B	non-standard equipment or procedures followed but deviations documented; test intervals > 5 feet for SPT and > 10 cm for Dutch Cone
C	unclear equipment or procedures for test; little or no documentation; inappropriate equipment or procedure

Table 6.3b: Interpretation Index for Field Tests

RATING	DESCRIPTION
I	in situ pore pressures available; or supporting data on grain size, permeability and/or excess pore pressures during test available; available data indicate test is either drained or undrained; test quality A or B
II	only depth to free standing water is known; little or no supporting data (grain size, limits or sample descriptions); available data make determination of drained or undrained test fuzzy or subject to interpretation; test quality A or B
III	no other data known; test results ambiguous; available data indicate test in between drained and undrained; test quality C

MINERAL	SITE	IN-SITU TEST	QUALITY	INTERP.	LAB TEST	QUALITY
Ur	Colorado	SPT*	A	II	TRIAXIAL	B
Ur	Shiprock	SPT	A	I	NONE	NA
Ur	Grand Junction	SPT	A	I	DS**	C
Ur	Ambrosia Lake	NONE	NA	NA	DS	C
Ur	Durango	NONE	NA	NA	DS	C
Ur	Falls City	NONE	NA	NA	DS	C
Ur	Green River	NONE	NA	NA	DS	C
Ur	Maybell	NONE	NA	NA	DS	C
Ur	Monument Valley	NONE	NA	NA	DS	C
Ur	New Rifle	NONE	NA	NA	DS	C
Ur	Old Rifle	NONE	NA	NA	DS	C
Ur	Riverton	NONE	NA	NA	DS	C
Ur	Slick Rock	NONE	NA	NA	DS	C
Ur	Spook	NONE	NA	NA	DS	C
Ur	Tuba City	NONE	NA	NA	DS	C
Cu	Morenci	Dutch Cone	A	II	TRIAXIAL	A
Cu	Morenci	SPT	NA	NA	TRIAXIAL	NA
Cu	Chino	SPT	A	II	TRIAXIAL	A
Cu	Magna	SPT	A	III	TRIAXIAL	A
Cu	Magna	Dutch Cone	A	I	TRIAXIAL	NA
Cu	Mindola	Dutch Cone	A	III	TRIAXIAL	A
Cu	Chingola	Dutch Cone	B	II	NONE	NA
Cu	Brenda	Dutch Cone	A	II	NONE	NA
Cu	Chambishi	Dutch Cone	B	III	NONE	NA
Cu	Chibuluma	Dutch Cone	B	II	NONE	NA
Cu	Japan Mine A	Dutch Cone	A	I	TRIAXIAL	A
Cu	Japan Mine B	Dutch Cone	A	I	TRIAXIAL	A
Cu	Japan Mine D	Dutch Cone	A	I	TRIAXIAL	A
Cu	Japan Mine E	Dutch Cone	A	I	TRIAXIAL	A
Cu	Japan Mine F	Dutch Cone	A	I	TRIAXIAL	A
Cu	Japan Mine G	Dutch Cone	A	I	TRIAXIAL	A
Cu	Japan Mine I	Dutch Cone	A	I	TRIAXIAL	A
Cu	Japan Mine J	Dutch Cone	A	I	TRIAXIAL	A
G	Texas	SPT	A	I	TRIAXIAL	A
G	Louisiana1	SPT	NA	I	TRIAXIAL	A
G	Florida1	SPT	B	II	TRIAXIAL	C
G	Vick Article	SPT	A	III	CD-DS,CU	A
G	Florida4	NONE	NA	NA	TRIAXIAL	A
G	Louisiana2	NONE	NA	NA	TRIAXIAL	A
G	Florida2	NONE	NA	NA	TRIAXIAL	A
G	North Carolina	NONE	NA	NA	TRIAXIAL	A
G	Florida3	NONE	NA	NA	TRIAXIAL	A
G	Piney Point	Dutch Cone	A	I	TRIAXIAL	B

*Standard Penetration Test **Direct Shear Test

Table 6.4: SUMMARY OF QUALITY AND INTERPRETATION RATINGS OF FIELD AND LABORATORY TESTS

7. DATA ANALYSIS PROCEDURE

The data analysis procedure followed seven (7) steps, with certain varitions given the uniqueness of each data set.

STEP 1--Data from the entire site were reviewed to form a concept of the tailings materials and the structure of the embankment or pond in which strength measurements were made. Materials processing and handling techniques were reviewed for their influence either on physical properties or on spatial variation, zonation, and other structural aspects.

STEP 2--Individual borings, penetrations or other soundings were studied to identify zonations within the embankment that from an engineering point of view would be treated as homogeneous for the purposes of stability analysis. Clearly, even within such zones the tailings materials can be quite variable. The intent was to perform statistical analyses on units of the same type as are used in geotechnical analysis, and in this way to have the statistical results be of use in common applications. As most people recognize, the spatial scale over which statistical analyses are made influences results. Typically, the less a site is divided into zones, the greater the variability in material properties that results. For the same reason, when stability analyses are performed without first differentiating the profile or embankment into "homogeneous" zones, the uncertainty or variability in material properties is large. Thus, the statistical analysis to infer variability and the engineering analysis in which that variability is used must be compatible.

STEP 3--Individual data records were reviewed to eliminate outliers, small scale inhomogeneities (e.g., small sand layers in silty or clayey materials), and other corrupting features in the data sets. Careful attention was paid to the importance of such features for stability, and attempts were made to interpret the connectivity of such features from one boring or penetration to another.

STEP 4--The data were digitized using an electronic digitizer and were stored within a computerized data bank. Computer graphics figures of the data profiles were drawn at the same scale as the original data plots and overlayed on a light table to assure the quality of the digitization. Tabulated data were entered by keyboard.

STEP 5--Data quality indices were assigned to all data

after inspection and study, as described in section 6.6.

STEP 6--Statistical analyses were performed on the data from each site. These analyses consisted of (1) spatial trends, (2) statistical moments for raw and residual (i.e., deviations from trend) data, (3) fitting and testing of analytical distribution forms to raw and residual data, (4) estimation of autocovariance functions where data permitted, and (5) estimation of cross correlations among different physical properties where data permitted.

STEP 7--Results of the statistical analyses were reviewed for consistency and accuracy.

8. RESULTS

The results presented in this section summarize the data analyses performed on each site. The results are organized by commodity, beginning with a summary table of average strengths and the variability of strengths from one site to another. This summary is intended to describe the sometimes large differences among materials at different sites, and is not intended to provide guidance in selecting strength properties a priori. This summary is followed by data and plots for each individual site.

The results for each site begin with an aggregate profile and data summary table. The aggregate profile shows the mean trend of the data with depth taken (1) as a linear regression, and (2) as depth interval means. The envelopes about the depth interval means indicate depth interval standard deviations. For profiles where only a few data were available the data themselves are plotted rather than means and standard de iations. These cases are clear from context. The data tables summarize the data base for each site, basic statistics of the data, and the results of goodness-of-fit testing. Two goodness-of-fit statistics are given for each distribution tested, the chi-square and the Kolmogorov-Smirnov maximum deviation from the theoretical frequency curve. For the raw data five distributions are tested; for the residual data (i.e., deviations from a linear trend with depth) two distributions are tested (pdf's defined on zero-infinity are inadmissable for residuals).

Pearson diagrams (Fig. 4.4) for individual borings or penetrations follow the profile and summary table. In each case, the first diagram summarizes raw data; the second diagram summarizes residual data.

Histograms and cumulative frequency plots for raw and residual data from the entire site follow the Pearson diagrams. The cumulative frequency data are plotted on normal probability grid, with best fitting theoretical distributions plotted as continuous curves, and denoted, respectively,

N ... normal (not shown on figs.)

B ... beta

E ... exponential

L ... lognormal

G ... gamma

Where in situ data were sufficiently numerous and appropriately arrayed to allow estimation of autocovariance functions, these estimates follow the histograms and cdf's. For convenience, these estimates are presented both as autocovariance and as variograms. With the exception of the Mindola site, the autocovariances pertain to vertical variations. In general, either too few in situ data were collected, the spacings among data were too great, or the data were too noisy to allow horizontal autocovariances to be estimated.

SITE Commodity: Copper

DATA Type Inferred friction angle

Number 26

Quality Index

TREND WITH DEPTH N/A

DATA SCATTER

	mean	SD	β_1	β_2
Raw Data	30.4	2.56	0.0015	2.17
Residual Data	--	--	--	--

GOODNESS OF FIT STATISTICS

	Raw		Residual	
	χ^2	D_m	χ^2	D_m
normal				
beta				
exponential				
lognormal				
gamma				
5% confidence limit				

INTERPRETED STRENGTH PARAMETERS

Table 8.2 - Table of copper global averages for inferred friction angles

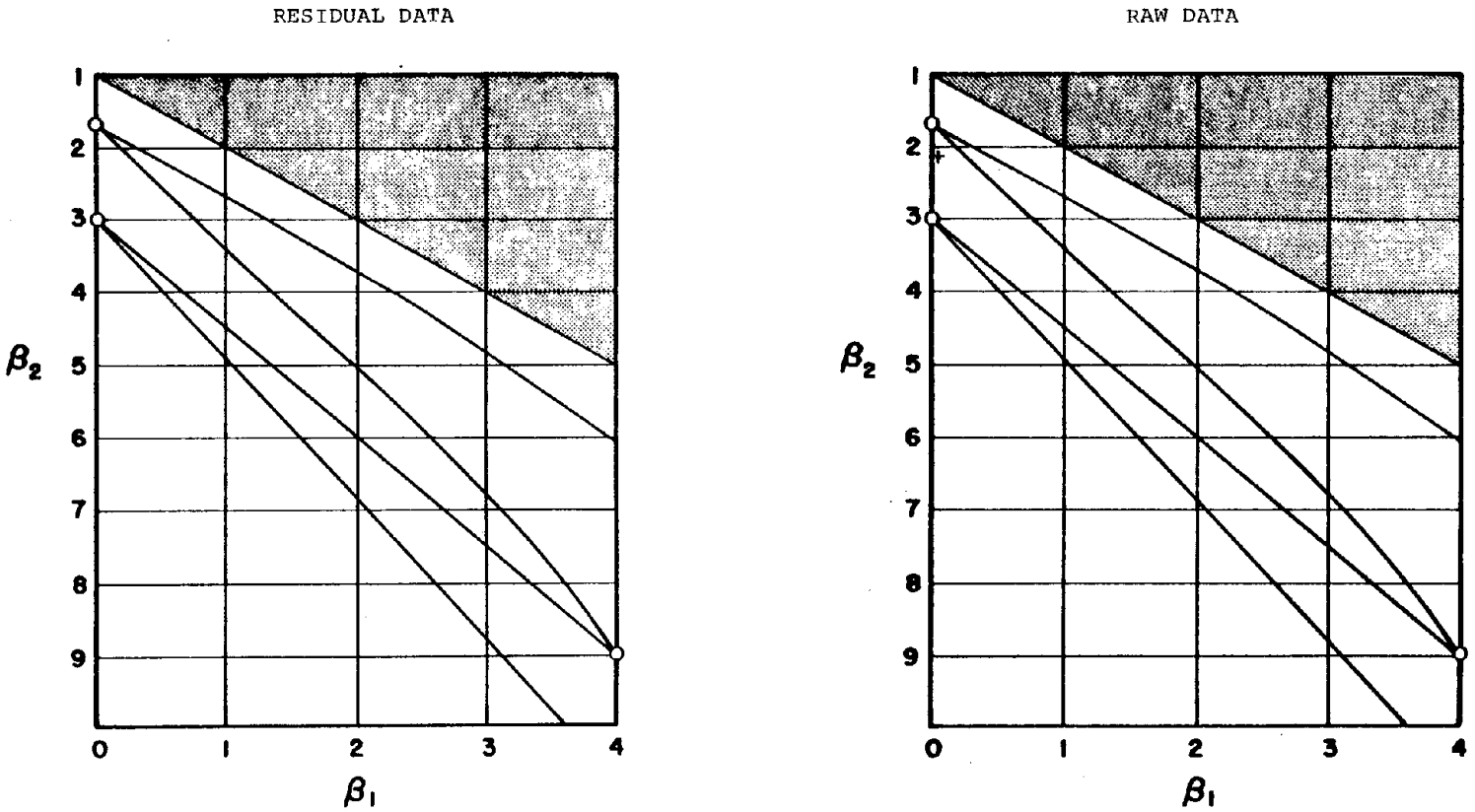

Figure 8.1 - Pearson diagrams of raw and residual inferred friction angles for global copper averages

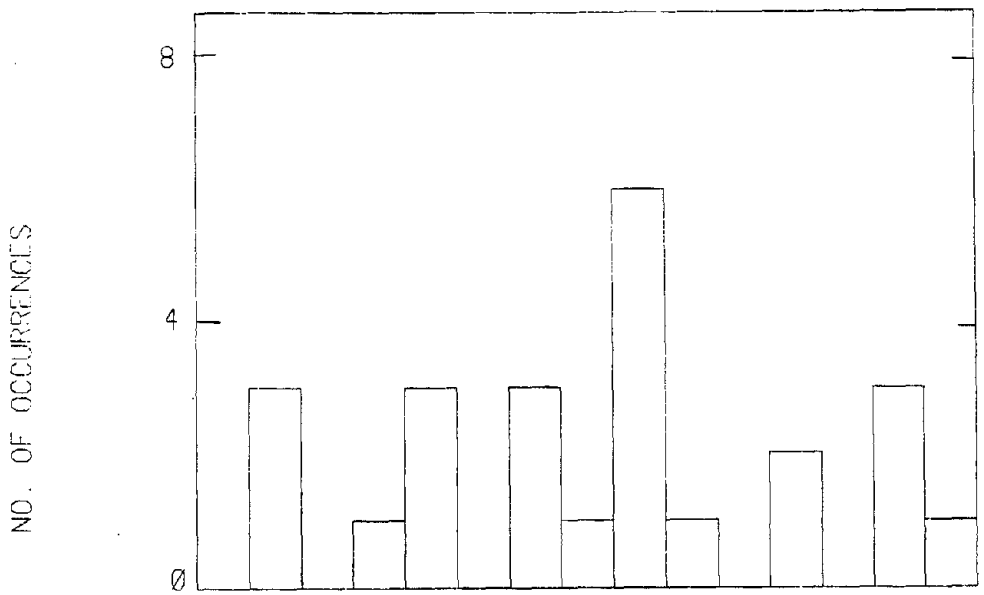

Figure 8.2 - Histogram of inferred friction angles for copper global averages

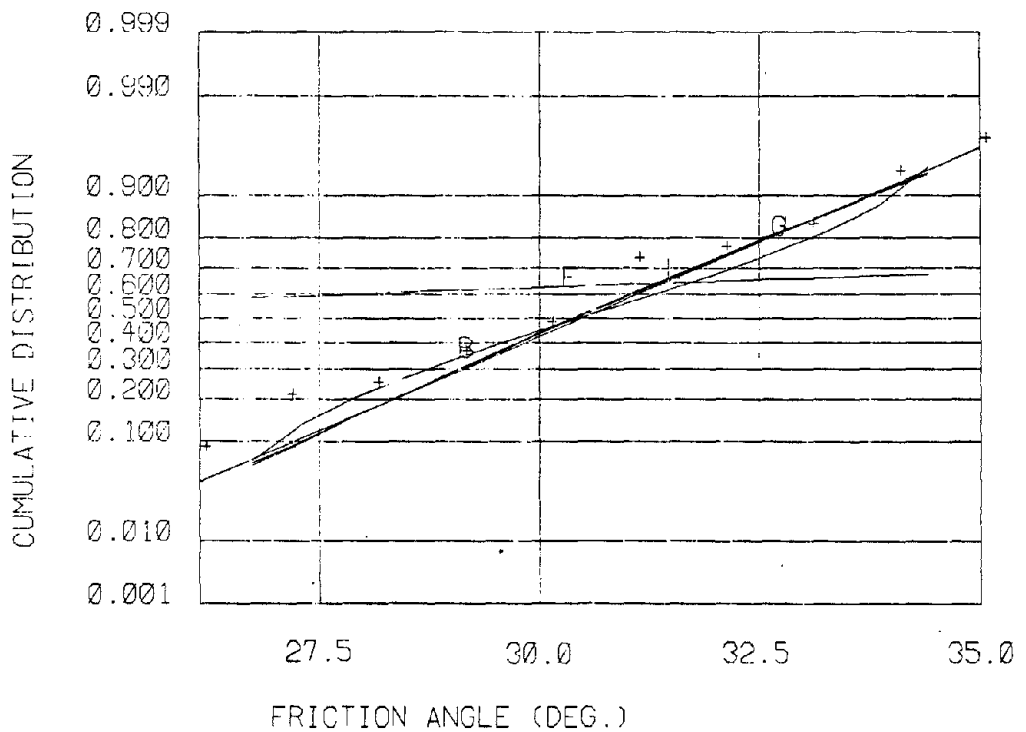

Figure 8.3 - CDF of inferred friction angles for global copper averages compared to standard CDF plots

SITE Commodity: copper

DATA Type friction angle

Number 16

Quality Index

TREND WITH DEPTH N/A

DATA SCATTER

	mean	SD	β_1	β_2
Raw Data	35.7	2.9	0.75	3.99
Residual Data	--	--	--	--

GOODNESS OF FIT STATISTICS

	Raw		Residual	
	χ^2	D_m	χ^2	D_m
normal	15.25	0.15		
beta	21.4	0.18		
exponential	277	0.48		
lognormal	14.7	0.14		
gamma	14.9	0.14		
5% confidence limit	23.7	0.33		

INTERPRETED STRENGTH PARAMETERS

Table 8.3 - Table of copper global averages for friction angles

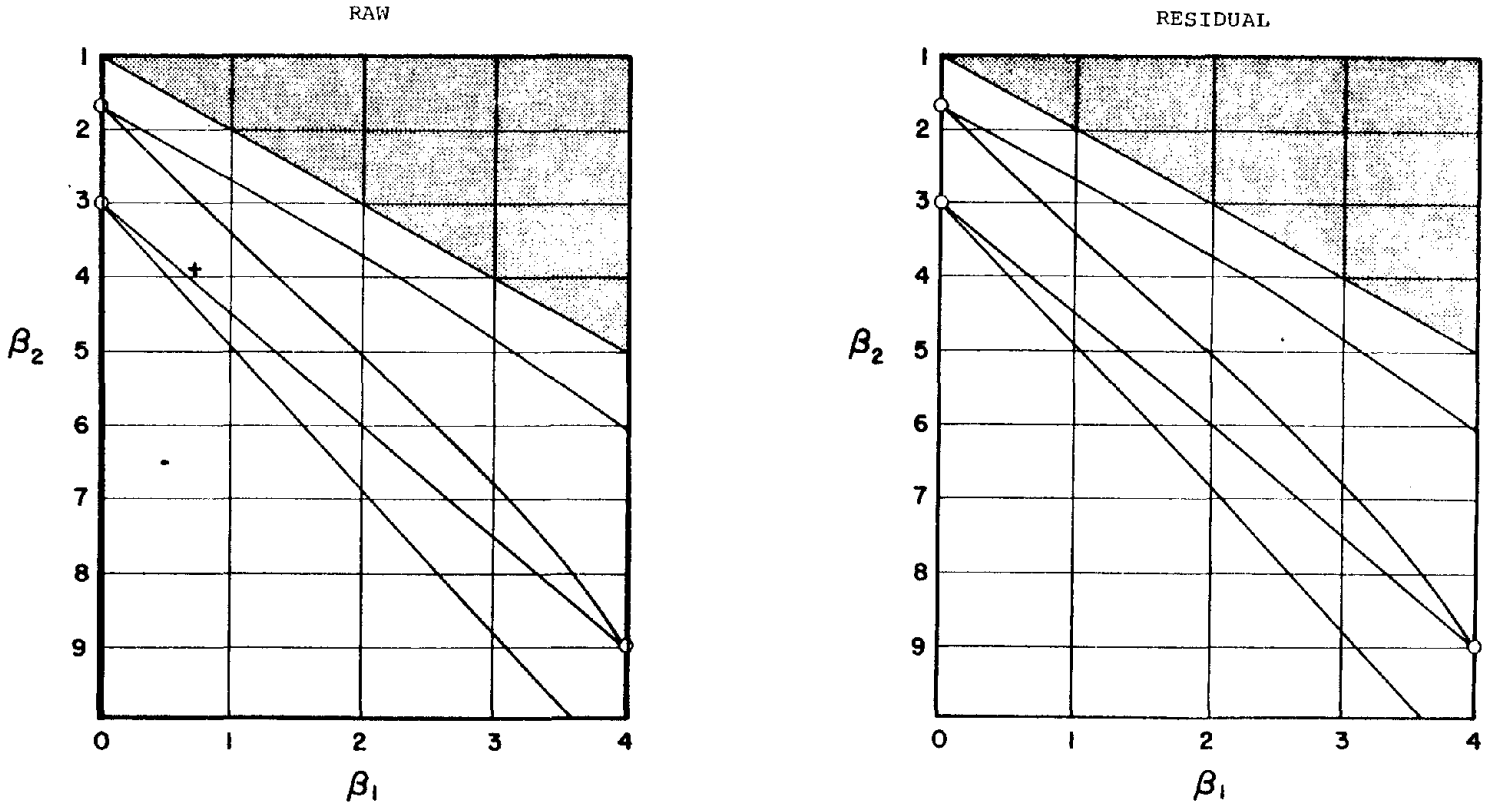

Figure 8.4 - Pearson diagrams of raw and residual friction angle data for global copper averages

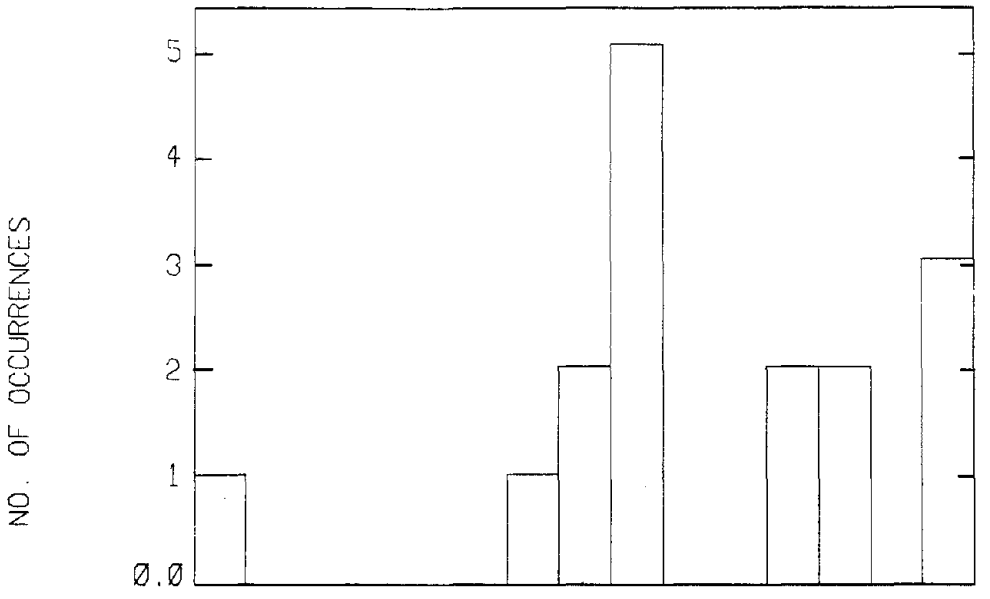

Figure 8.5 - Histogram of friction angles for copper global averages

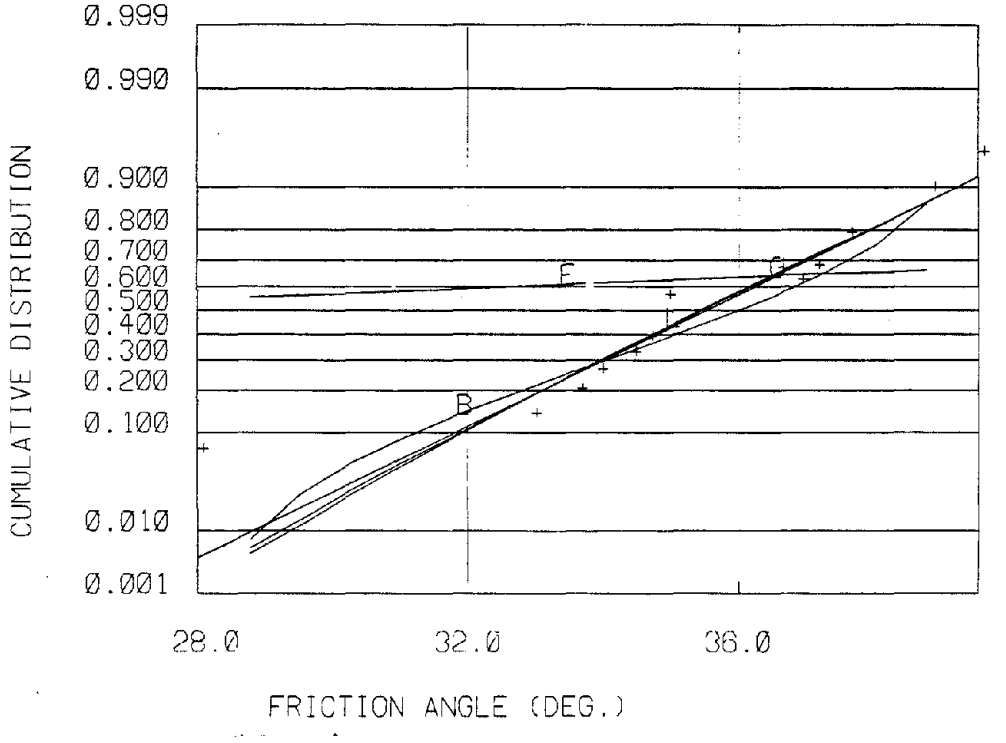

Figure 8.6 - CDF of friction angles for global copper averages compared to standard CDF plots

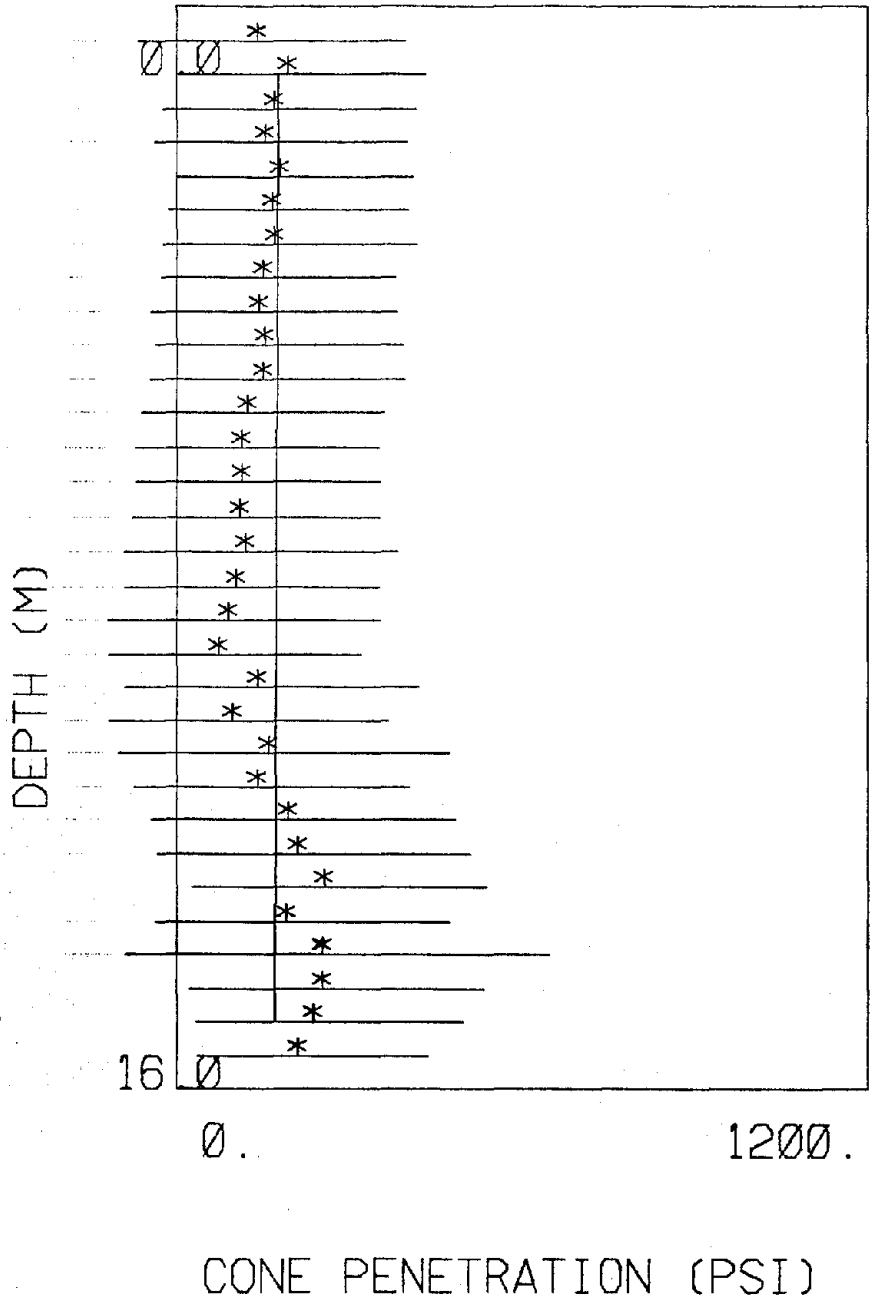

Figure 8.7 - Cone penetration resistance v. depth for Chambishi copper

SITE	Chambishi (Copper) Zambia	
DATA	Type	30 Cone Penetrations
	Number	697
	Quality Index	B
TREND WITH DEPTH	q_c(psi) = 178 - 0.4z(m)	

DATA SCATTER

	mean	SD	β_1	β_2
Raw Data	175.4	164	1.55	6.20
Residual Data	--	163	1.57	6.26

GOODNESS OF FIT STATISTICS

	Raw		Residual	
	χ^2	D_m	χ^2	D_m
normal	48.8	0.142	47.7	0.138
beta	85.9	0.132	85.6	0.093
exponential	143	0.168	--	--
lognormal	569	0.24	--	--
gamma	160	0.181	--	--
5% confidence limit	23.7	0.052	--	--

INTERPRETED STRENGTH PARAMETERS III

Table 8.4 - Table of Chambishi copper cone penetration data

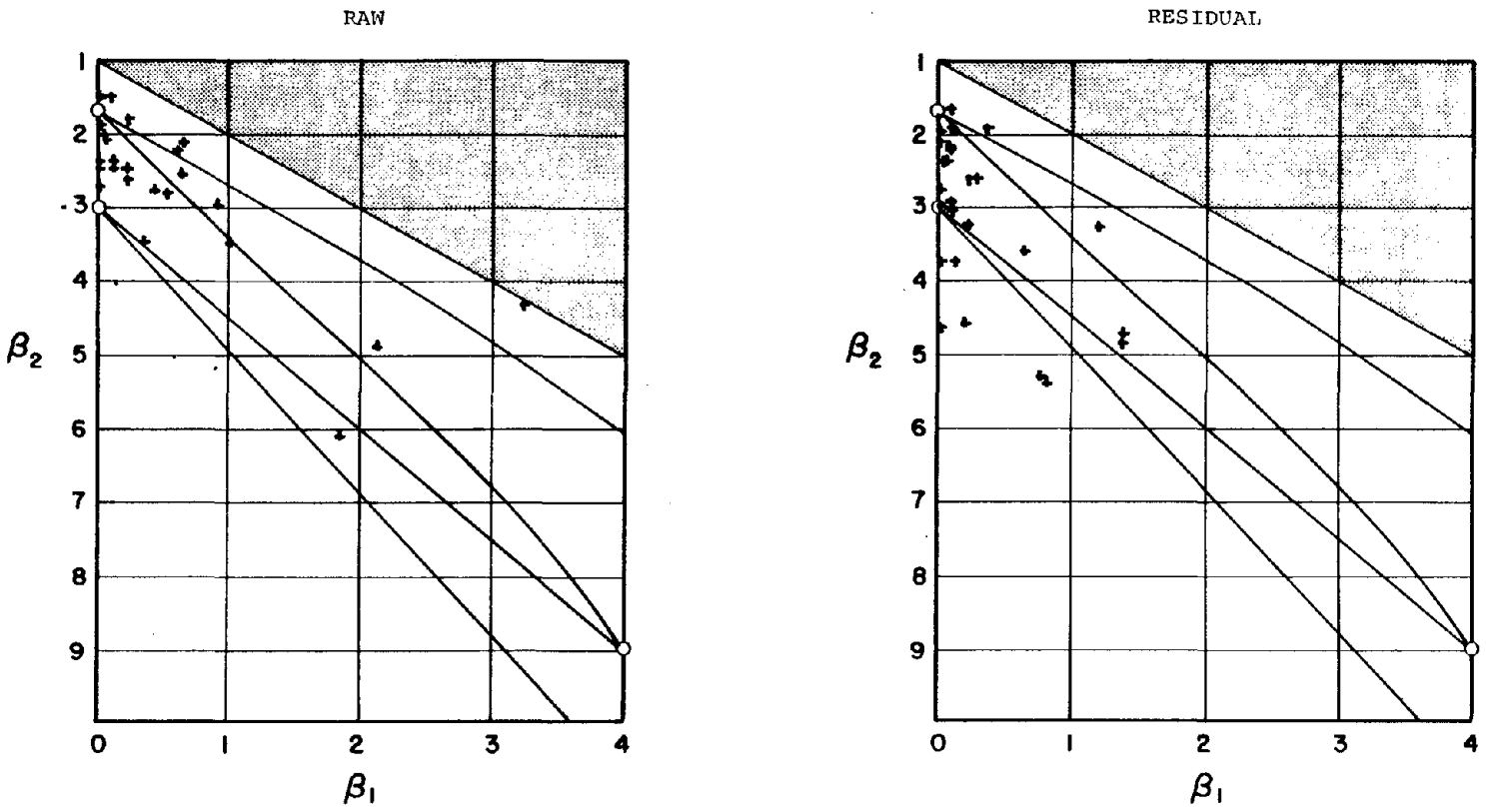

Figure 8.8 - Pearson diagrams of raw and residual Dutch Cone data for Chambishi copper

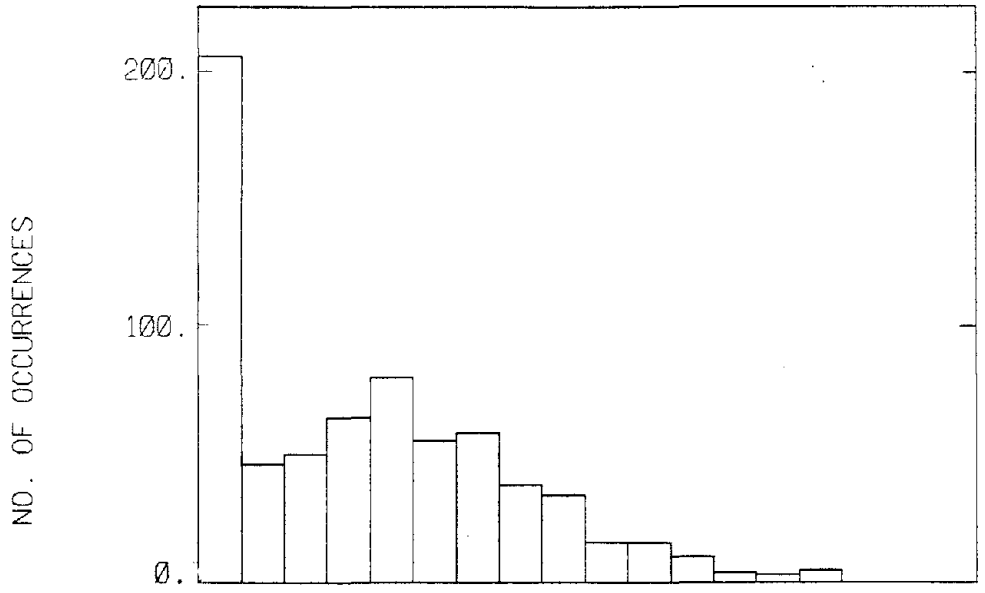

Figure 8.9 - Histogram of cone penetration resistance for raw Chambishi copper data

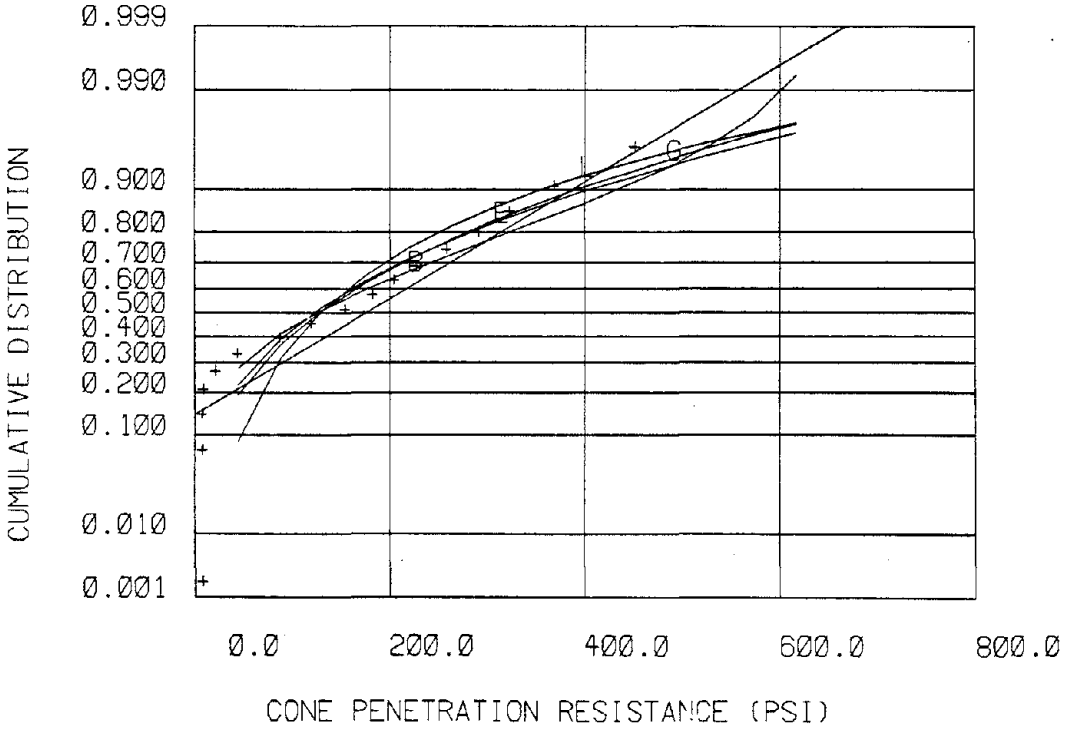

Figure 8.10 - CDF of cone penetration resistance for raw Chambishi copper data

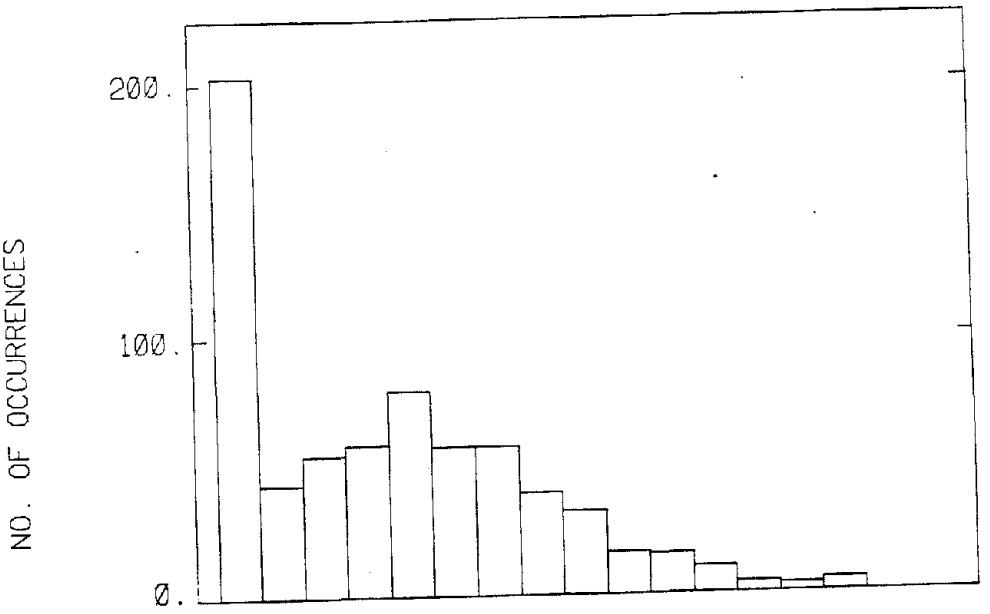

Figure 8.11 - Histogram of cone penetration resistance for residual Chamishi copper data

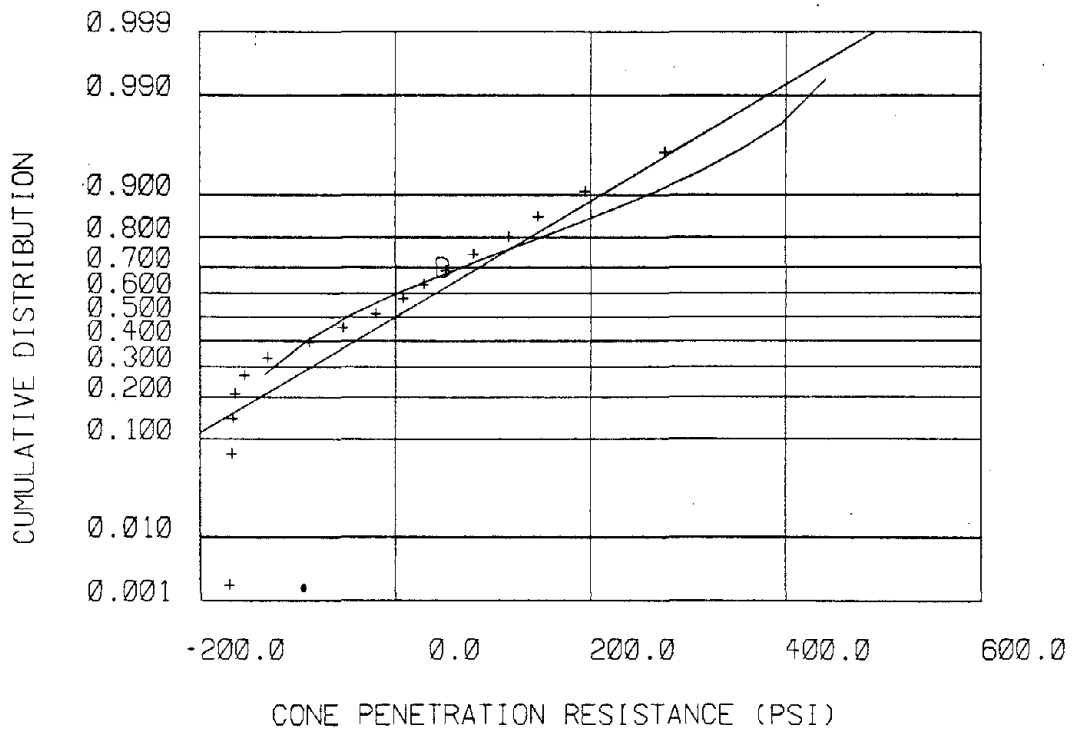

Figure 8.12 - CDF of cone penetration resistance for residual Chambishi copper data compared to standard CDF plots

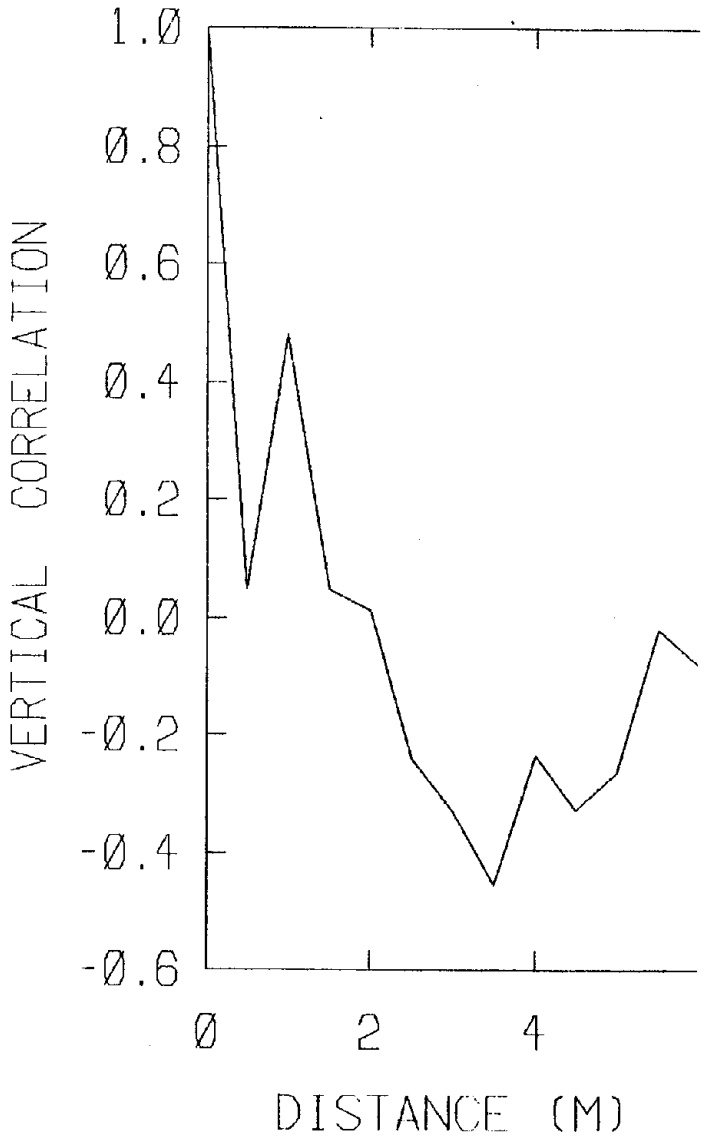

Figure 8.13 - Vertical correlation for residual Chambishi copper cone resistance

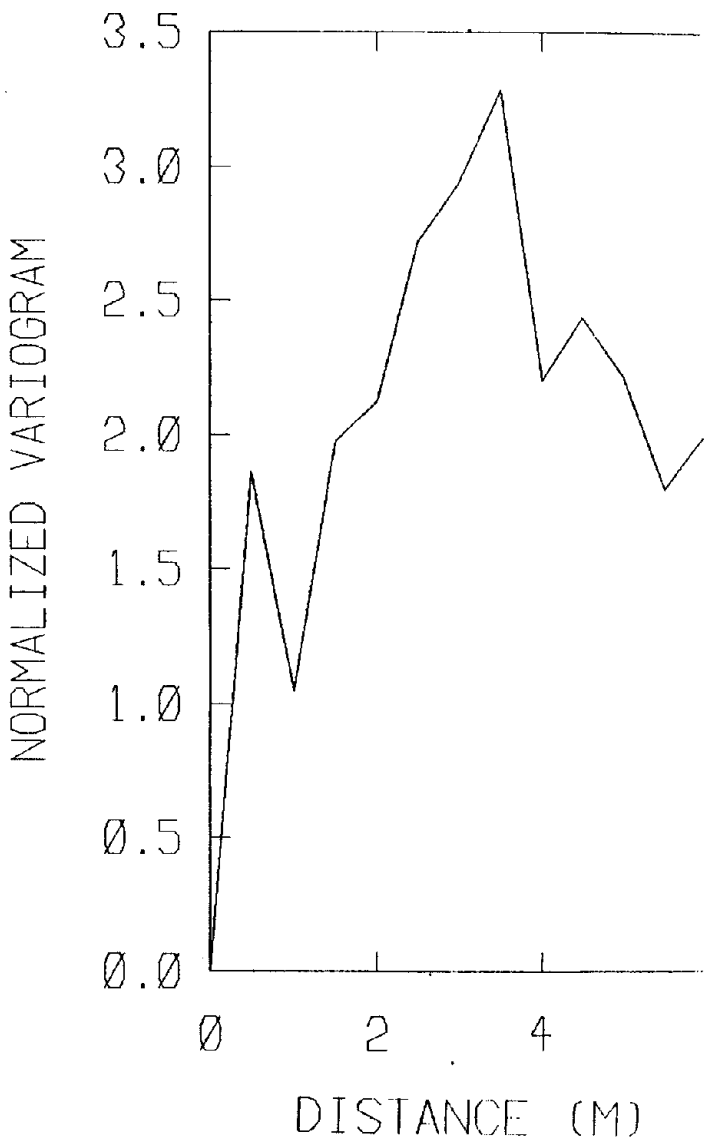

Figure 8.14 - Normalized variogram for residual Chambishi copper cone resistance

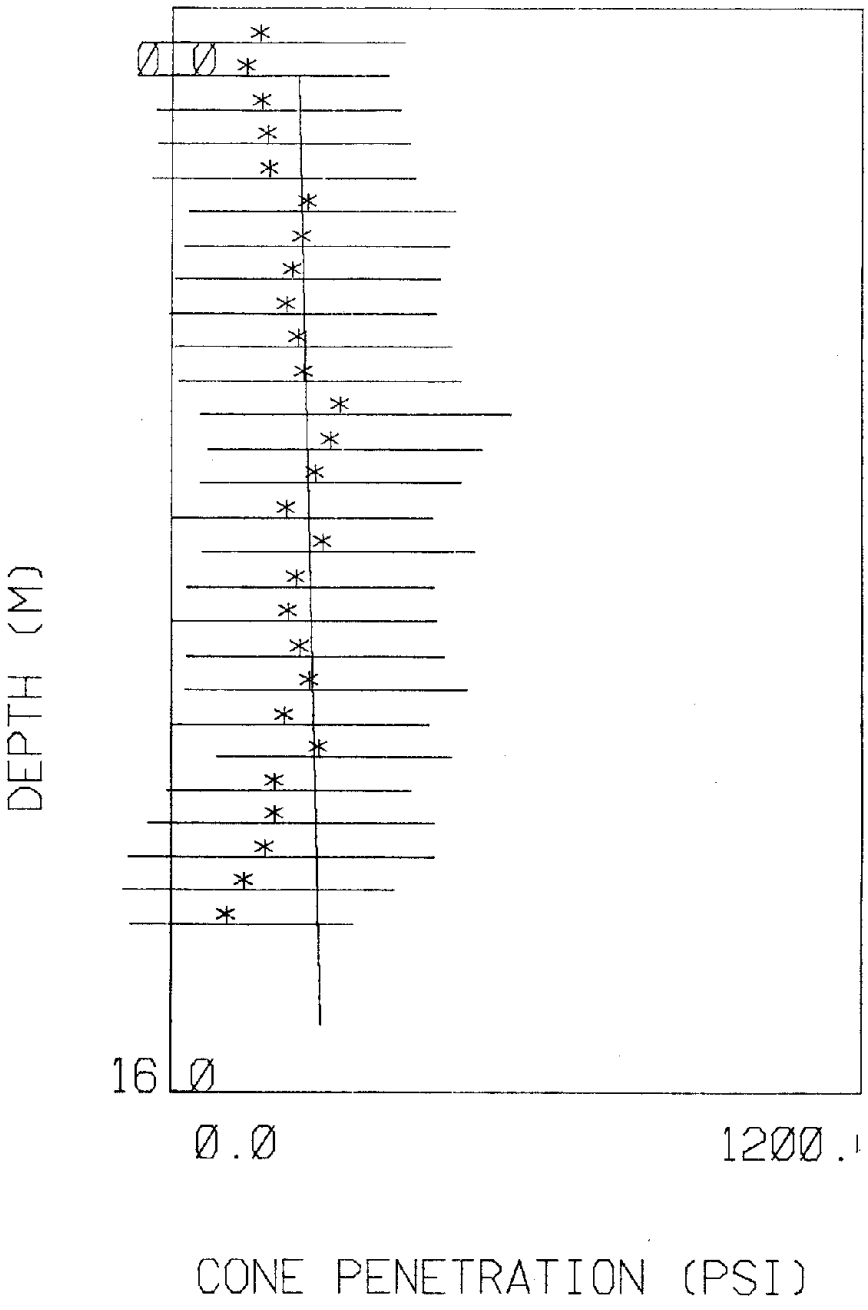

Figure 8.15 - Cone penetration resistance v. depth for Chibuluma copper

SITE	Chibuluma (Copper) Zambia	
DATA	Type	24 Cone Penetrations
	Number	488
	Quality Index	B

TREND WITH DEPTH $q_c(psi) = 220 + 2.7z(m)$

DATA SCATTER

	mean	SD	β_1	β_2
Raw Data	235	170	0.29	2.77
Residual Data	--	169	0.28	2.73

GOODNESS OF FIT STATISTICS

	Raw		Residual	
	χ^2	D_m	χ^2	D_m
normal	41.4	0.08	65.6	0.07
beta	22.4	0.04	27.4	0.03
exponential	111	0.11	--	--
lognormal	920	0.15	--	--
gamma	127	0.09	--	--
5% confidence limit	23.7	0.062	--	--

INTERPRETED STRENGTH PARAMETERS II

Table 8.5 - Table of Chinbumuma copper cone penetration data

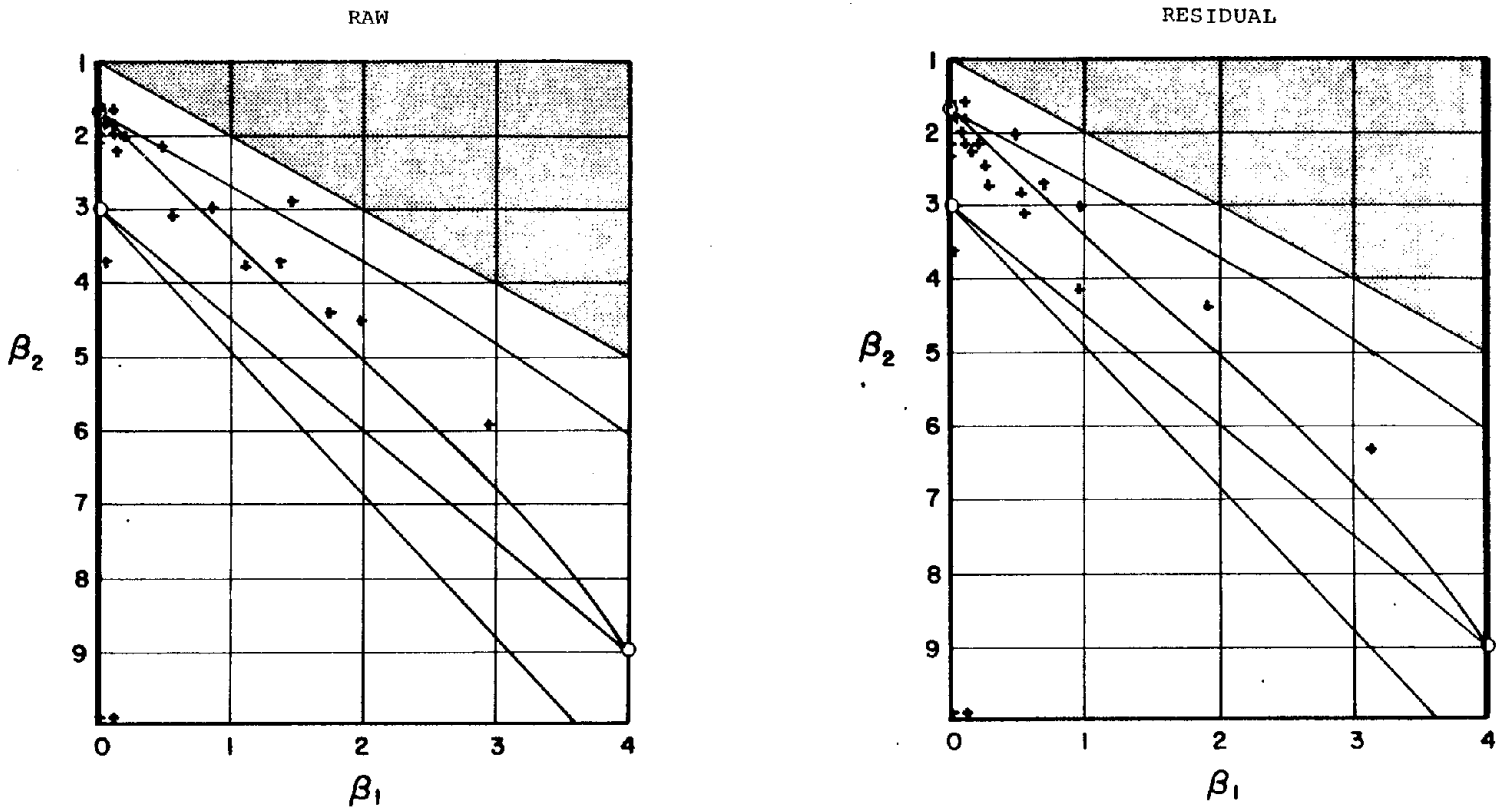

Figure 8.16 - Pearson diagrams of raw and residual cone data for Chibuluma copper

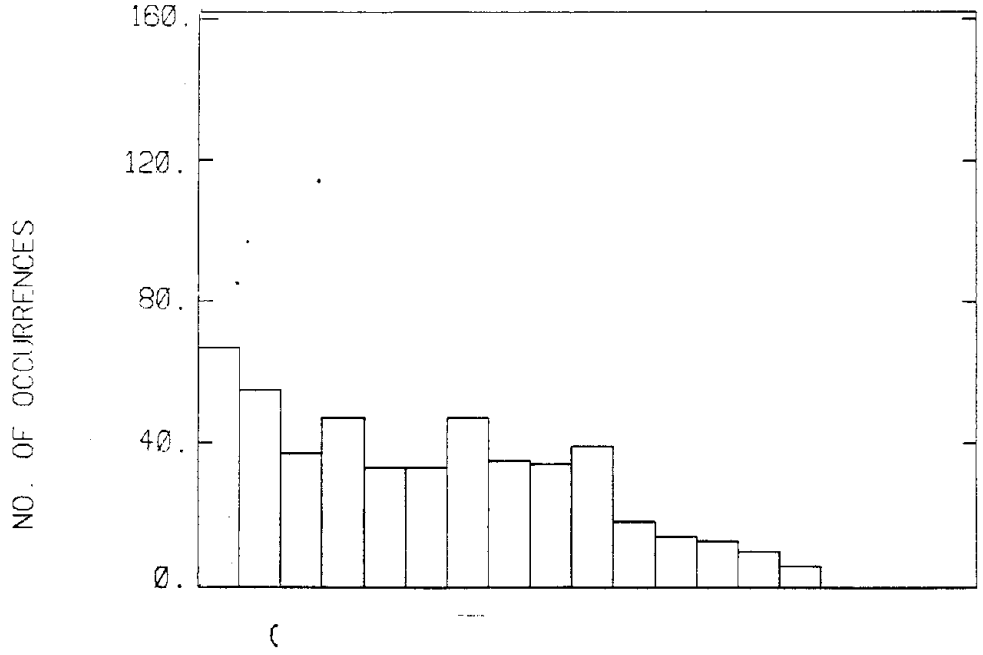

Figure 8.17 - Histogram of cone penetration resistance for raw Chibuluma copper data

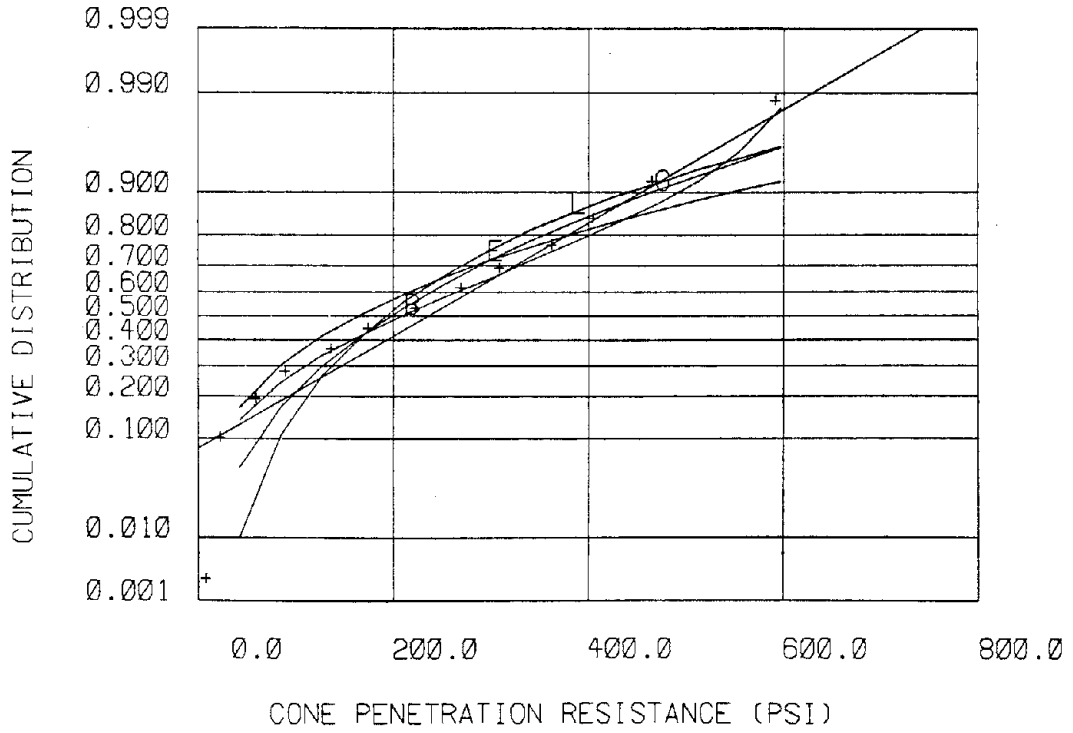

Figure 8.18 - CDF of cone penetration resistance for raw Chibuluma copper data compared to standard CDF plots

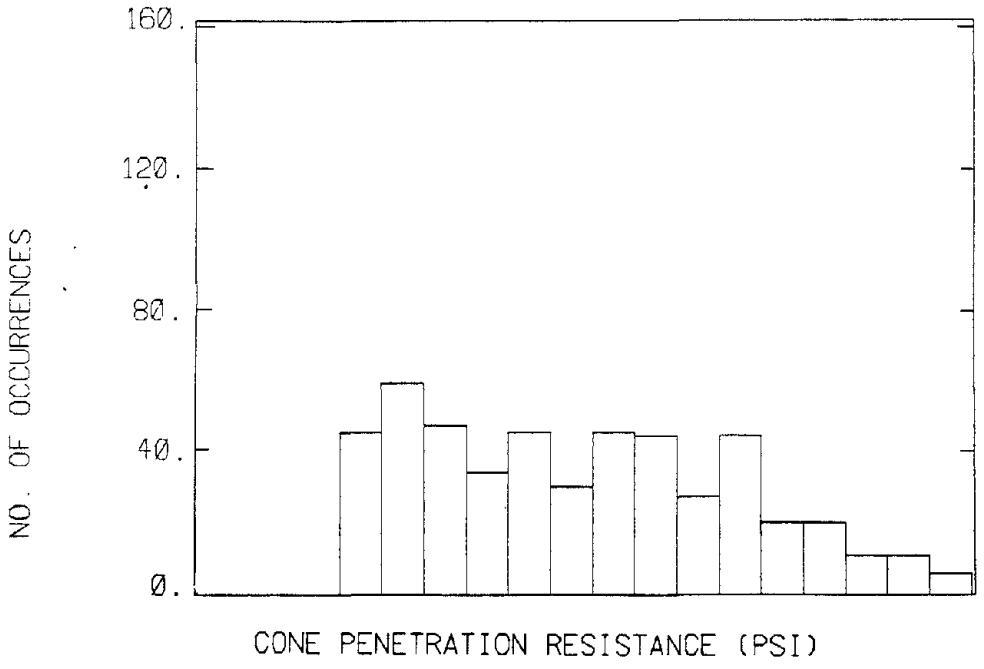

Figure 8.19 - Histogram of cone penetration resistance for raw Chibuluma copper data compared to standard CDF plots

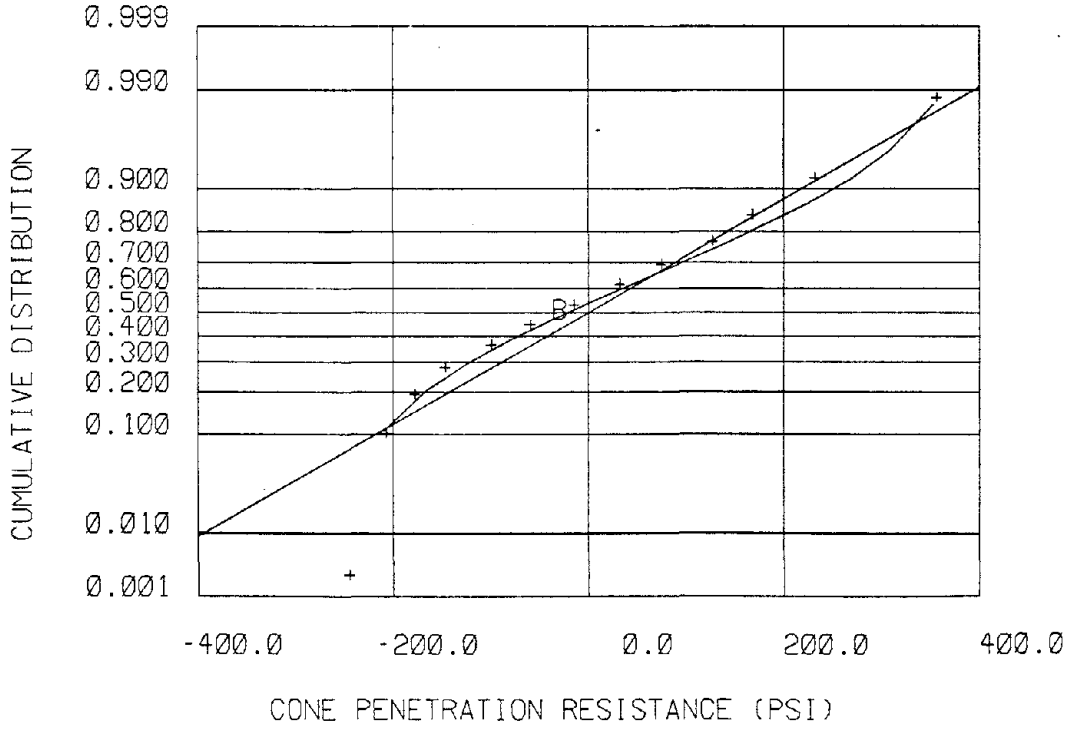

Figure 8.20 - CDF of cone penetration resistance for residual Chibuluma copper data compared to standard CDF plots

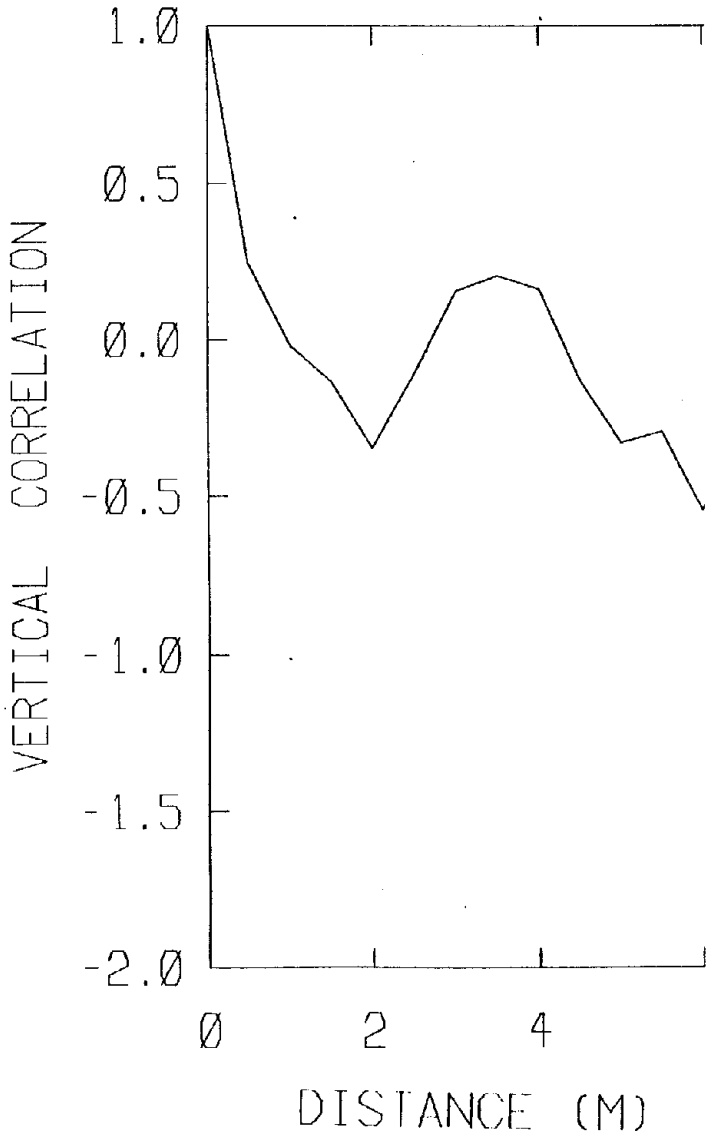

Figure 8.21 - Vertical correlation for residual Chibuluma copper cone penetration

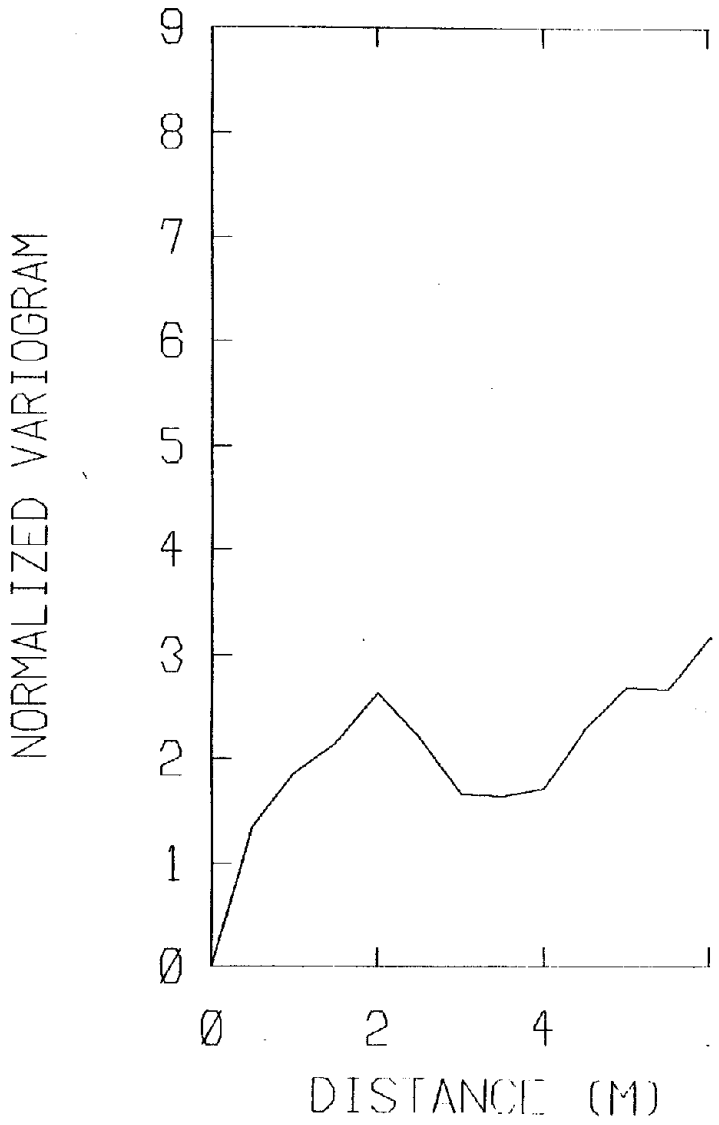

Figure 8.22 - Normalized variogram for residual Chibuluma copper cone penetration

SITE Chino Dam (Copper)

DATA Type SPT (Combined)

Number 19

Quality Index A

TREND WITH DEPTH N = 13.1 + 0.462z(ft)

DATA SCATTER

	mean	SD	β_1	β_2
Raw Data	38.4	19.2	0.61	3.00
Residual Data	--	12.8	0.88	5.76

GOODNESS OF FIT STATISTICS

	Raw		Residual	
	χ^2	D_m	χ^2	D_m
normal	13.2	0.15	22.1	0.18
beta	13.9	0.12	54.0	0.17
exponential	28.3	0.23	--	--
lognormal	10.9	0.08	--	--
gamma	10.8	0.09	--	--
5% confidence limit	23.7	0.30	--	--

INTERPRETED STRENGTH PARAMETERS II

Table 8.6 - Table of Chino copper SPT data

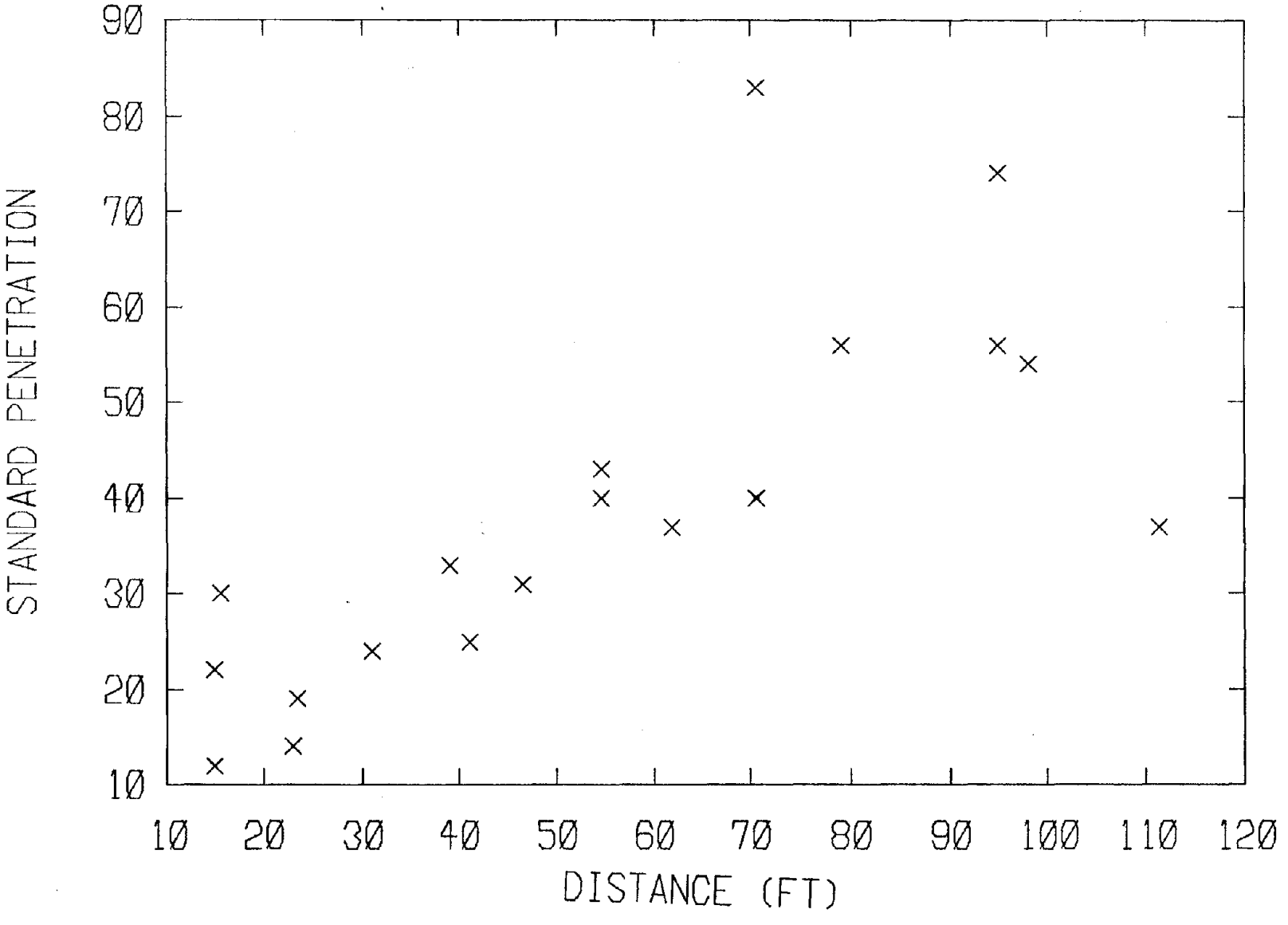

Figure 8.23 - SPT v. depth for Chino copper

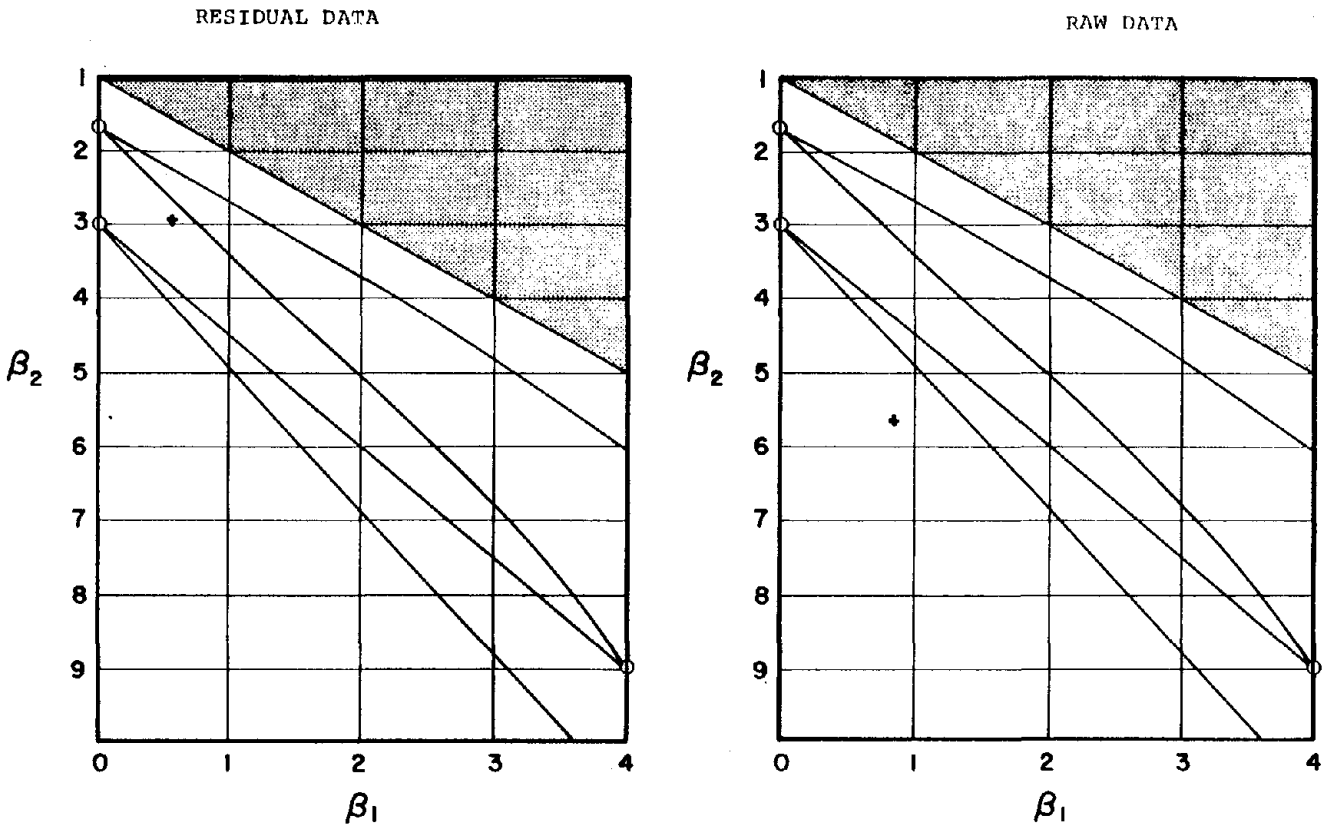

Figure 8.24 - Pearson diagrams of raw and residual SPT data for Chino copper

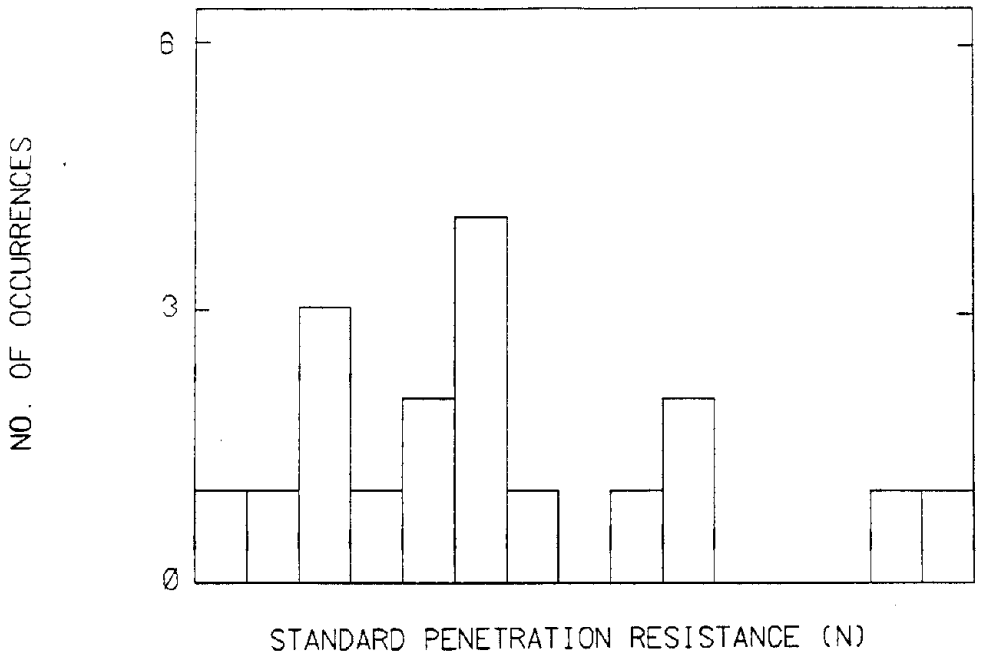

Figure 8.25 - Histogram of SPT (N) values for raw Chino copper data

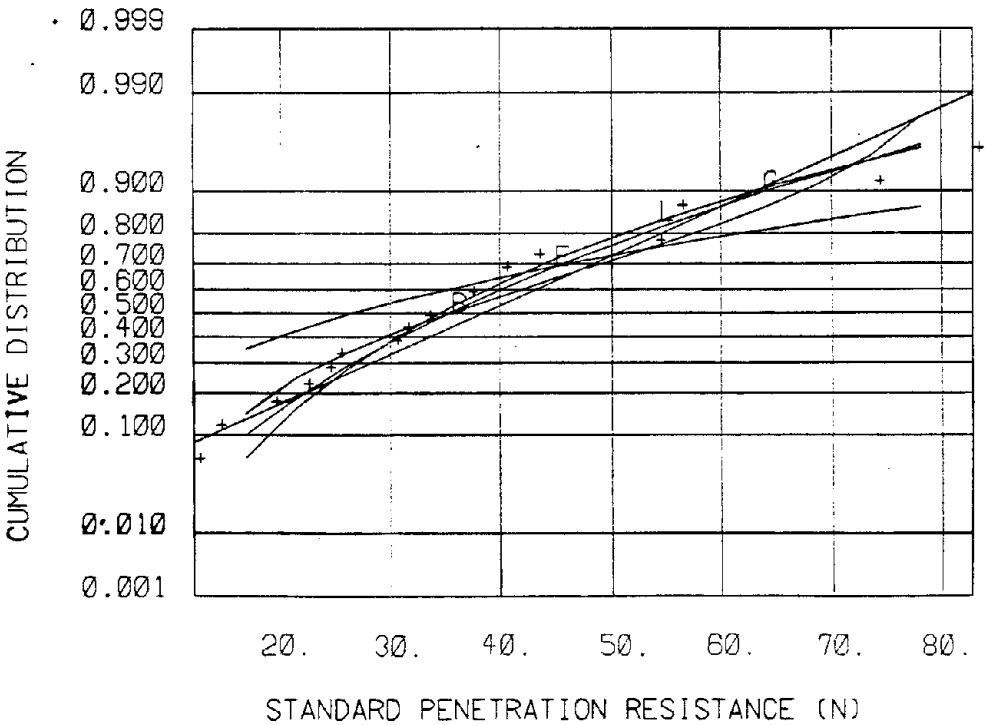

Figure 8.26 - CDF of SPT (N) values for raw Chino copper data compared to standard CDF plots

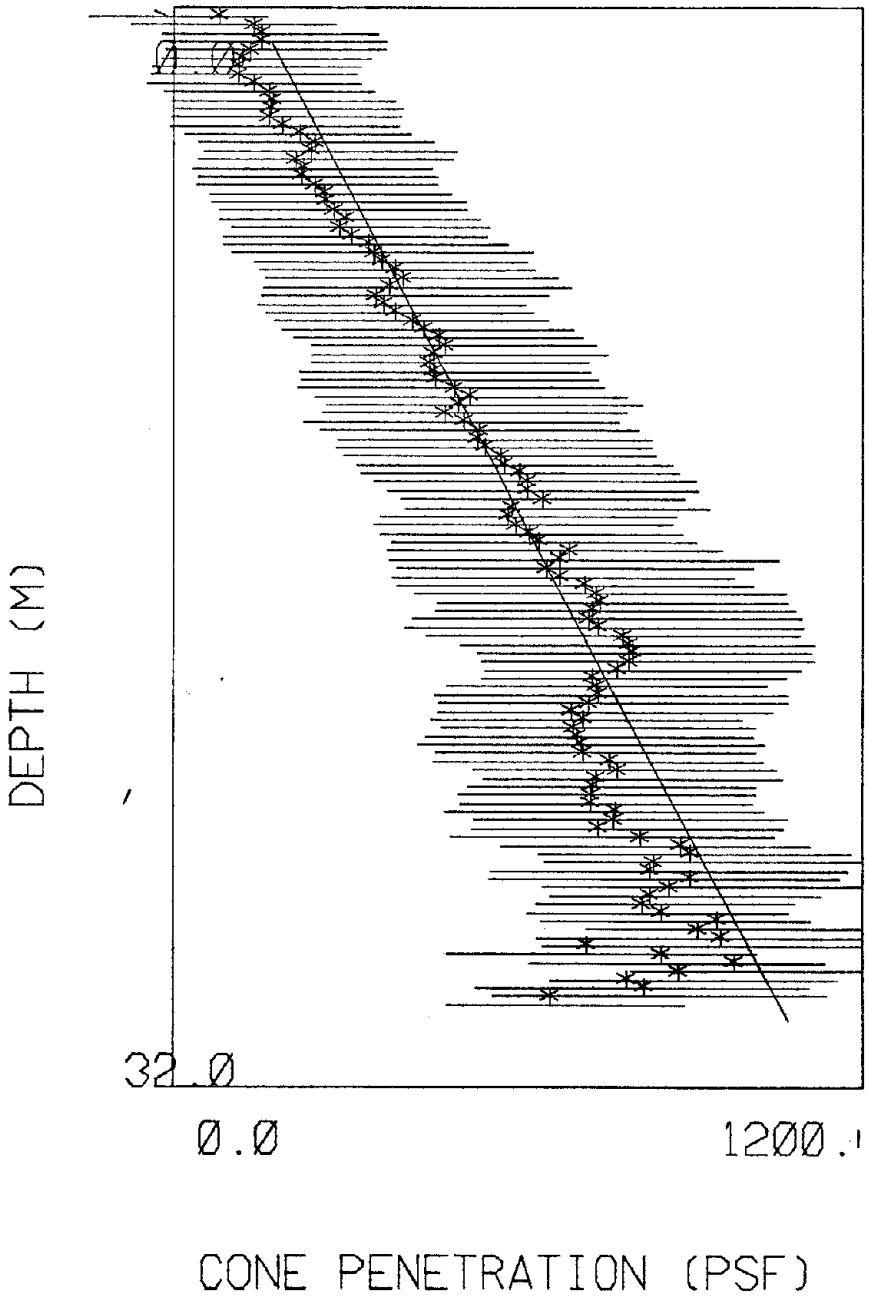

Figure 8.27 - Cone penetration resistance v. depth for Chingola copper

SITE	Chingola (Copper) Zambia	
DATA	Type	Cone Penetration
	Number	2387
	Quality Index	B

TREND WITH DEPTH $q_c = 142 + 31z(m)$

DATA SCATTER

	mean	SD	β_1	β_2
Raw Data	518	324	0.29	3.83
Residual Data	--	230	0.10	3.82

GOODNESS OF FIT STATISTICS

	Raw		Residual	
	χ^2	D_m	χ^2	D_m
normal	262	0.08	52.3	0.04
beta	98.9	0.05	234	0.04
exponential	645	0.13	--	--
lognormal	5060	0.11	--	--
gamma	317	0.06	--	--
5% confidence limit	23.7	0.028	--	--

INTERPRETED STRENGTH PARAMETERS II

Table 8.7 - Table of Chingola copper cone penetration data

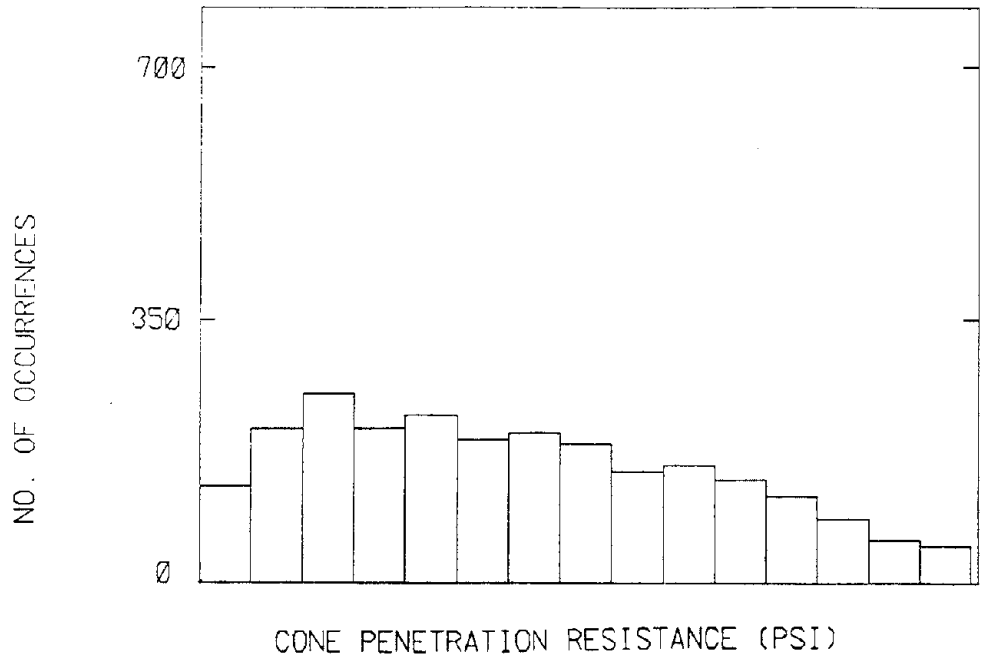

Figure 8.29 - Histogram of cone penetration resistance for raw Chingola copper data

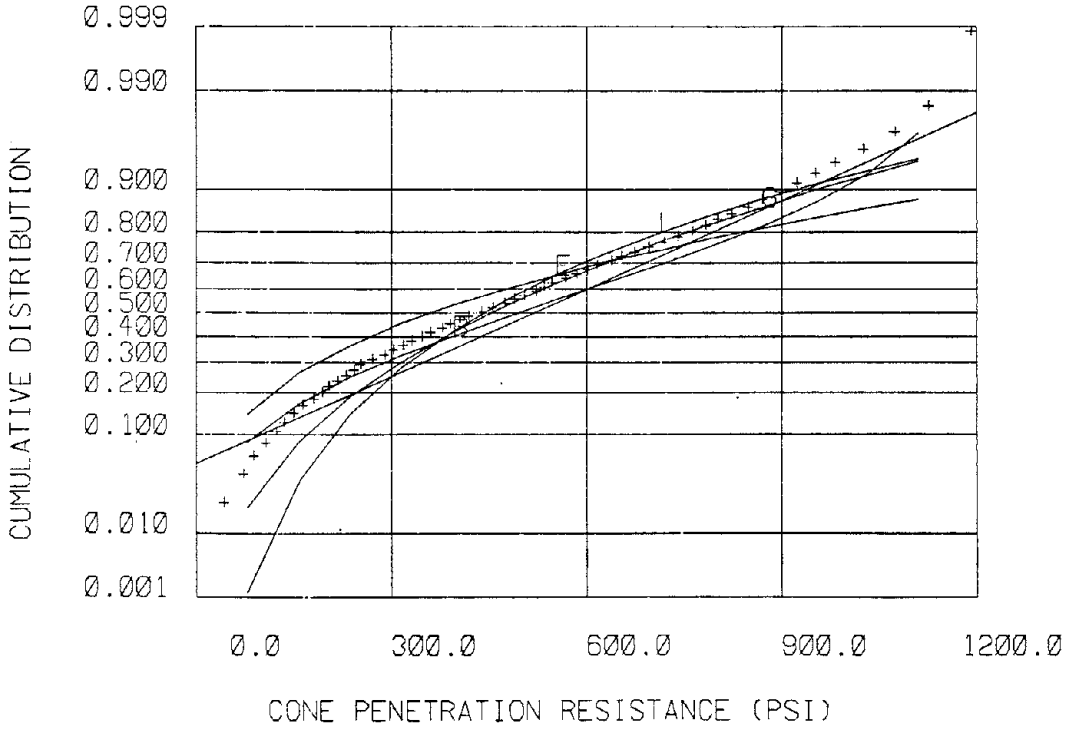

Figure 8.30 - CDF of cone penetration resistance for raw Chingola copper data compared to standard CDF plots

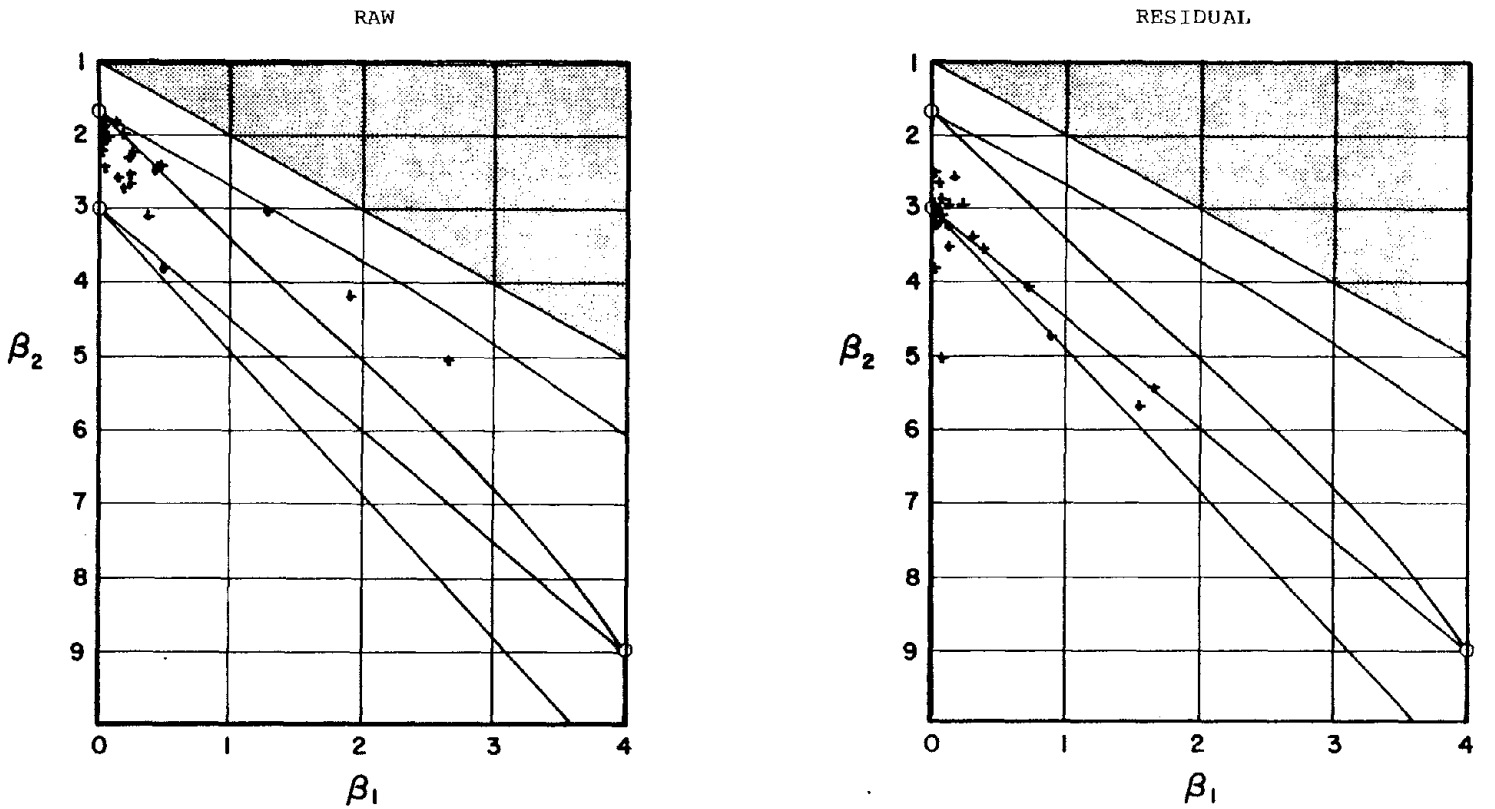

Figure 8.28 - Pearson diagrams of raw and residual cone data for Chingola copper

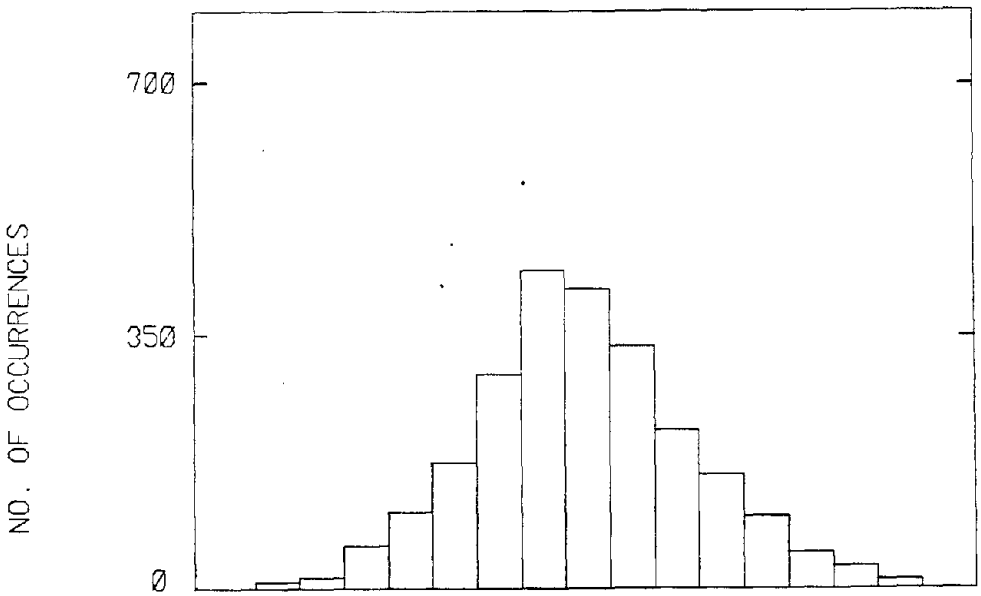

Figure 8.31 - Histogram of cone penetration resistance for residual Chingola copper data

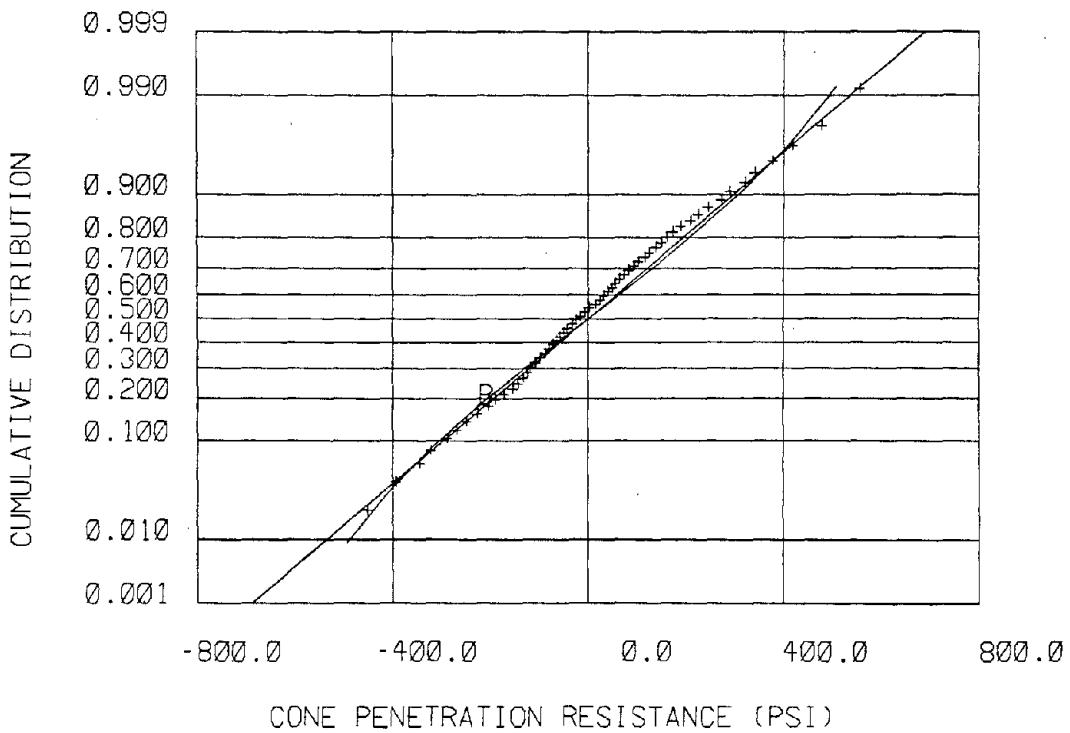

Figure 8.32 - CDF of cone penetration resistance for residual Chingola copper data compared to standard CDF plots

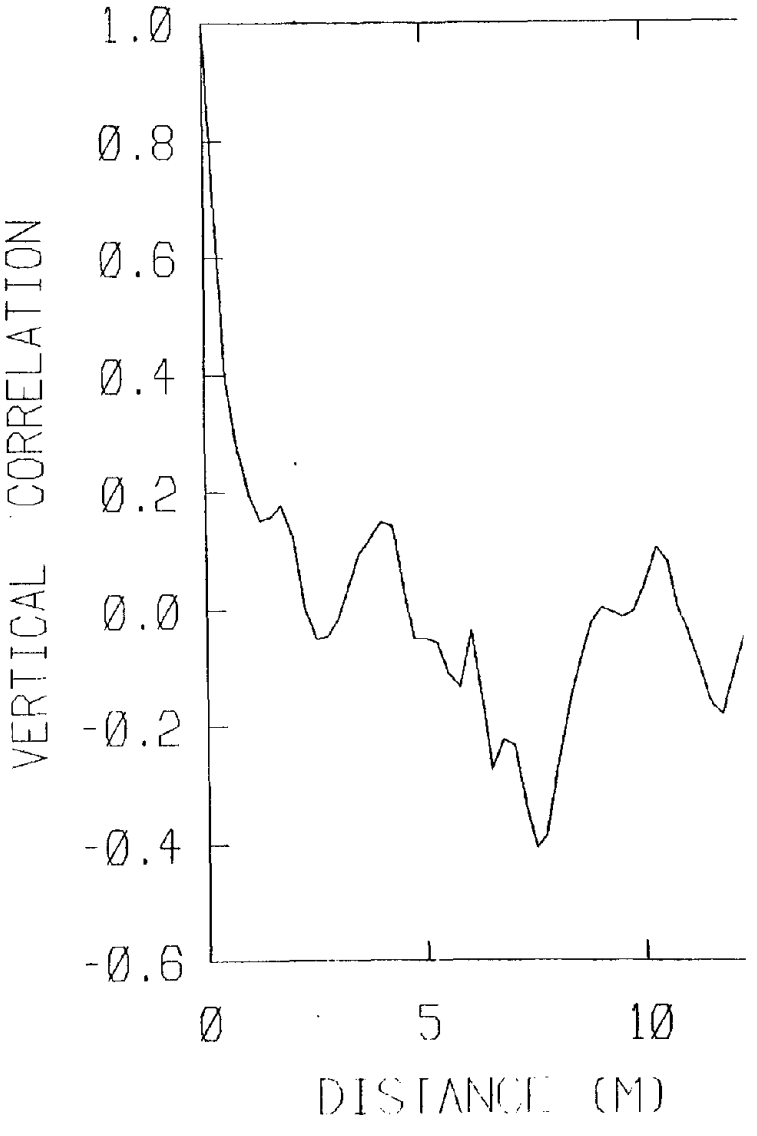

Figure 8.33 - Vertical correlation for residual Chingola copper cone penetration

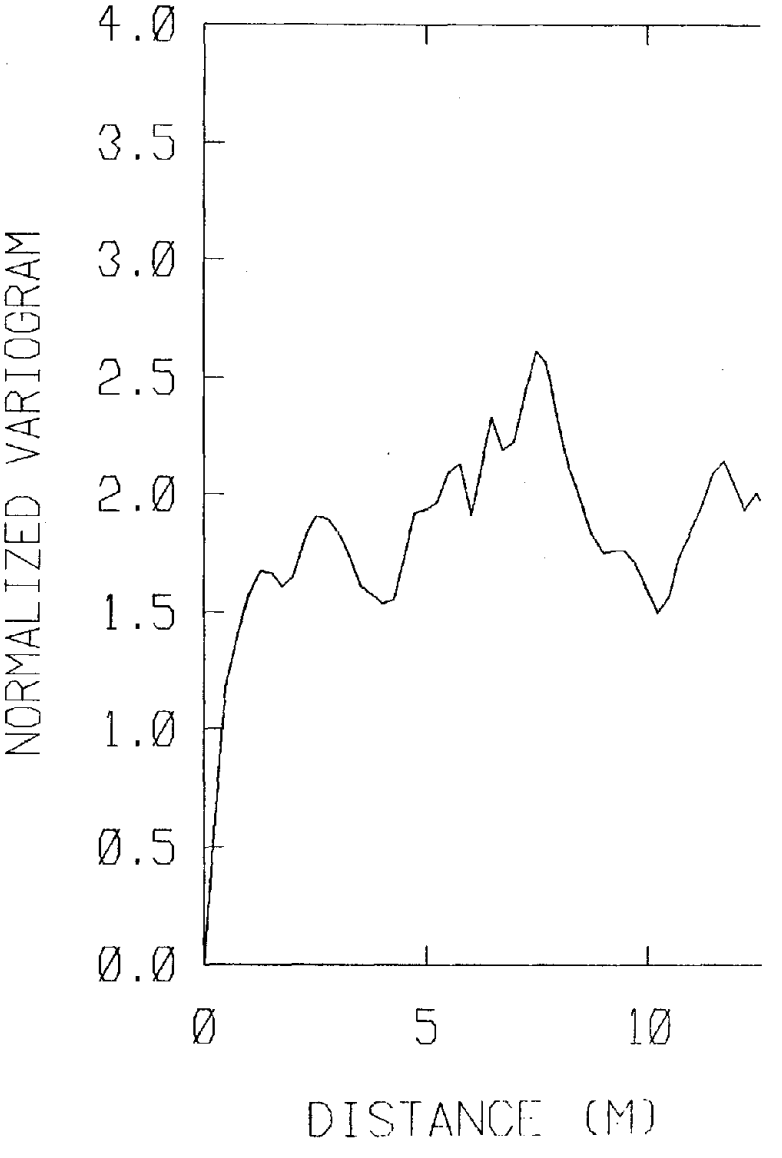

Figure 8.34 - Normalized variogram for residual Chingola copper cone penetration

SITE	Japanese Sites (Copper)	
DATA	Type	Friction Angles
	Number	21
	Quality Index	A
TREND WITH DEPTH	N/A	

DATA SCATTER

	mean	SD	β_1	β_2
Raw Data	36.2	4.35	0.10	3.01
Residual Data	--	--	--	--

GOODNESS OF FIT STATISTICS

	Raw		Residual	
	χ^2	D_m	χ^2	D_m
normal	17.2	0.17	--	--
beta	21.8	0.20	--	--
exponential	--	--	--	--
lognormal	--	--	--	--
gamma	--	--	--	--
5% confidence limit	23.7	0.28	--	--

INTERPRETED STRENGTH PARAMETERS I

Talbe 8.8 - Table of Japanese copper friction angle data

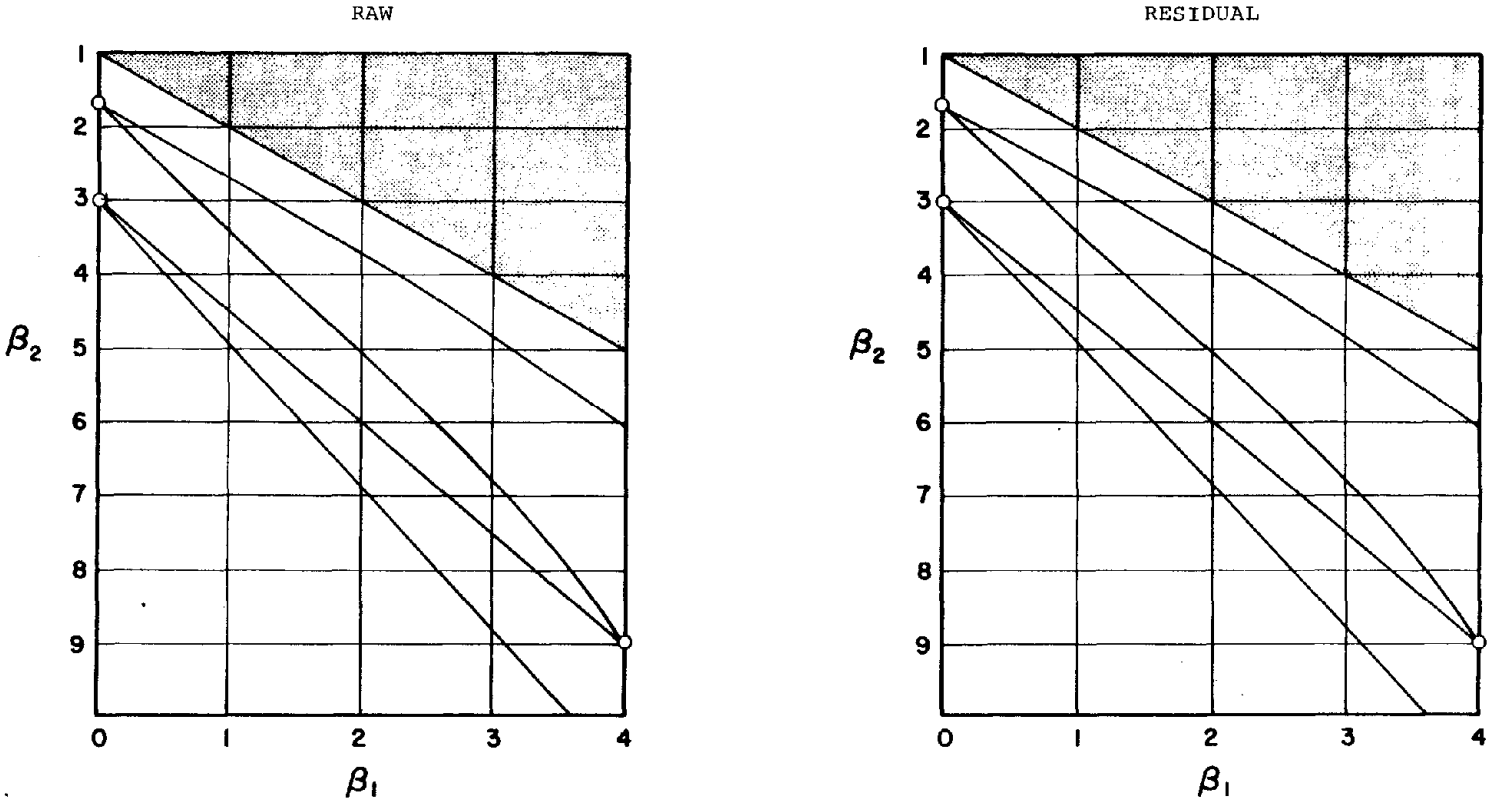

Figure 8.35 - Pearson diagrams of raw and residual friction angle data for Japanese copper

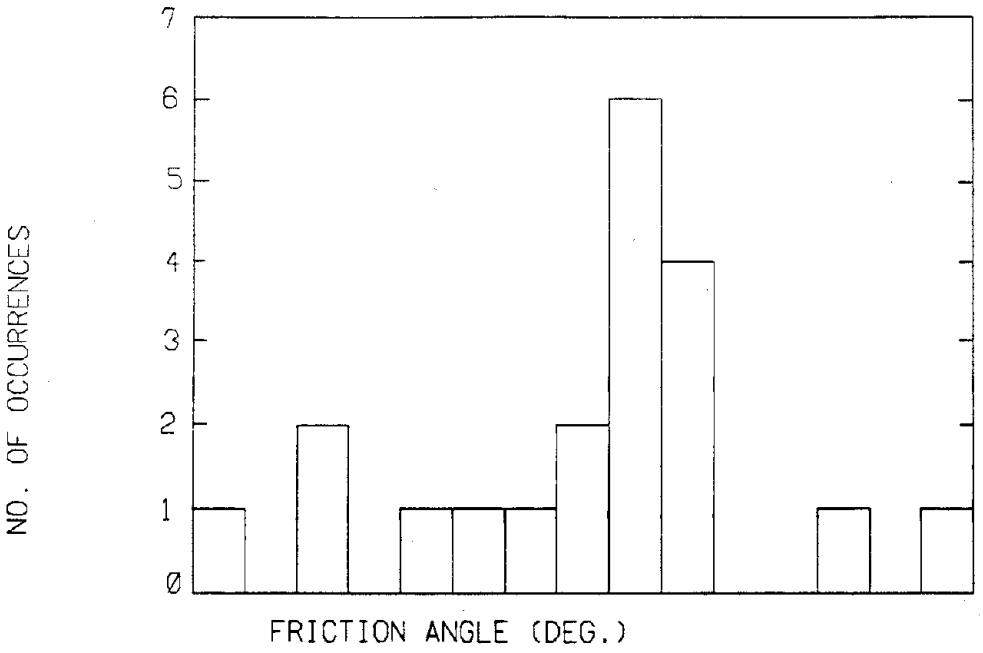

Figure 8.36 - Histogram of Japanese copper friction angle data

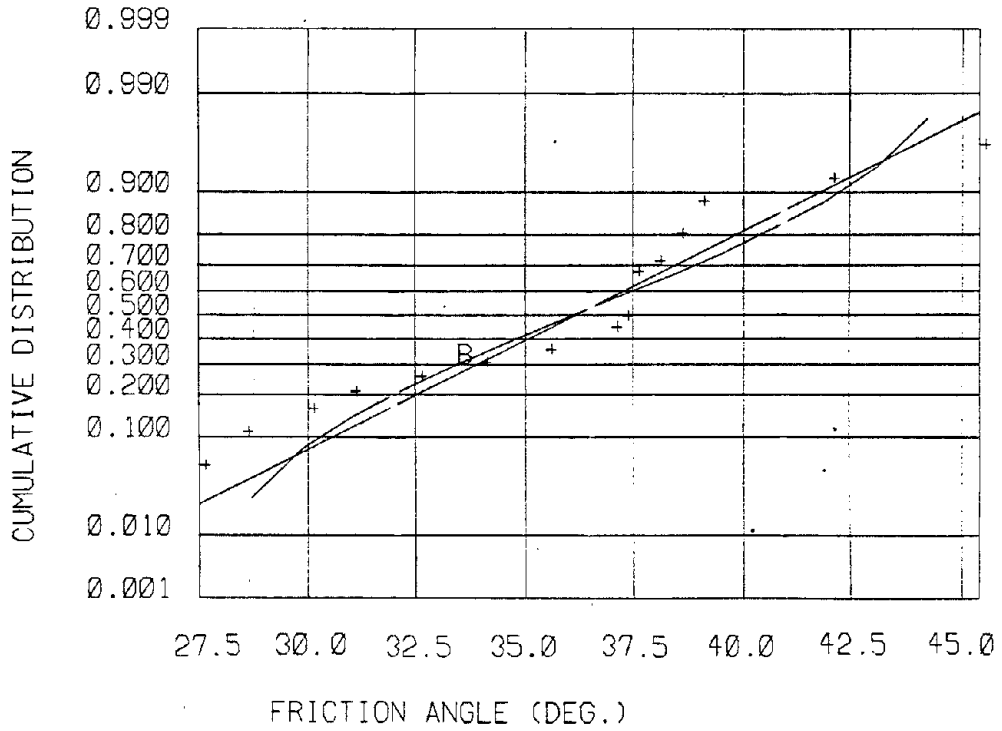

Figure 8.37 - CDF of Japanese Copper friction angle data compared to standard CDF plots

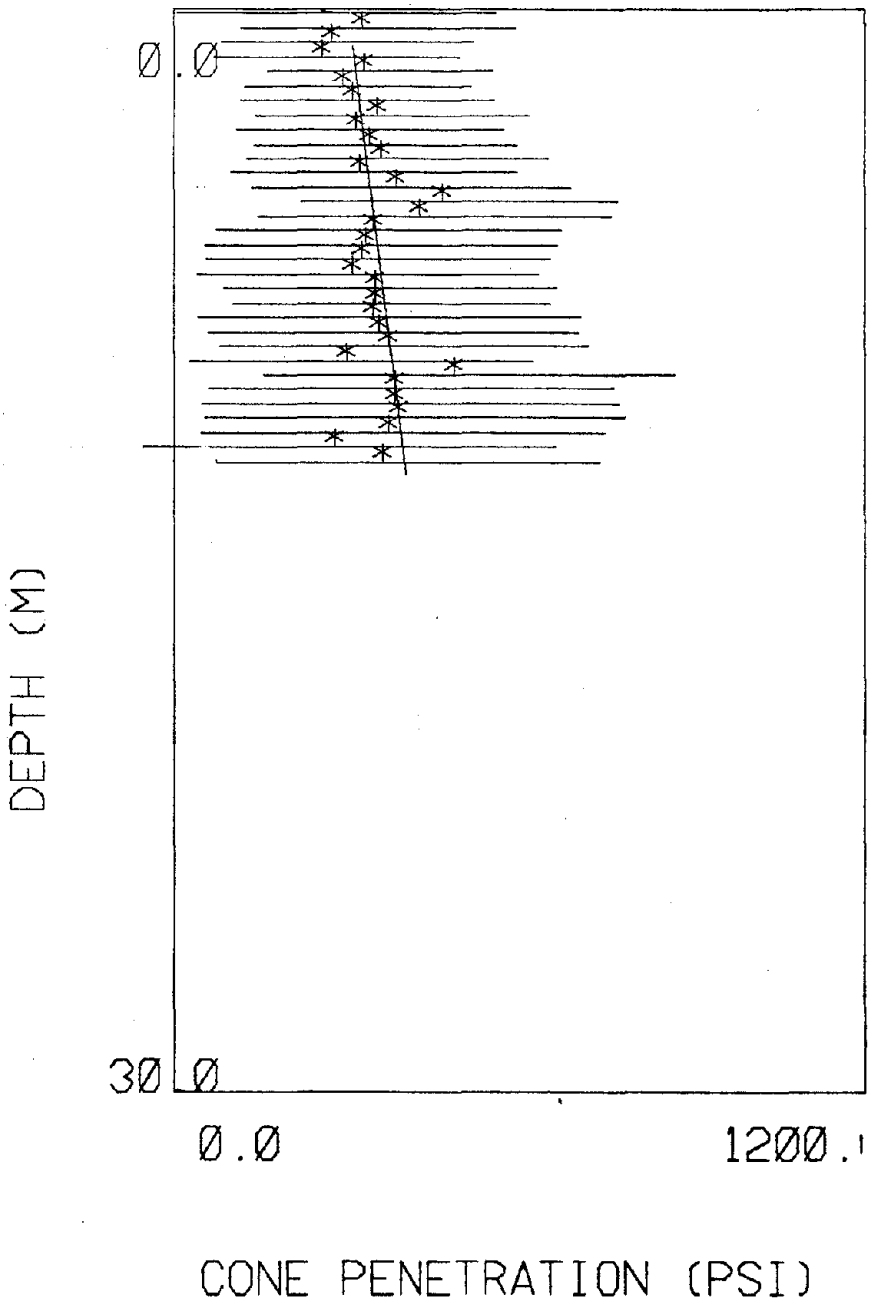

Figure 8.38 - Cone penetration resistance v. depth for Japanese copper

SITE	Japanese Copper all sites	
DATA	Type	Piezocone (drained portion)
	Number	726
	Quality Index	A
TREND WITH DEPTH	q_c(psi) = 302.6 + 7.95z(m)	

DATA SCATTER

	mean	SD	β_1	β_2
Raw Data	360	246	0.14	2.10
Residual Data	--	244	0.03	1.97

GOODNESS OF FIT STATISTICS

	Raw		Residual	
	χ^2	D_m	χ^2	D_m
normal	117.6	0.08	117.6	0.09
beta	86.5	0.05	148.6	0.09
exponential	247.2	0.14	--	--
lognormal	2213.8	0.17	--	--
gamma	372.8	0.12	--	--
5% confidence limit	23.7	0.050	--	--

INTERPRETED STRENGTH PARAMETERS I

Table 8.9 - Table of Japanese copper piezocone resistance data (drained portion)

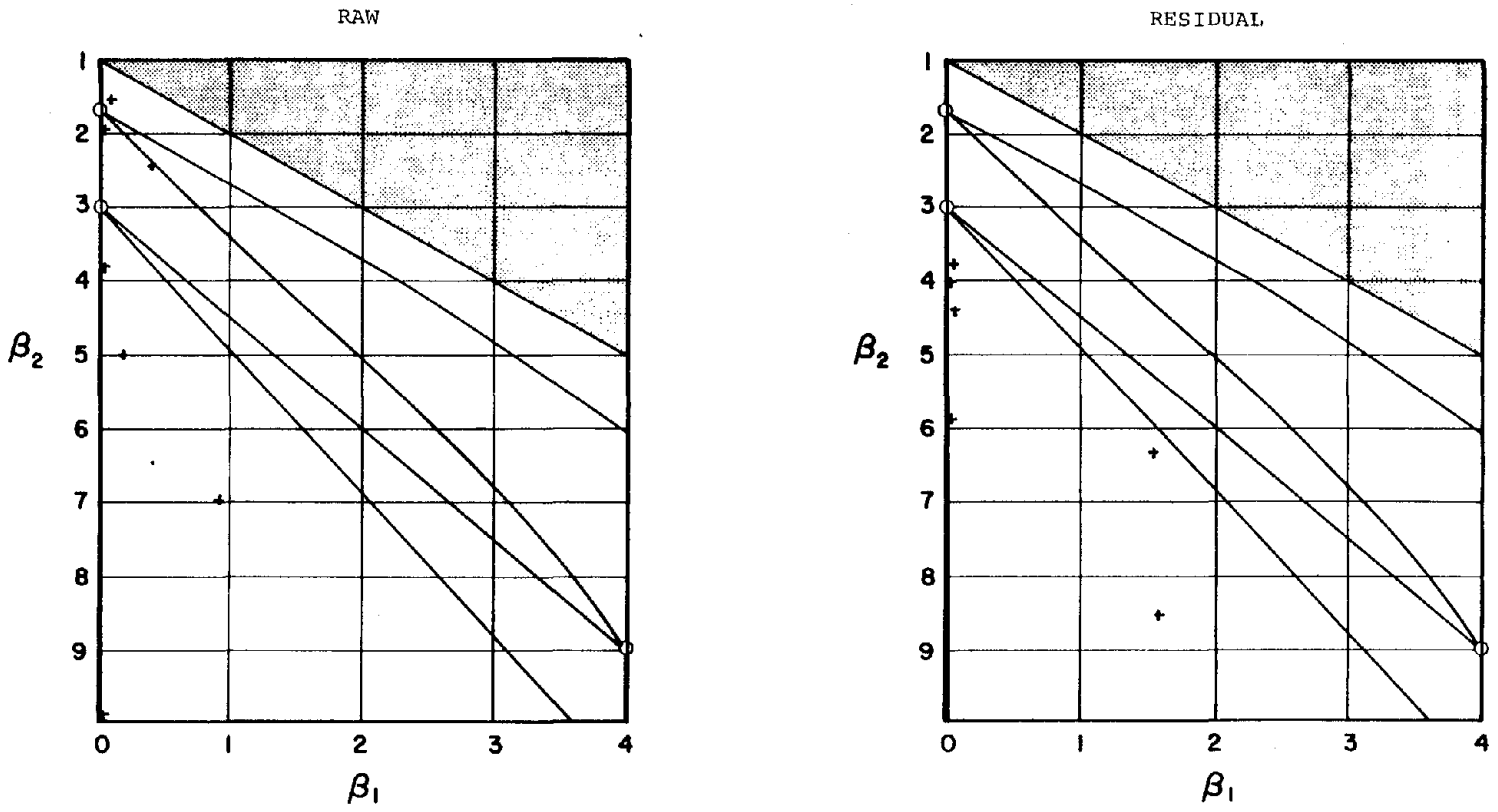

Figure 8.39 - Pearson diagrams of raw and residual piezocone data (drained portion) for Japanese copper

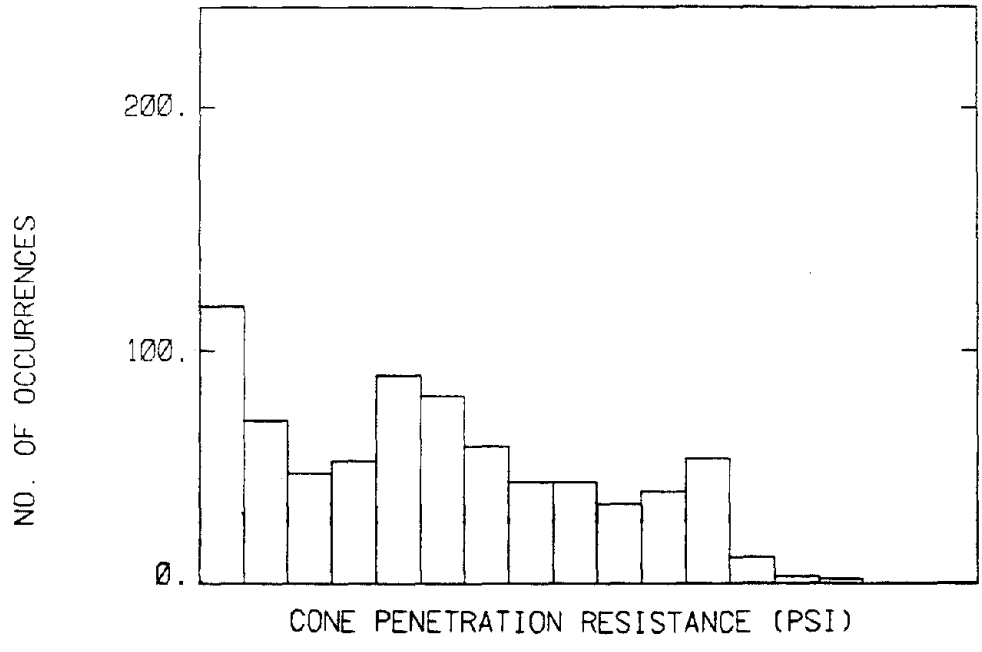

Figure 8.40 - Histogram of Japanese copper drained piezocone raw data

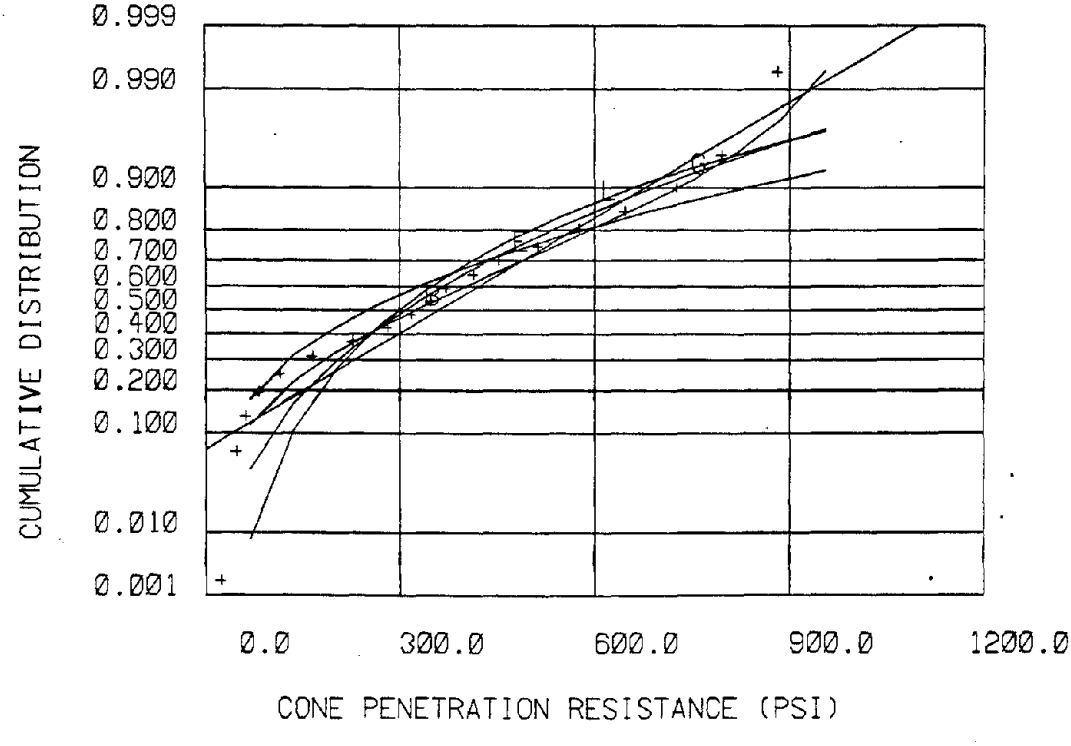

Figure 8.41 - CDF of Japanese copper drained piezocone raw data compared to standard CDF plots

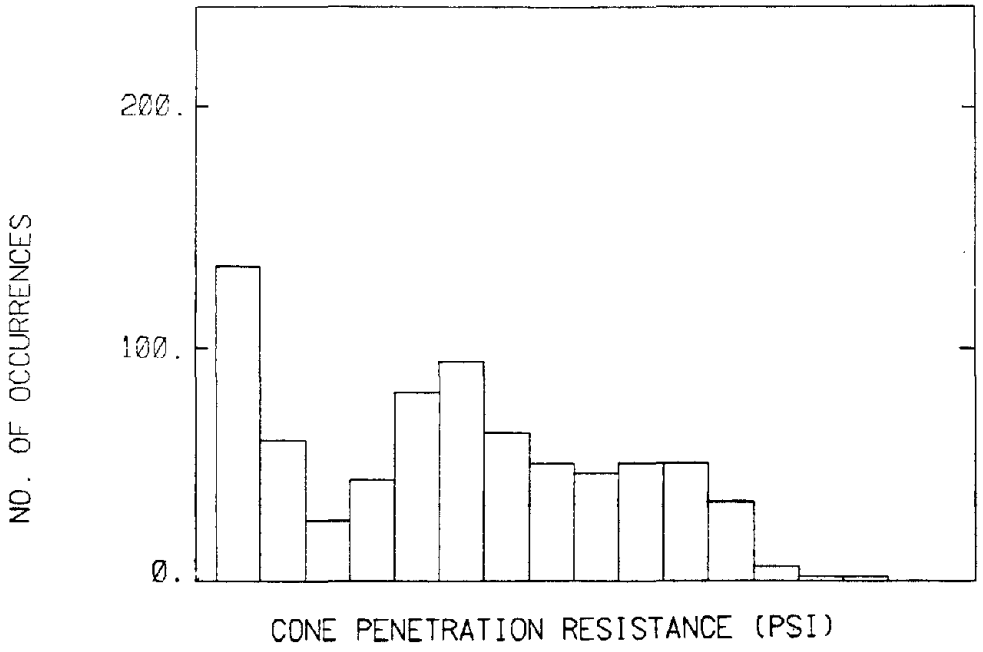

Figure 8.42 - Histogram of Japanese copper drained piezocone residual data

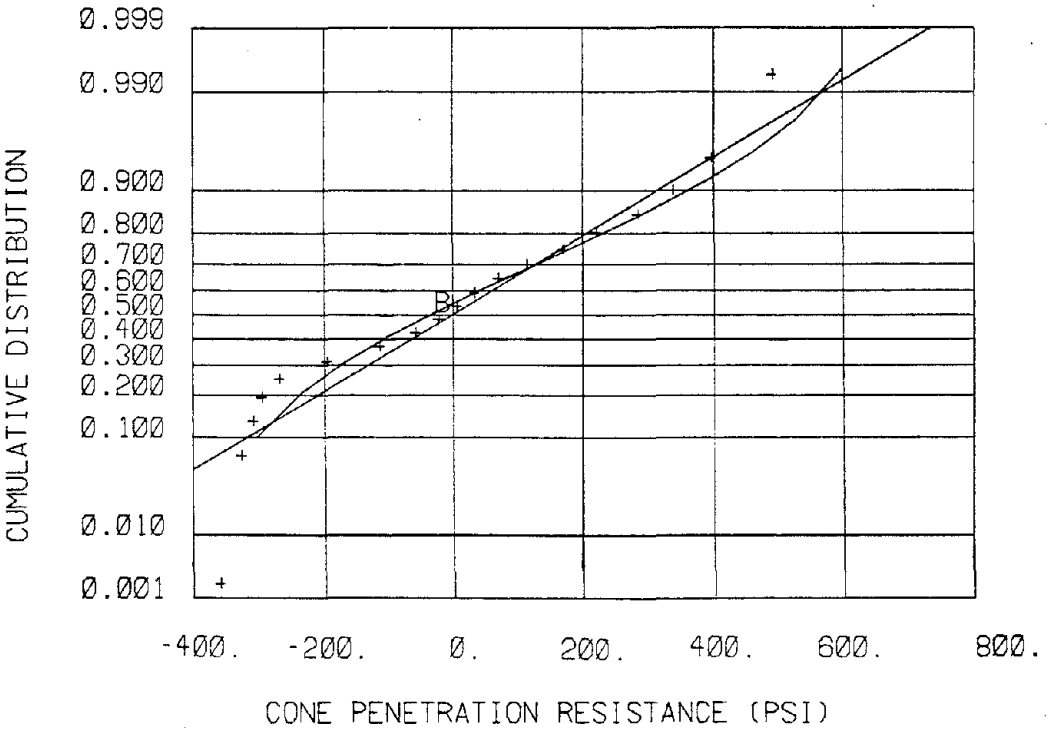

Figure 8.43 - CDF of Japanese copper drained piezocone residual data compared to standard CDF plots

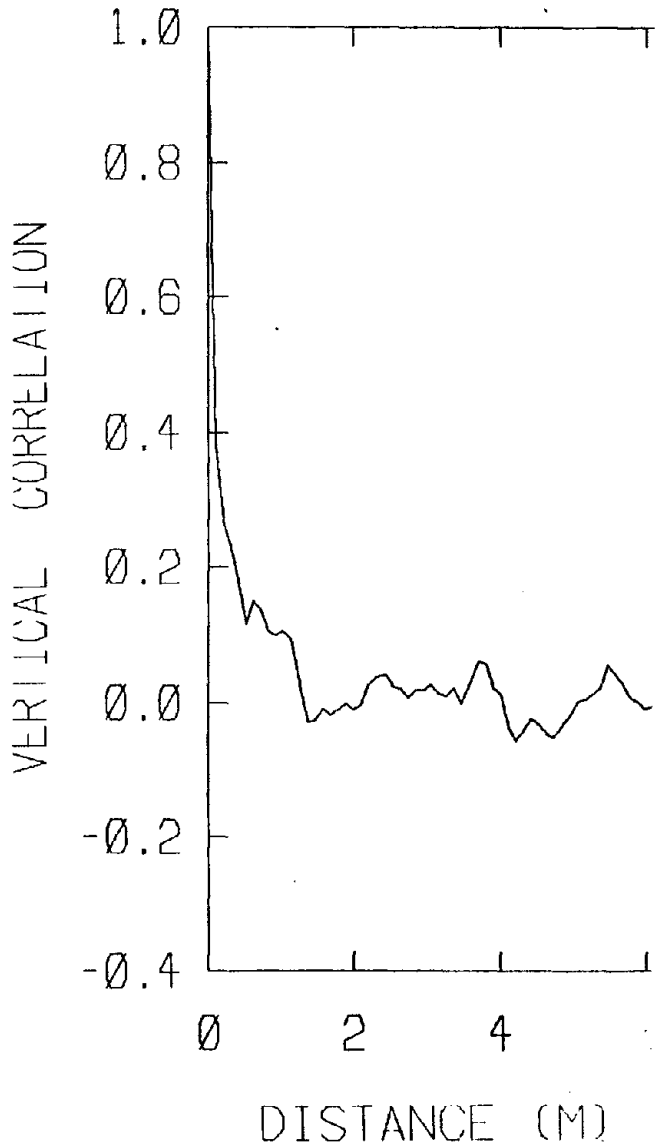

Figure 8.44 - Vertical correlation for residual Japanese copper piezocone data

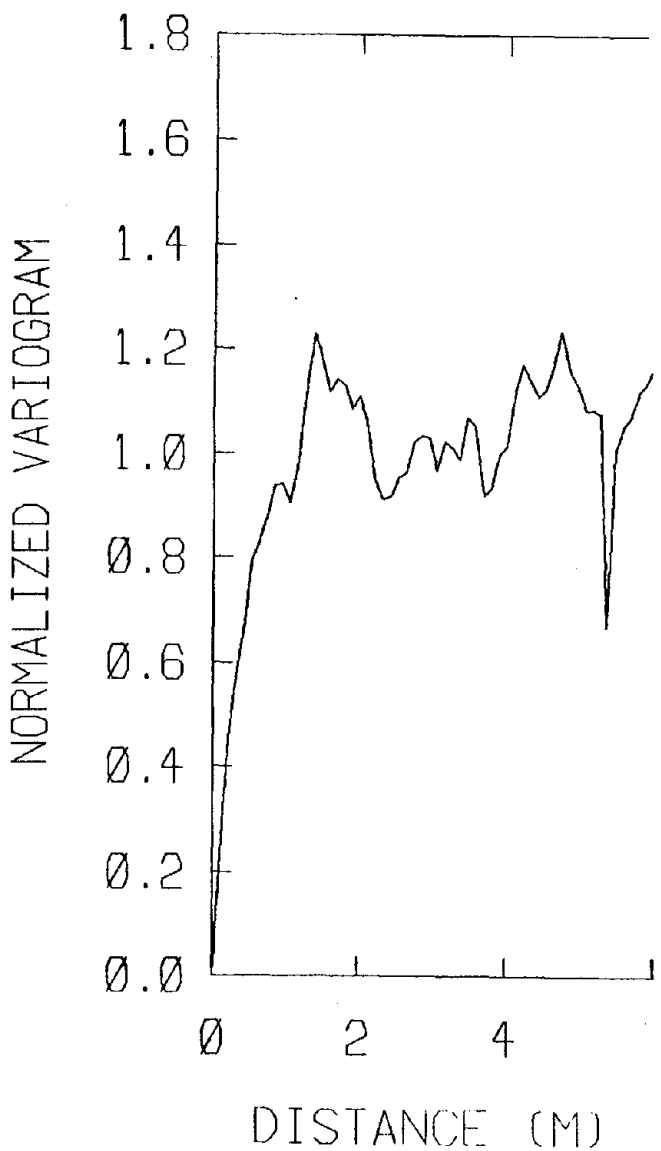

Figure 8.45 - Normalized variogram residual Japanese piezocone data

SITE Magna (Copper)

DATA Type: Cone penetration (3 individual holes)
Number: 378
Quality Index: A

TREND WITH DEPTH $q_c(psi) = -37.6 + 22.1 \cdot z(m)$

DATA SCATTER

	mean	SD	β_1	β_2
Raw Data	445.8	352.4	0.881	3.22
Residual Data	--	253.9	0.282	2.82

GOODNESS OF FIT STATISTICS

	Raw		Residual	
	χ^2	D_m	χ^2	D_m
normal	80.3	0.102	44.2	0.071
beta	19.7	0.045	31.9	0.050
exponential	33.9	0.051	--	--
lognormal	179.4	0.128	--	--
gamma	25.8	0.054	--	--
5% confidence limit	23.7	0.07	--	--

INTERPRETED STRENGTH PARAMETERS I

Table 8.10 - Table of Magna copper cone penetration resistance data

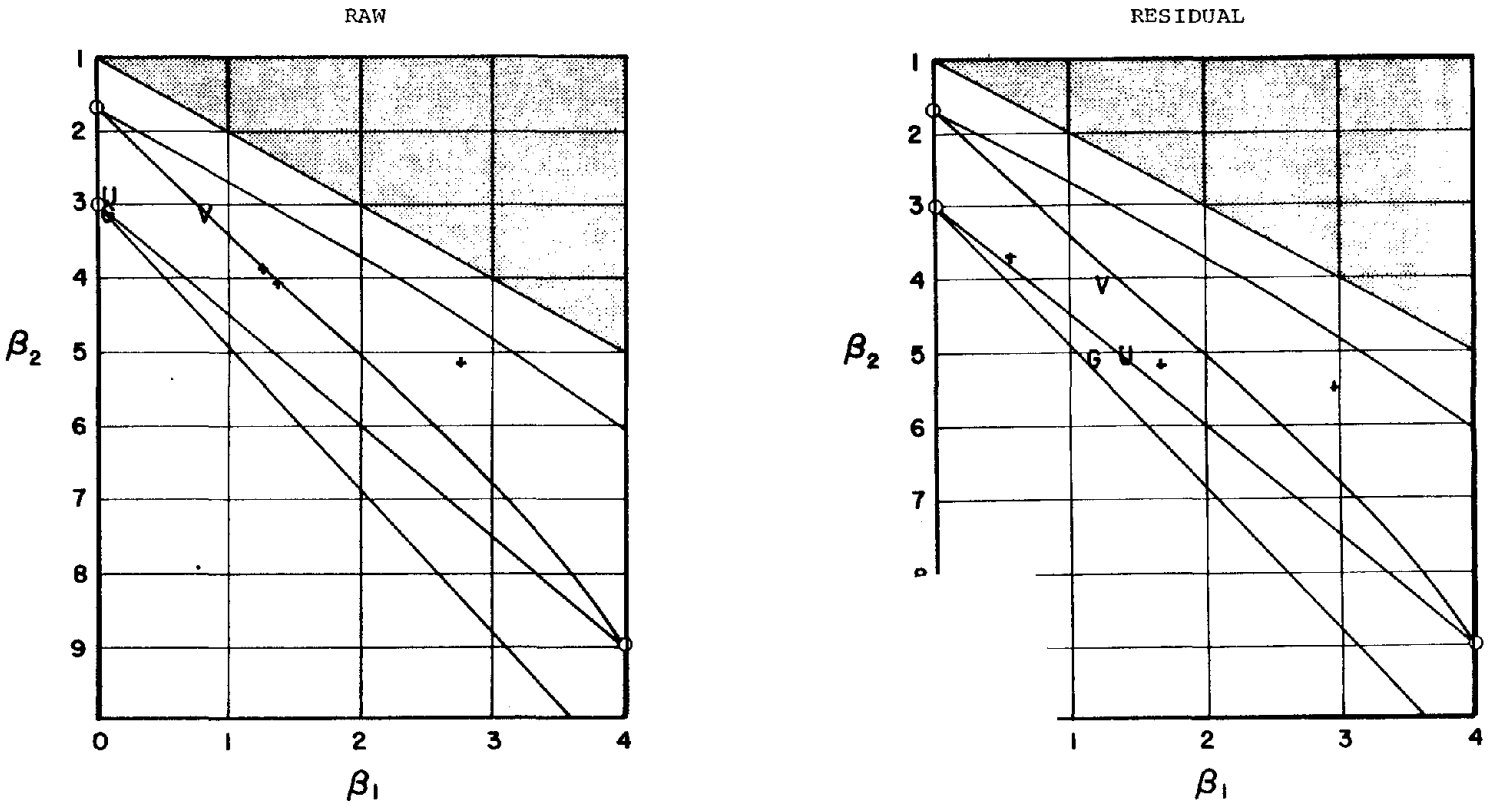

Figure 8.46 - Pearson diagrams of raw and residual cone penetration resistance data for Magna copper

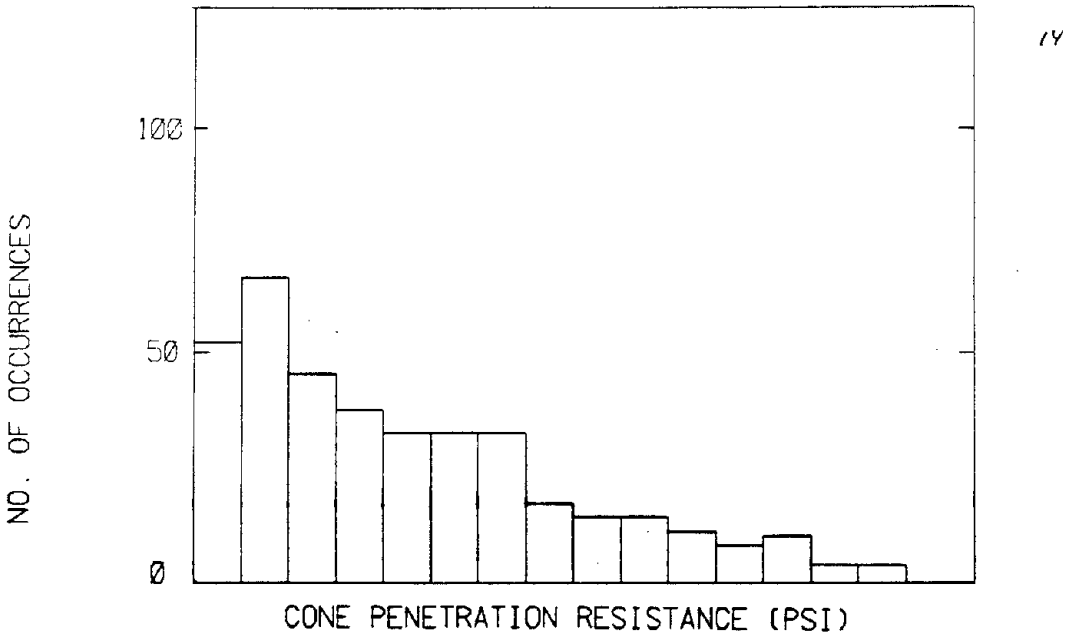

Figure 8.47 - Histogram of Magna copper raw cone penetration resistance data

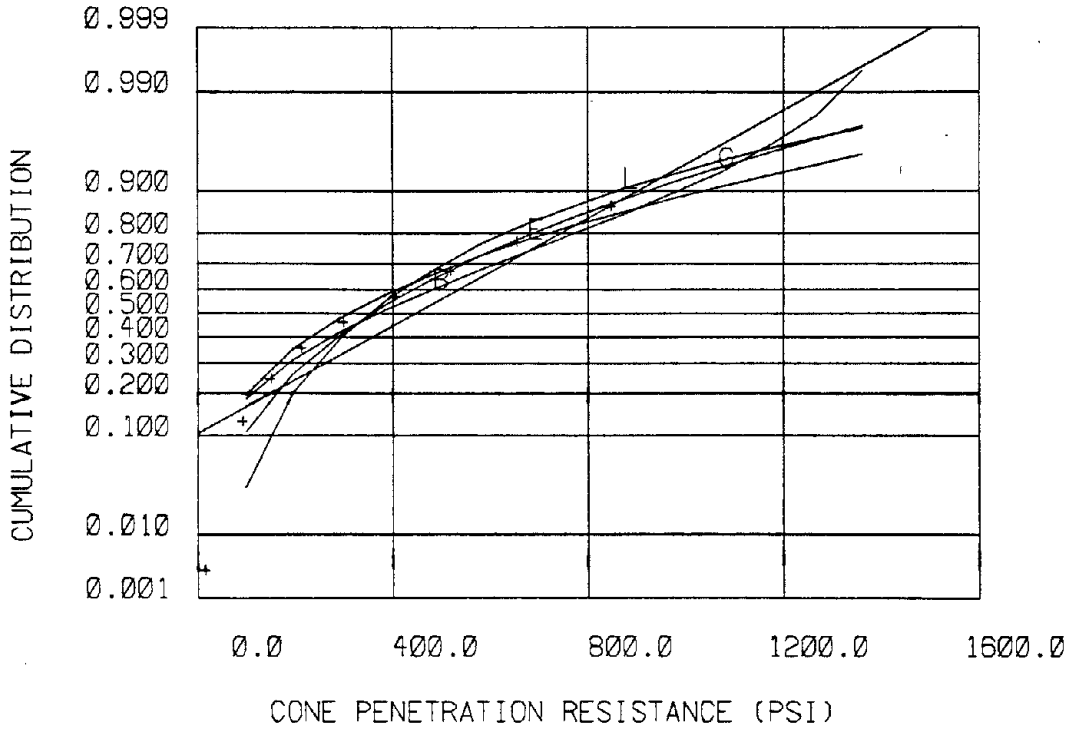

Figure 8.48 - CDF of Magna copper raw cone penetration resistance compared to standard CDF plots

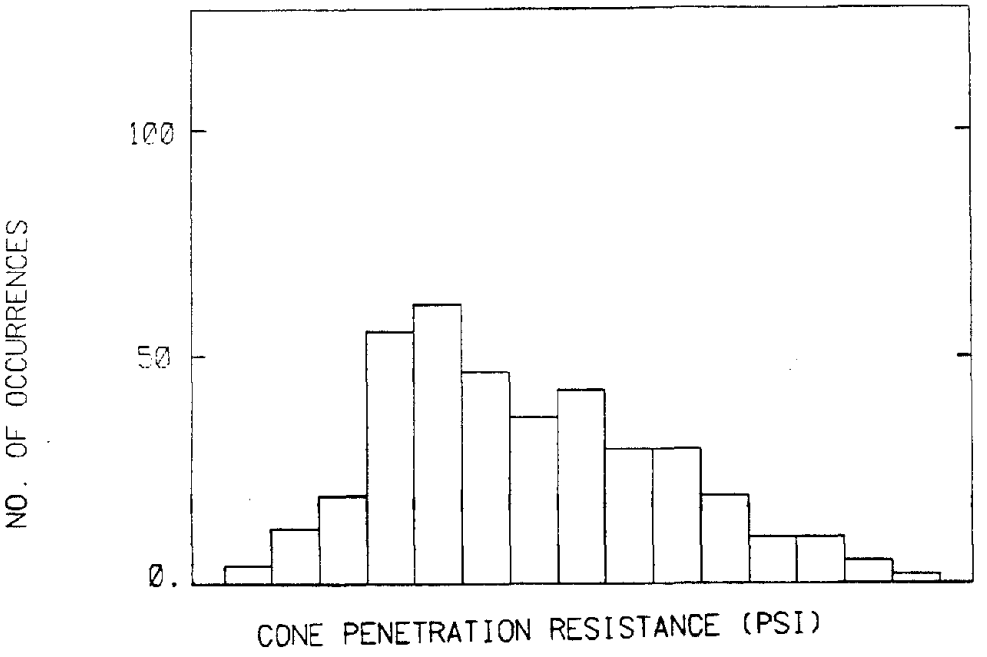

Figure 8.49 - Histogram of Magna copper residual cone penetration resistance data compared to standard CDF plots

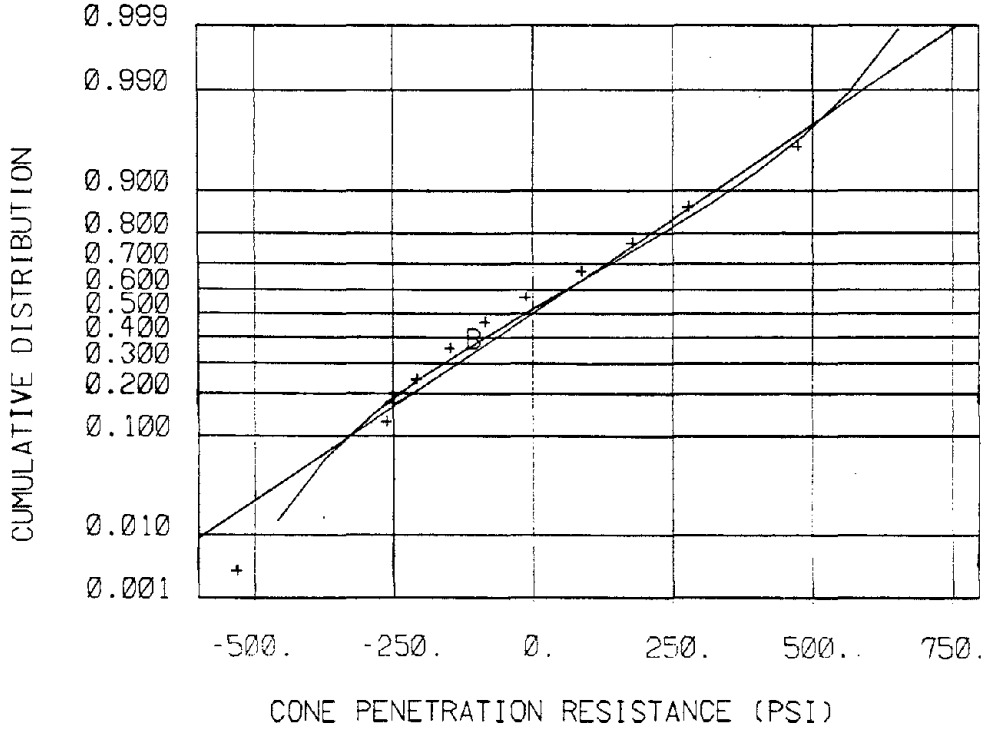

Figure 8.50 - CDF of Magna copper residual cone penetration resistance data compared to standard CDF plots

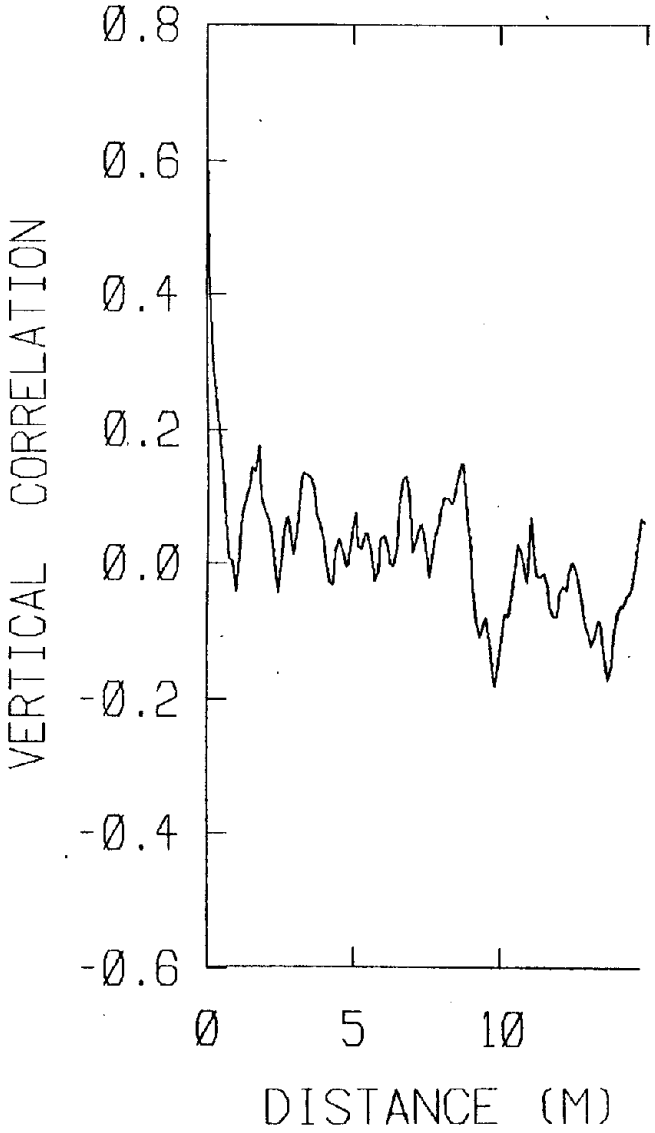

Figure 8.51 - Vertical correlation for residual magna copper cone penetration resistance data

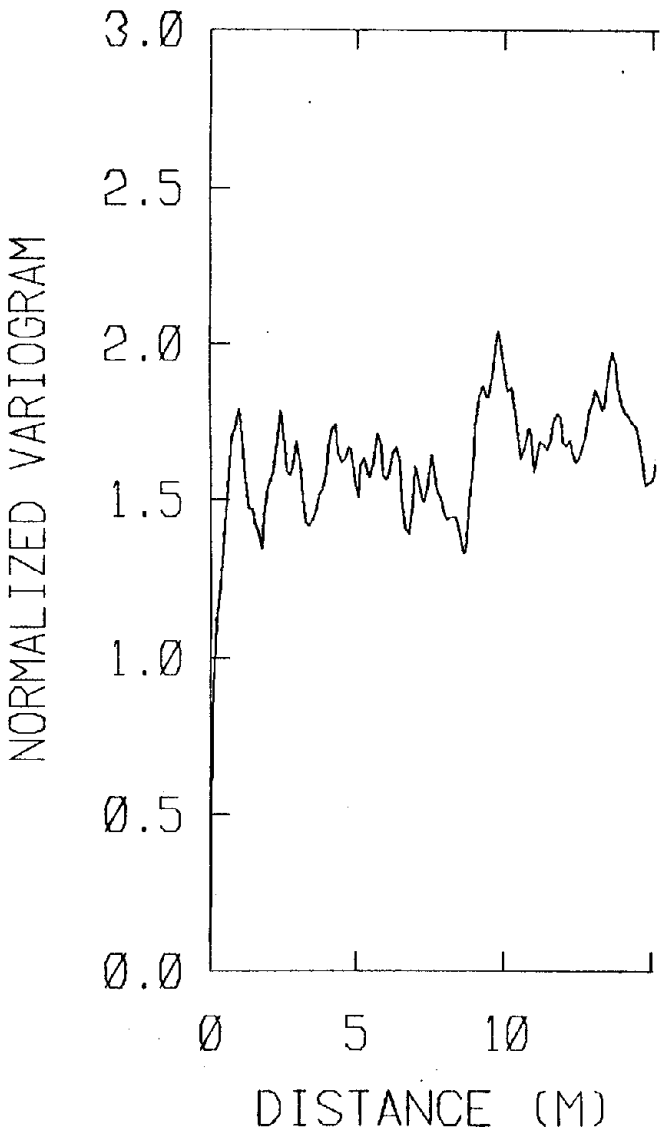

Figure 8.52 - Normal variogram for residual Magna copper cone penetration resistance data

SITE	Magna (Copper)	
DATA	Type	Water Contents (2 borings)
	Number	74
	Quality Index	NA
TREND WITH DEPTH	w/c(%) = 43.9 - 0.27z(m)	

DATA SCATTER

	mean	SD	β_1	β_2
Raw Data	39.3	8.04	0.129	2.97
Residual Data	--	7.5	1.45	5.14

GOODNESS OF FIT STATISTICS

	Raw		Residual	
	χ^2	D_m	χ^2	D_m
normal	14.4	0.088	31.4	0.119
beta	15.7	0.067	25.4	0.113
exponential	269	0.440	--	--
lognormal	24.2	0.119	--	--
gamma	18.3	0.106	--	--
5% confidence limit	23.7	0.158	--	--

INTERPRETED STRENGTH PARAMETERS NA

Table 8.11 - Table of Magna copper water content data

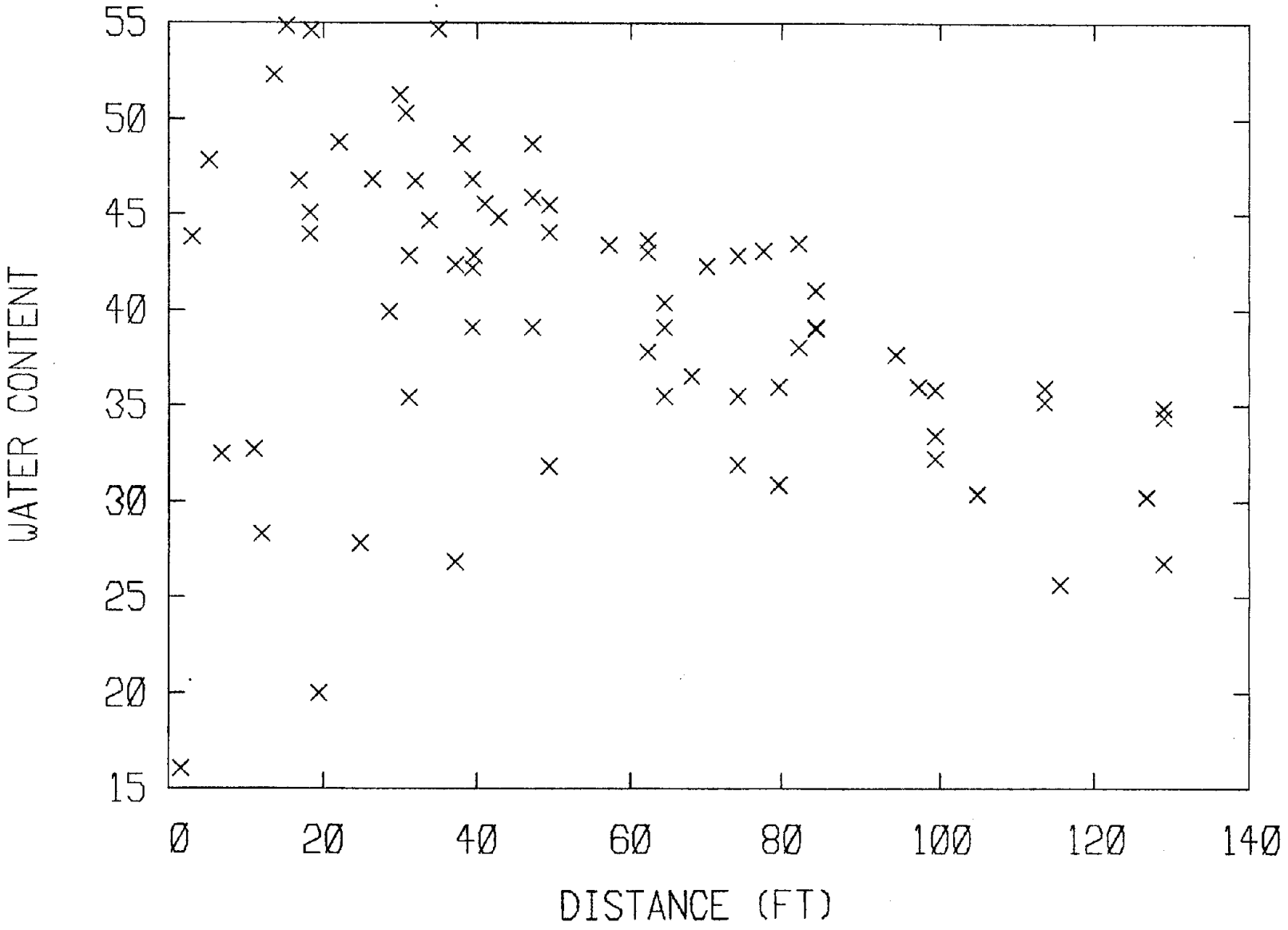

Figure 8.53 - Water content v. depth for Magna copper

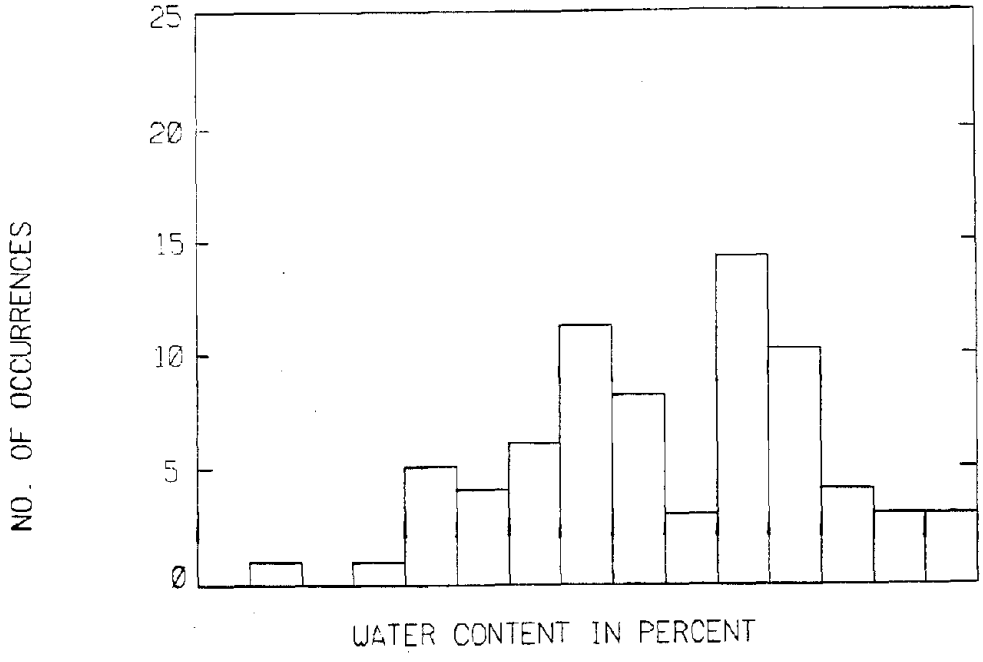

Figure 8.54 - Histogram of raw Magna copper water content data

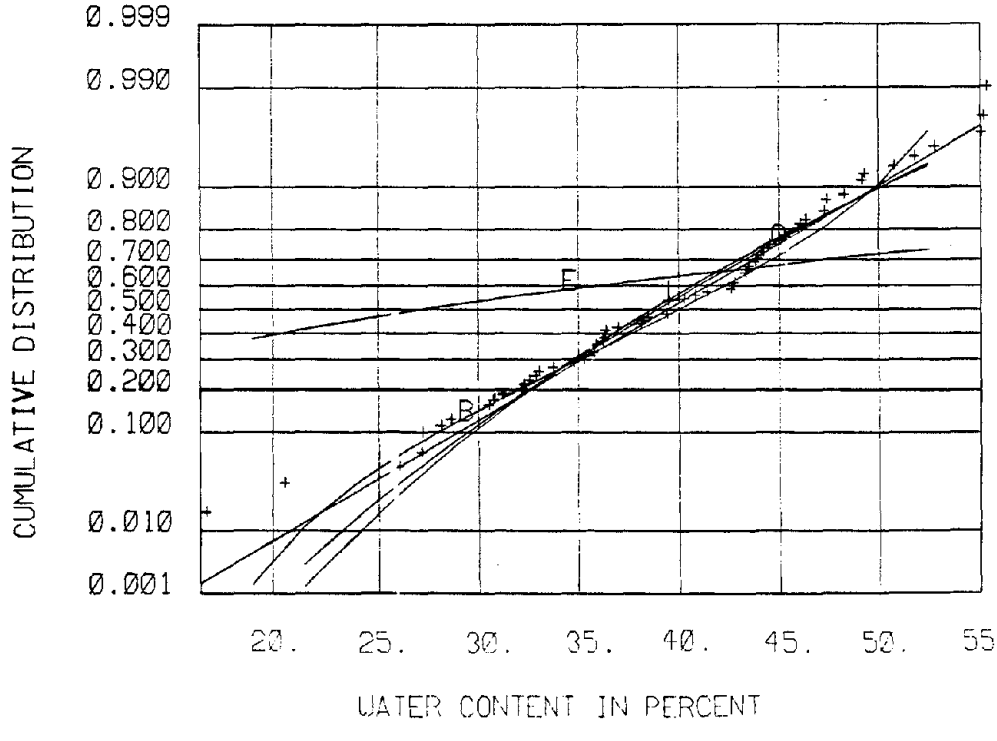

Figure 8.55 - CDF of raw Magna copper water content compared to standard CDF plots

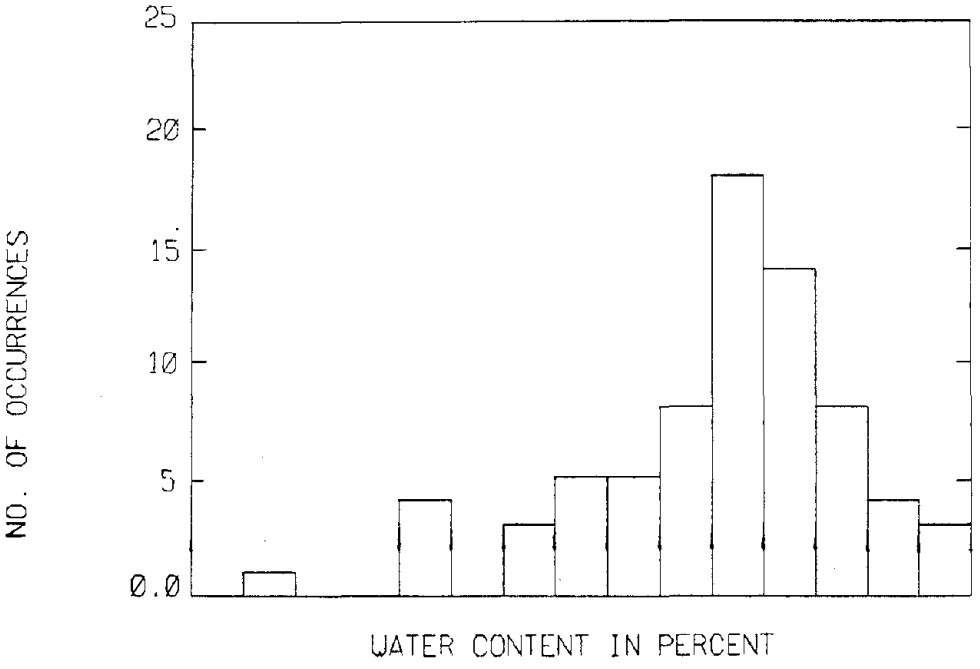

Figure 8.56- Histogram of residual Magna copper water content

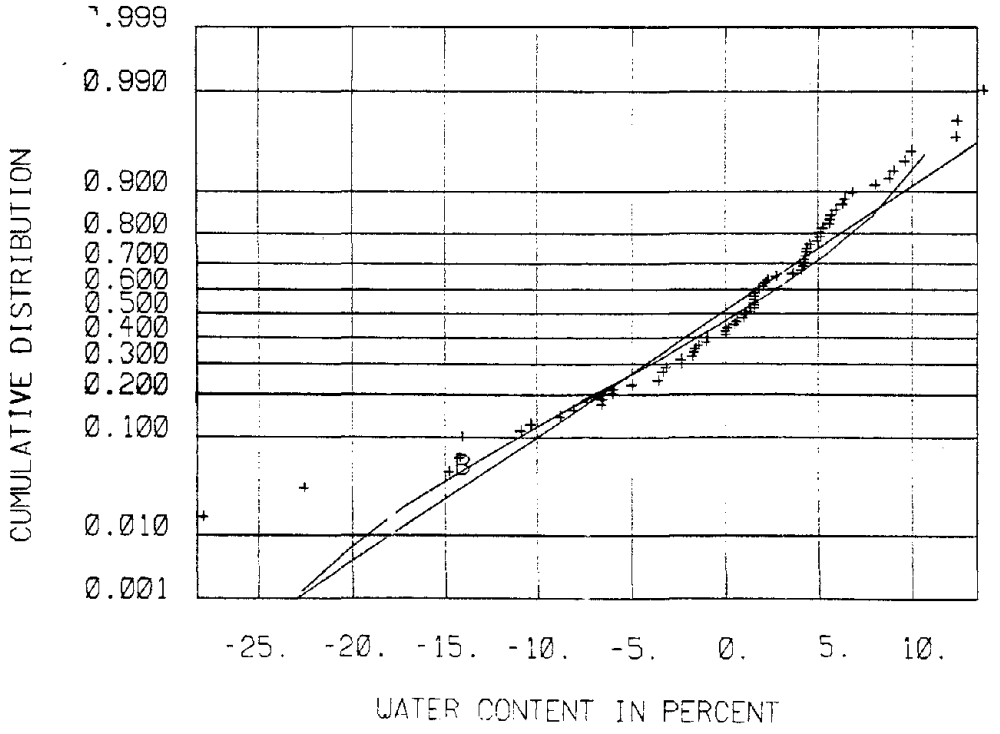

Figure 8.57 - CDF of residual Magna copper water content data compared to standard CDF plots

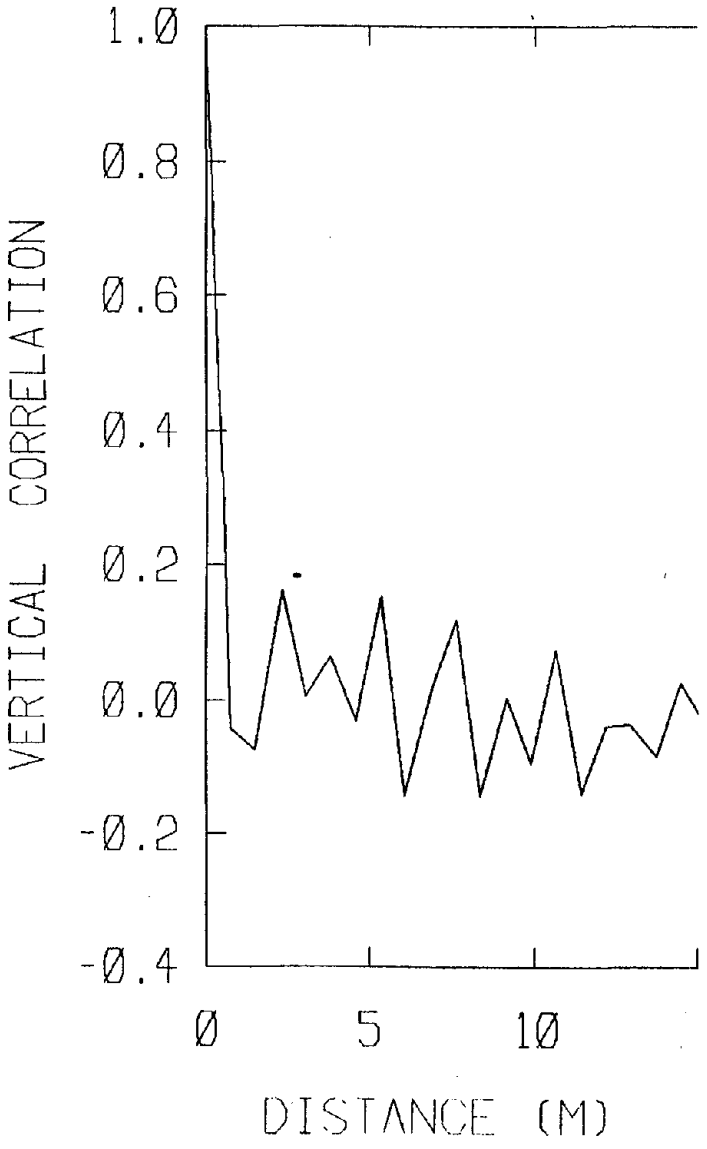

Figure 8.58 - Vertical correlation residual Magna copper water content data

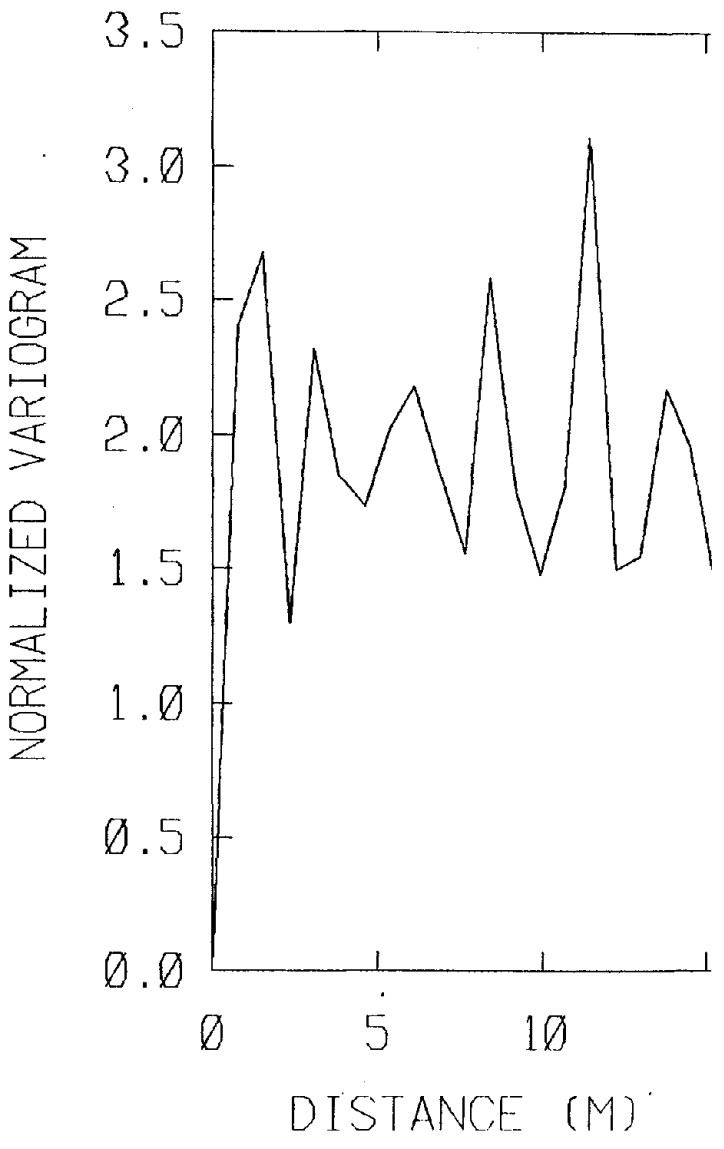

Figure 8.59 - Normalized variogram residual Magna copper water content data

SITE Magna (Copper)

DATA Type Field Vane

Number 80

Quality Index NA

TREND WITH DEPTH S_u(psf) = 188 + 25z(ft)

DATA SCATTER

	mean	SD	β_1	β_2
Raw Data	999	609	0.85	3.24
Residual Data	--	431	1.27	4.17

GOODNESS OF FIT STATISTICS

	Raw		Residual	
	χ^2	D_m	χ^2	D_m
normal	45.0	0.136	34.6	0.127
beta	35.4	0.09	27.7	0.117
exponential	48.8	0.227	--	--
lognormal	24.8	0.088	--	--
gamma	21.4	0.07	--	--
5% confidence limit	23.6	0.152	--	--

INTERPRETED STRENGTH PARAMETERS NA

Table 8.12 - Table of Magna copper field vane data

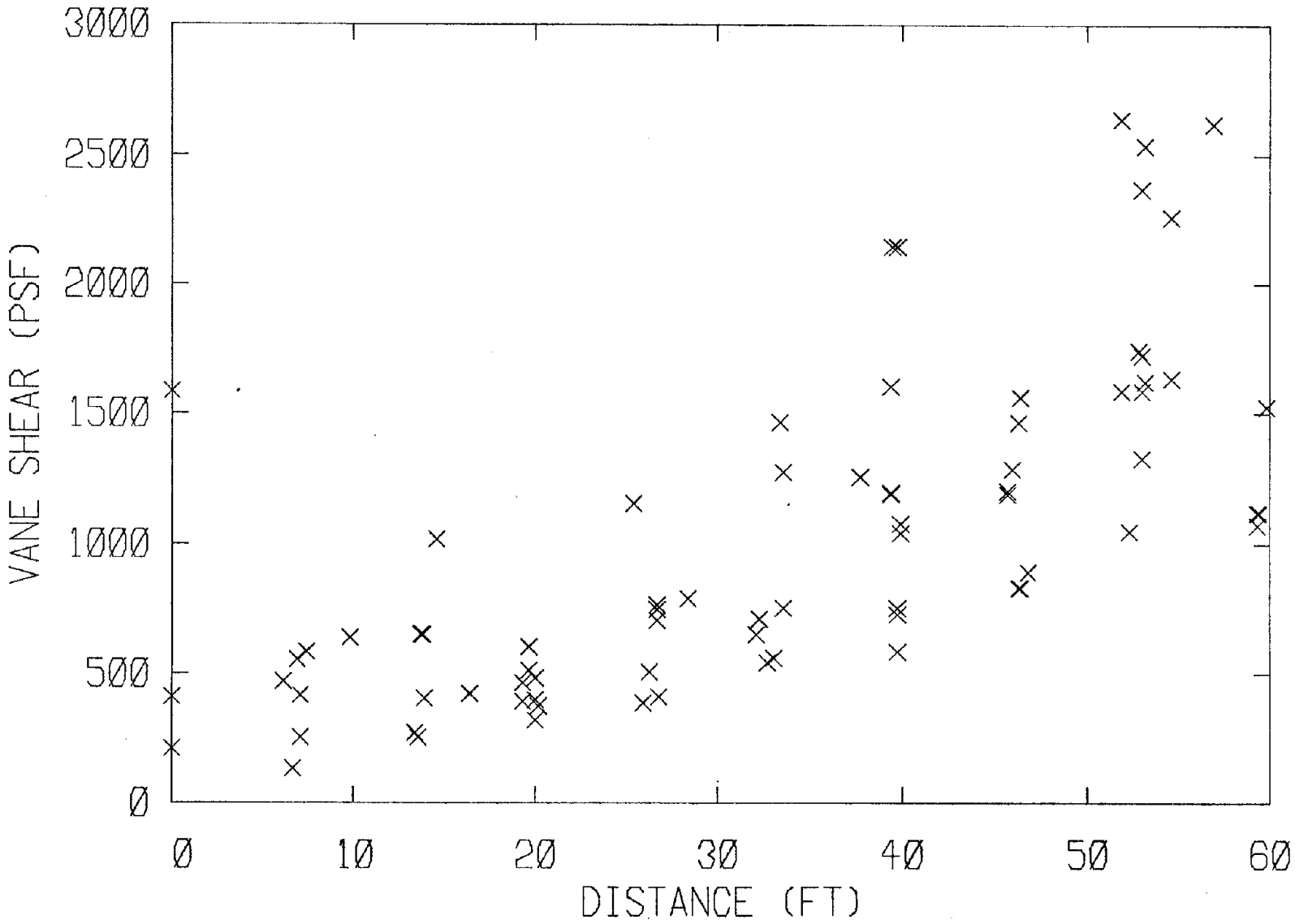

Figure 8.60 - Vane shear v. depth for Magna copper field vane data

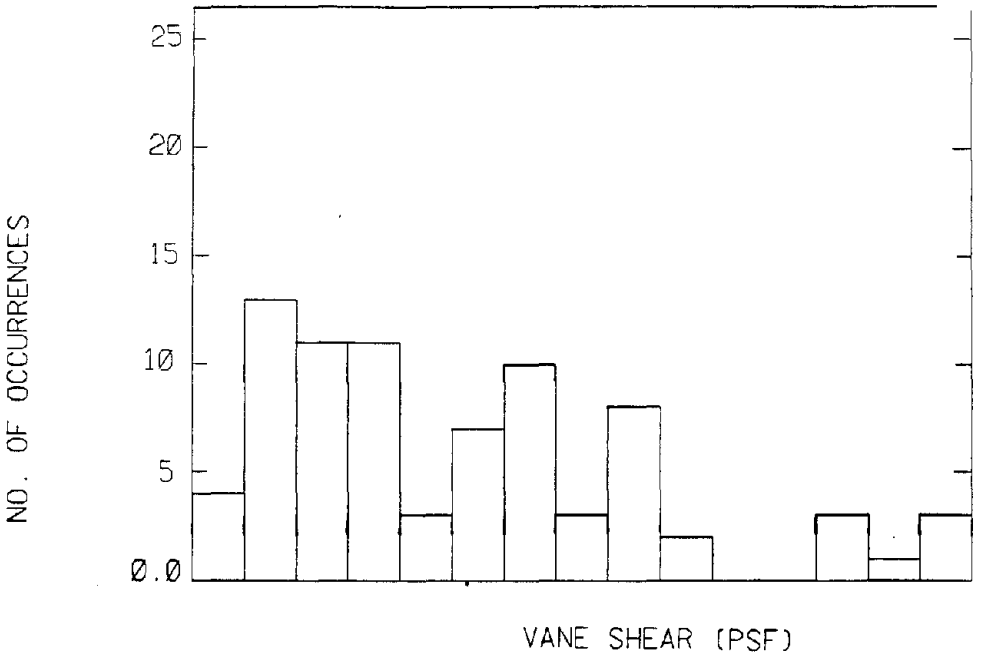

Figure 8.61 - Histogram of raw Magna copper field vane data

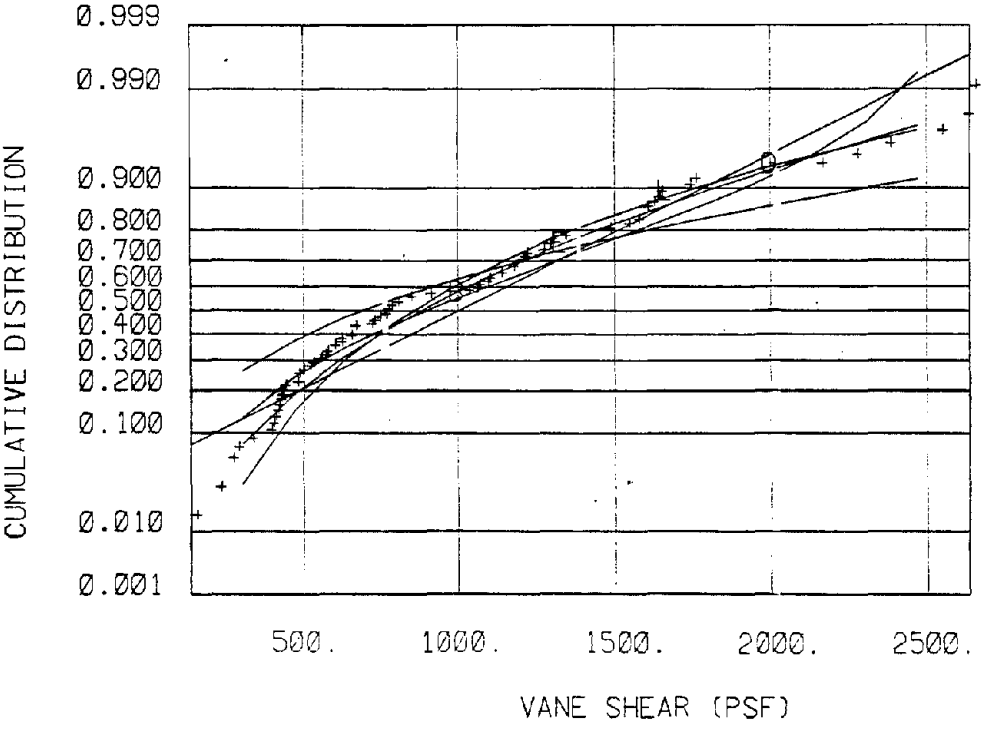

Figure 8.62 - CDF of raw Magna copper field vane data compared to standard CDF plots

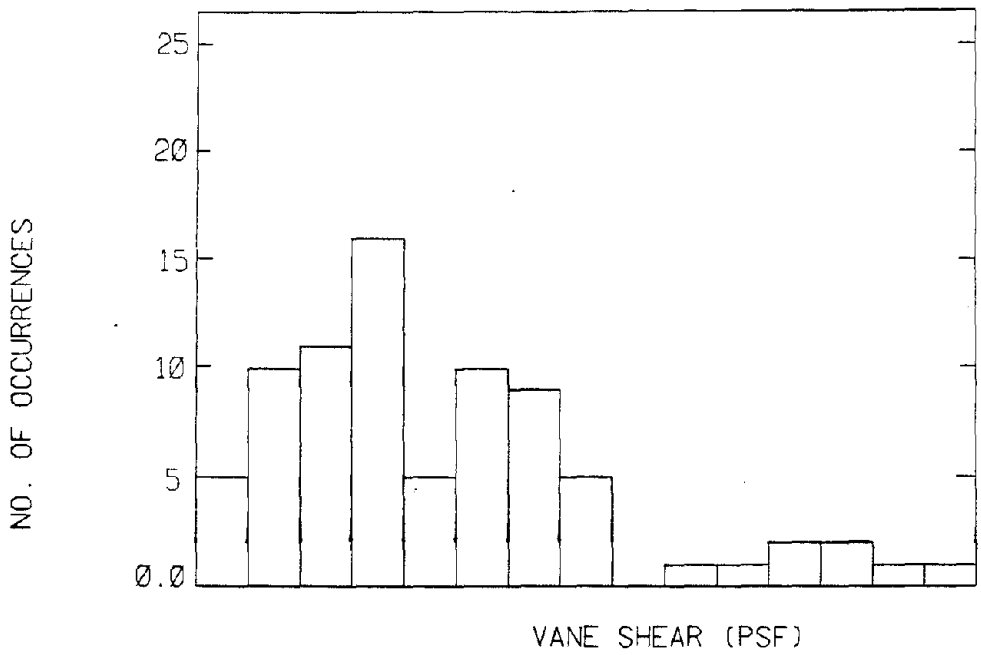

Figure 8.63 - Histogram of residual Magna copper field vane data

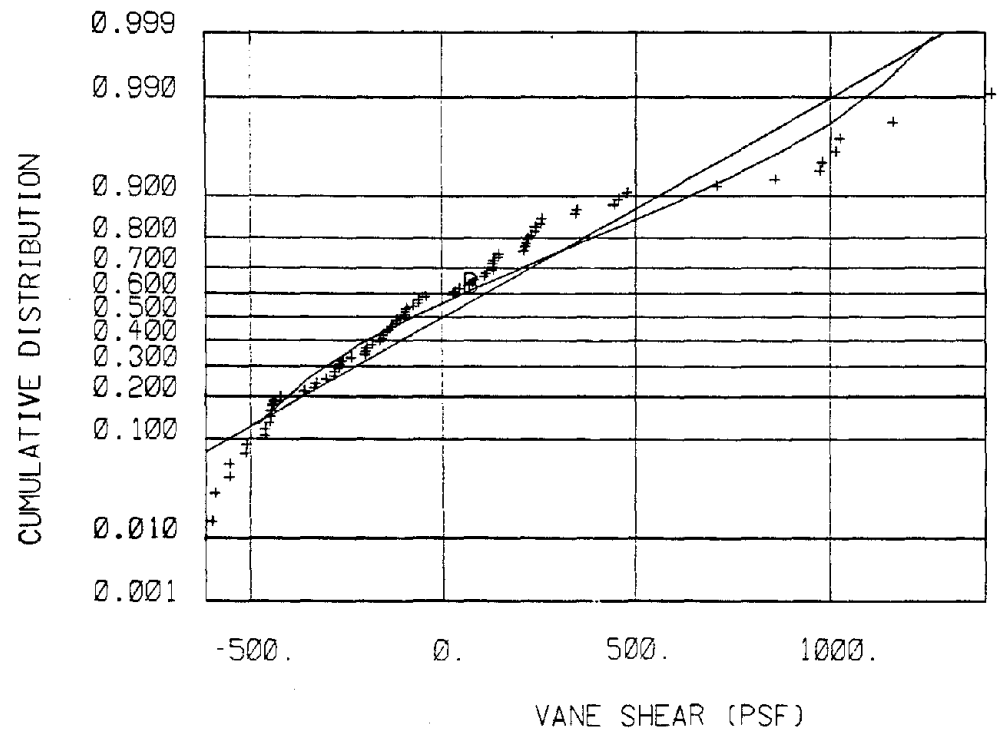

Figure 8.64 - CDF of residual Magna copper field vane data compared to standard CDF plots

SITE Magna (Copper)

DATA Type Dry density

Number 154

Quality Index NA

TREND WITH DEPTH γ_d(pcf) = 75.8 + 0.75z(ft)

DATA SCATTER

	mean	SD	β_1	β_2
Raw Data	79.8	7.45	0.117	3.22
Residual Data	--	6.91	1.21	5.19

GOODNESS OF FIT STATISTICS

	Raw		Residual	
	χ^2	D_m	χ^2	D_m
normal	17.2	0.069	162	0.134
beta	112	0.049	3045	0.113
exponential	1154	0.548	--	--
lognormal	10.4	0.052	--	--
gamma	11.7	0.058	--	--
5% confidence limit	23.7	0.11	--	--

INTERPRETED STRENGTH PARAMETERS NA

Table 8.13 - Table of Magna copper dry density data

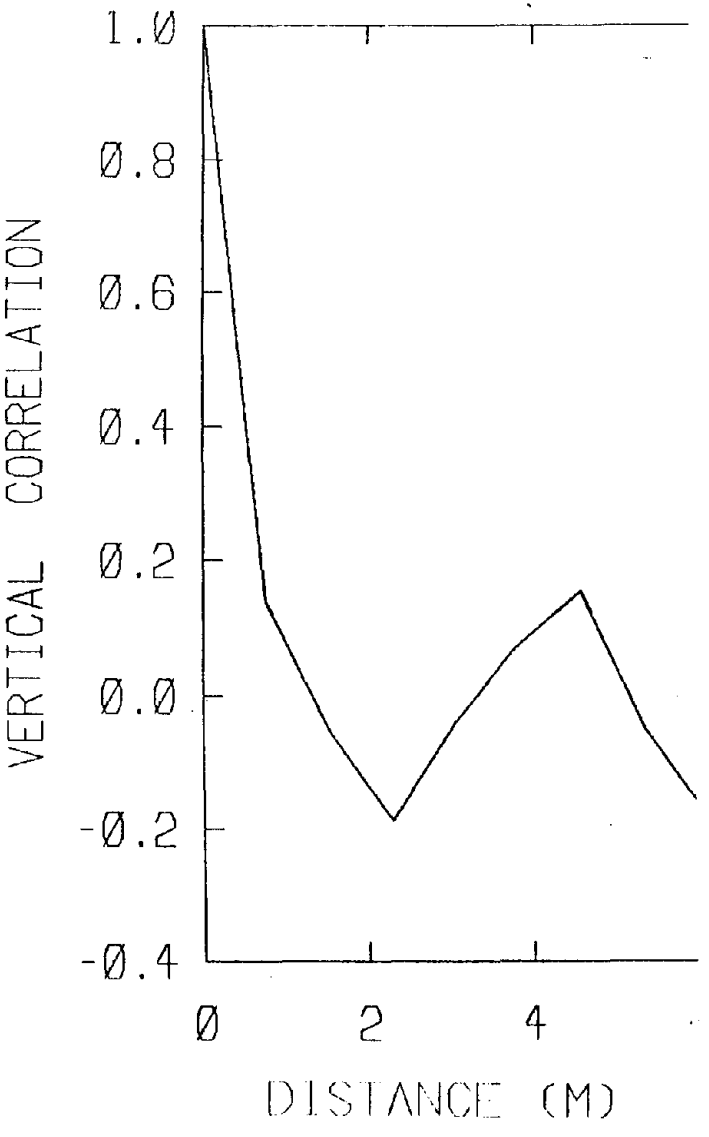

Figure 8.65 - Vertical correlation for raw Magna copper dry density data

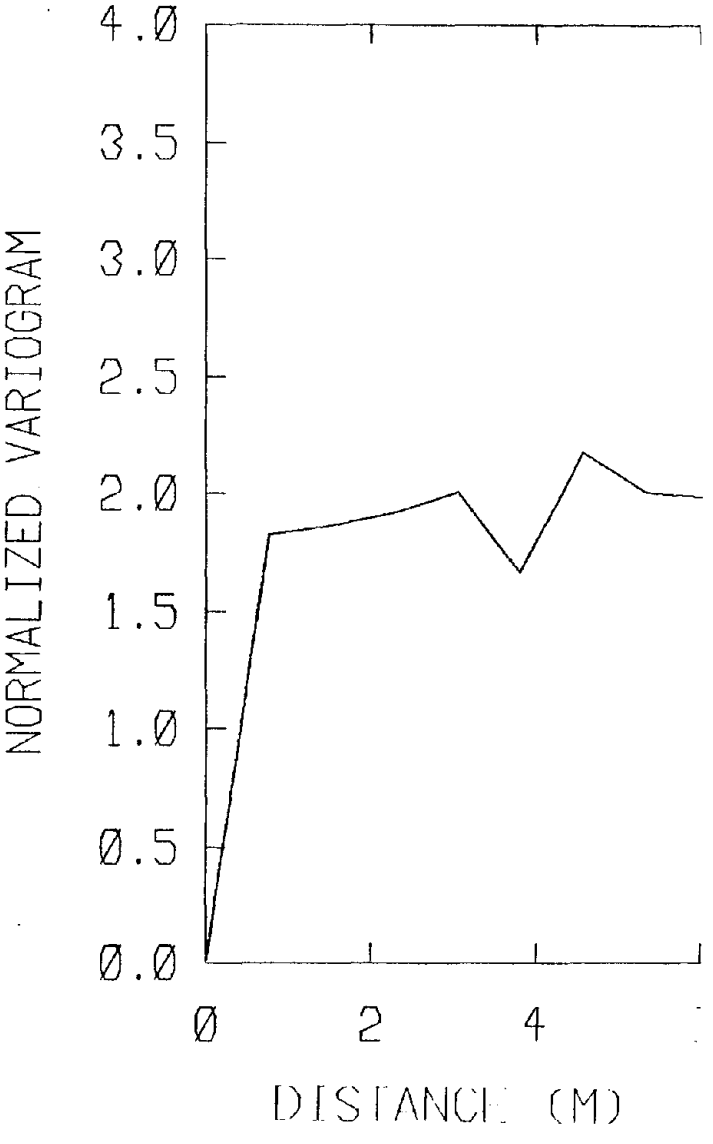

Figure 8.66 - Normalized variogram raw Magna copper dry density data

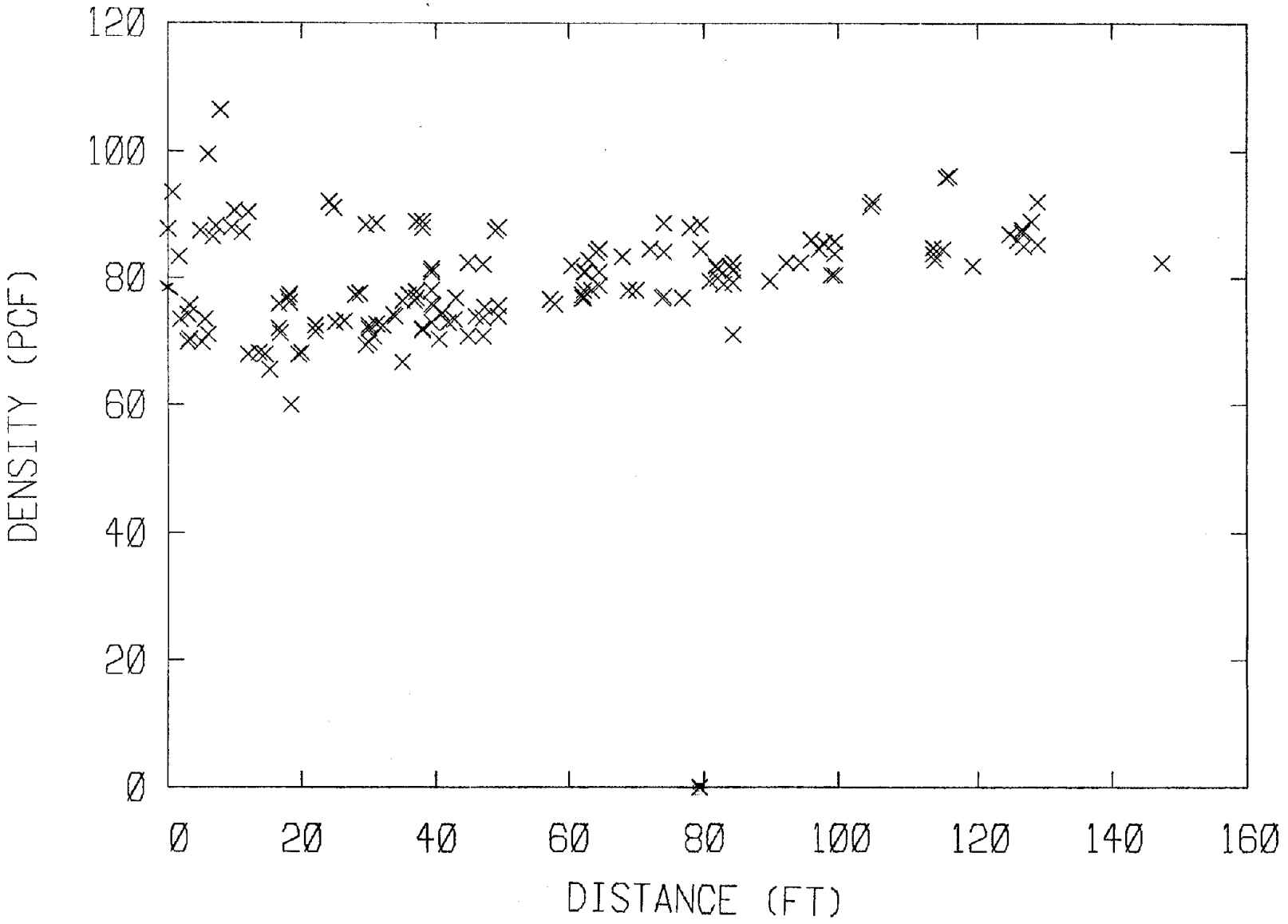

Figure 8.67 - Dry density v. depth for Magna copper

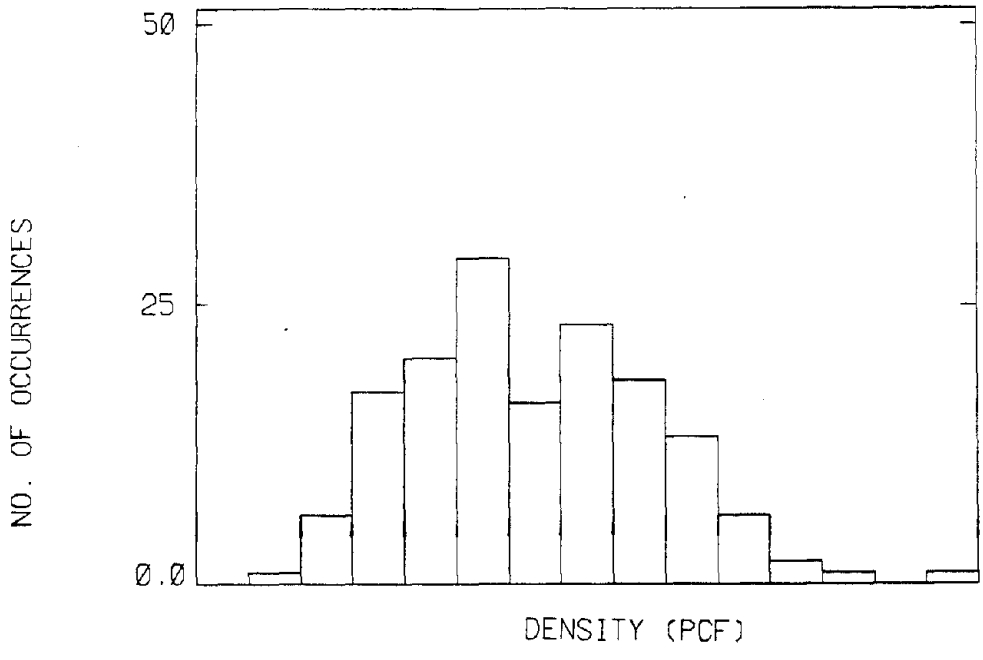

Figure 8.68 - Histogram of raw Magna copper dry density data

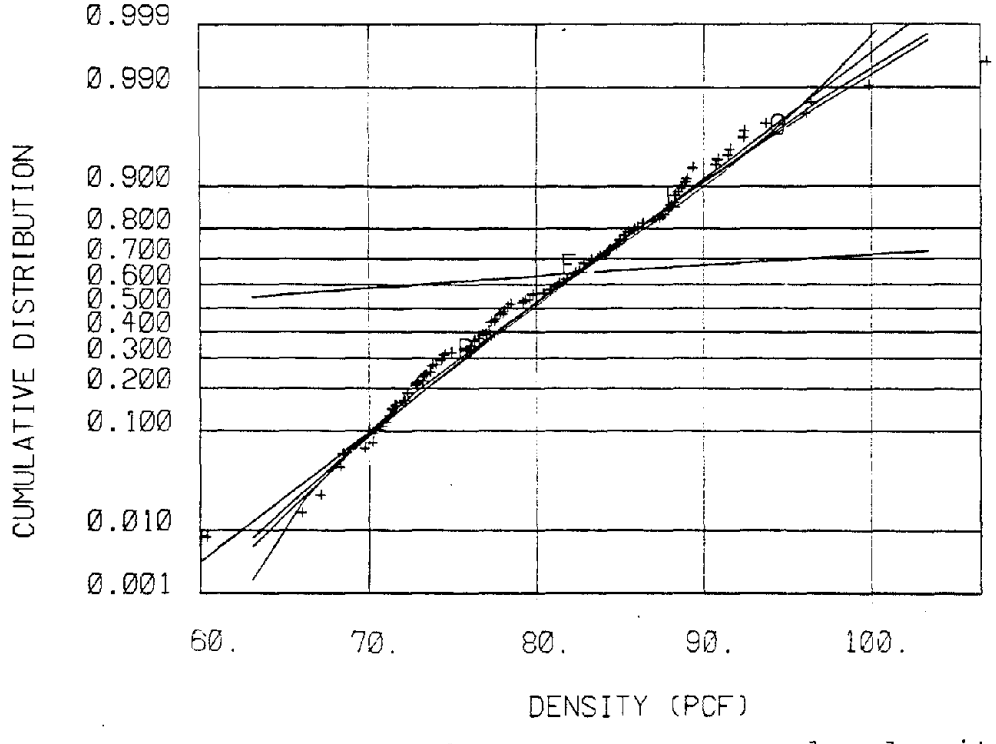

Figure 8.69 - CDF of raw Magna copper dry density data compared to standard CDF plots

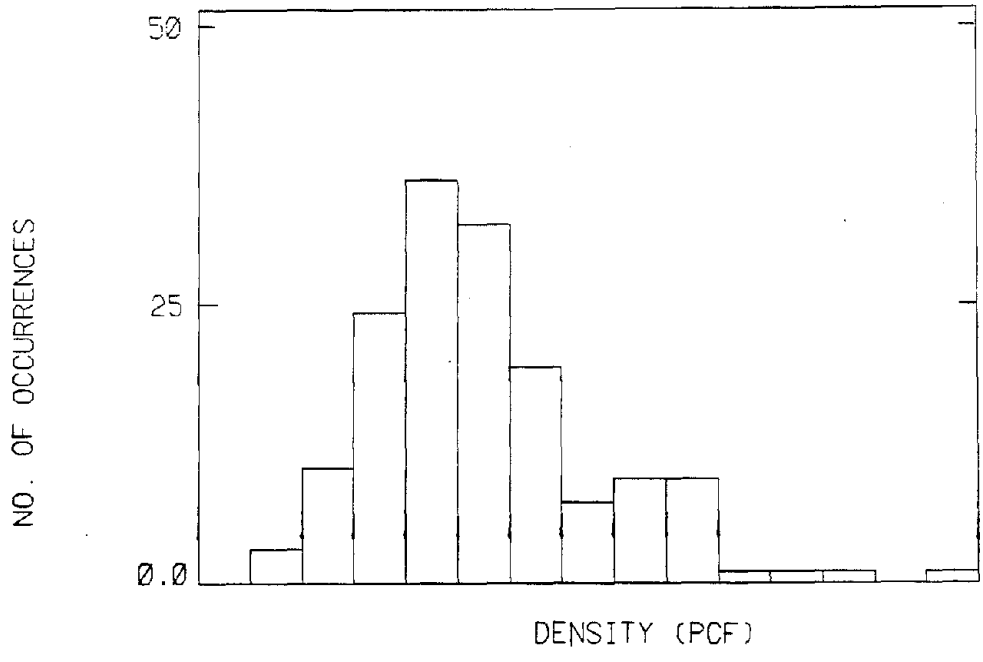

Figure 8.70 - Histogram of residual Magna copper dry density data

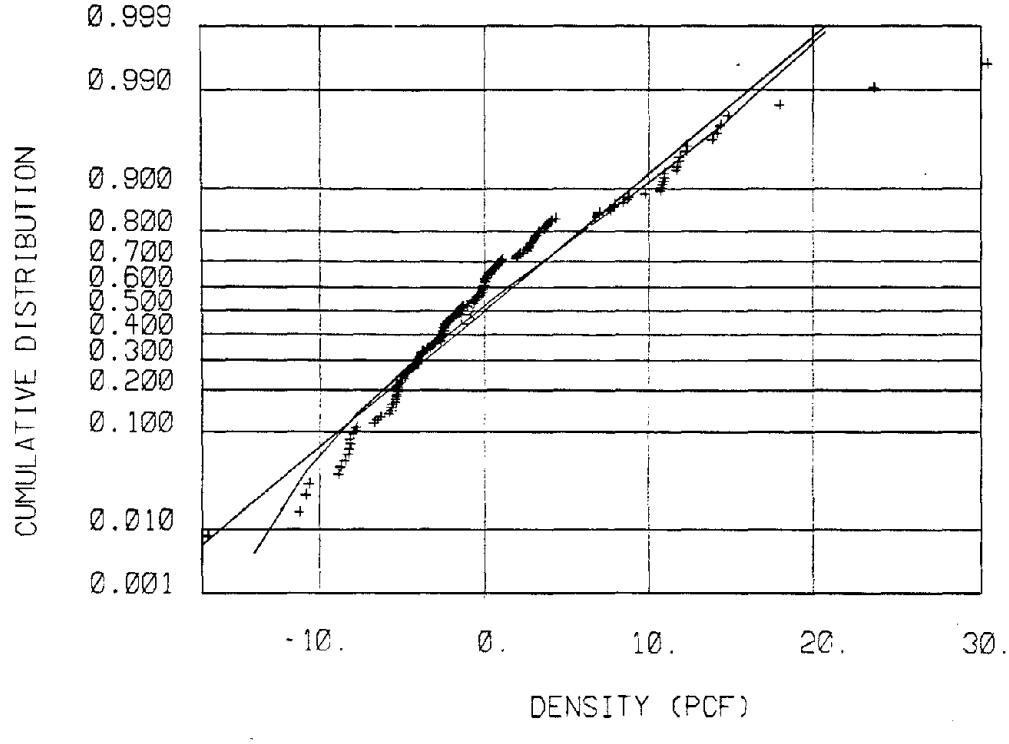

Figure 8.71 - CDF of raw Magna copper dry density data compared to standard CDF plots

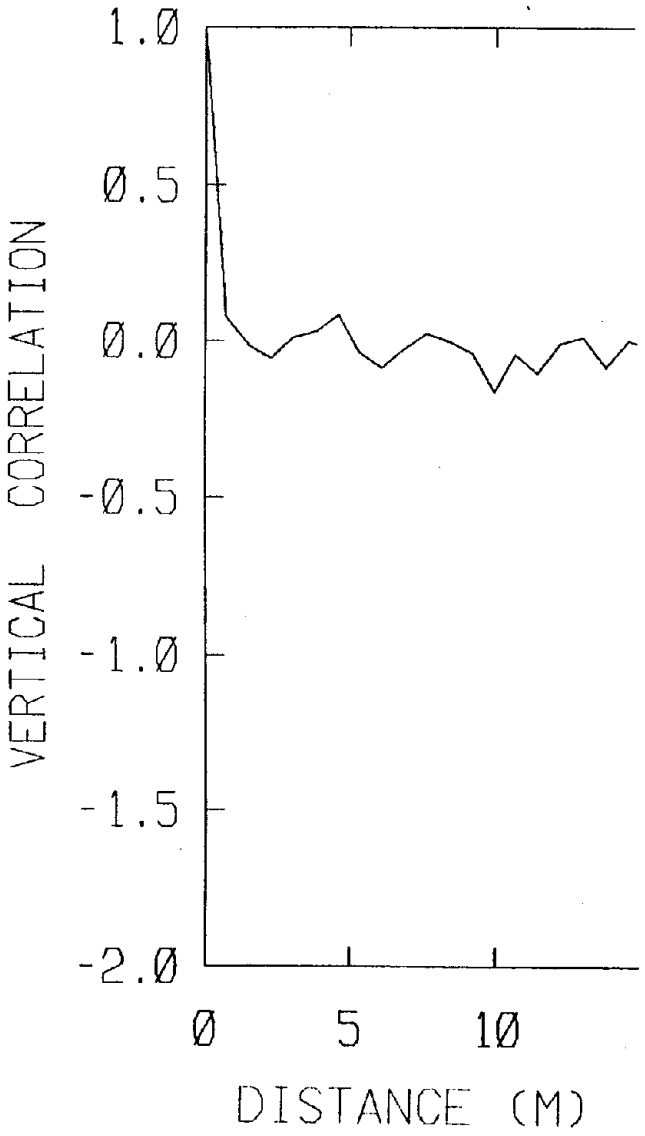

Figure 8.72 - Vertical correlation for residual Magna copper dry density data

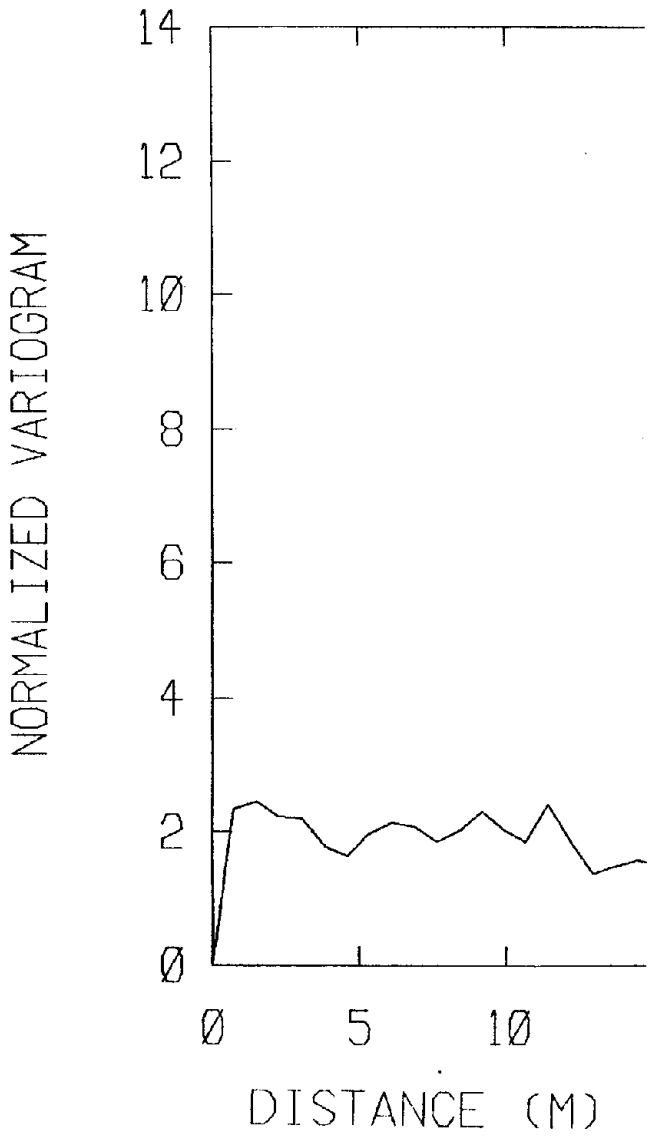

Figure 8.73 - Normalized variogram residual Magna copper density data

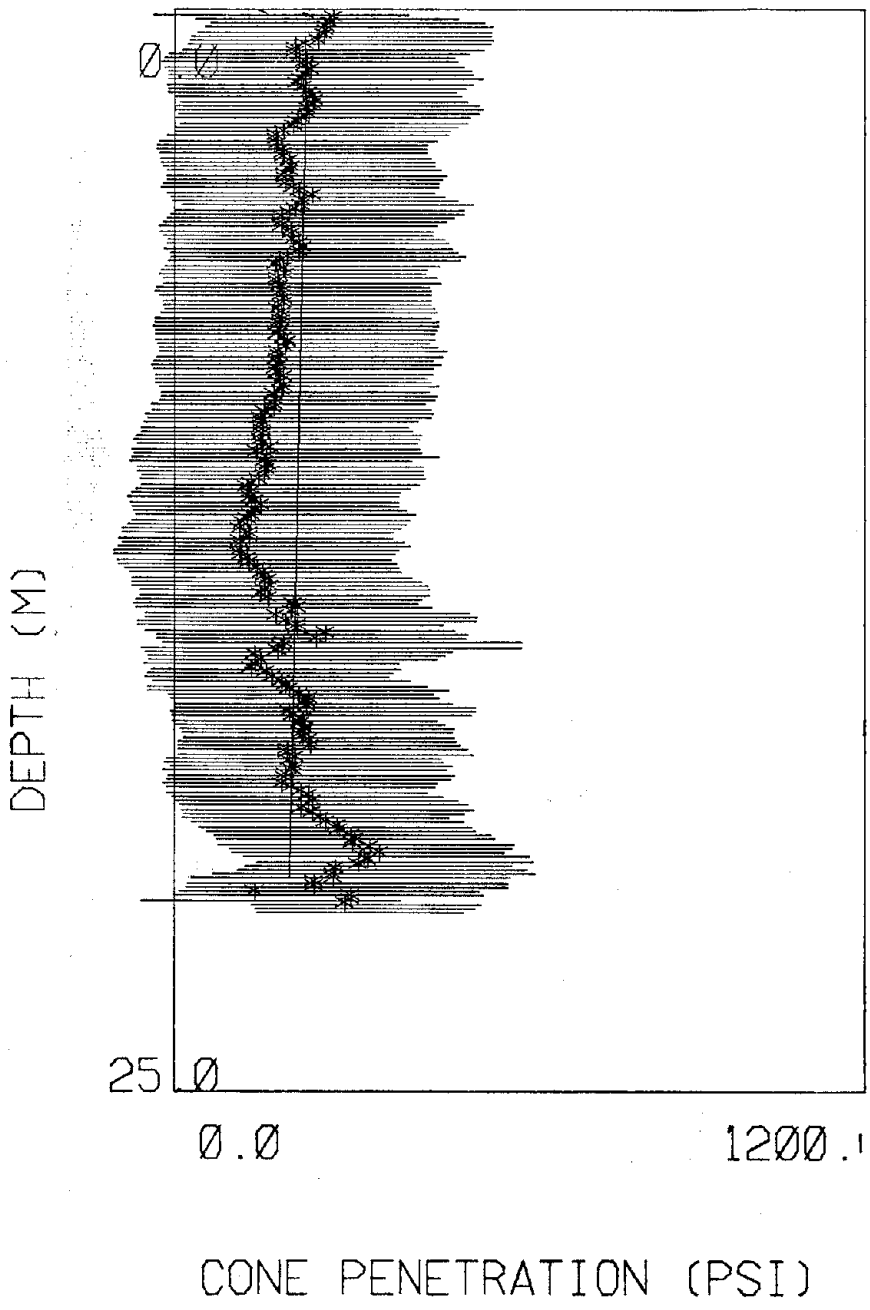

Figure 8.74 - Cone penetration resistance data v. depth for Mindola copper

SITE	Mindola (Copper) Zambia	
DATA	Type	43 Cone Penetrations
	Number	6593
	Quality Index	A

TREND WITH DEPTH $q_c(psi) = 234 - 1.6z(m)$

DATA SCATTER

	mean	SD	β_1	β_2
Raw Data	222	198	1.13	3.77
Residual Data	--	198	1.14	3.79

GOODNESS OF FIT STATISTICS

	Raw		Residual	
	χ^2	D_m	χ^2	D_m
normal	703	0.133	761	0.120
beta	123	0.053	108	0.056
exponential	399	0.070	--	--
lognormal	3477	0.166	--	--
gamma	552	0.080	--	--
5% confidence limit	23.7	0.017	--	--

INTERPRETED STRENGTH PARAMETERS III

Table 8.14 - Table of Mindola copper cone penetration resistance data

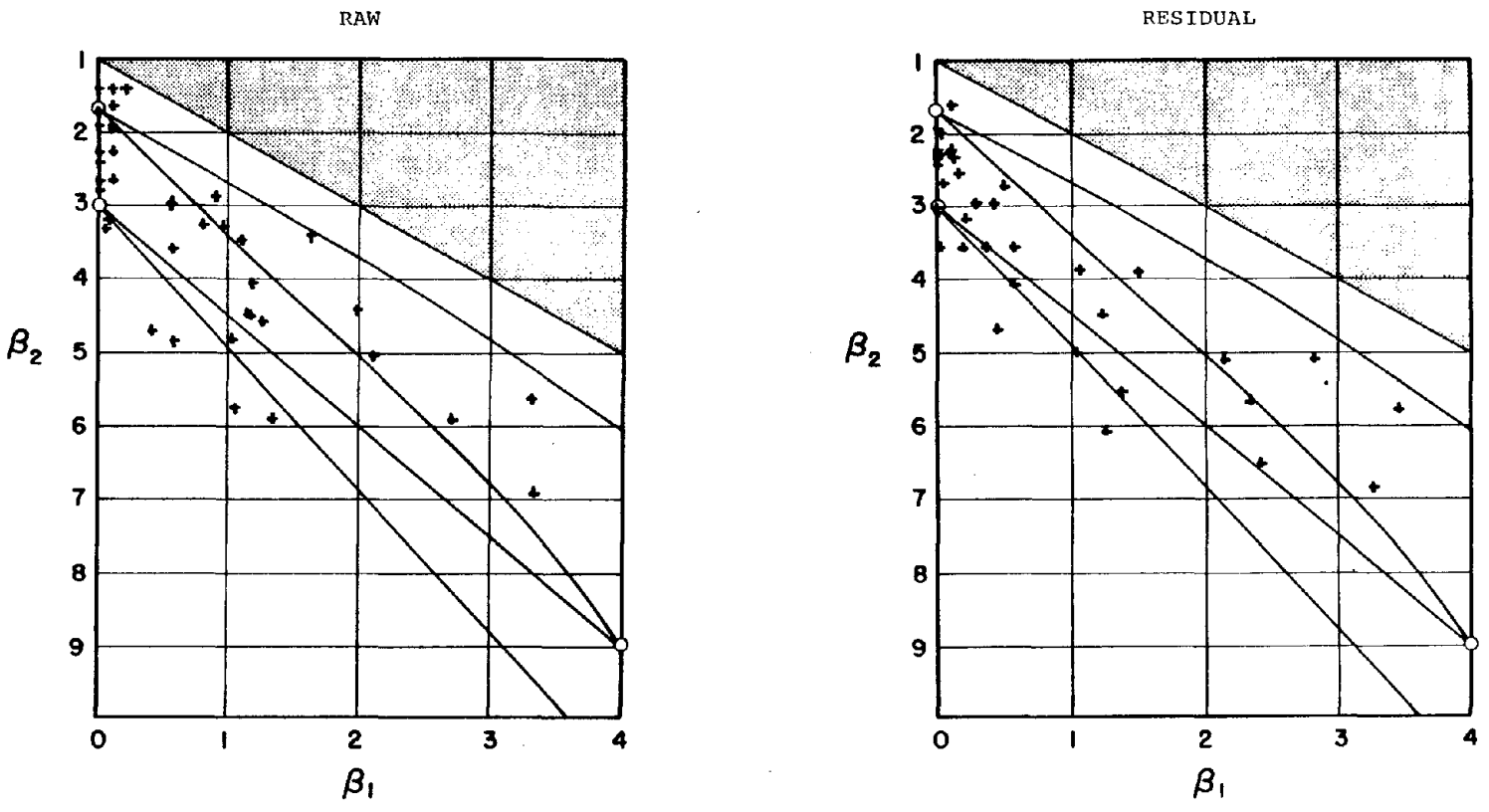

Figure 8.75 - Pearson diagrams of raw and residual cone penetration resistance data

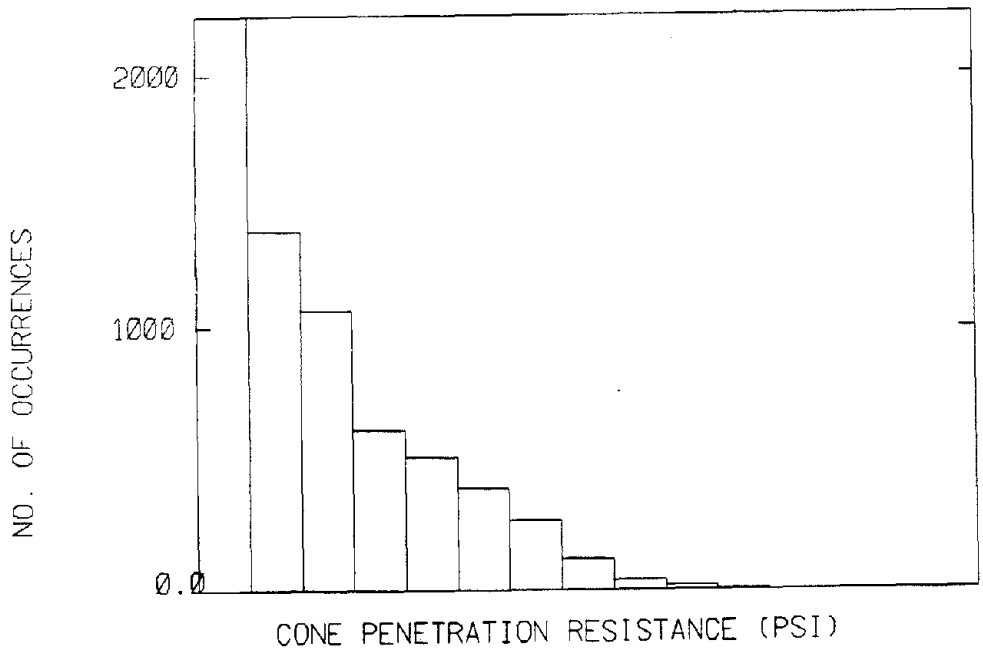

Figure 8.76 - Histogram of raw Mindola copper cone penetration resistance data

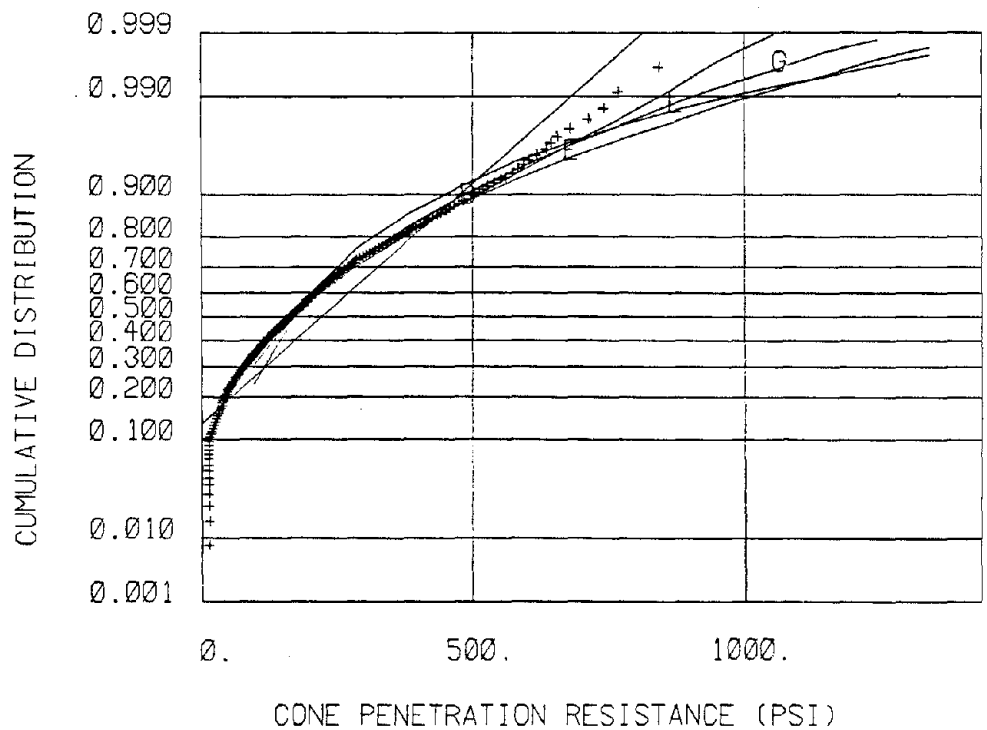

Figure 8.77 - CDF of raw Mindola copper cone penetration resistance data

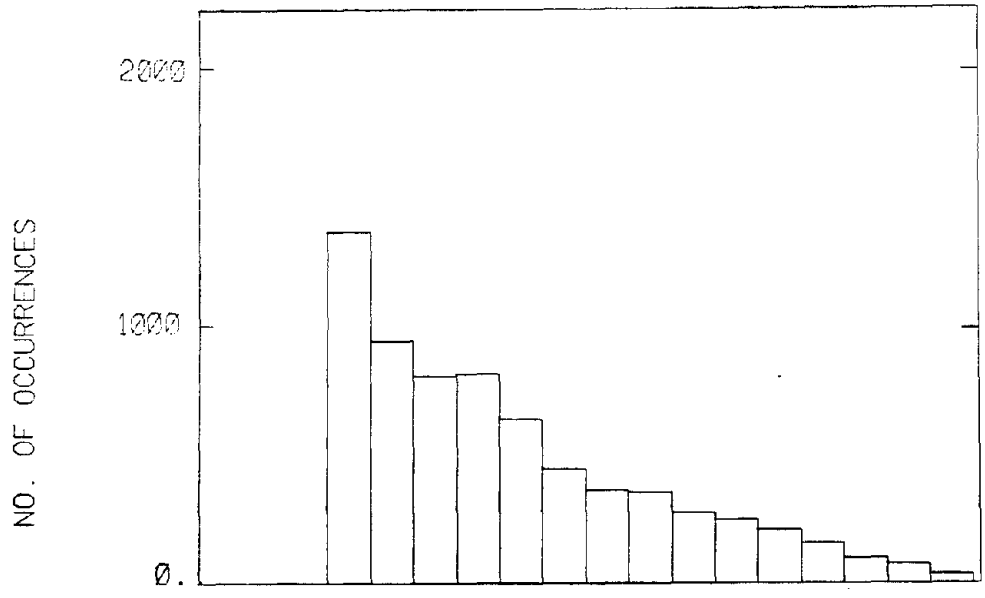

Figure 8.78 - Histogram of residual Mindola copper cone penetration resistance data

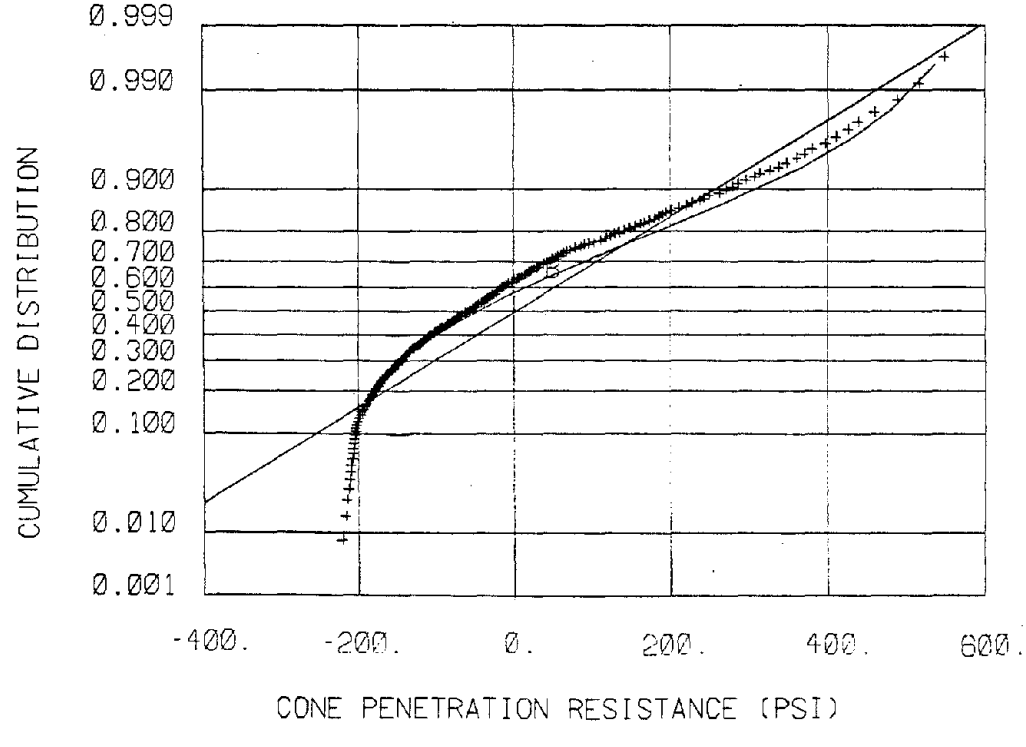

Figure 8.79 - CDF of residual Mindola copper cone penetration resistance data compared to standard CDF plots

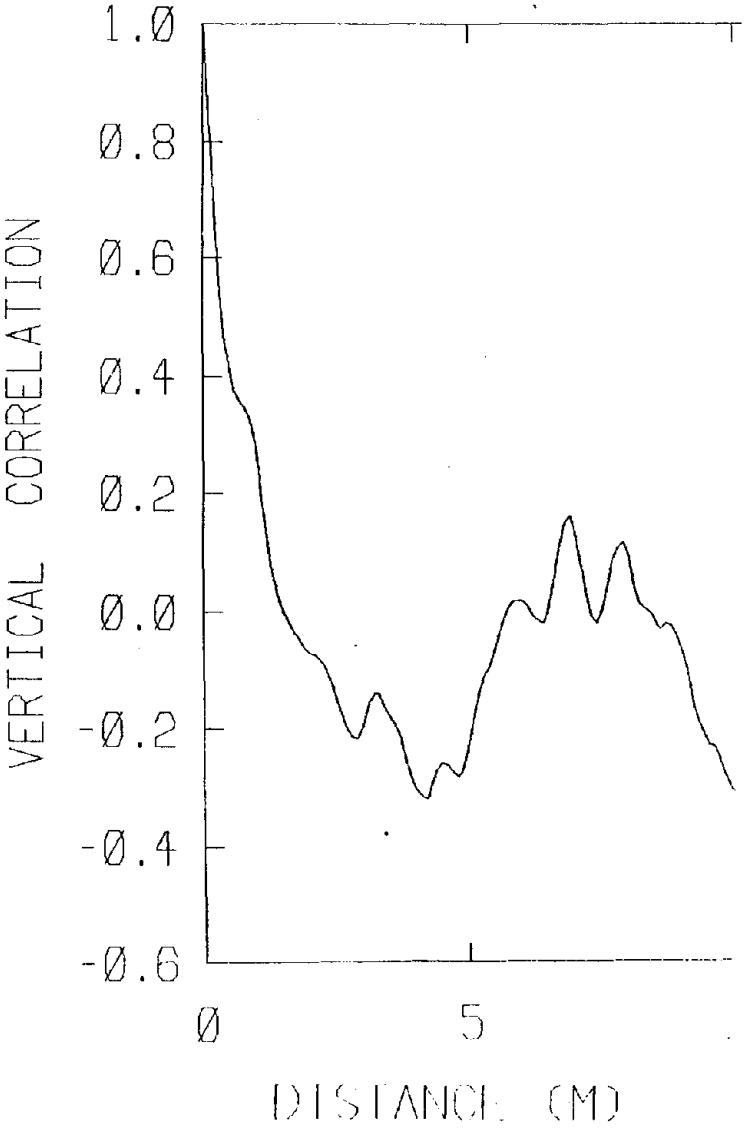

Figure 8.80 - Vertical correlation of Mindola copper residual cone penetration resistance data

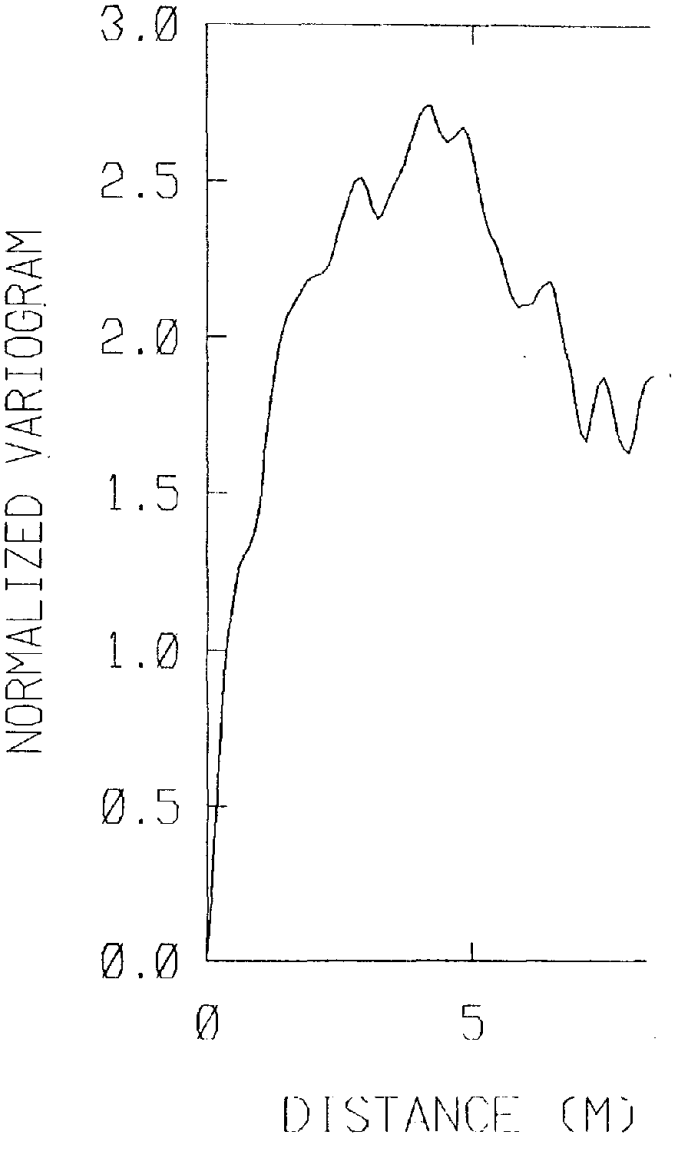

Figure 8.81 - Normalized variogram Mindola copper residual cone penetration

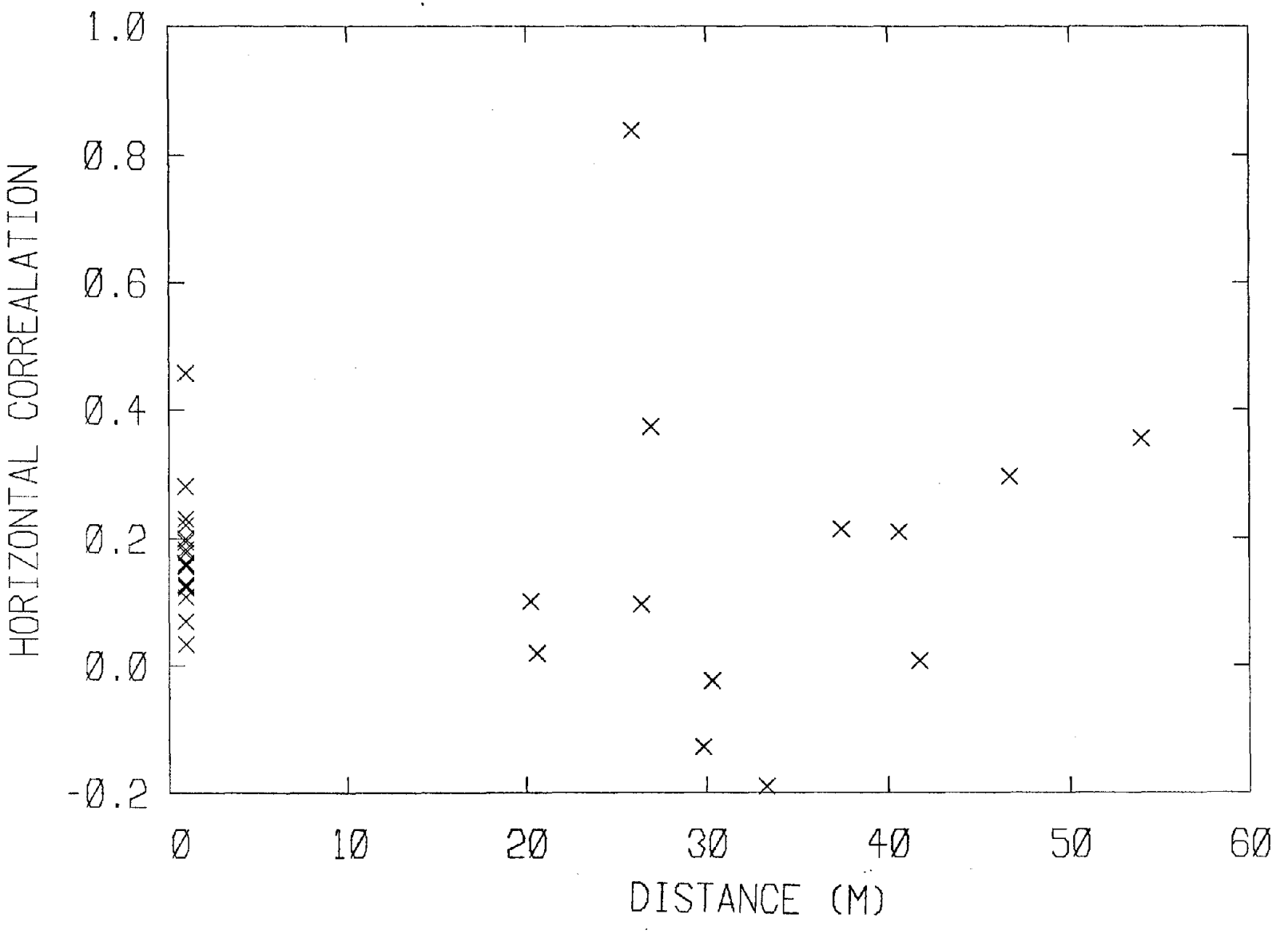

Figure 8.82 Horizontal correlation for Mindola copper cone penetration resistance data

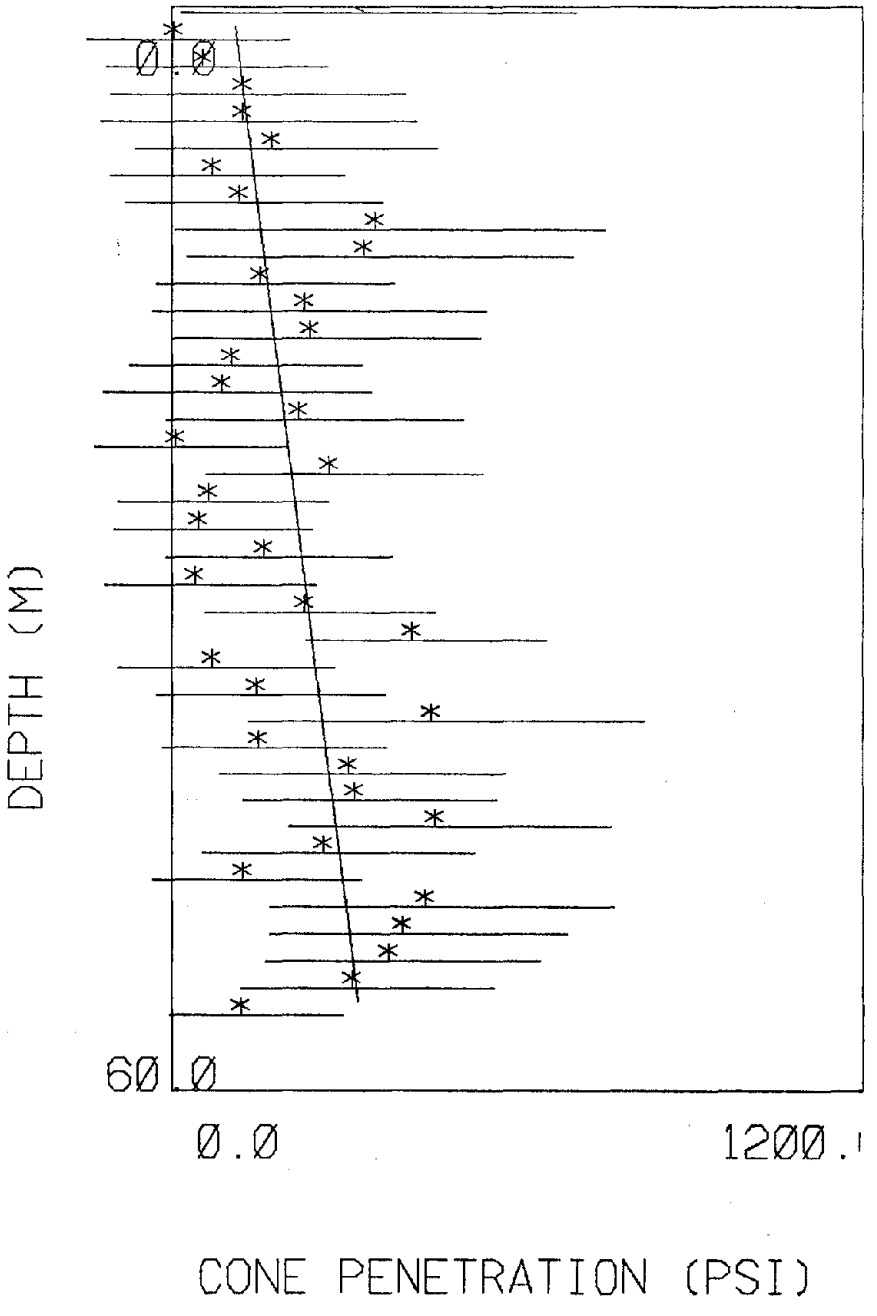

Figure 8.83 - Cone penetration resistance v. depth for Morenci copper

SITE	Morenci (Copper)	
DATA	Type	Cone Penetration (4 individual holes)
	Number	564
	Quality Index	A

TREND WITH DEPTH q_c(psi) = 108.3 + 3.96z(m)

DATA SCATTER

	mean	SD	β_1	β_2
Raw Data	202.4	228	2.19	4.87
Residual Data	--	219.6	2.69	5.60

GOODNESS OF FIT STATISTICS

	Raw		Residual	
	χ^2	D_m	χ^2	D_m
normal	89.2	0.187	341.7	0.181
beta	120.3	0.196	220.2	0.150
exponential	50.6	0.195	--	--
lognormal	169.5	0.229	--	--
gamma	29.0	0.174	--	--
5% confidence limit	23.6	0.057	--	--

INTERPRETED STRENGTH PARAMETERS NA

Table 8.15 - Table of Morenci copper cone penetration resistance data

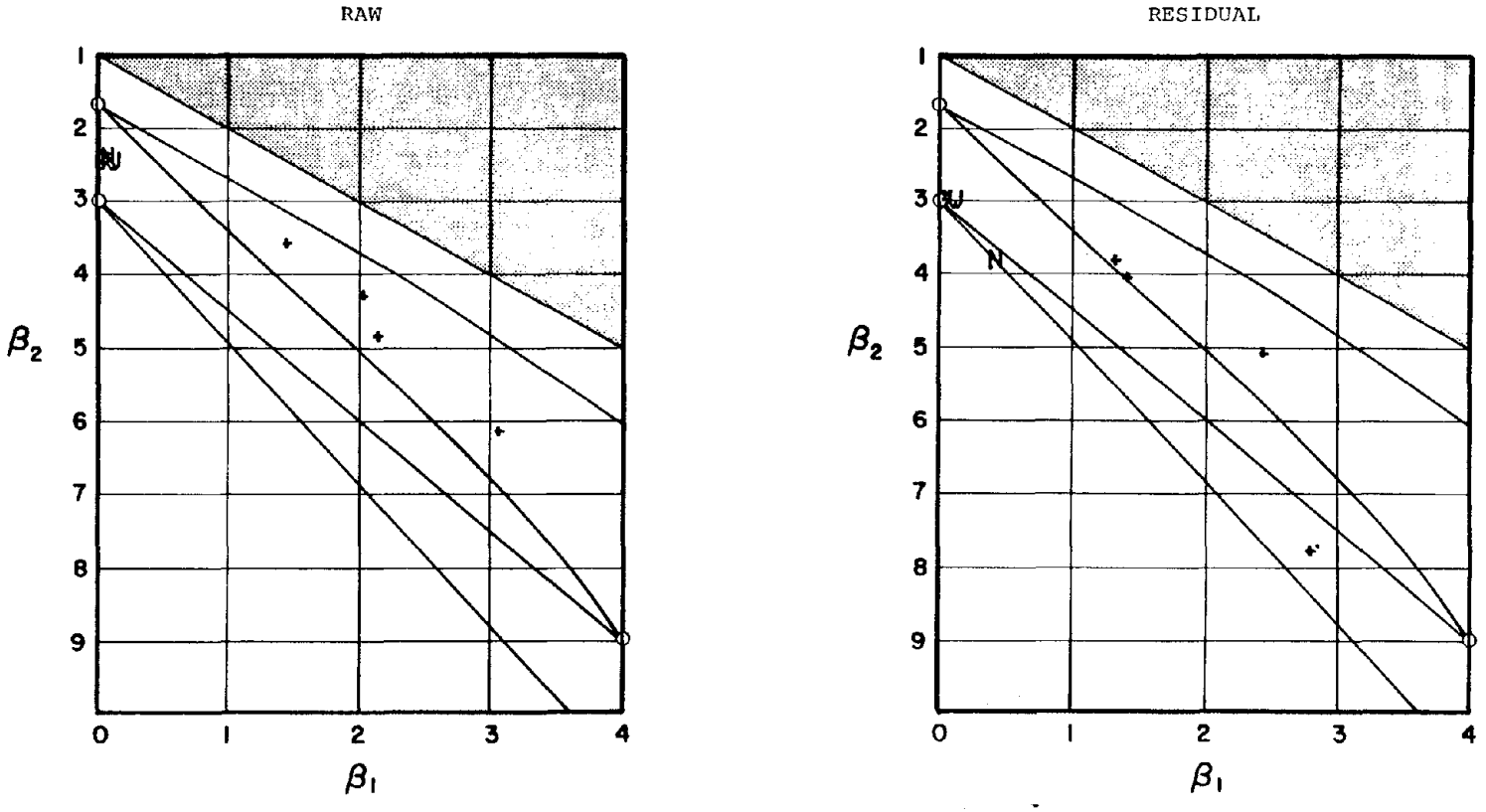

Figure 8.84 - Pearson diagram of raw and residual cone penetration resistance data for Morenci copper

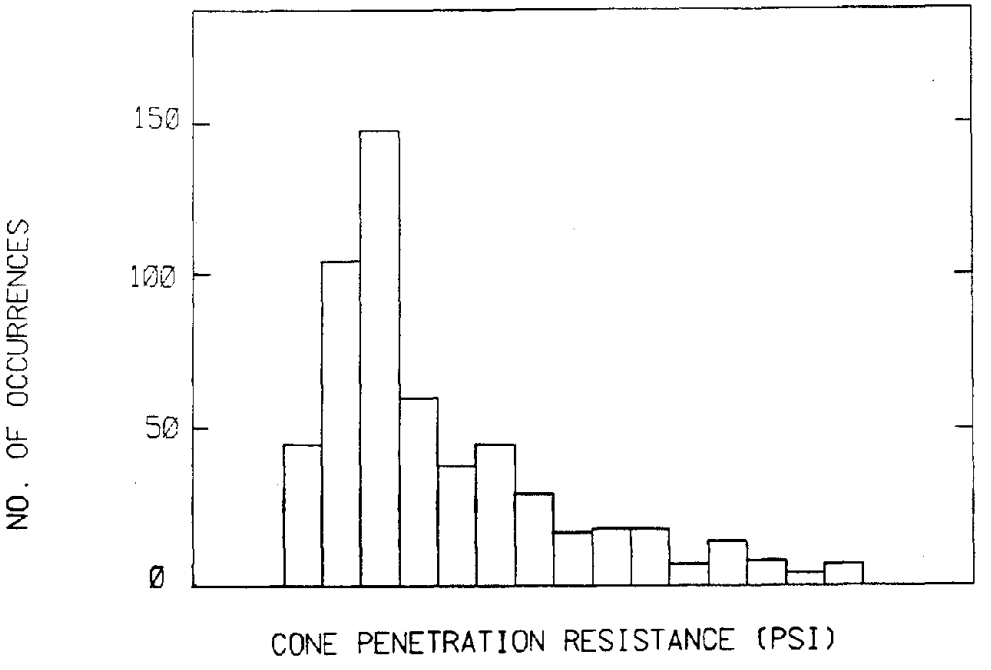

Figure 8.85 - Histogram of residual Morenci copper cone penetration resistance data

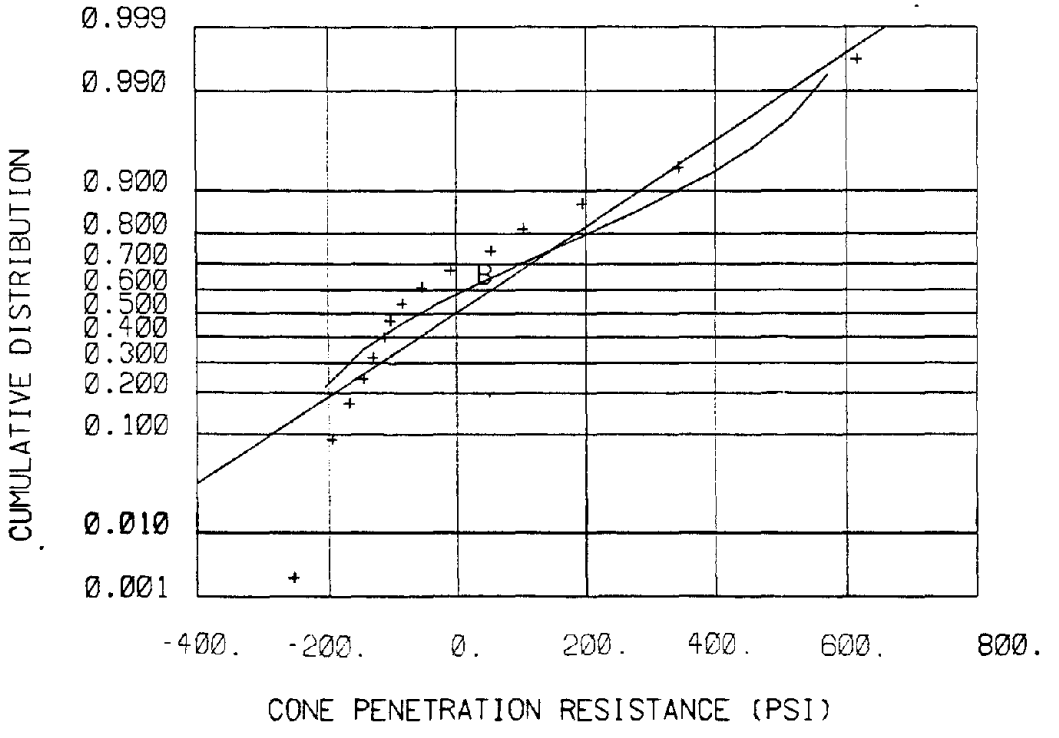

Figure 8.86 - CDF of residual Morenci copper cone penetration resistance data compared to standard CDF plots

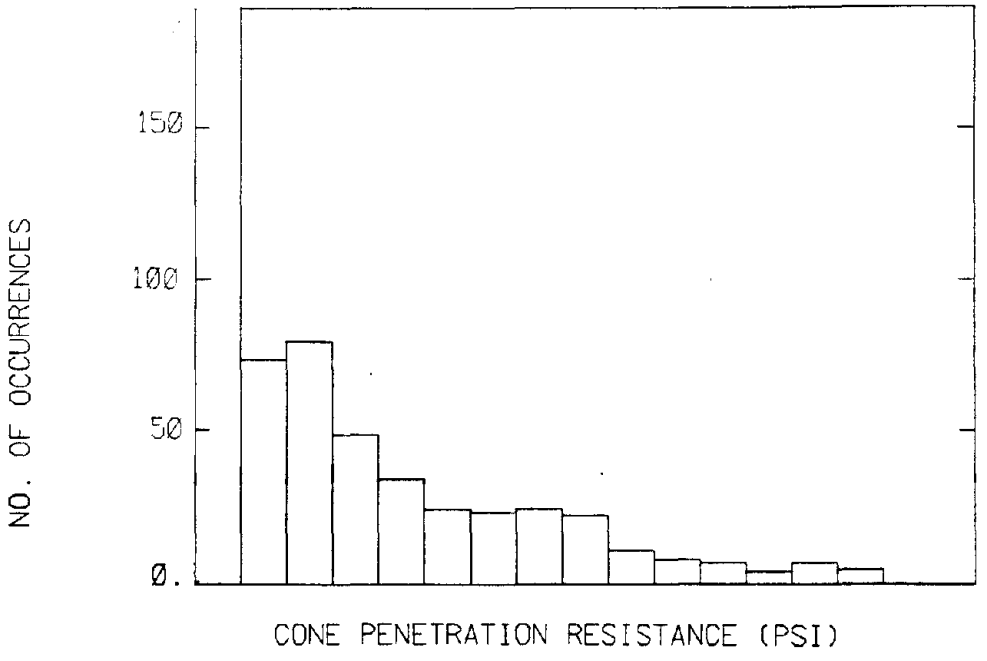

Figure 8.87 - Histogram of raw Morenci copper cone penetration resistance data

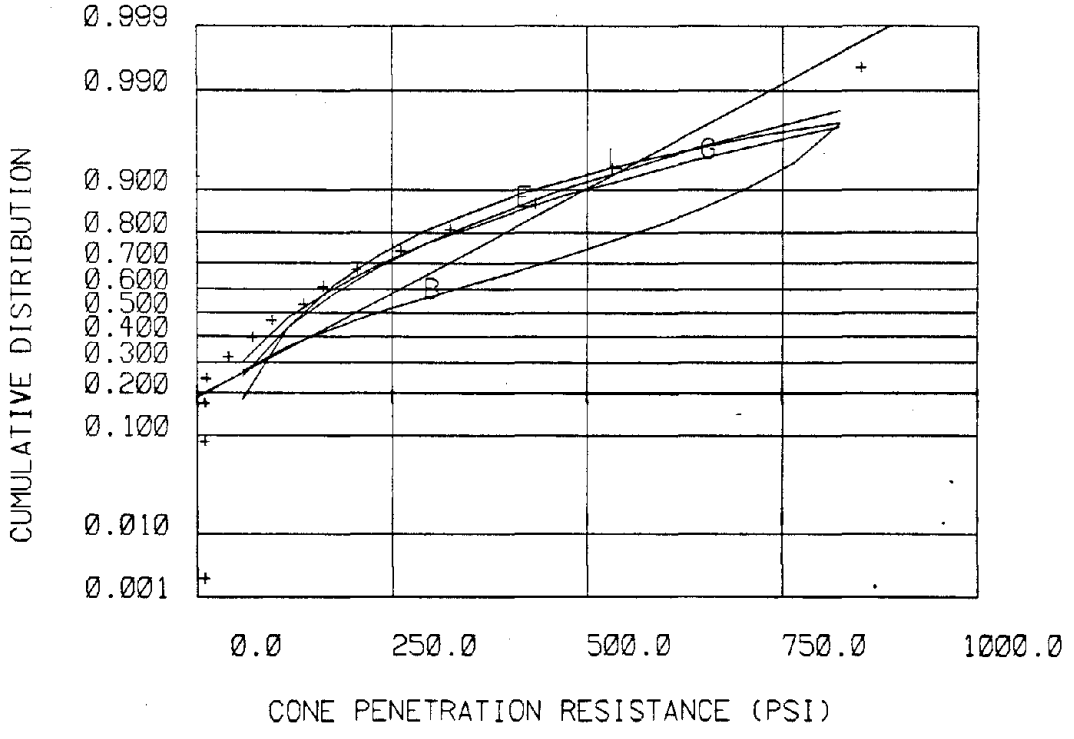

Figure 8.88 - CDF of raw Morenci copper cone penetration resistance data compared to standard CDF

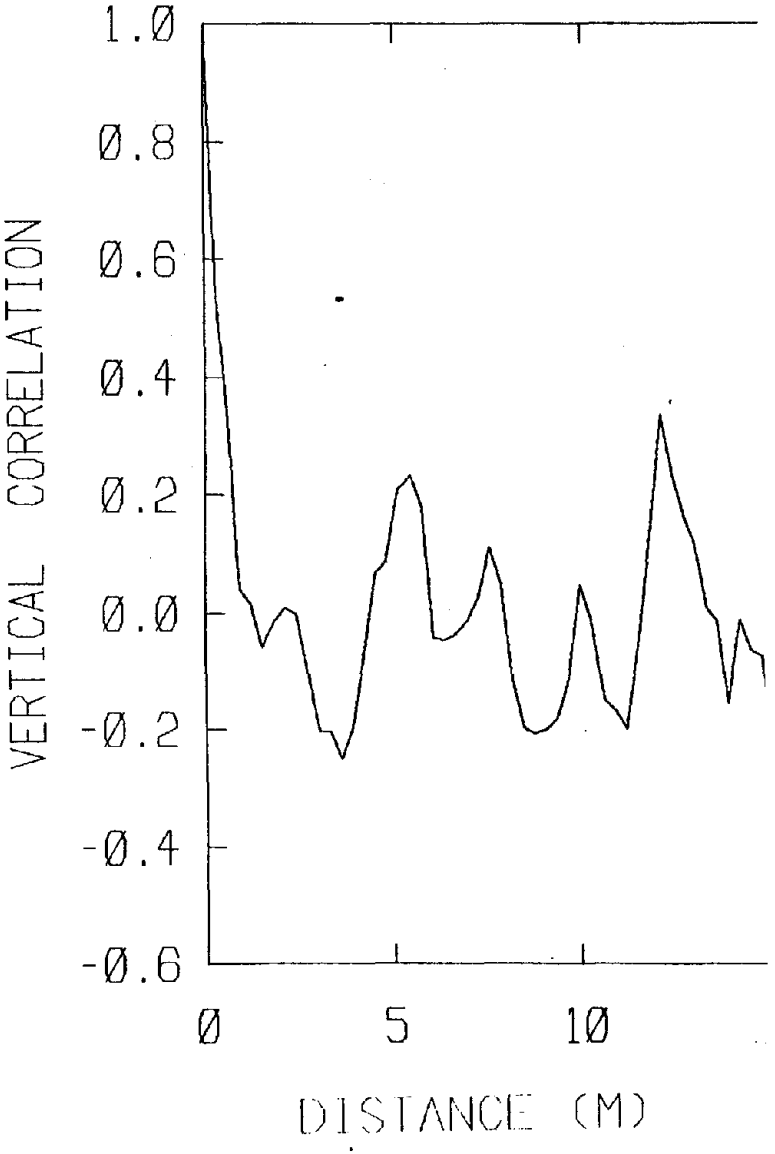

Figure 8.89 - Vertical correlation of residual Morenci copper cone penetration resistance data

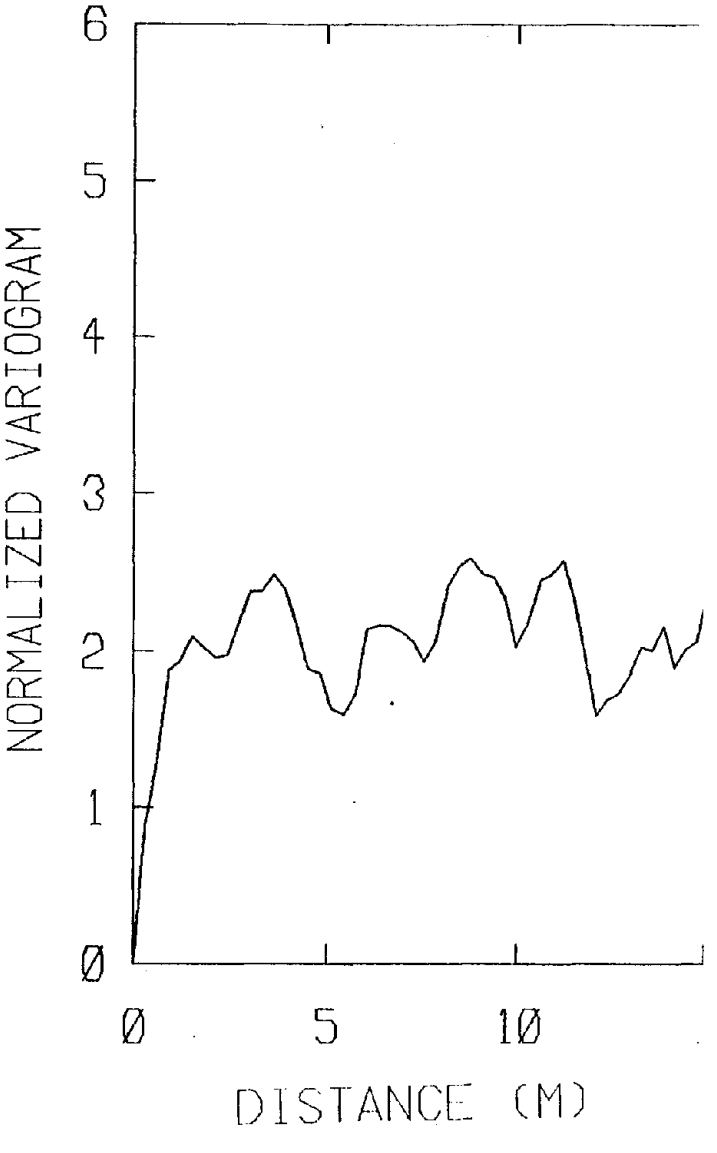

Figure 8.90 - normalized variogram residual Morenci cone penetration data

SITE Morenci Copper

DATA Type Standard Penetration

Number 60

Quality Index NA

TREND WITH DEPTH $N = 6.96 + 0.63z(m)$

DATA SCATTER

	mean	SD	β_1	β_2
Raw Data	17.2	10.6	0.131	2.46
Residual Data	--	7.49	0.462	3.85

GOODNESS OF FIT STATISTICS

	Raw		Residual	
	χ^2	D_m	χ^2	D_m
normal	14.9	0.113	8.90	0.103
beta	14.7	0.073	14.3	0.098
exponential	35.5	0.152	--	--
lognormal	75.6	0.158	--	--
gamma	18.9	0.125	--	--
5% confidence limit	23.7	0.176	--	--

INTERPRETED STRENGTH PARAMETERS NA

Table 8.16 - Table of Morenci copper SPT data

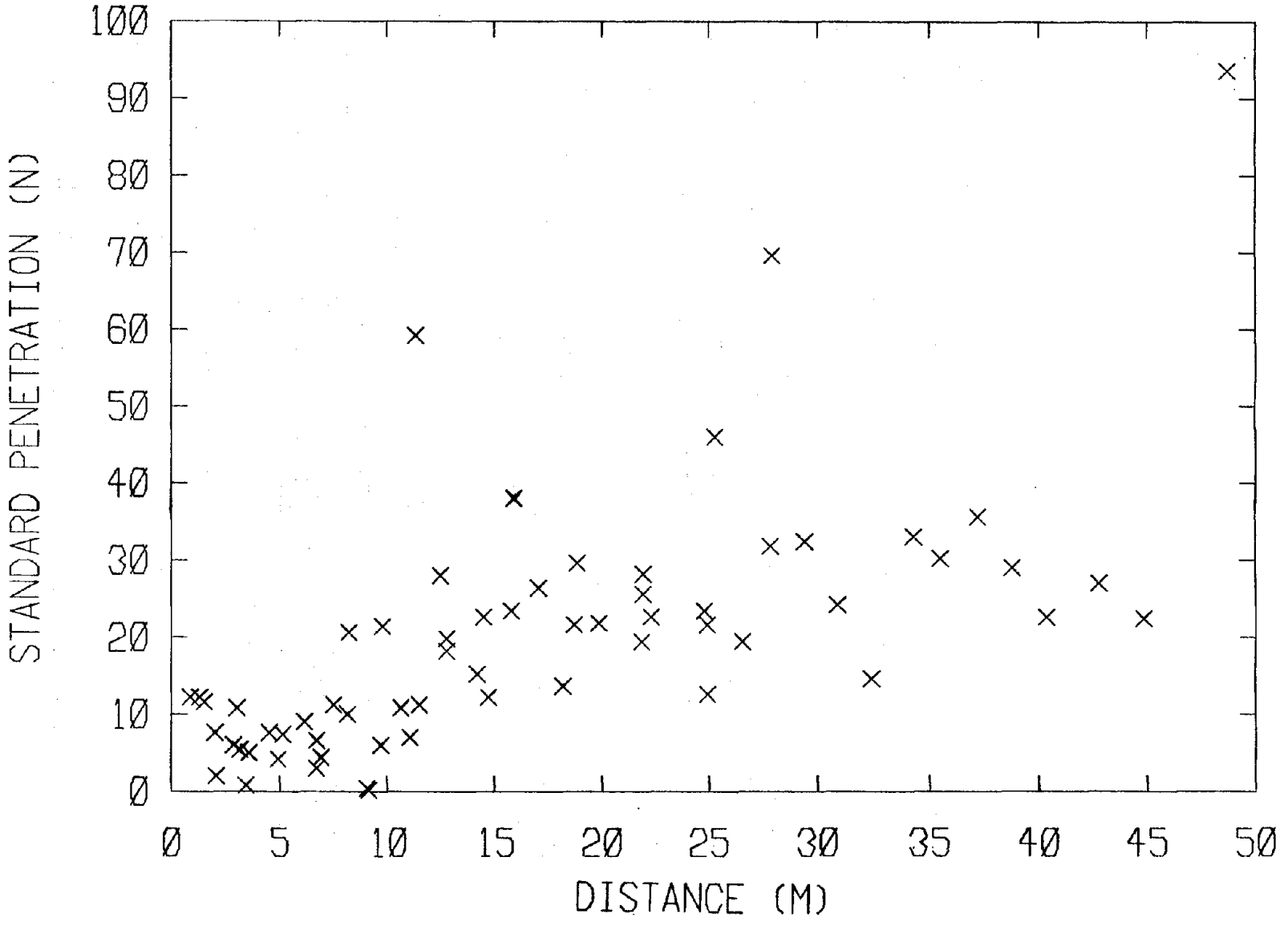

Figure 8.91 - Standard penetration (N) v. depth for Morenci copper

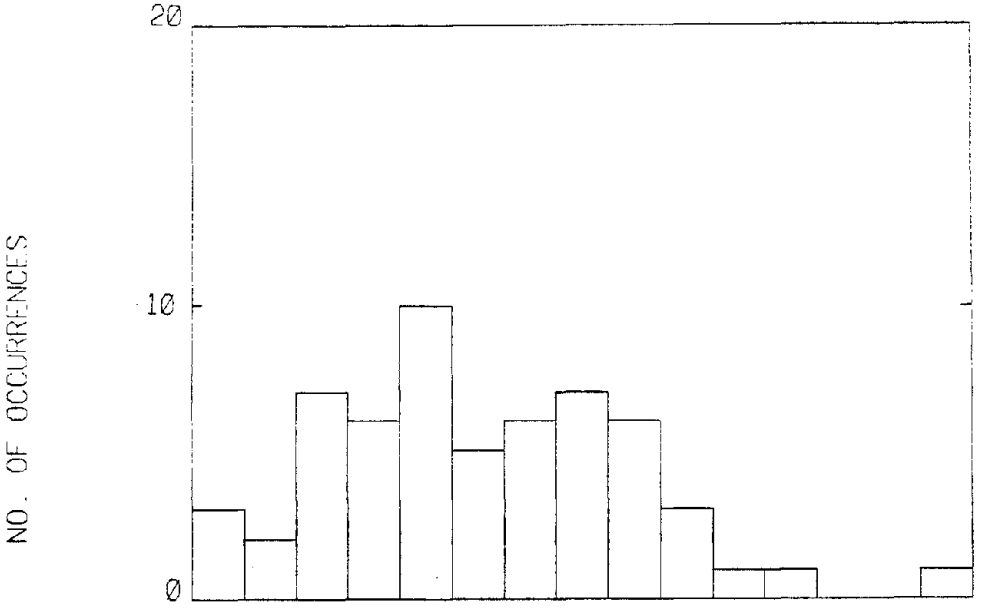

Figure 8.92 - Histogram of Morenci copper raw SPT data

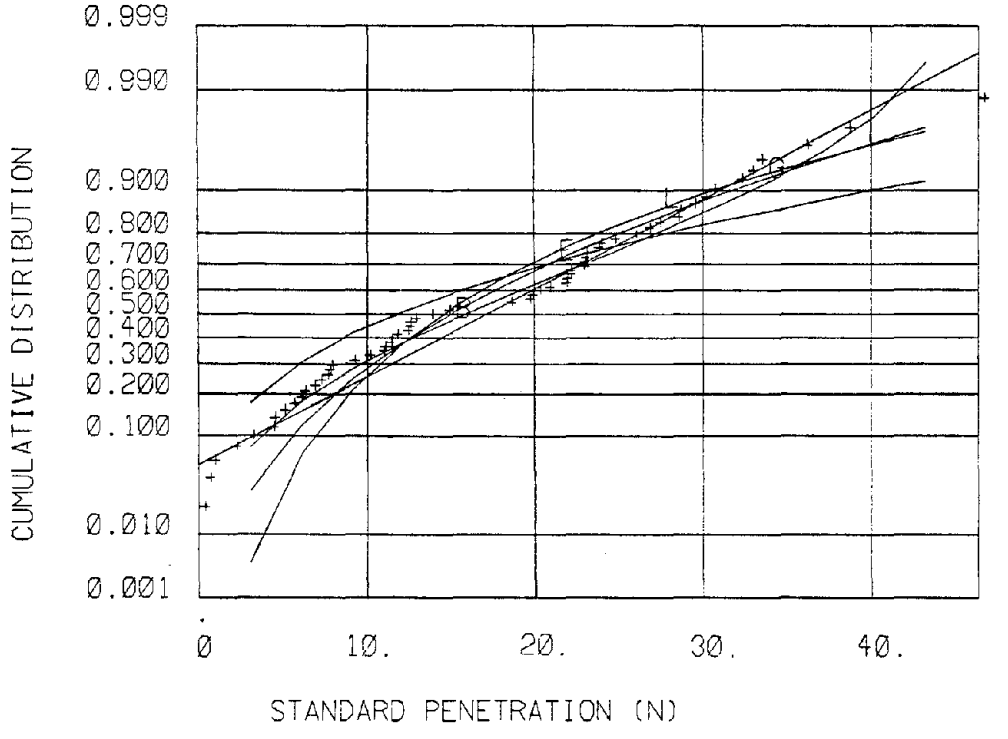

Figure 8.93 - CDF of raw Morenci copper STP data compared to standard CDF plots

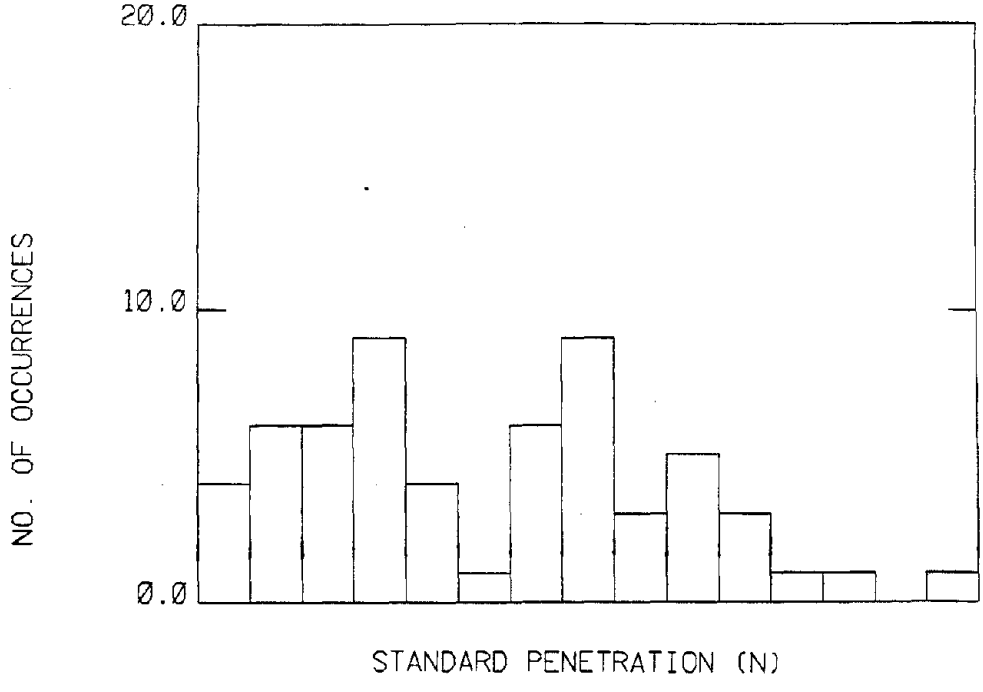

Figure 8.94 - Histogram of Morenci copper residual SPT data

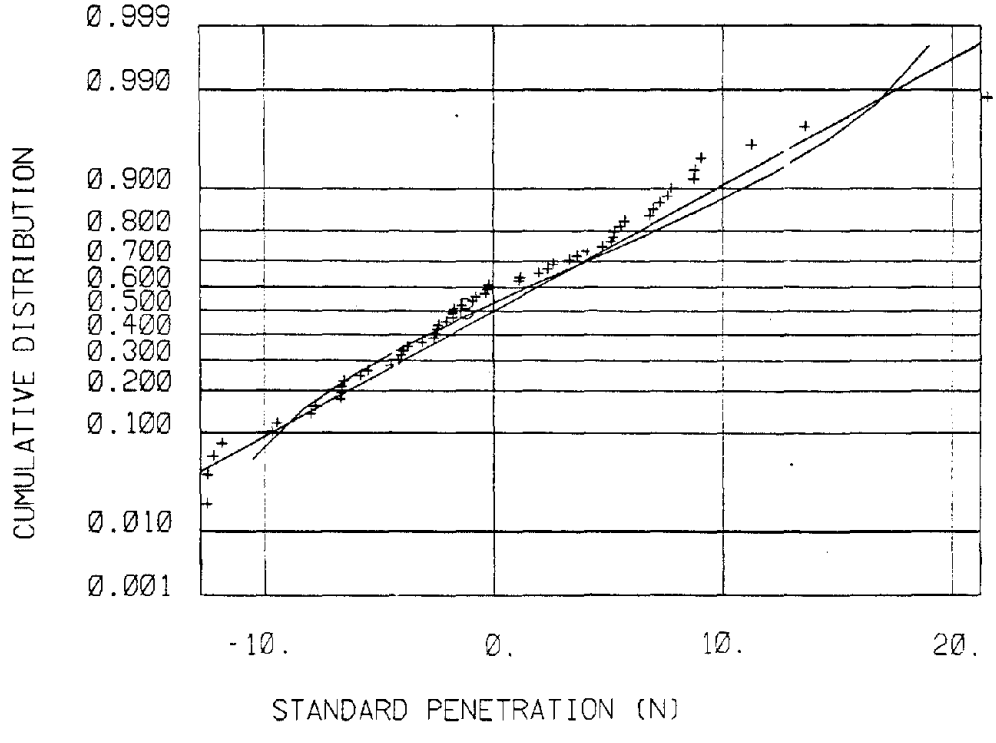

Figure 8.95 - CDF of residual Morenci copper STP data compared to standard CDF plots

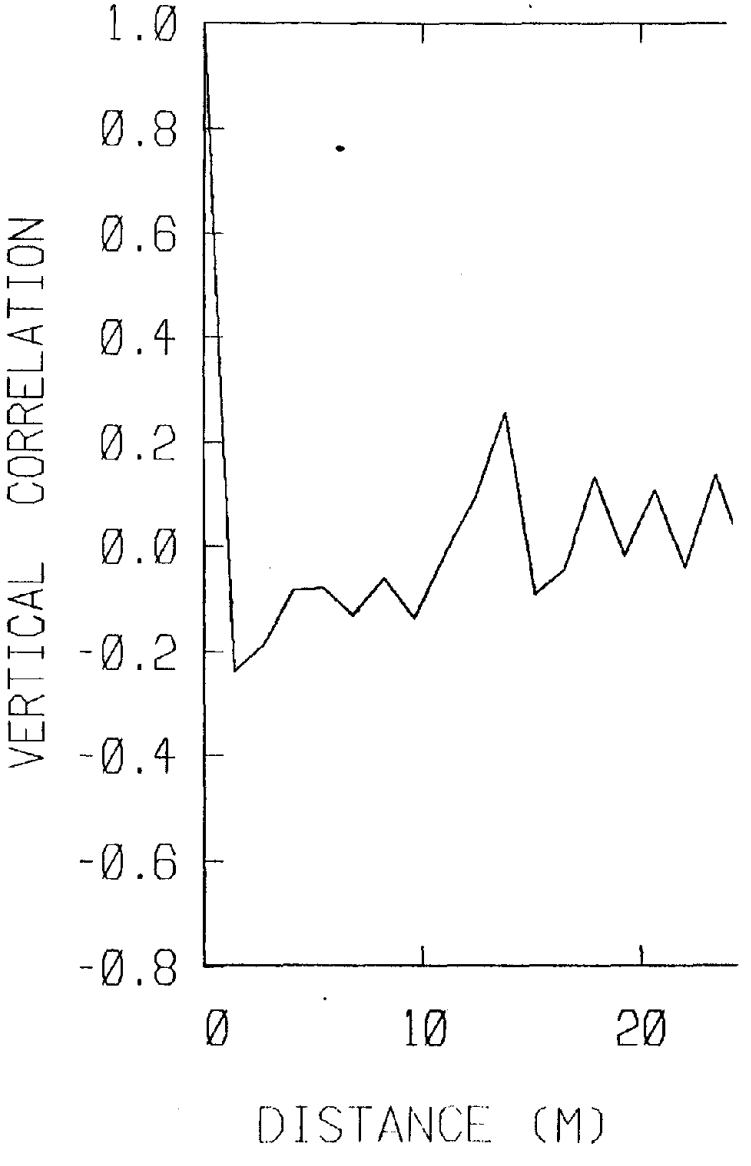

Figure 8.96 - Vertical correlation of residual Morenci copper SPT data

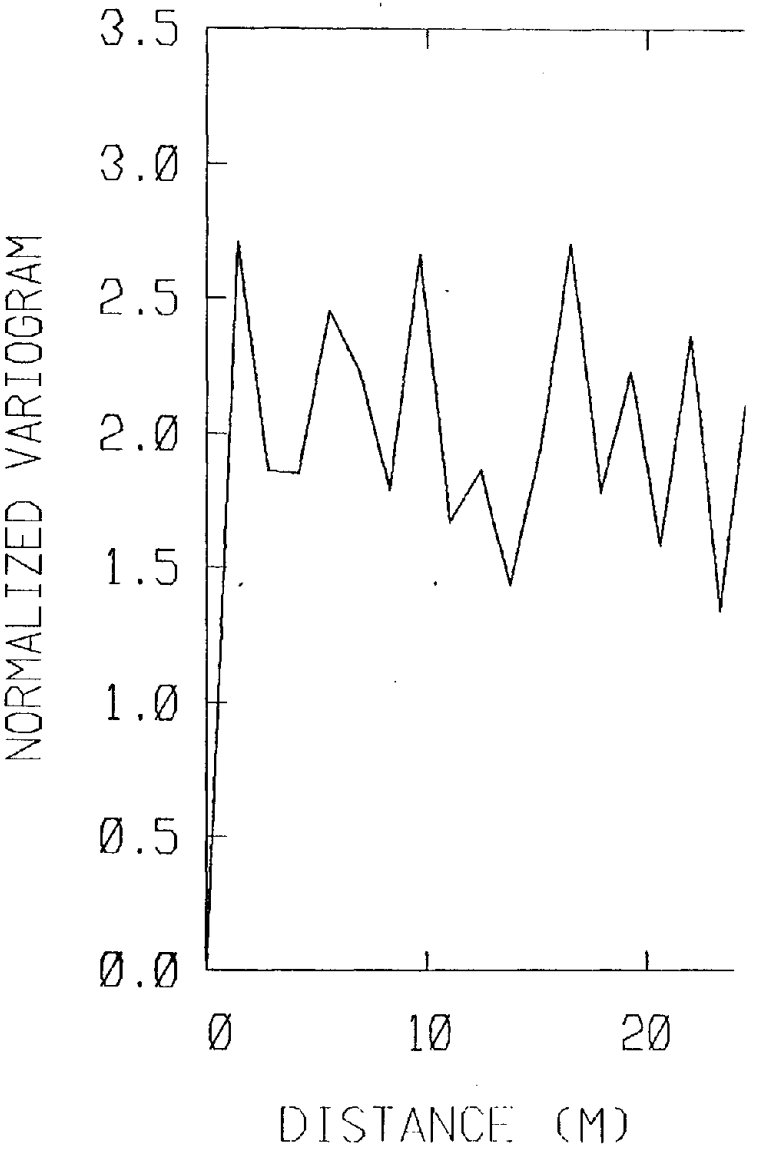

Figure 8.97 - Normalized variogram of residual Morenci copper SPT data

SITE Morenci (Copper)

DATA Type density (combined)

Number 62

Quality Index NA

TREND WITH DEPTH γ(pcf) = 99.6 + 0.07z(m)

DATA SCATTER

	mean	SD	β_1	β_2
Raw Data	101.1	3.83	0.008	2.61
Residual Data	--	3.70	0.013	2.92

GOODNESS OF FIT STATISTICS

	Raw		Residual	
	χ^2	D_m	χ^2	D_m
normal	10.9	0.054	18.9	0.088
beta	8.44	0.053	19.9	0.091
exponential	1249.2	0.577	--	--
lognormal	10.9	0.047	--	--
gamma	10.9	0.049	--	--
5% confidence limit	23.7	0.173	--	--

INTERPRETED STRENGTH PARAMETERS NA

Table 8.17 - Table of Morenci copper dry density data

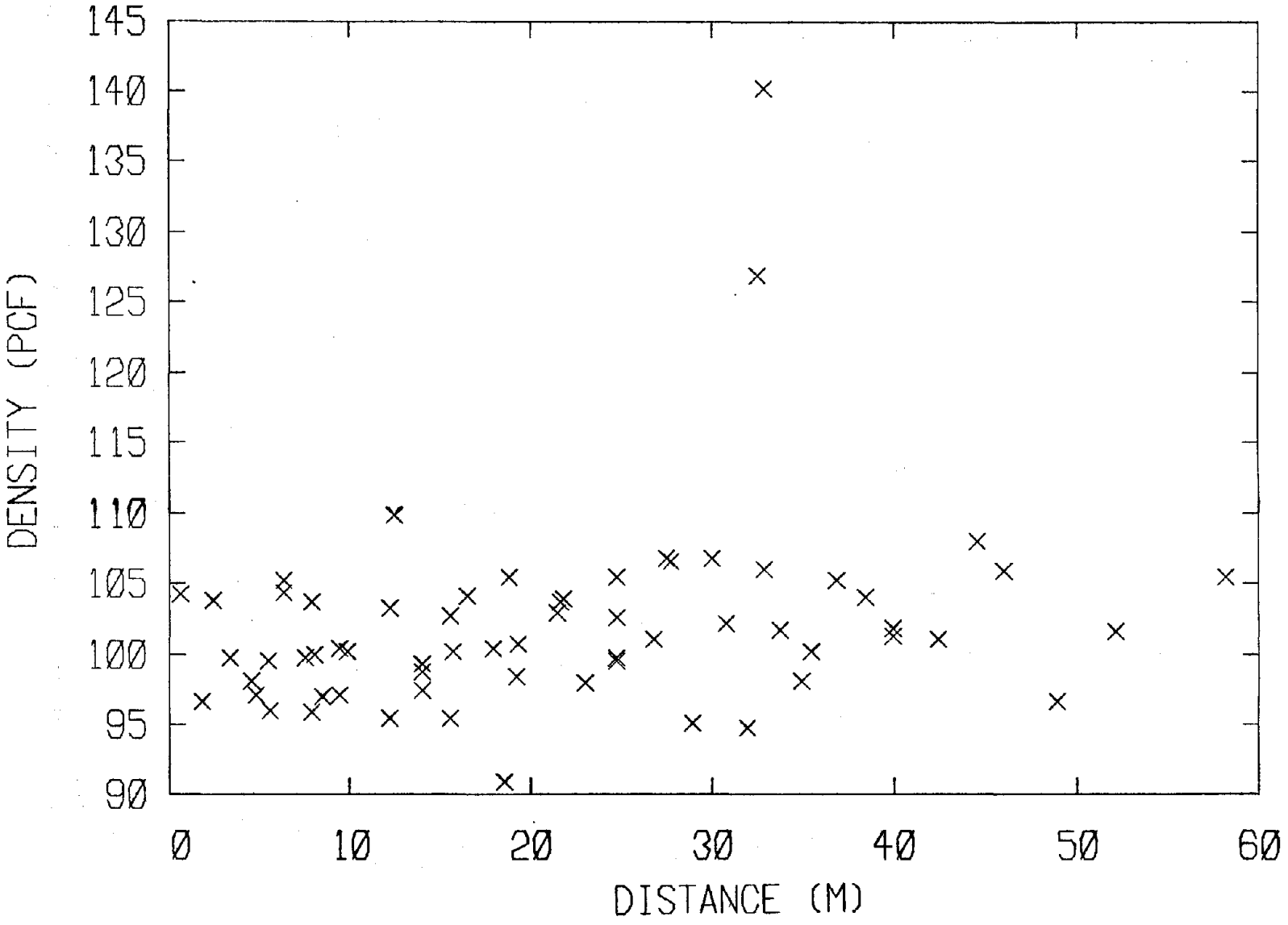

Figure 8.98 - Dry density v. depth for Morenci copper

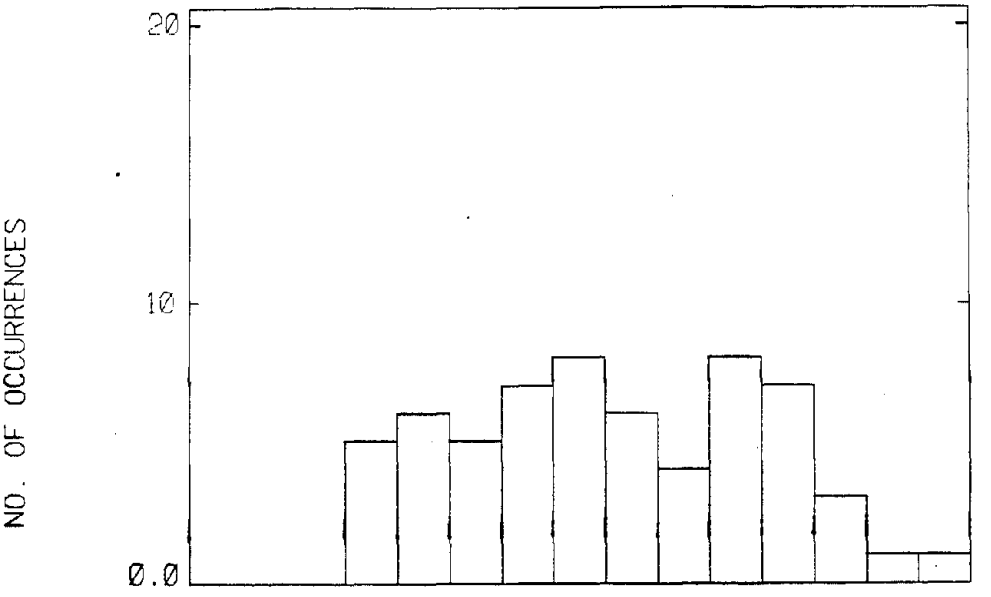

Figure 8.99 - Histogram of Morenci copper raw dry density data

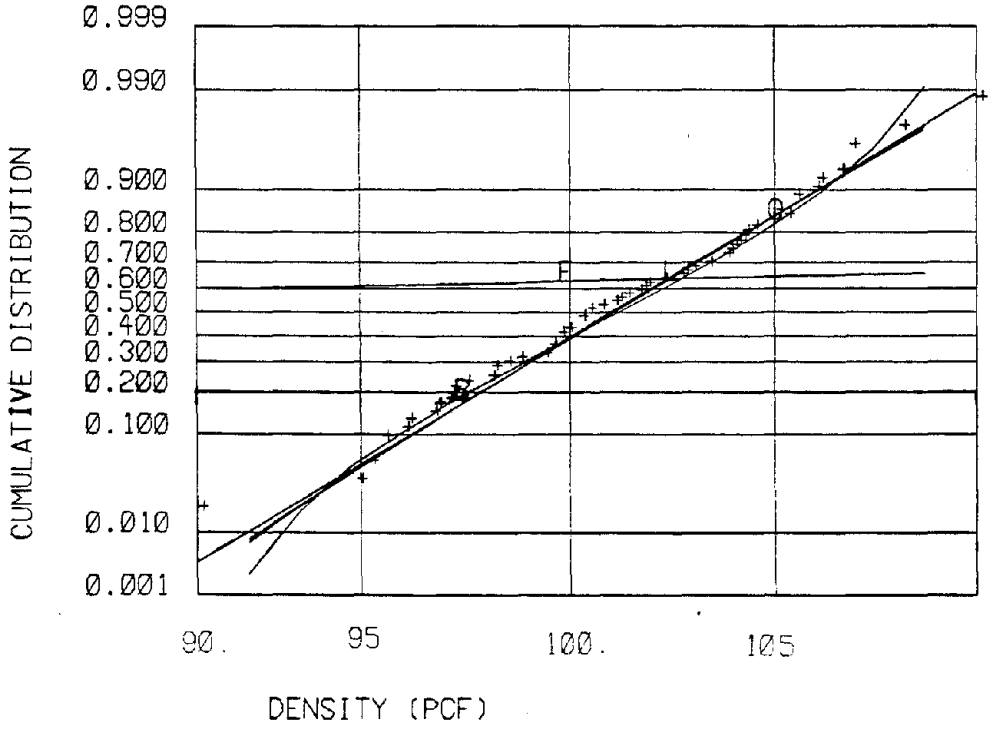

Figure 8.100- CDF of raw Morenci copper dry density data compared to standard CDF plots

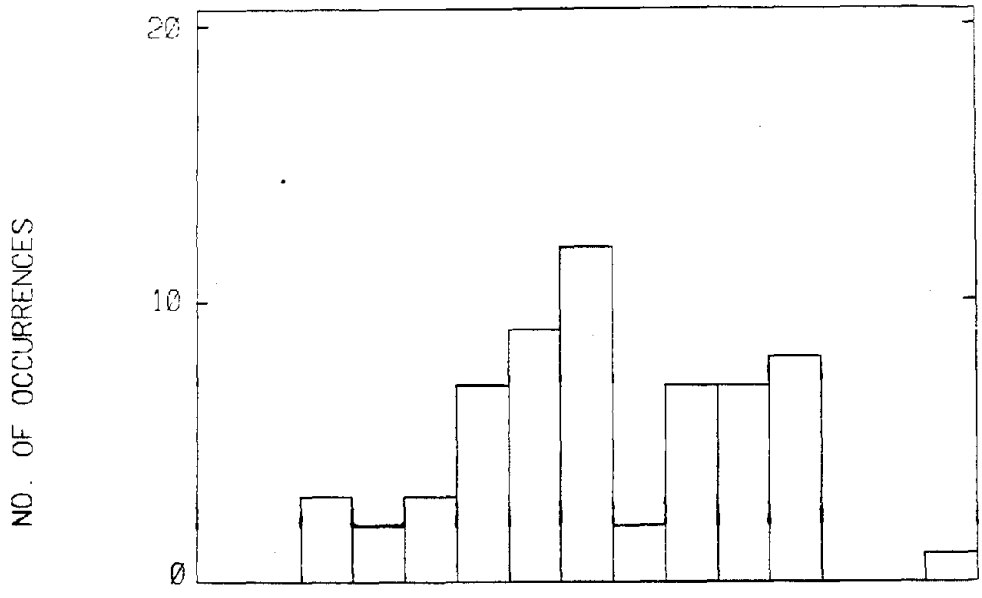

Figure 8.101 - Histogram of Morenci copper residual dry density data

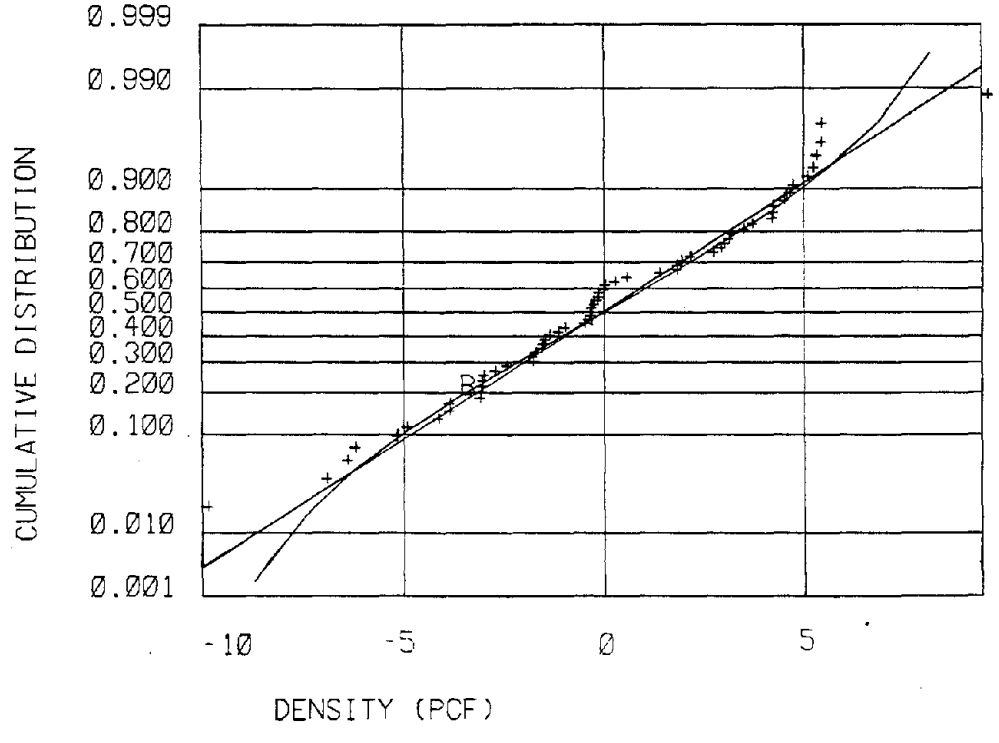

Figure 8.102 - CDF of residual Morenci copper dry density compared to standard CDF plots

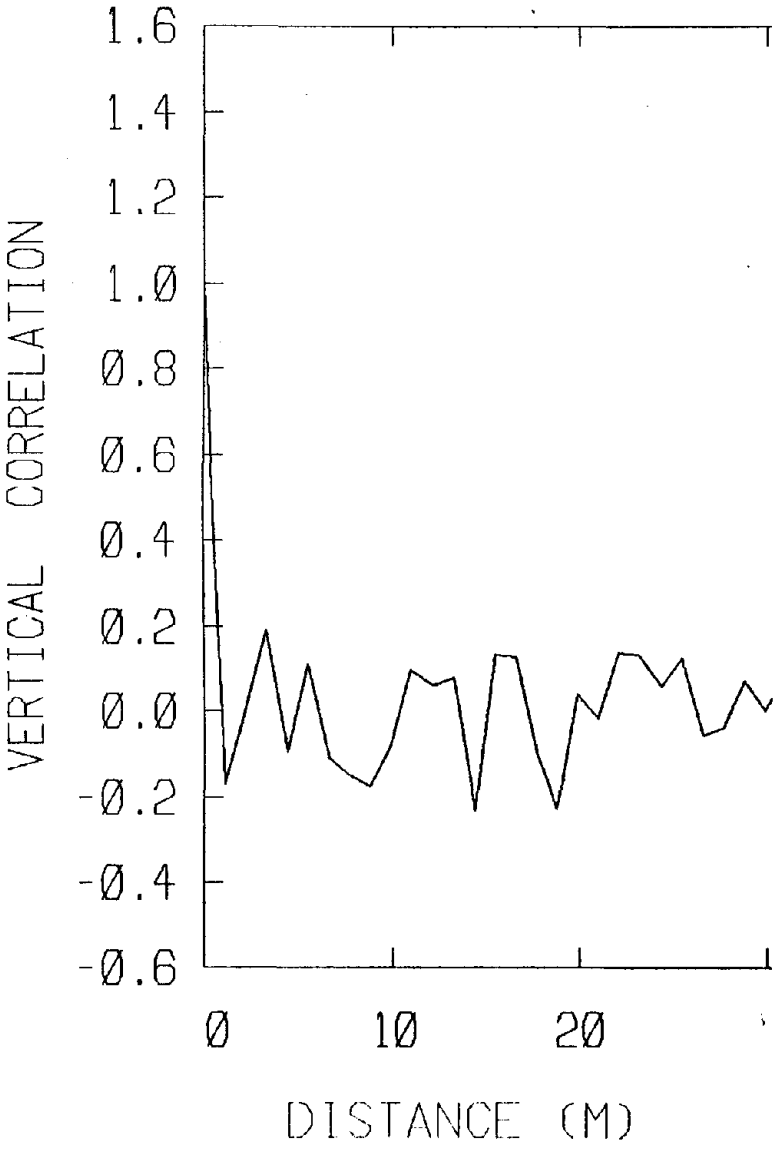

Figure 8.103 - Vertical correlation of residual Morenci copper dry density area

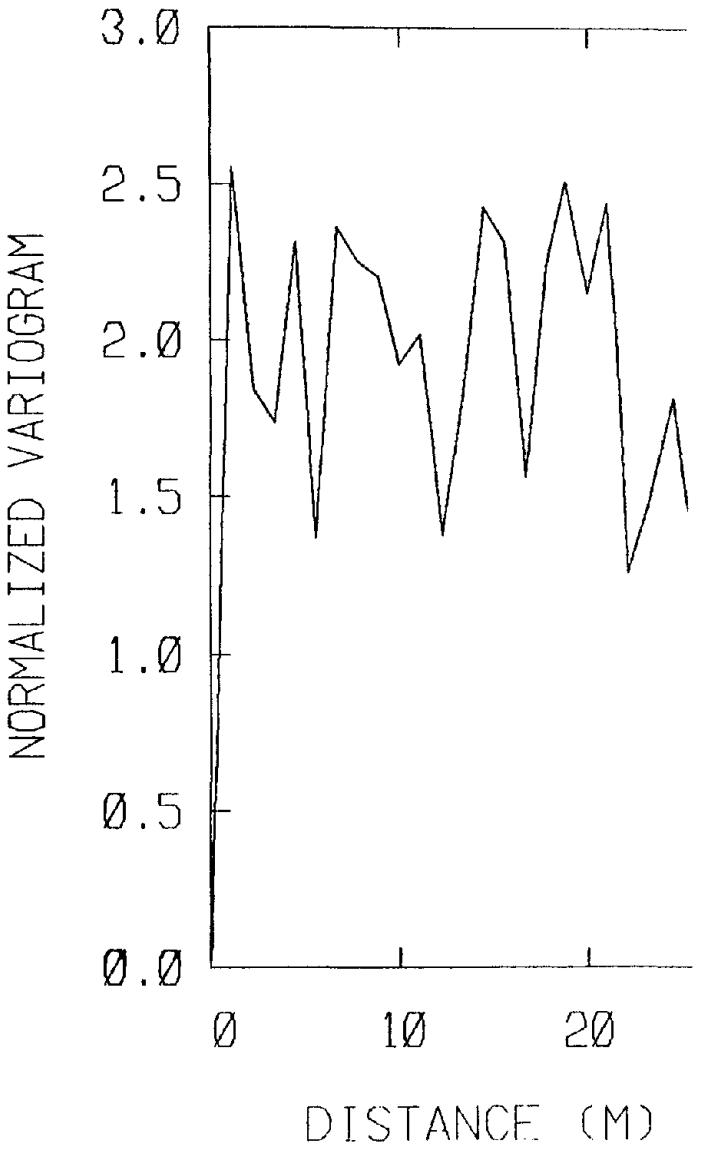

Figure 8.104 - Normalized variogram of residual Morenci copper dry density area

SITE Morenci (Copper)

DATA Type Water Content (combined)

Number 64

Quality Index NA

TREND WITH DEPTH w/c(%) = 2.26 + 0.02z(m)

DATA SCATTER

	mean	SD	β_1	β_2
Raw Data	22.8	2.24	0.017	2.66
Residual Data	--	2.21	0.0001	2.41

GOODNESS OF FIT STATISTICS

	Raw		Residual	
	χ^2	D_m	χ^2	D_m
normal	10.4	0.049	12.3	0.075
beta	16.7	0.079	13.6	0.079
exponential	457.1	0.518	--	--
lognormal	9.75	0.051	--	--
gamma	9.83	0.047	--	--
5% confidence limit	23.7	0.17	--	--

INTERPRETED STRENGTH PARAMETERS NA

Table 8.18 - Table of Morenci copper water content data

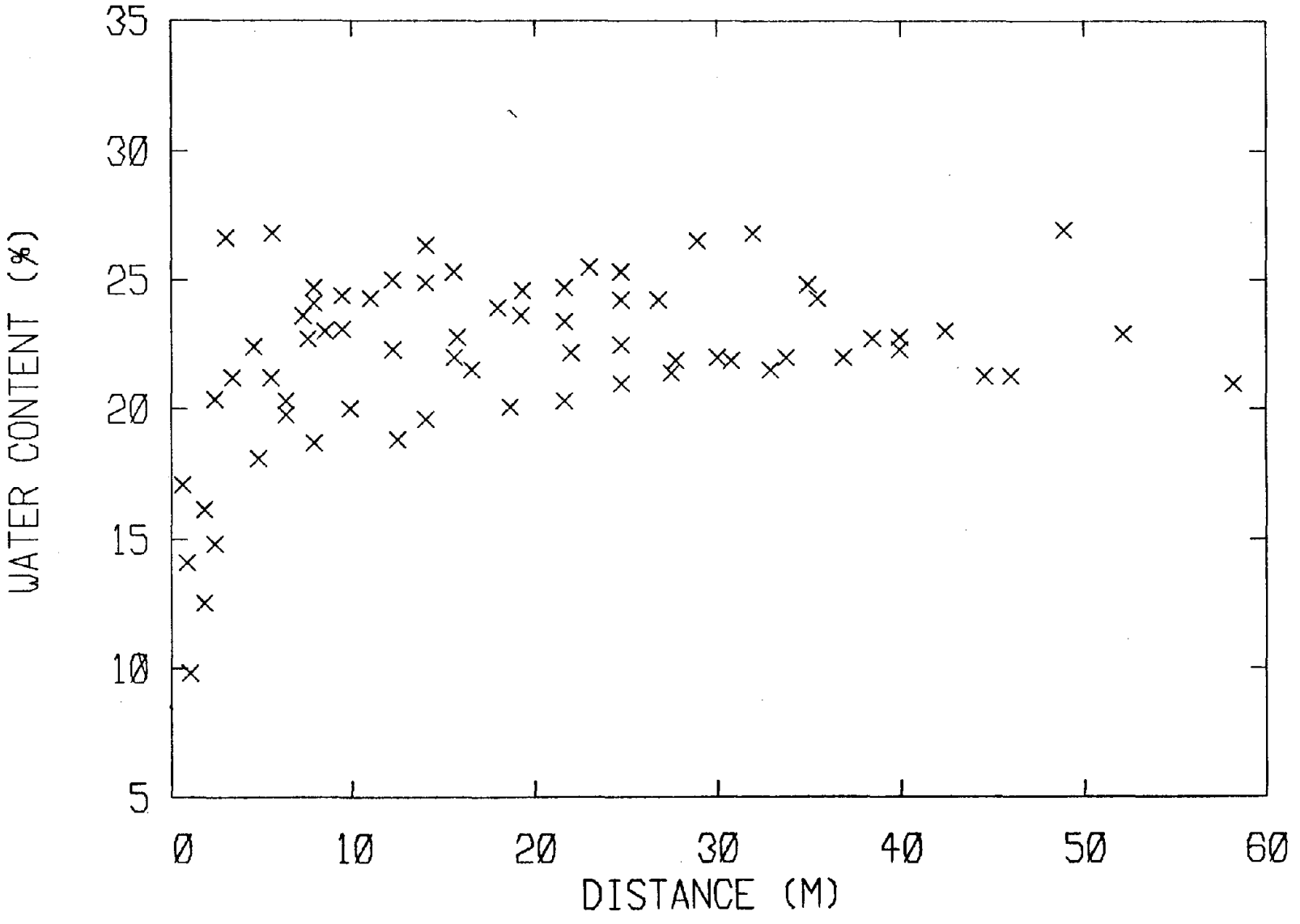

Figure 8.105 - Water content v. depth for Morenci copper

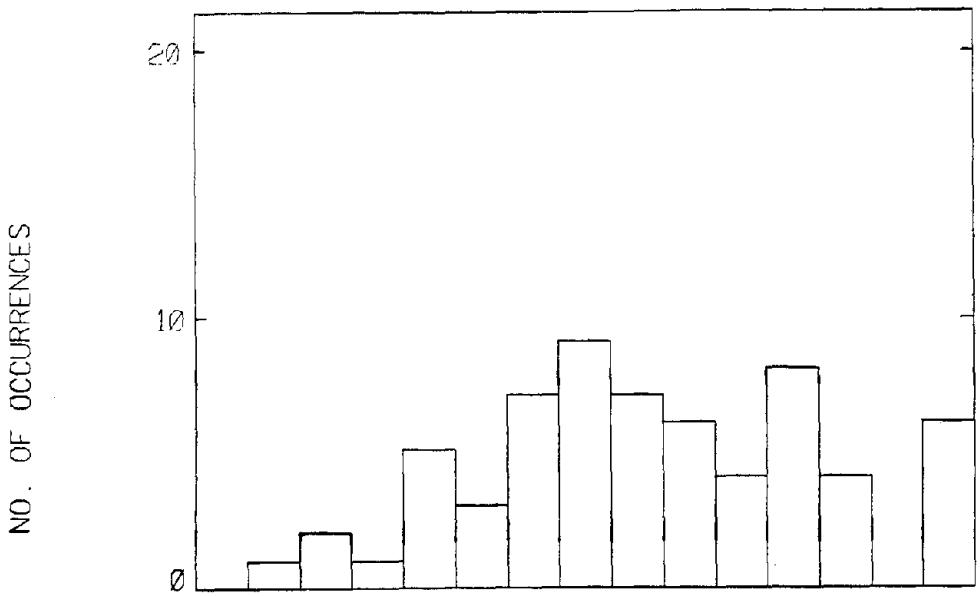

Figure 8.106 - Histogram of Morenci copper raw water content data

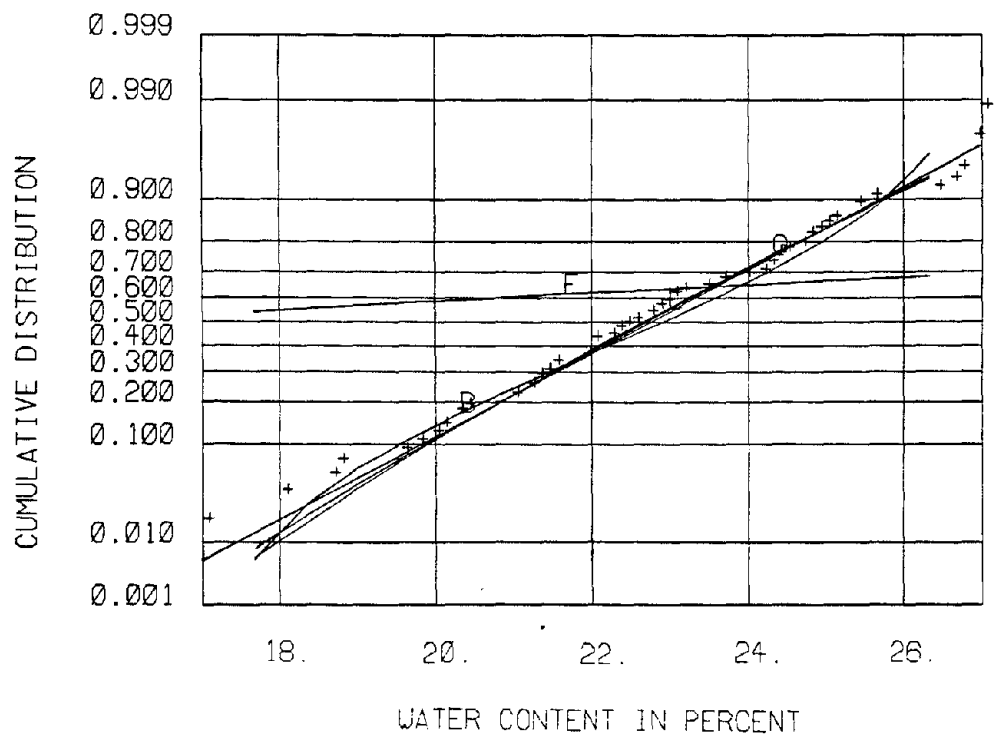

Figure 8.107 - CDF of raw Morenci copper water content data compared to standard CDF plots

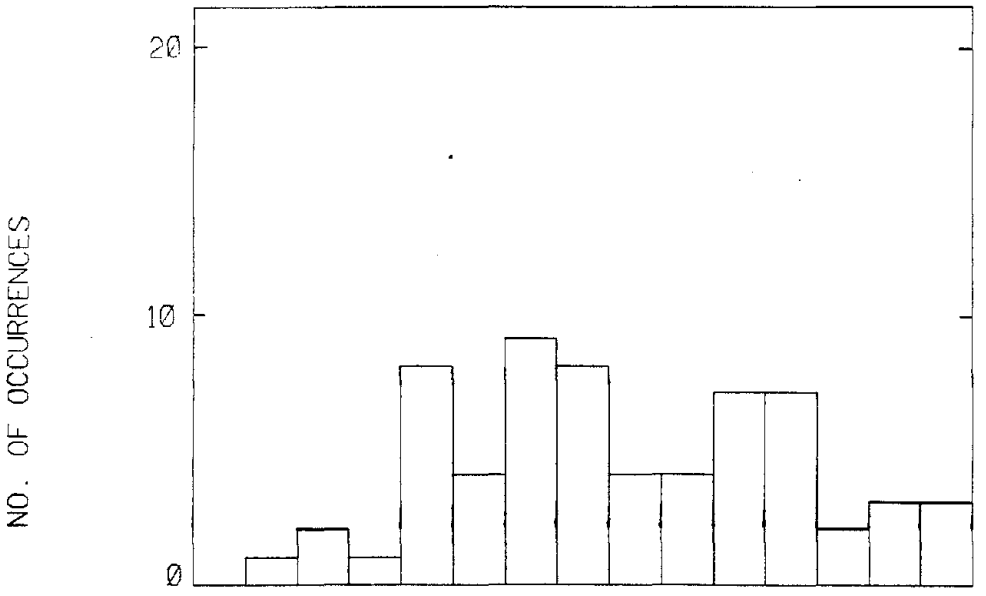

Figure 8.108 - Histogram of residual Morenci copper water content data

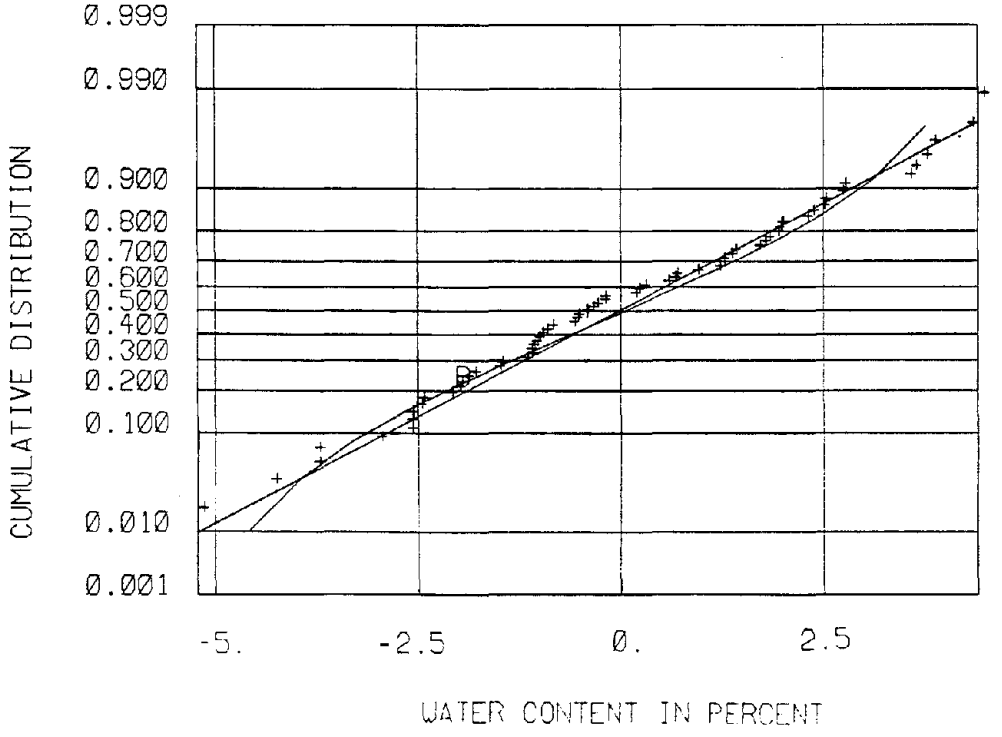

Figure 8.109 - CDF of residual Morenci copper water content data compared to standard CDF plots

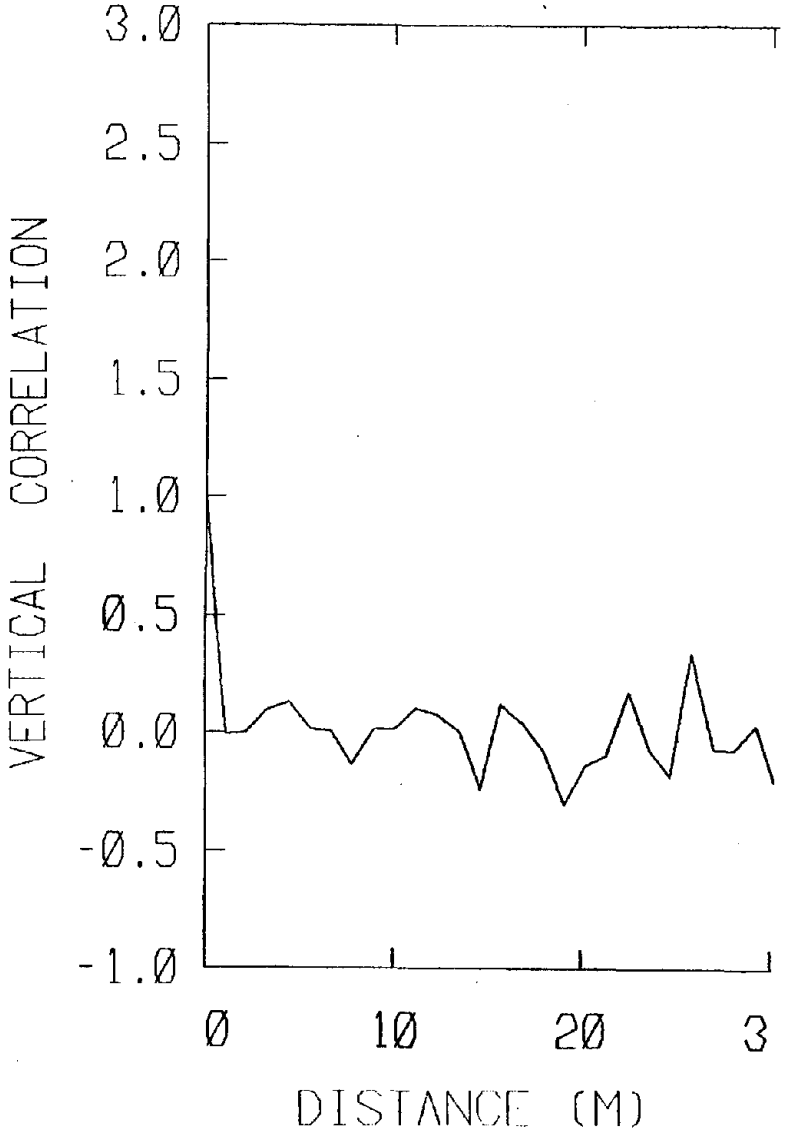

Figure 8.110 - Vertical correlation of residual Morenci copper water content data

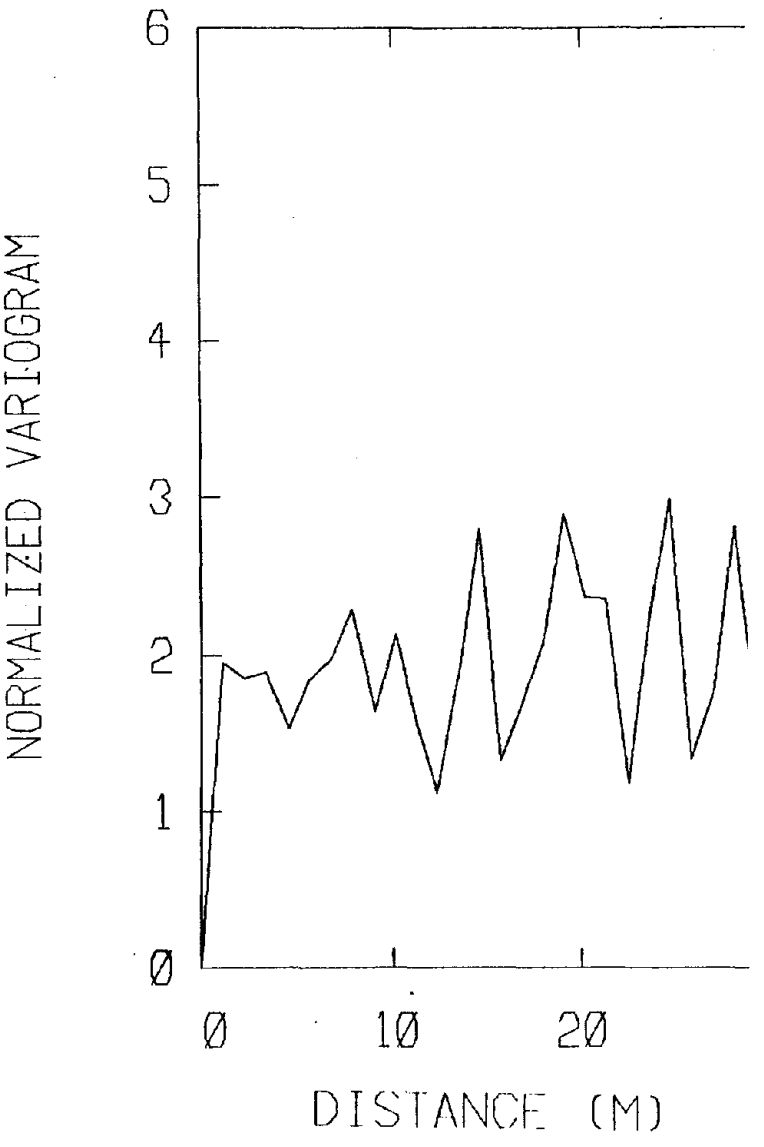

Figure 8.111 - Normalized variogram of residual Morenci copper water content data

Table 8.19 - Uranium tailings summary data

SITE	DATA TYPE	NO. TESTS	MEAN	COV*
Colorado	SPT#	785	13.6	0.52

*Coefficient of Variation #Standard Penetration Test

SITE	Global (Uranium) Triaxial Friction Angles, $\bar{\phi}$	
DATA	Type	Triaxial Tests
	Number	23
	Quality Index	
TREND WITH DEPTH	N/A	

DATA SCATTER

	mean	SD	β_1	β_2
Raw Data	35.8	6.04	0.202	3.02
Residual Data	--	--	--	--

GOODNESS OF FIT STATISTICS

	Raw		Residual	
	χ^2	D_m	χ^2	D_m
normal	11.2	0.150	--	--
beta	16.2	0.157	--	--
exponential	115	0.459	--	--
lognormal	8.88	0.115	--	--
gamma	9.44	0.125	--	--
5% confidence limit	23.7	0.284	--	--

INTERPRETED STRENGTH PARAMETERS

Table 8.20 - Table of uranium global averages for triaxial friction angles

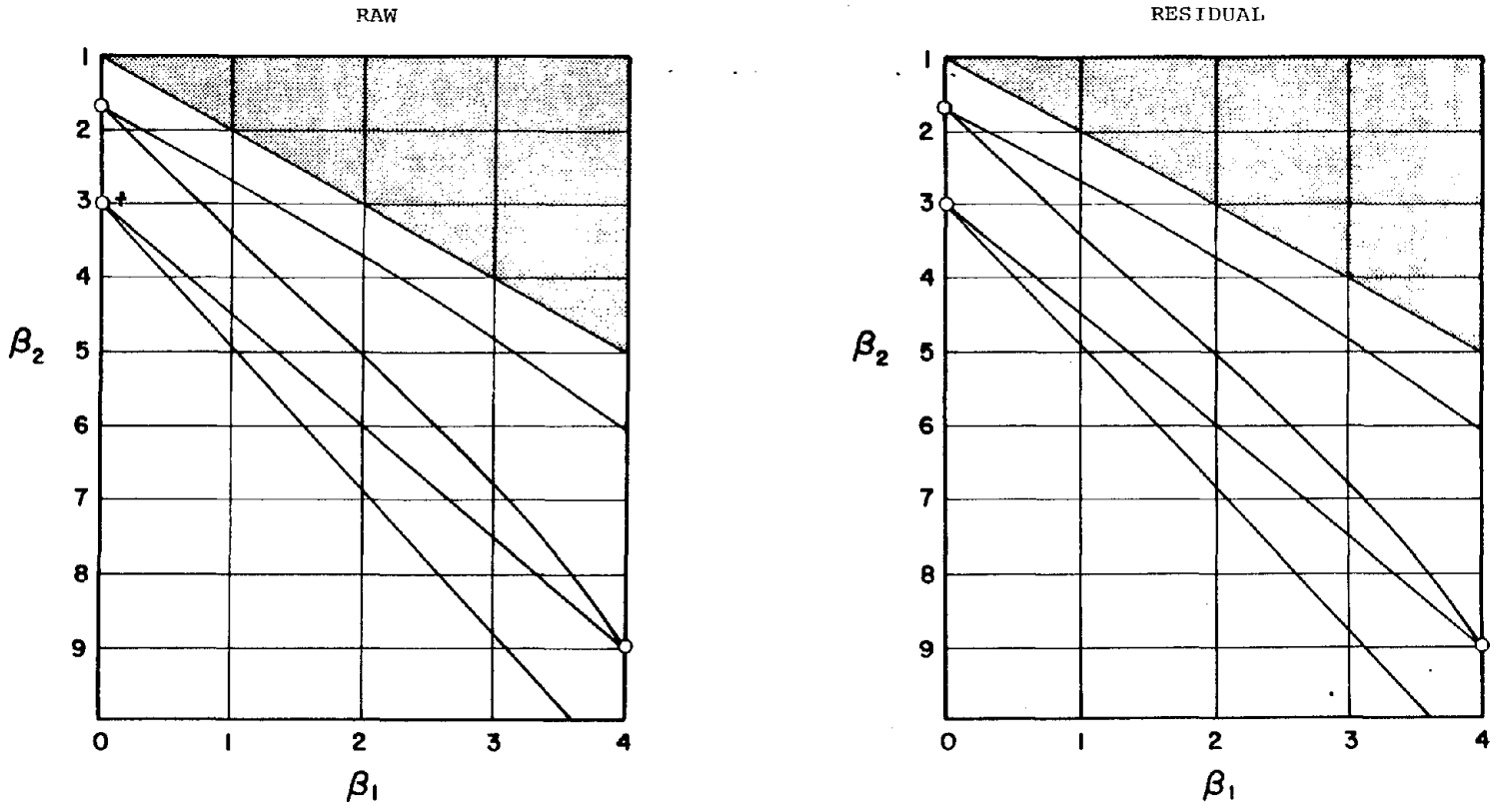

Figure 8.112 - Pearson diagram of raw and residual triaxial friction angle data for global uranium results

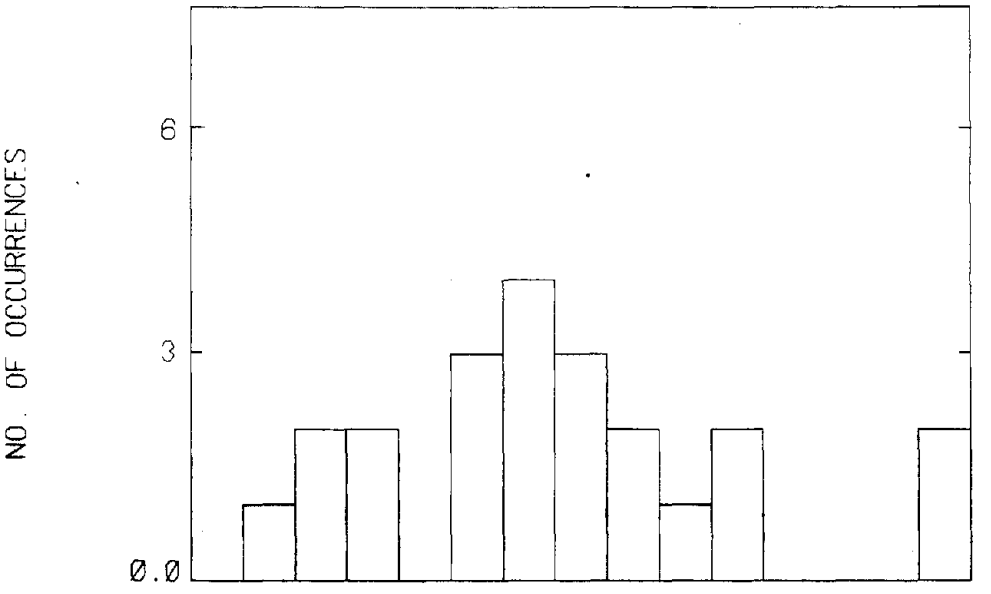

Figure 8.113 - Histogram of raw global uranium triaxial friction angle data

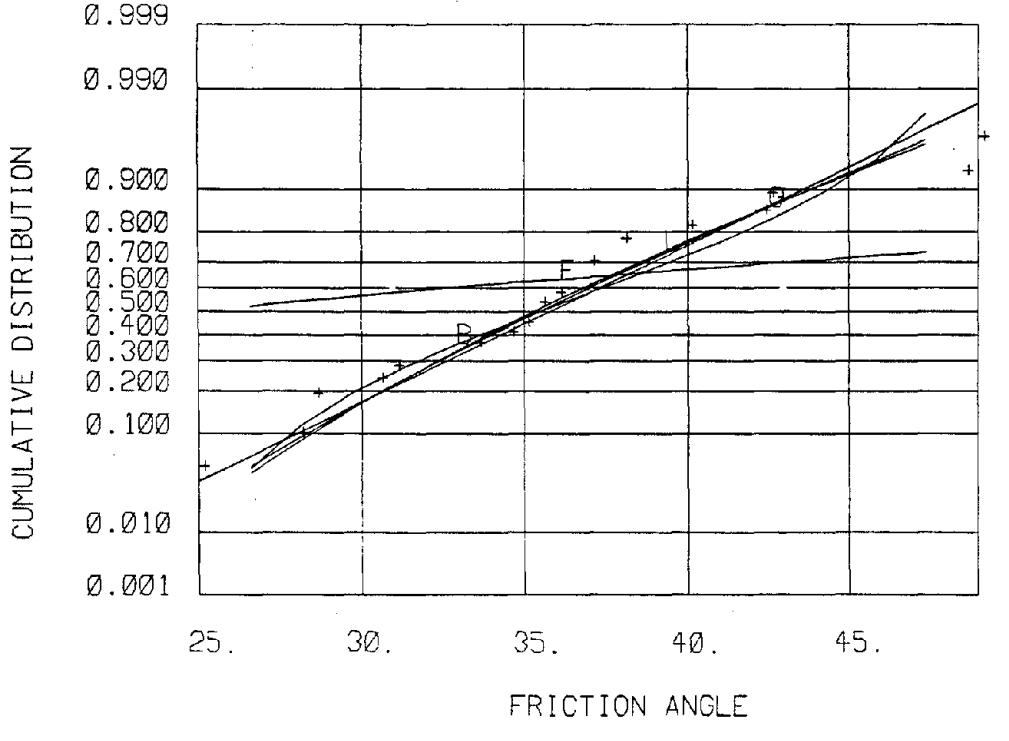

Figure 8.114 - CDF of raw global uranium triaxial friction angle data compared to standard CDF plots

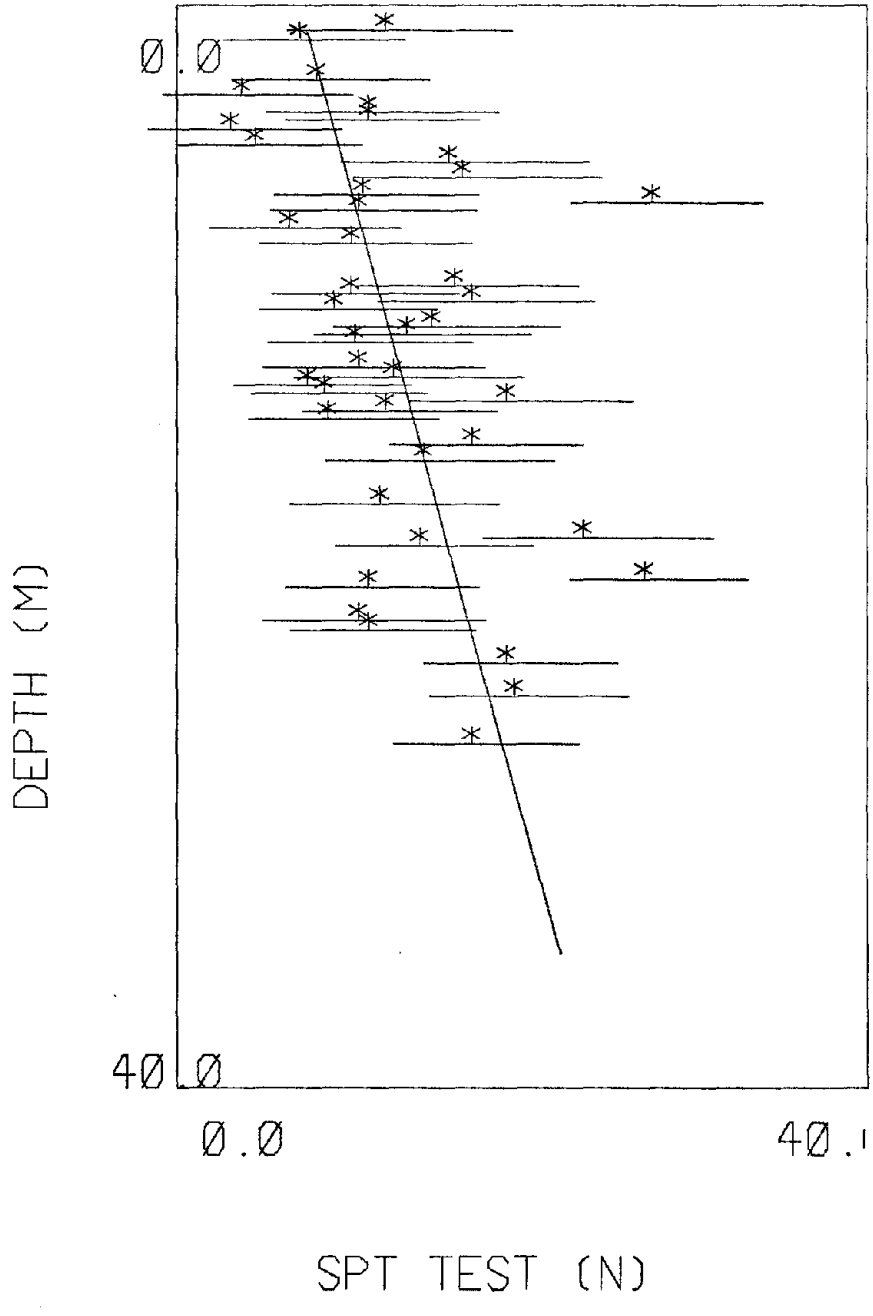

Figure 8.115 - SPT (N) v. depth for Colorado uranium data

SITE	Colorado (Uranium) USA	
DATA	Type	26 SPT Borings
	Number	785
	Quality Index	A

TREND WITH DEPTH $N = 7.21 + 0.131z(m)$

DATA SCATTER

	mean	SD	β_1	β_2
Raw Data	13.6	8.18	0.88	3.82
Residual Data	--	7.08	1.18	4.80

GOODNESS OF FIT STATISTICS

	Raw		Residual	
	χ^2	D_m	χ^2	D_m
normal	252	0.074	182	0.094
beta	153	0.090	141	0.102
exponential	300	0.254	--	--
lognormal	183	0.118	--	--
gamma	38.1	0.091	--	--
5% confidence limit	23.7	0.049	--	--

INTERPRETED STRENGTH PARAMETERS II

Table 8.21 - Table of Colorado uranium SPT data

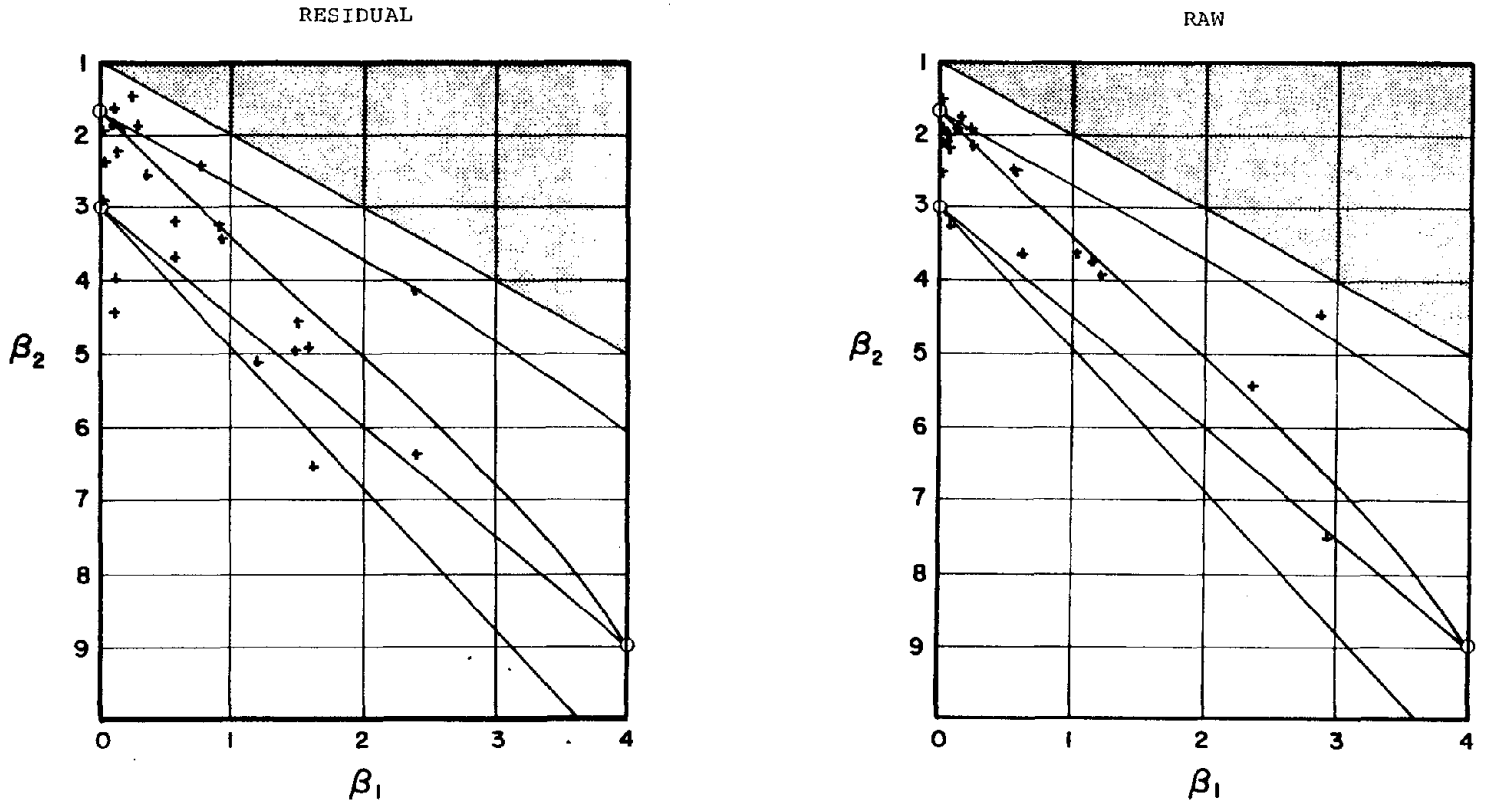

Figure 8.116 Pearson diagram of raw and residual SPT data for Colorado uranium

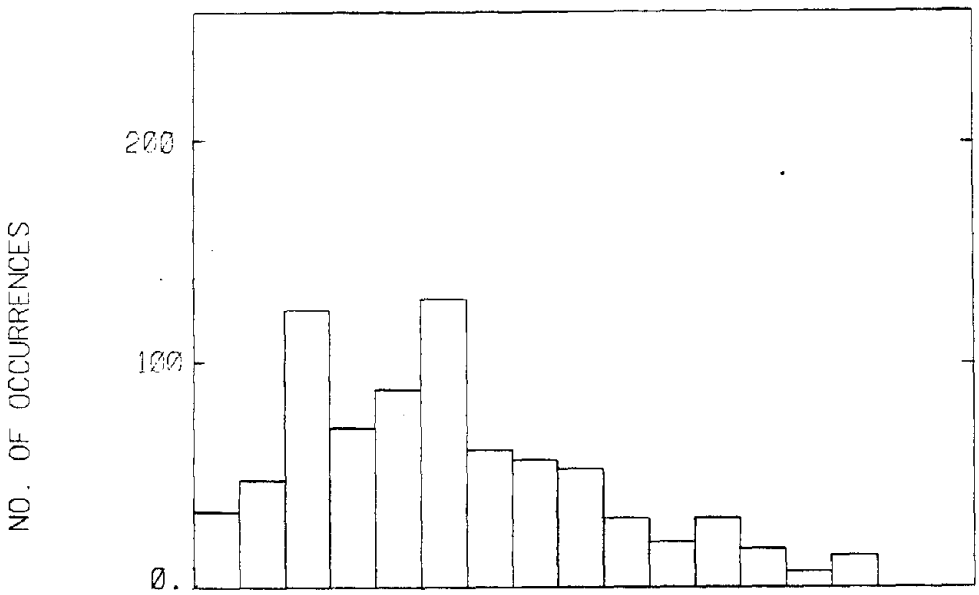

Figure 8.117 - Histogram of raw colorado uranium SPT data

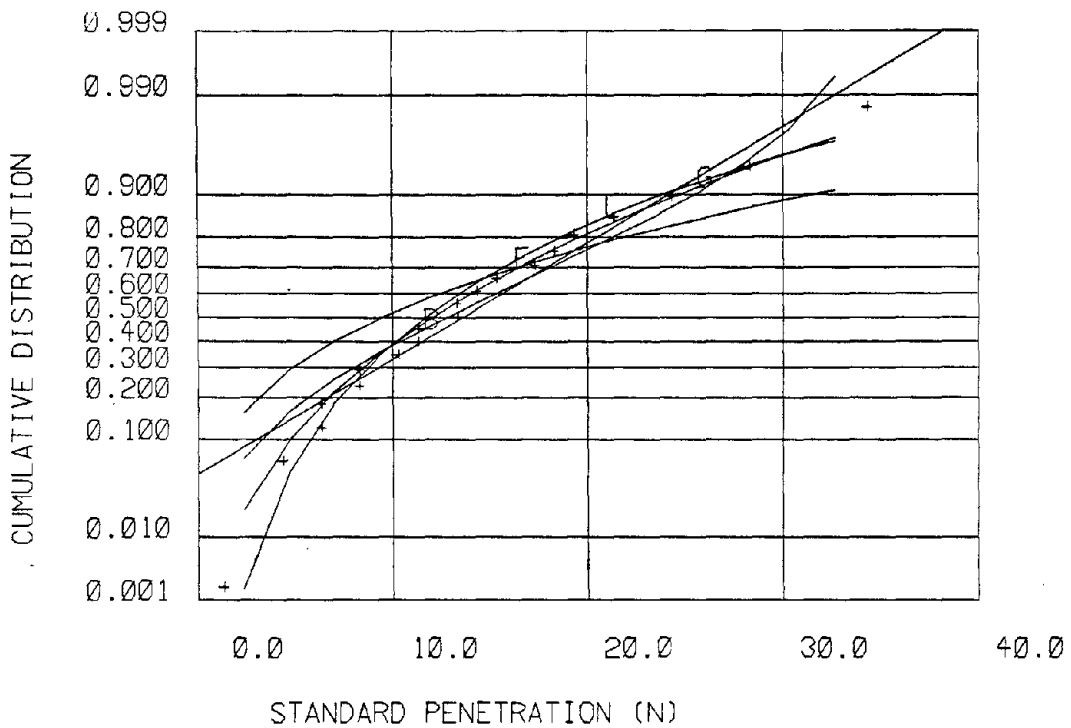

Figure 8.118 - CDF of raw Colorado uranium SPT data compared to standard CDF plots

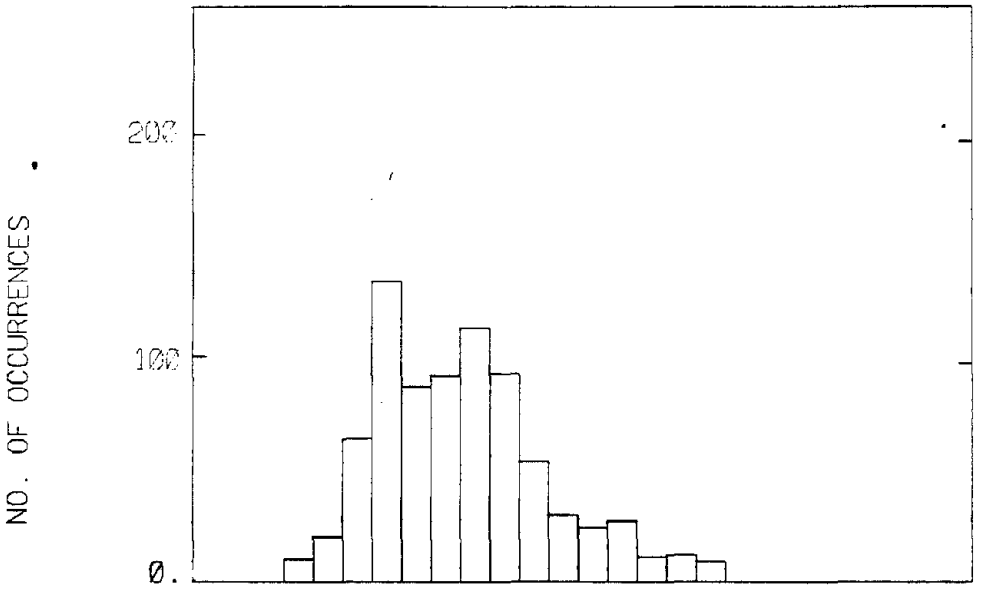

Figure 8.119 - Histogram of residual Colorado uranium SPT data

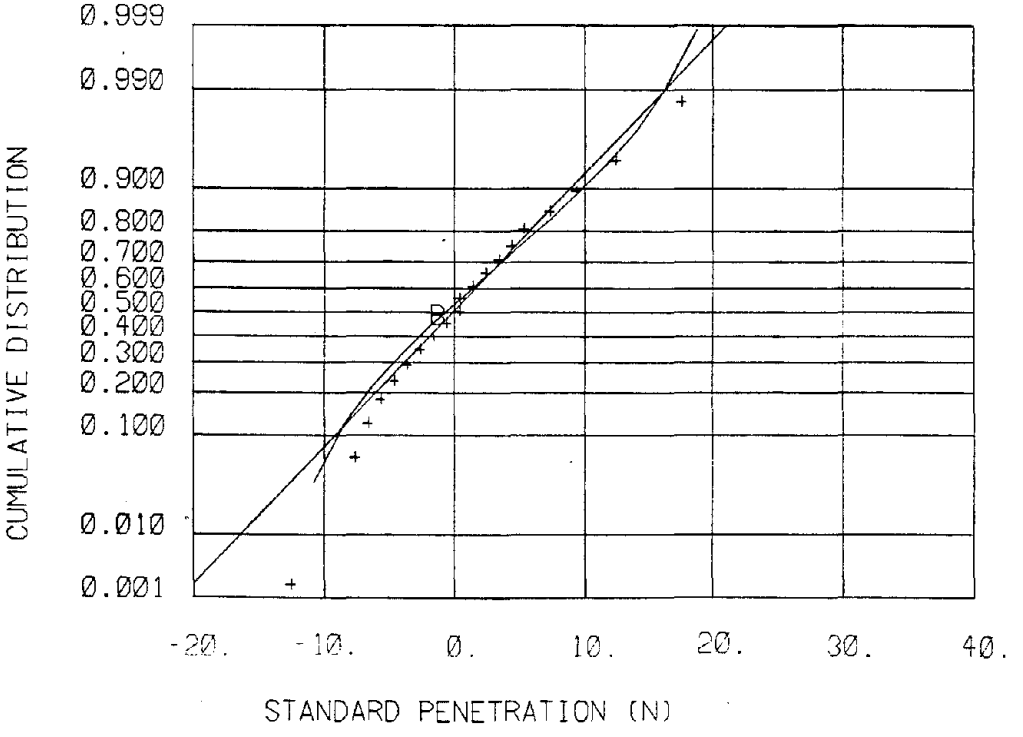

Figure 8.120 - CDF of residual Colorado uranium SPT data compared to standard CDF plots

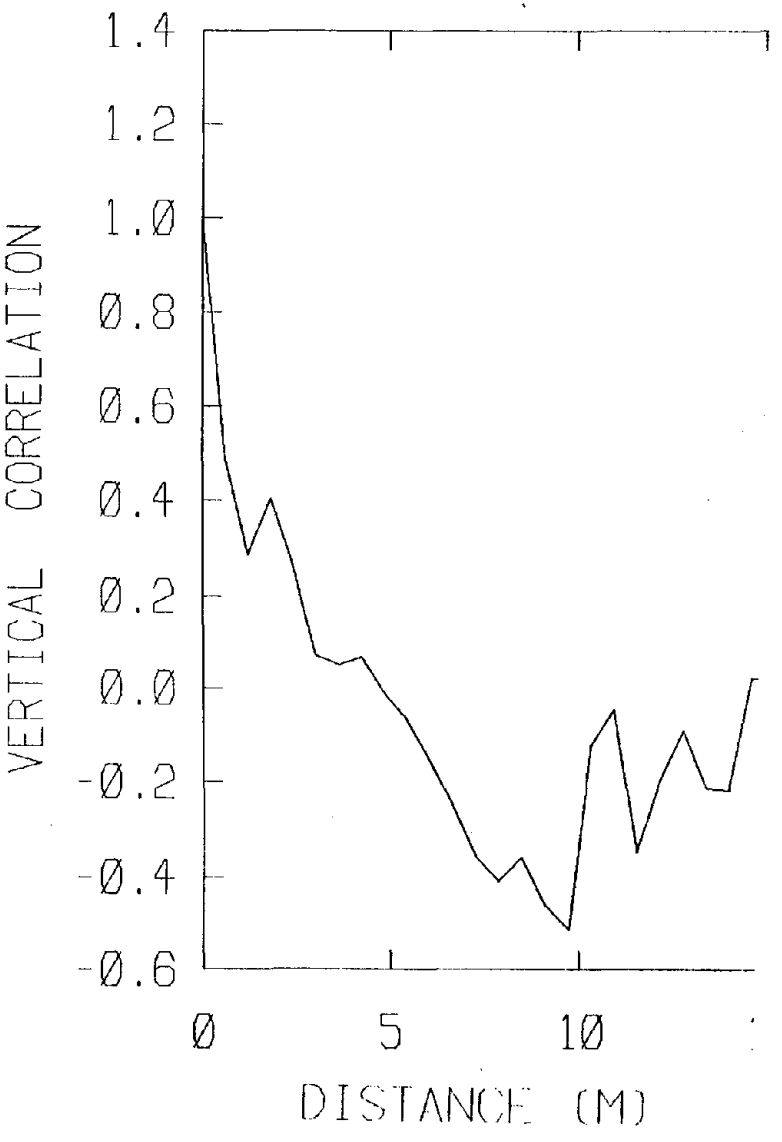

Figure 8.121 - Vertical correlation of residual Colorado uranium SPT data

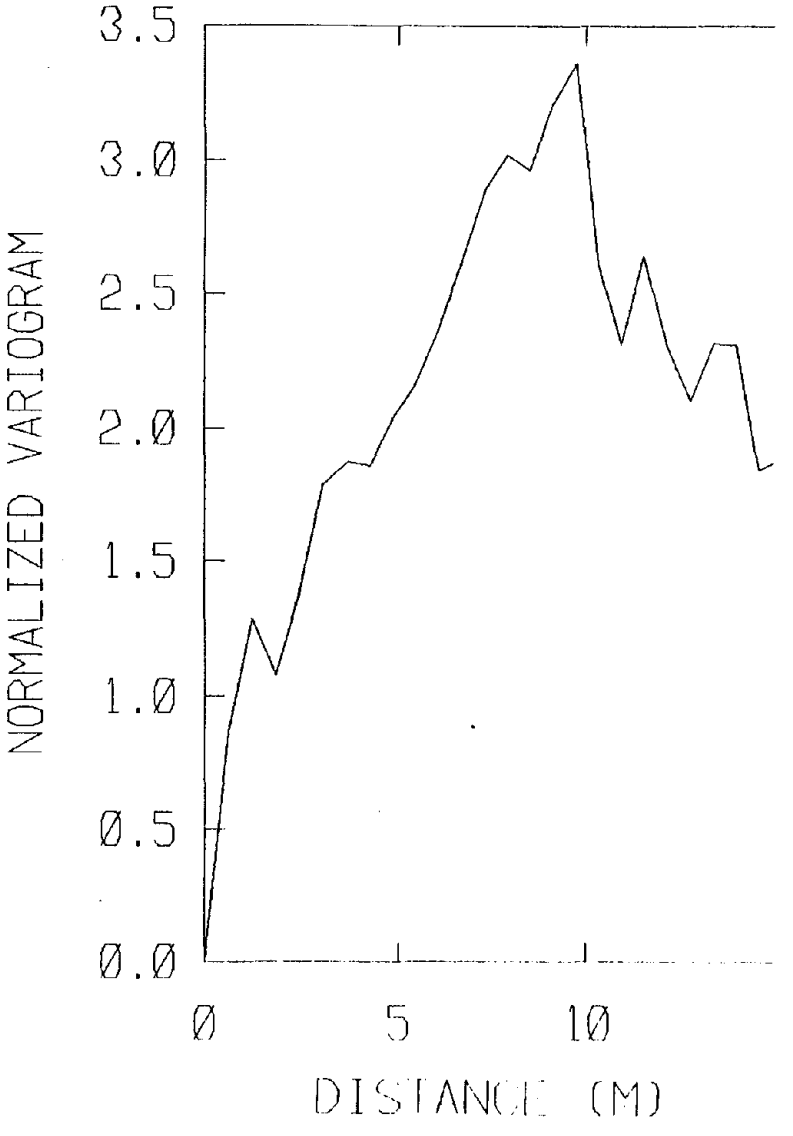

Figure 8.122 - Normalized variogram of residual Colorado uranium SPT data

Table 8.22 - Gypsum tailings summary data

SITE	DATA TYPE	NO. TESTS	MEAN	COV*
Texas	SPT#	40	24.7	0.42
Louisiana1 (lower)	SPT	89	4.3	0.50
Louisiana1 (upper)	SPT	91	21.2	0.66
Florida1	SPT	111	12.7	0.65
Vick	SPT	20	33.9	0.58
Piney Point	CPT&	92	161.0	0.52

*Coefficient of Variation #Standard Penetration Test
&Cone Penetration Test

SITE Commodity: Gypsum

DATA Type: Site Average Friction Angles

Number: 19

Quality Index:

TREND WITH DEPTH: N/A

DATA SCATTER

	mean	SD	β_1	β_2
Raw Data	41.6	5.8	0.146	2.68
Residual Data	--	--	--	--

GOODNESS OF FIT STATISTICS

	Raw		Residual	
	χ^2	D_m	χ^2	D_m
normal	15.0	0.158	--	--
beta	16.7	0.137	--	--
exponential	157	0.484	--	--
lognormal	13.9	0.153	--	--
gamma	14.2	0.154	--	--
5% confidence limit	23.7	0.30	--	--

INTERPRETED STRENGTH PARAMETERS

Table 8.23 - Table of gypsum global averages for site average friction angles

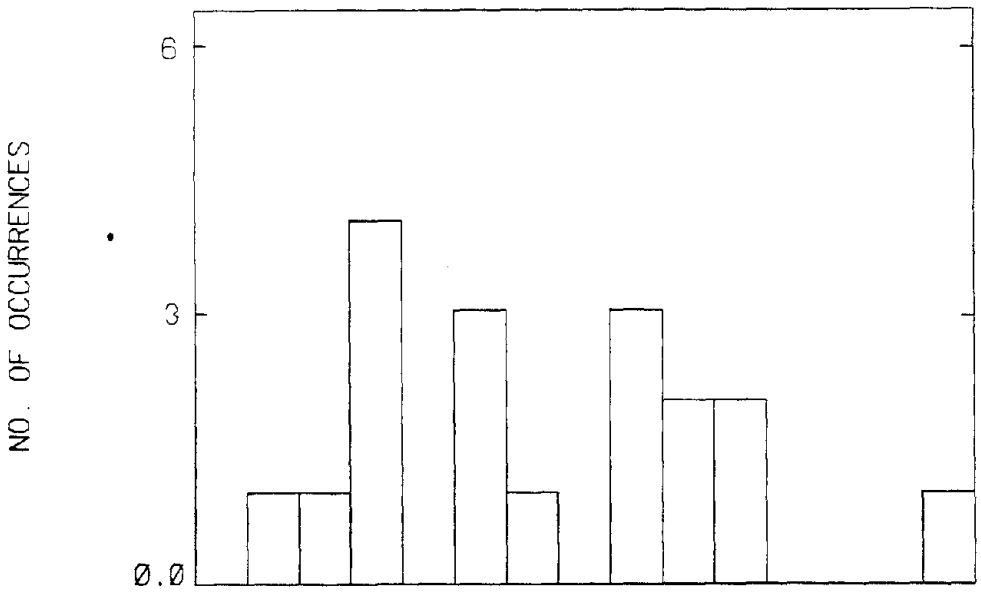

Figure 8.123 - Histogram of raw global gypsum site friction angles

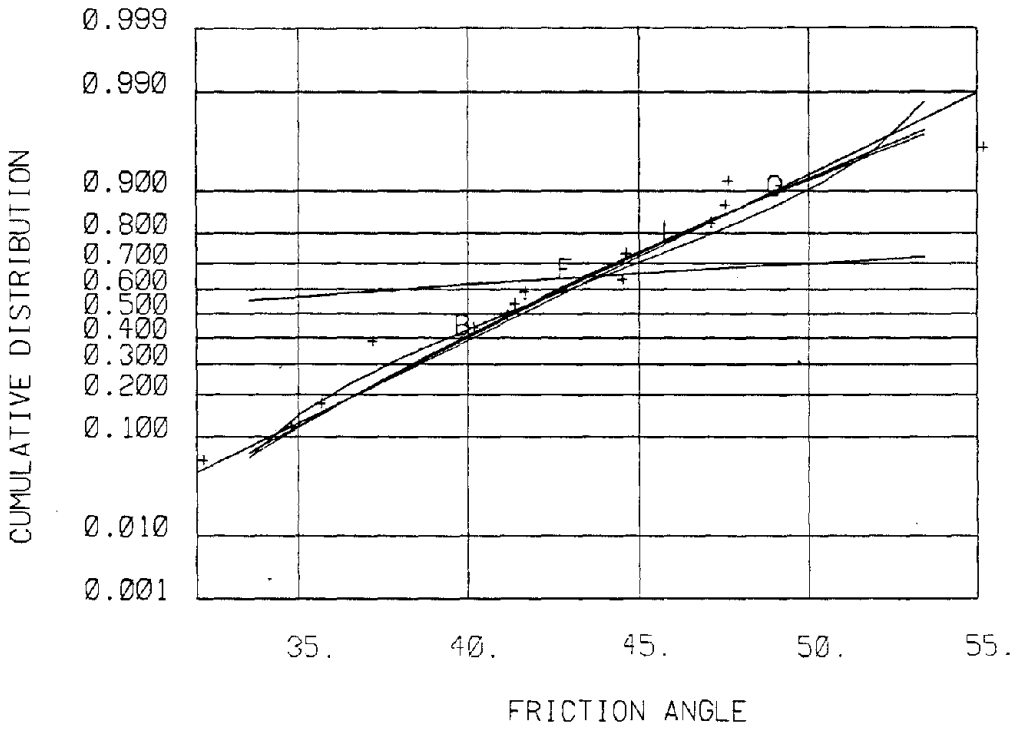

Figure 8.124 - CDF of raw global gypsum site friction angles compared to standard CDF plots

SITE	Commodity:	Gypsum Global Data
DATA	Type	Peak Friction Angles
	Number	34
	Quality Index	
TREND WITH DEPTH		N/A

DATA SCATTER

	mean	SD	β_1	β_2
Raw Data	45.6	5.61	0.752	2.84
Residual Data	--	--	--	--

GOODNESS OF FIT STATISTICS

	Raw		Residual	
	χ^2	D_m	χ^2	D_m
normal	34.4	0.144	--	--
beta	35.2	0.166	--	--
exponential	316	0.526	--	--
lognormal	28.3	0.133	--	--
gamma	30.1	0.136	--	--
5% confidence limit	23.7	0.23	--	--

INTERPRETED STRENGTH PARAMETERS NA

Table 8.24 - Table of gypsum global data for residual friction angles

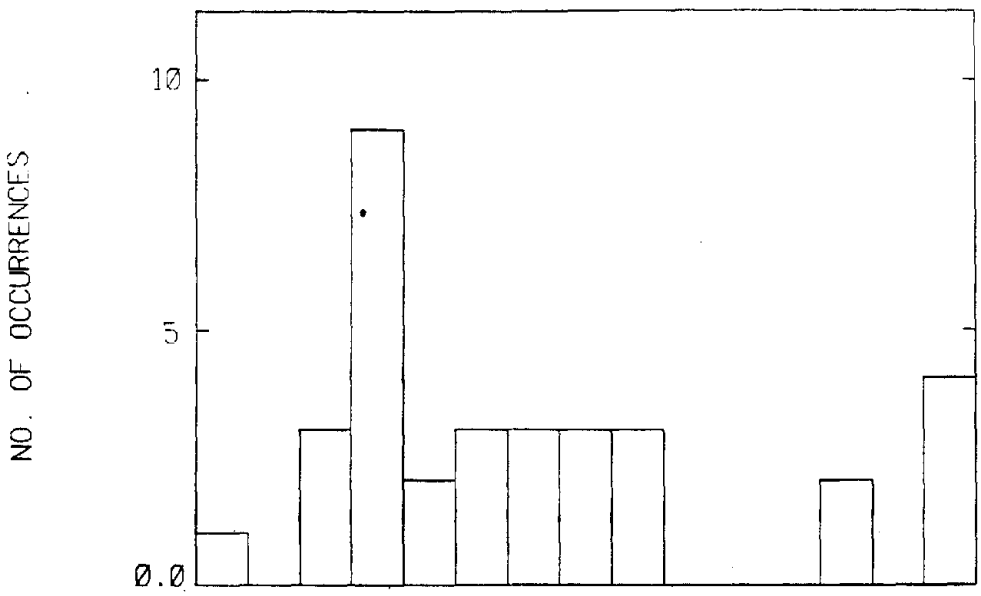

Figure 8.125 - Histogram of raw global gypsum peak friction angles

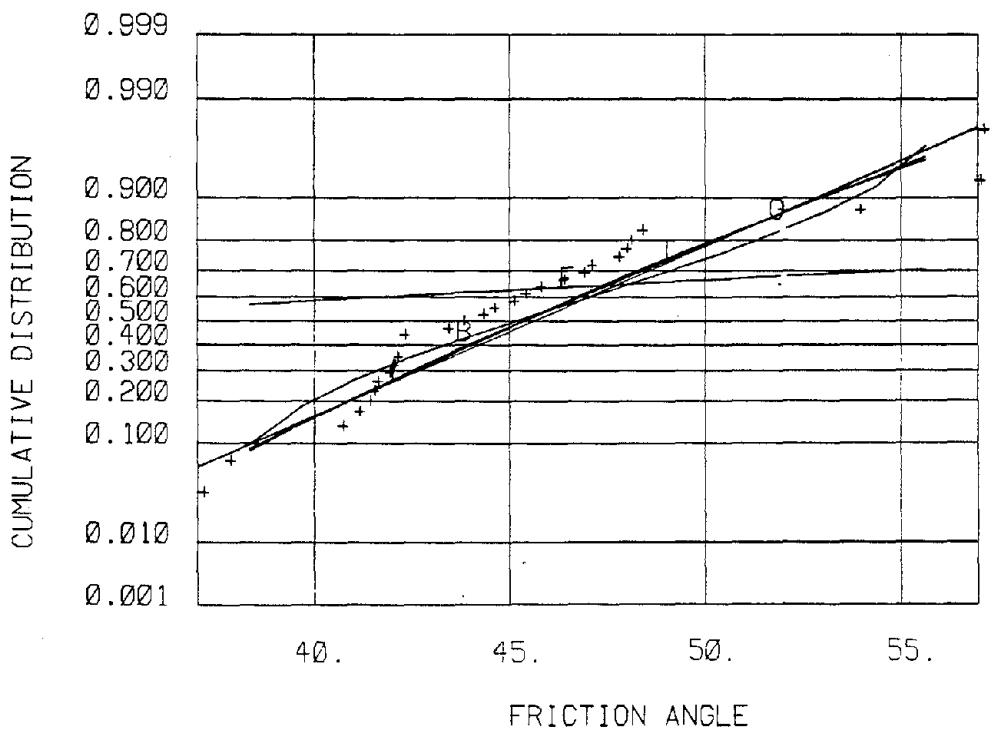

Figure 8.126 - CDF of raw global gypsum peak friction angles compared to standard CDF plots

SITE Commodity: Gypsum

DATA Type Residual Friction Angles

Number 18

Quality Index

TREND WITH DEPTH N/A

DATA SCATTER

	mean	SD	β_1	β_2
Raw Data	42.2	4.71	0.683	2.90
Residual Data	--	--	--	--

GOODNESS OF FIT STATISTICS

	Raw		Residual	
	χ^2	D_m	χ^2	D_m
normal	12.7	0.109	--	--
beta	11.7	0.121	--	--
exponential	179	0.471	--	--
lognormal	13.9	0.112	--	--
gamma	13.4	0.112	--	--
5% confidence limit	23.7	0.31	--	--

INTERPRETED STRENGTH PARAMETERS

Table 8.25 - Table of gypsum global data for residual friction angles

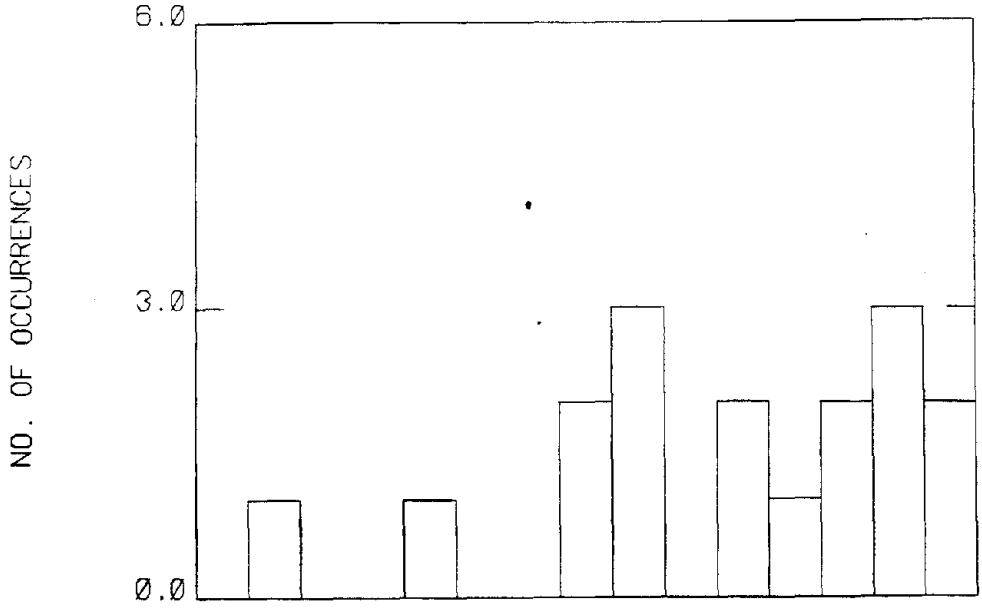

Figure 8.127 - Histogram of raw global gypsum residual friction angles

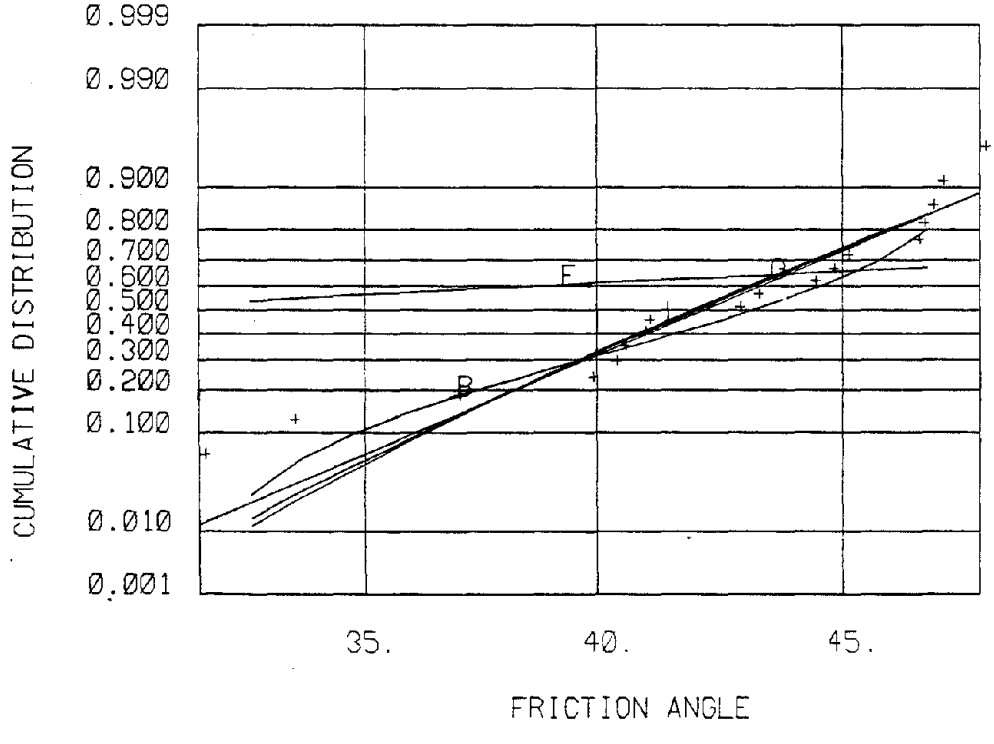

Figure 8.128 - CDF of raw global gypsum residual friction angles compared to standard CDF plots

SITE Texas (Gypsum)

DATA Type SPT Borings

Number 40

Quality Index A

TREND WITH DEPTH N = 22.2 + 0.032 (ft)

DATA SCATTER

	mean	SD	β_1	β_2
Raw Data	24.7	10.5	0.834	4.25
Residual Data	--	10.4	1.13	4.42

GOODNESS OF FIT STATISTICS

	Raw		Residual	
	χ^2	D_m	χ^2	D_m
normal	20.3	0.099	23.8	0.143
beta	30.0	0.102	27.9	0.092
exponential	51.2	0.281	--	--
lognormal	11.0	0.064	--	--
gamma	10.3	0.070	--	--
5% confidence limit	23.7	0.21	--	--

INTERPRETED STRENGTH PARAMETERS 35°

Table 8.26 - Table of Texas gypsum SPT data

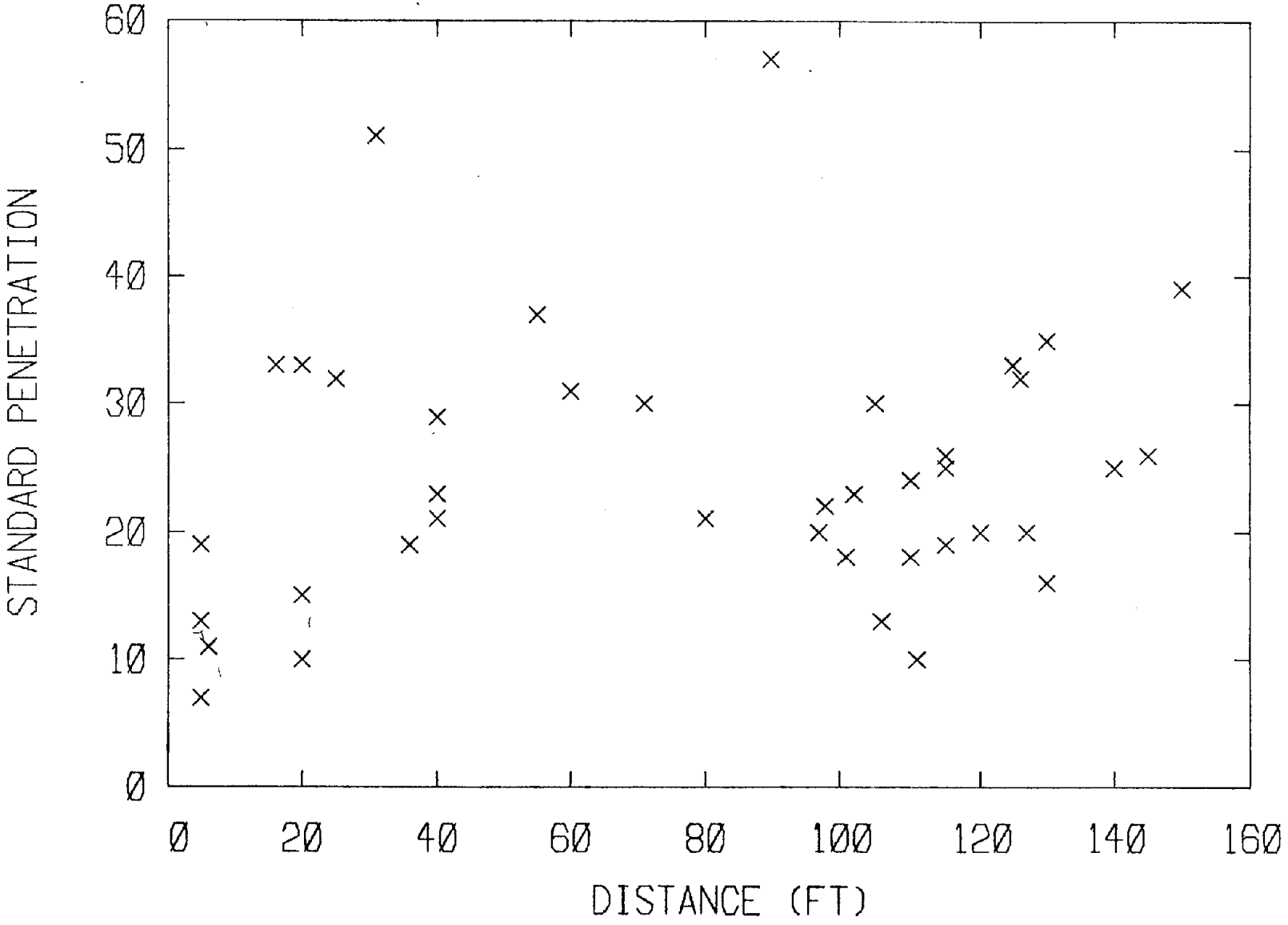

Figure 8.129 - SPT (N) v. depth for Texas gypsum

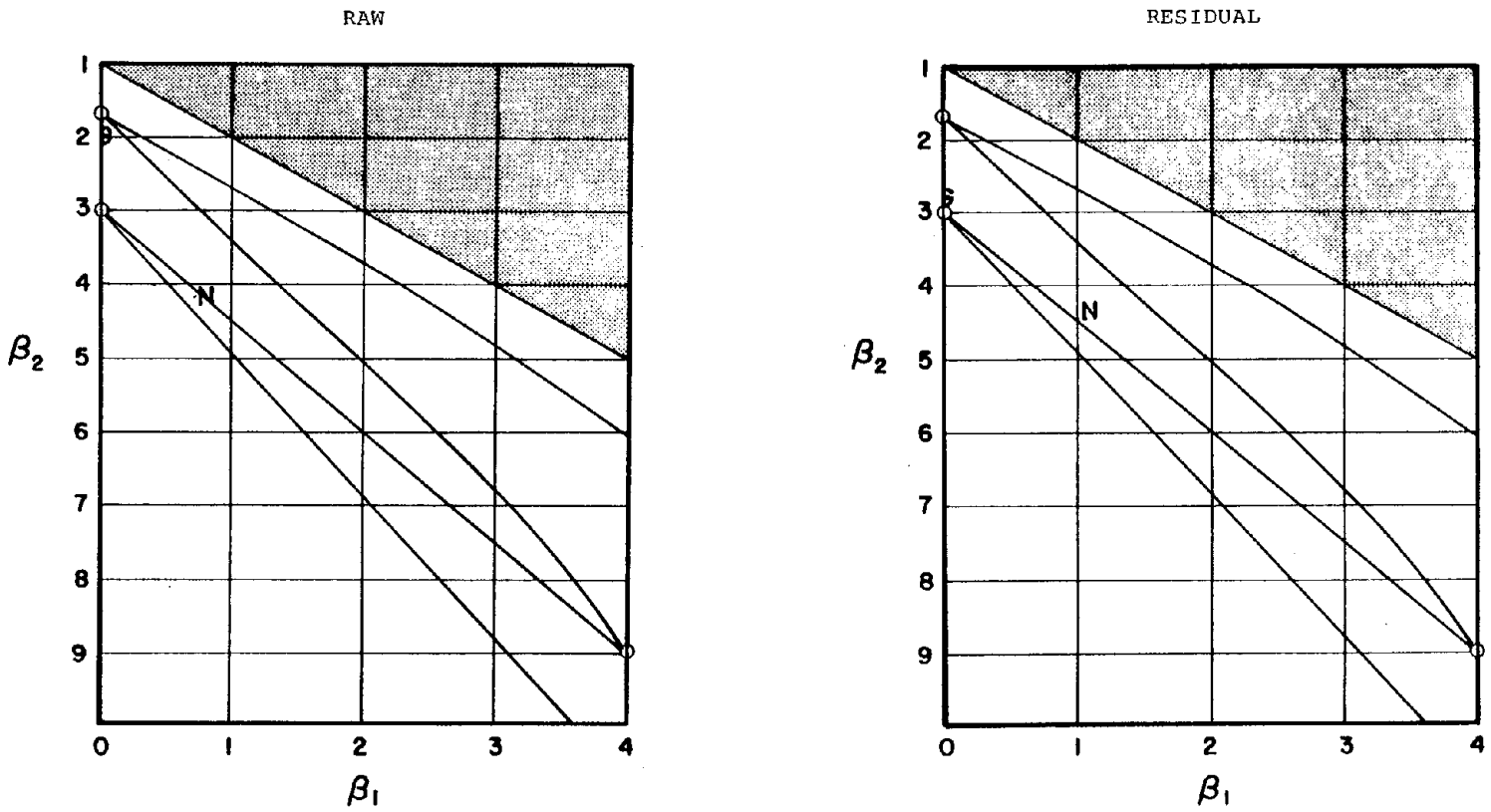

Figure 8.130 - Pearson diagrams of raw and residual SPT data for Texas gypsum

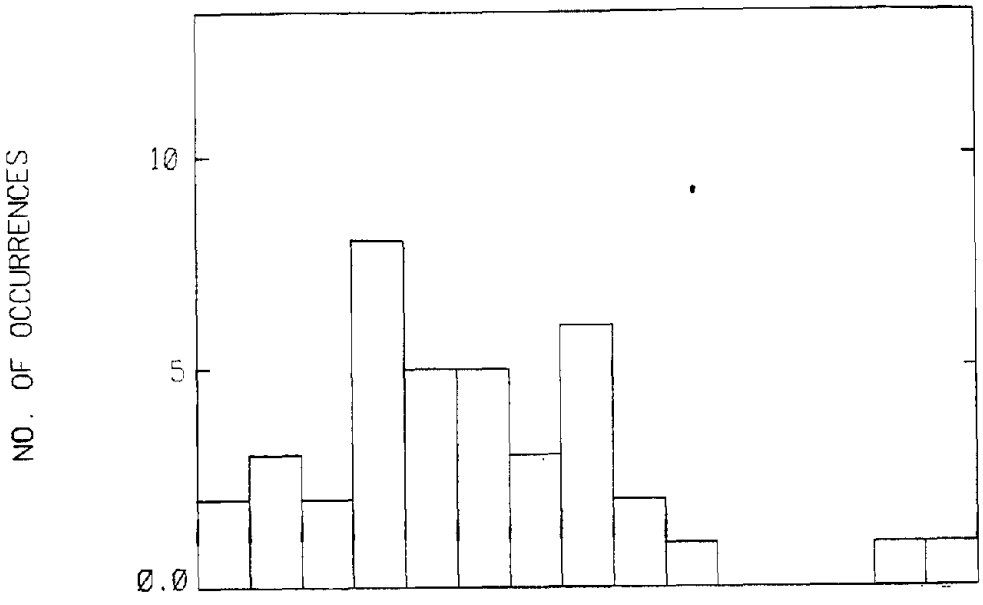

Figure 8.131 - Histogram of raw Texas gypsum SPT data

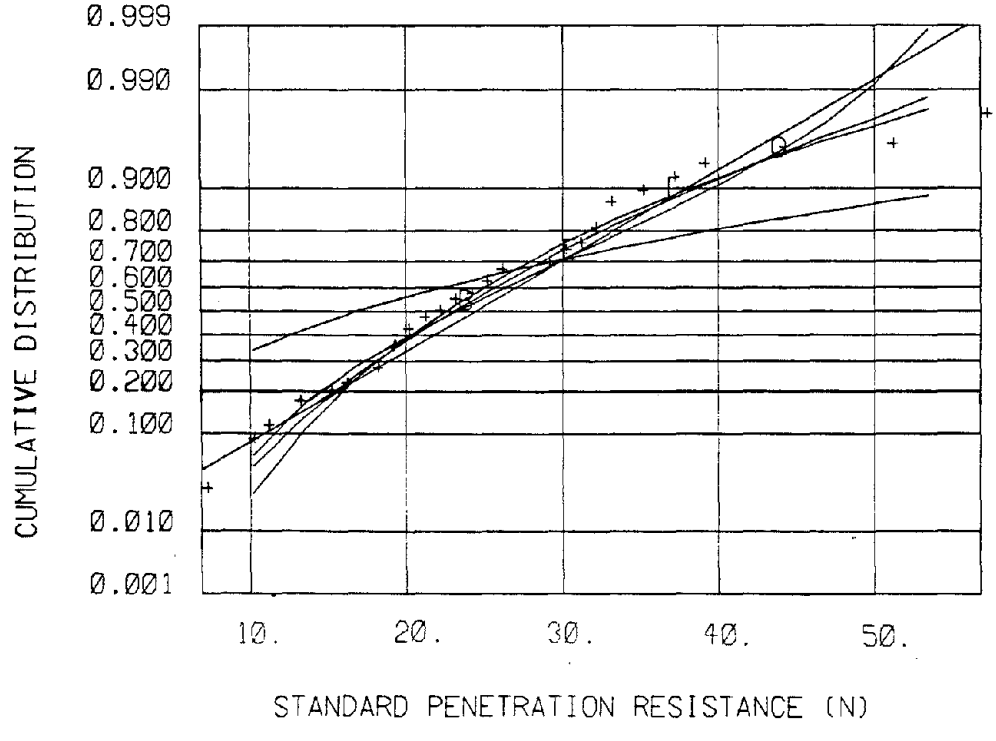

Figure 8.132 - CDF of raw Texas gypsum SPT data compared to standard CDF plots

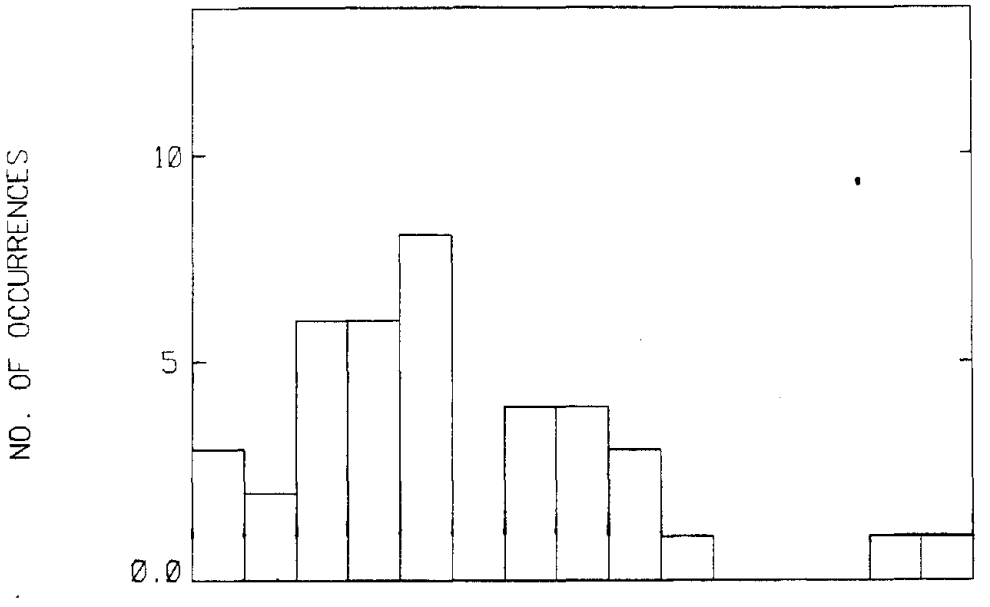

Figure 8.133 - Histogram of residual Texas gypsum SPT data

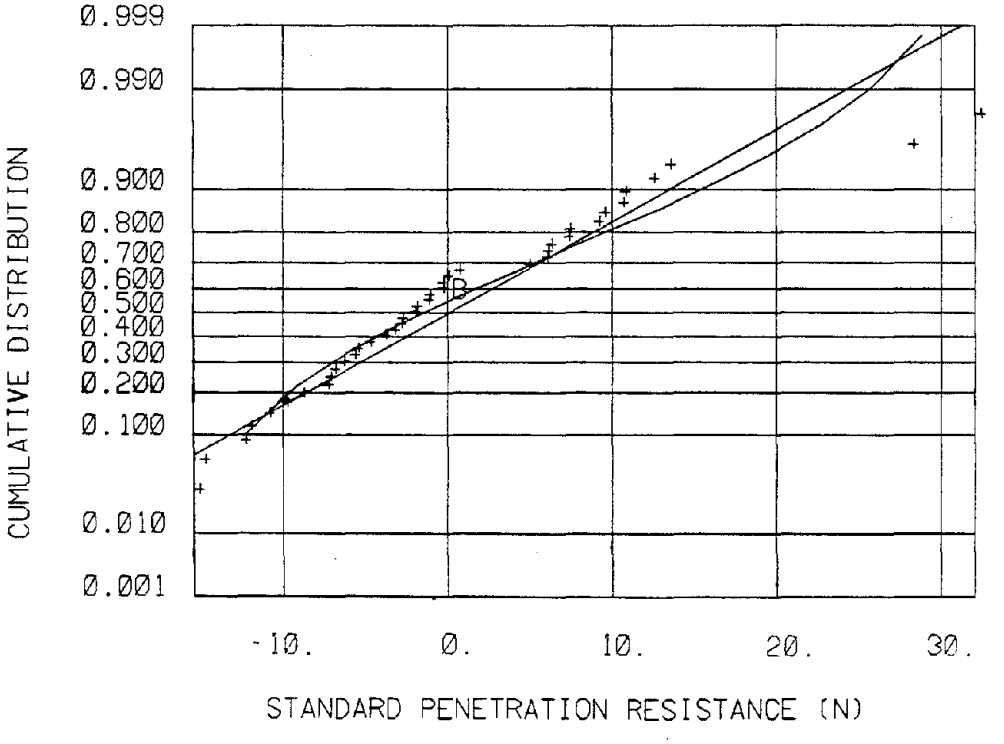

Figure 8.134 - CDF of residual Texas gypsum SPT data compared to standard CDF plots

SITE	Texas Texas	(Gypsum)
DATA	Type	Dry density
	Number	87
	Quality Index	NA
TREND WITH DEPTH	γ_d(pcf) = 83.5 + 0.183z(ft)	

DATA SCATTER

	mean	SD	β_1	β_2
Raw Data	97.2	13.5	0.037	2.00
Residual Data	--	11.3	0.001	2.76

GOODNESS OF FIT STATISTICS

	Raw		Residual	
	χ^2	D_m	χ^2	D_m
normal	39.4	0.093	9.37	0.057
beta	23.6	0.061	20.5	0.059
exponential	531	0.495	--	--
lognormal	44.1	0.097	--	--
gamma	41.9	0.095	--	--
5% confidence limit	23.7	0.146	--	--

INTERPRETED STRENGTH PARAMETERS NA

Table 8.27 - Table of Texas gypsum dry density data

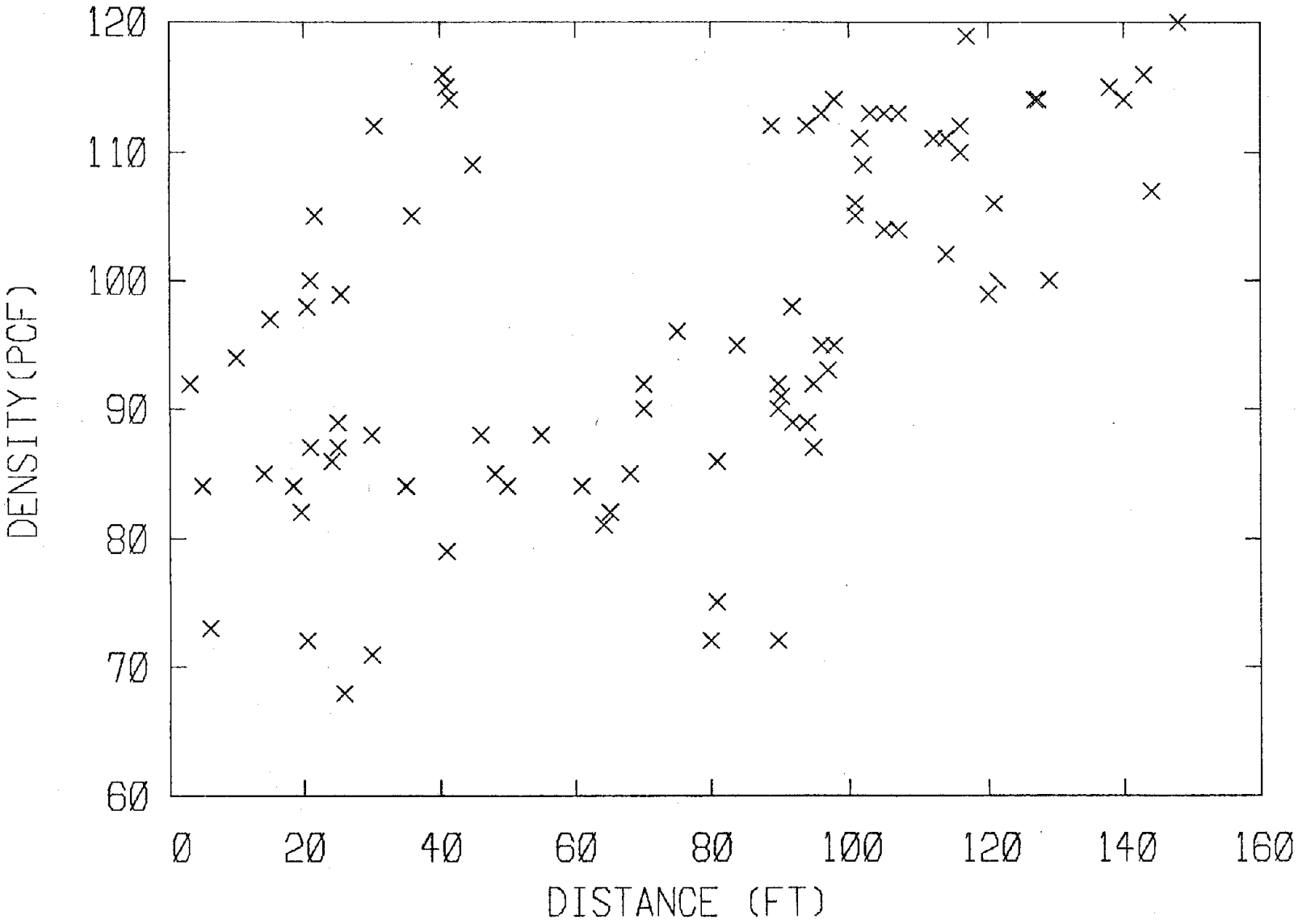

Figure 8.135 - Dry density v. depth for Texas Gypsum

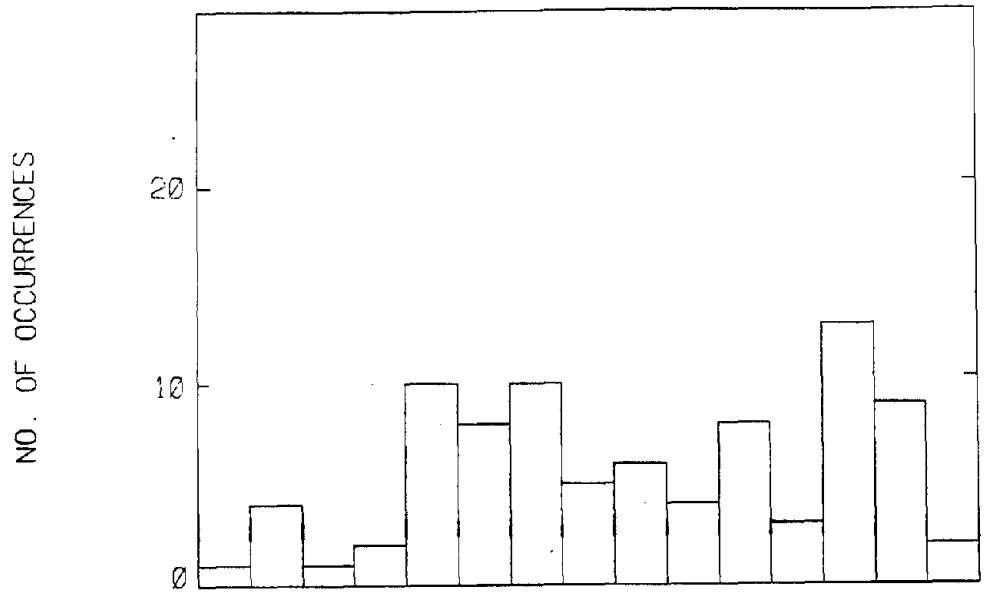

Figure 8.136 - Histogram of raw Texas gypsum dry density data

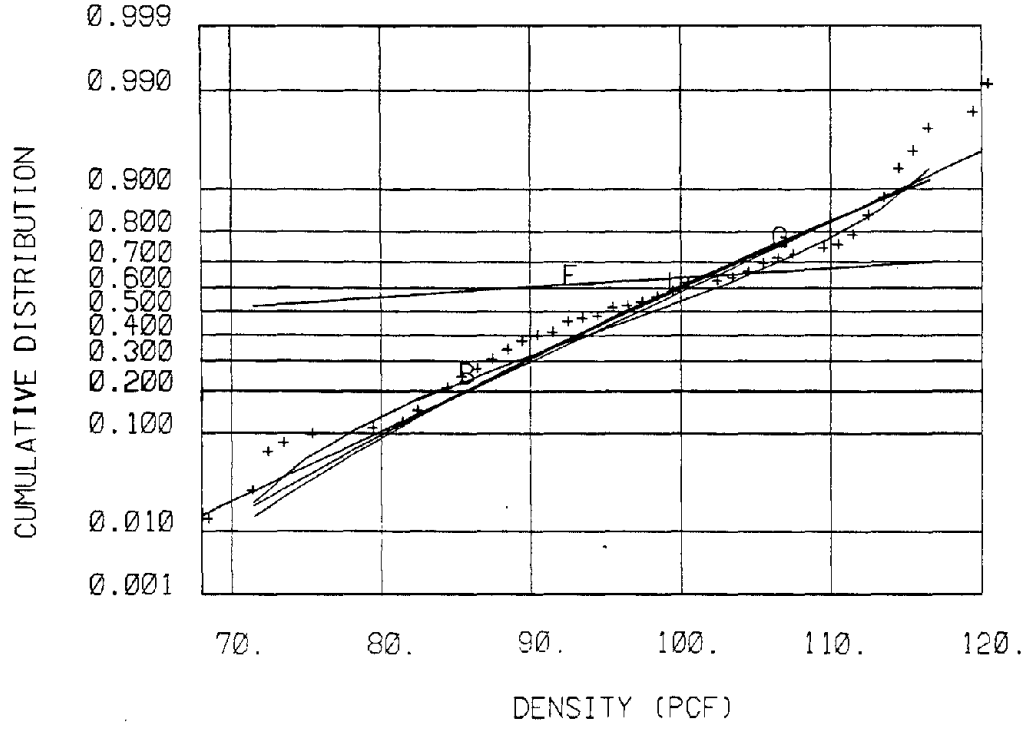

Figure 8.137 - CDF of raw Texas gypsum dry density data compared to standard CDF plots

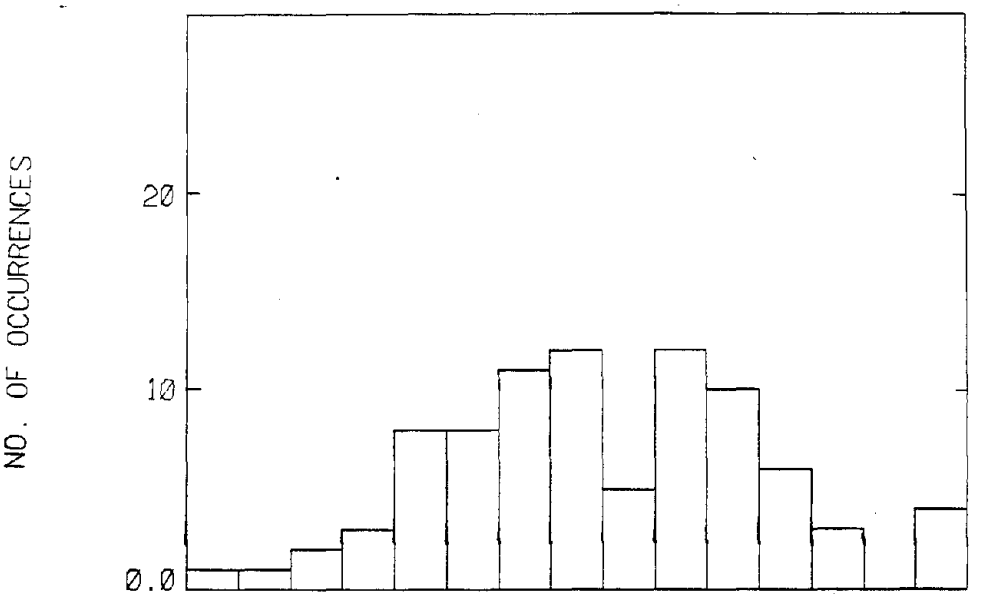

Figure 8.138 - Histogram of residual Texas gypsum dry density data

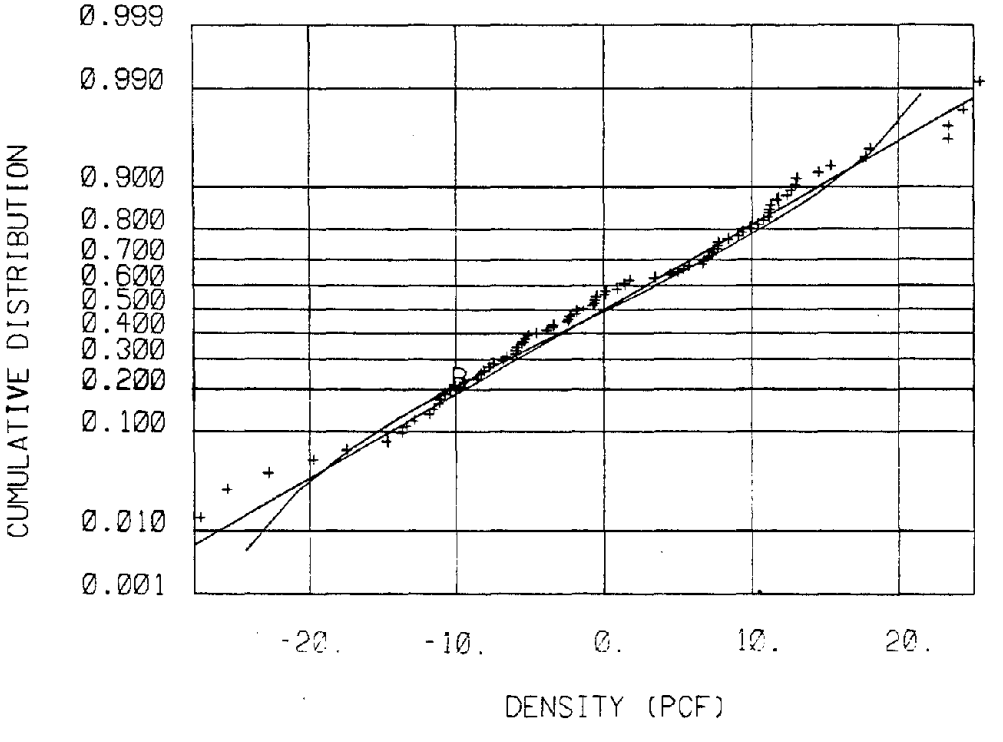

Figure 8.139 - CDF of residual Texas gypsum dry density data compared to standard CDF plots

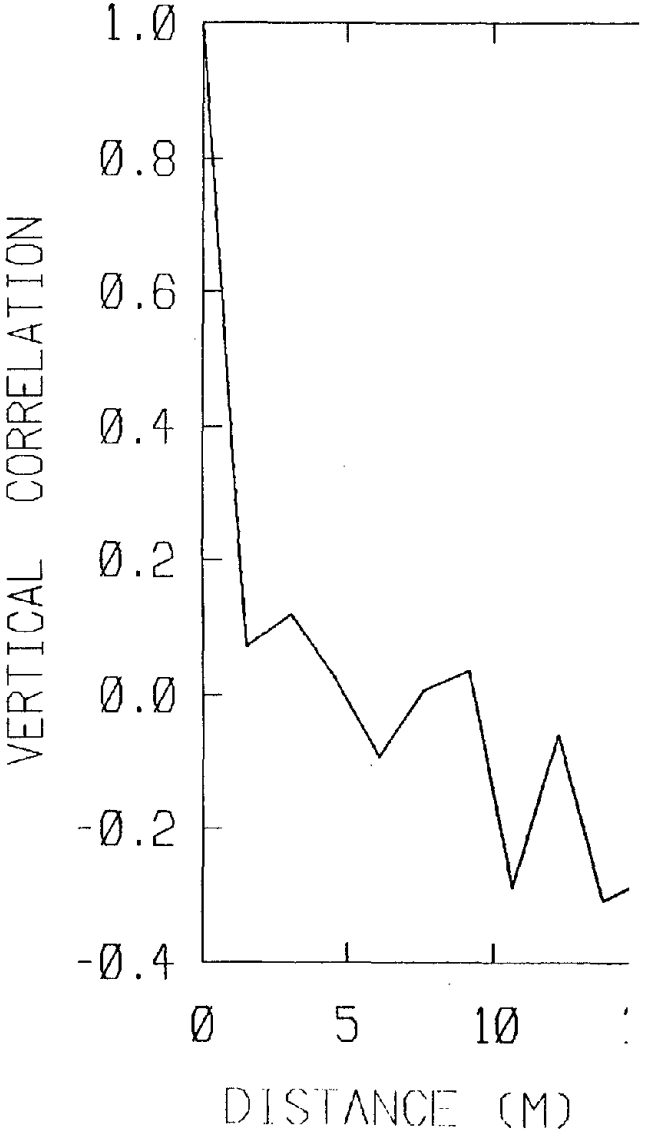

Figure 8.140 - Vertical correlation of residual Texas dry density data

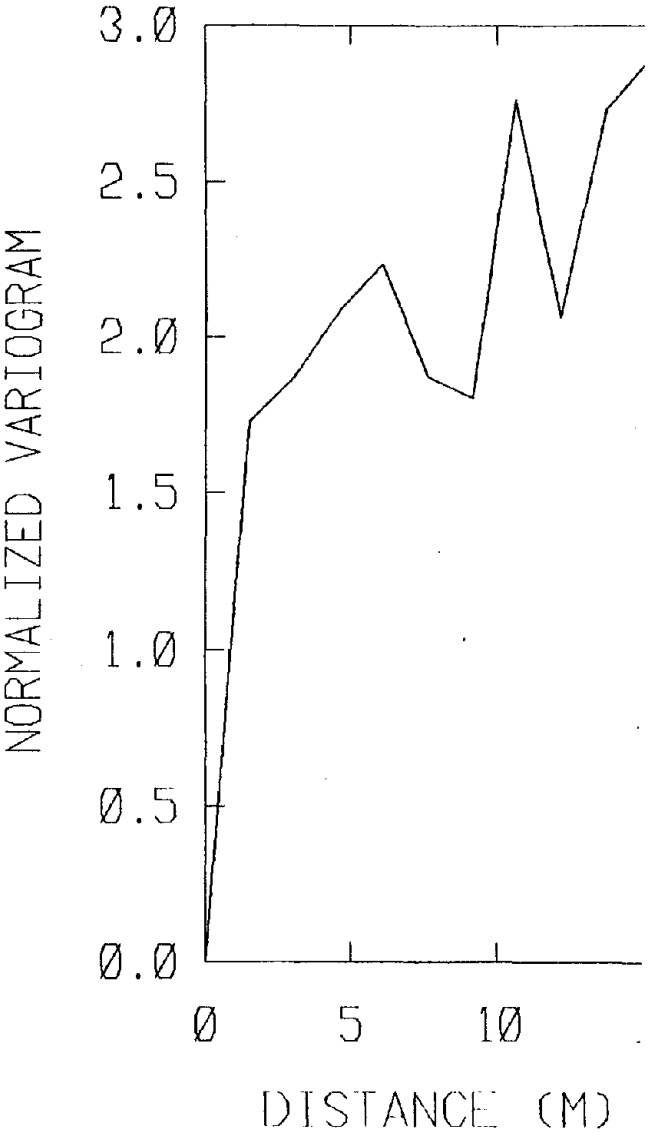

Figure 8.141 - Normalized variogram of residual Texas dry density data

SITE	Louisiana 1 Data-Gypsum Lower Strata (55 to 100 ft)	
DATA	Type	11 SPT Borings
	Number	89
	Quality Index	A
TREND WITH DEPTH	N = 2.9 + 0.018z(ft)	

DATA SCATTER

	mean	SD	β_1	β_2
Raw Data	4.28	2.14	1.14	5.05
Residual Data	--	2.12	1.19	5.18

GOODNESS OF FIT STATISTICS

	Raw		Residual	
	χ^2	D_m	χ^2	D_m
normal	121.2	0.153	139	0.095
beta	602	0.114	658	0.057
exponential	82.9	0.182	--	--
lognormal	12.5	0.125	--	--
gamma	17.0	0.119	--	--
5% confidence limit	23.7	0.144	--	--

INTERPRETED STRENGTH PARAMETERS 25^o

Table 8.28 - Table of Louisianal gypsum SPT data (lower strata)

SITE	Louisiana 1 Data-Gypsum Upper Strata (0 to 50 ft)	
DATA	Type	11 SPT Borings
	Number	91
	Quality Index	A
TREND WITH DEPTH	N = 22.2 - 0.034z(ft)	

DATA SCATTER

	mean	SD	β_1	β_2
Raw Data	21.2	14.0	0.093	2.01
Residual Data	--	13.9	0.102	2.01

GOODNESS OF FIT STATISTICS

	Raw		Residual	
	χ^2	D_m	χ^2	D_m
normal	14.8	0.095	10.5	0.099
beta	14.3	0.049	7.63	0.047
exponential	37.6	0.134	--	--
lognormal	241	0.183	--	--
gamma	46.1	0.134	--	--
5% confidence limit	23.7	0.143	--	--

INTERPRETED STRENGTH PARAMETERS 40^{o}

Table 8.29 - Table of Louisianal gypsum SPT data (upper strata)

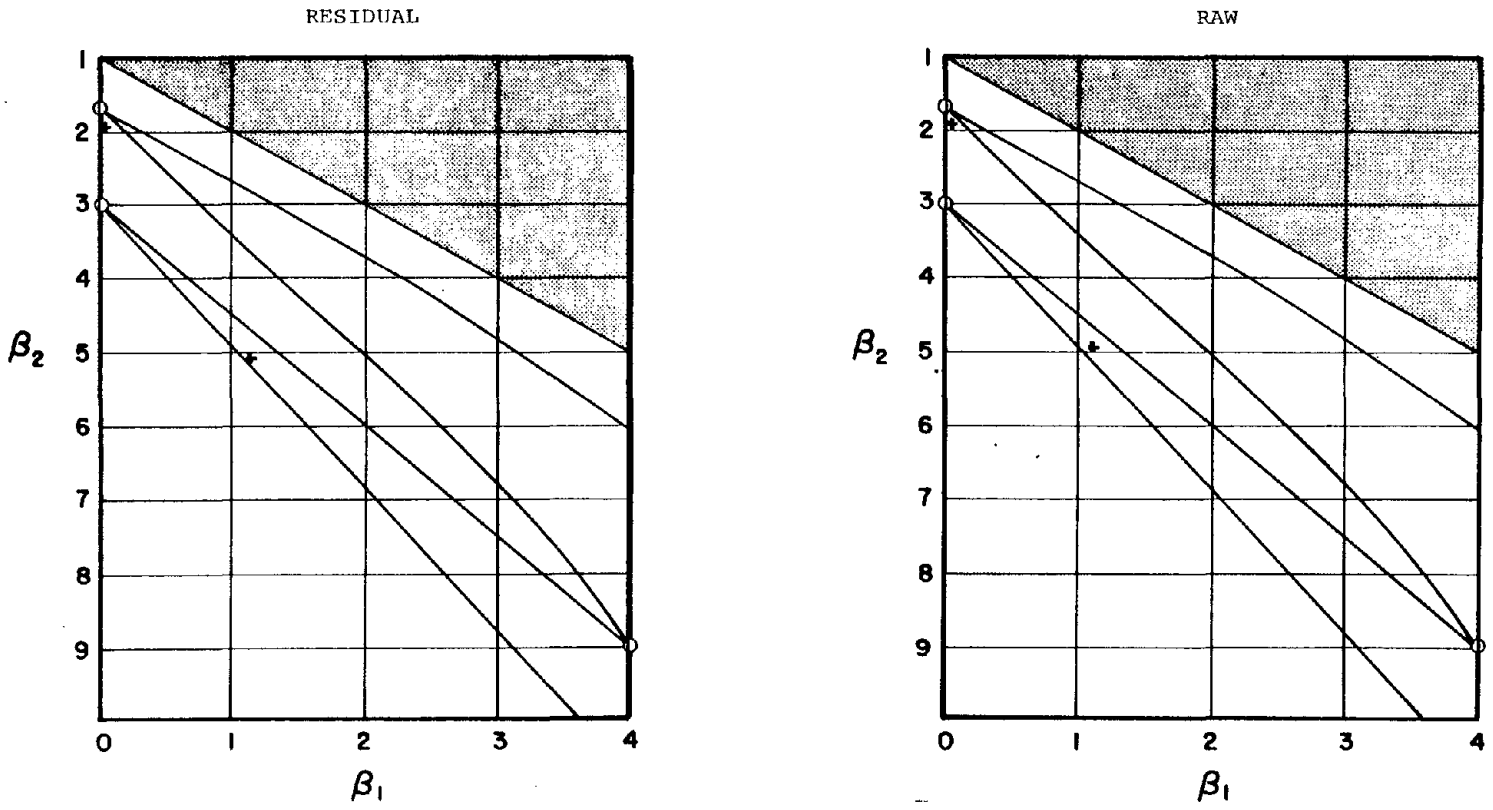

Figure 8.142 - Pearson diagrams of raw and residual SPT data for Louisianal gypsum

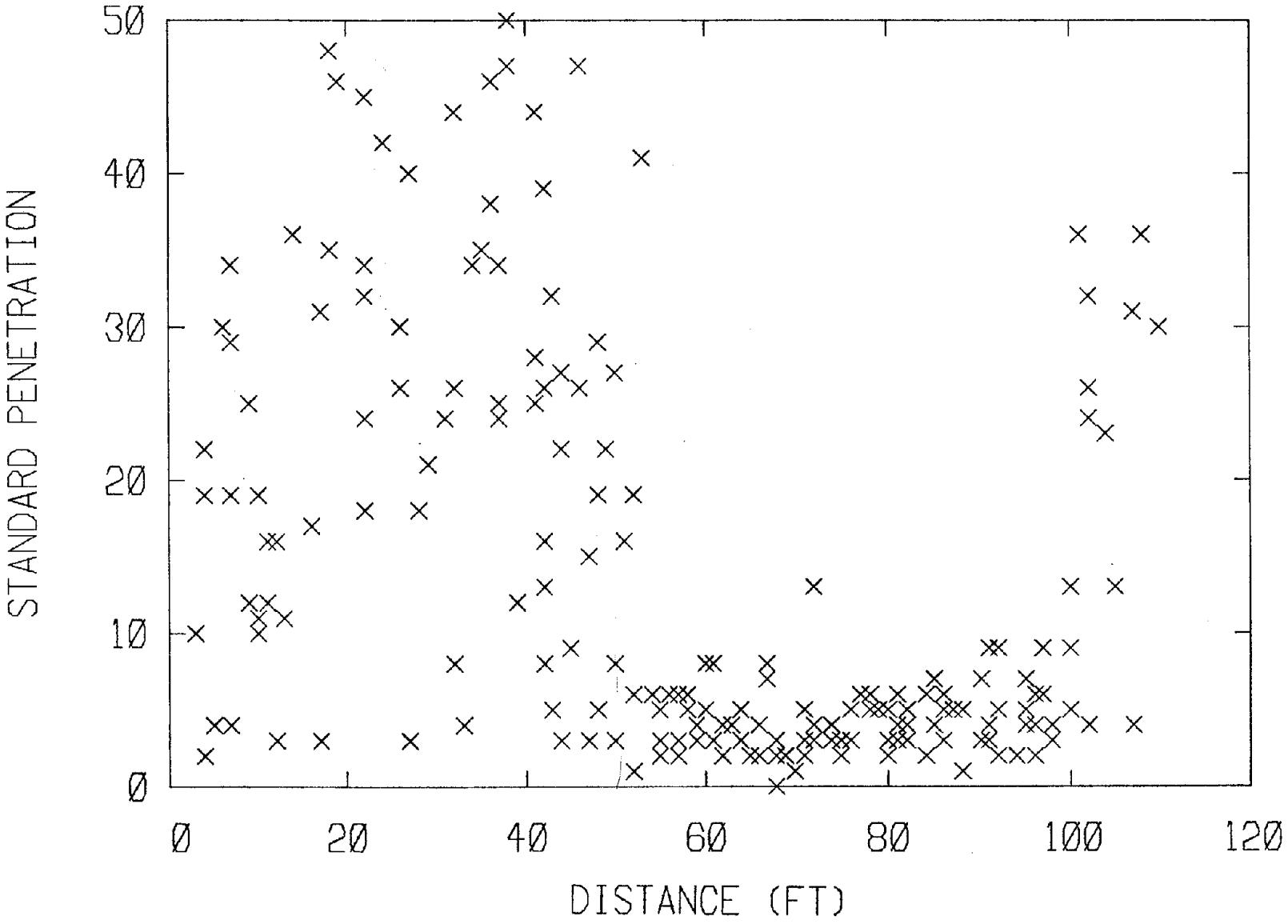

Figure 8.143 - SPT (N) v. depth for Louisianal gypsum (all)

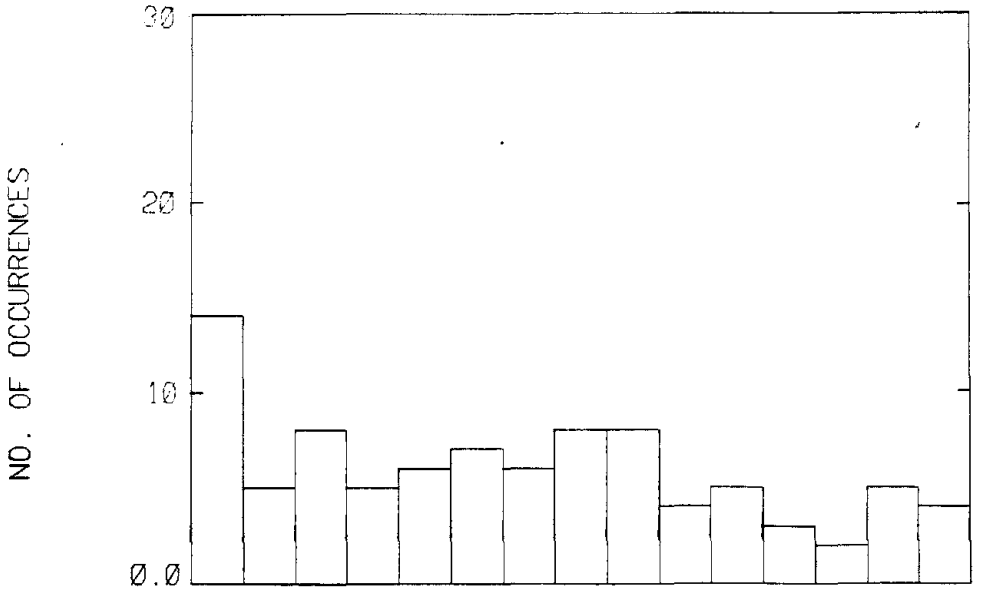

Figure 8.144 - Histogram of residual Louisianal gypsum SPT data (lower strata)

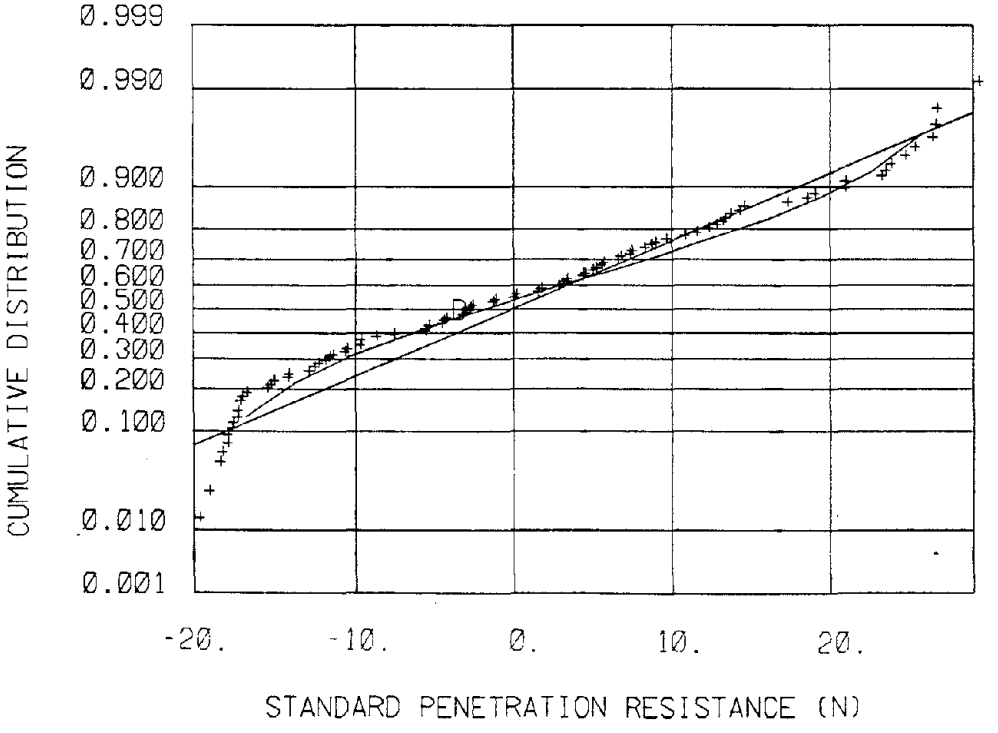

Figure 8.145 - CDF of residual Louisianal gypsum SPT data (lower) compared to standard CDF plots

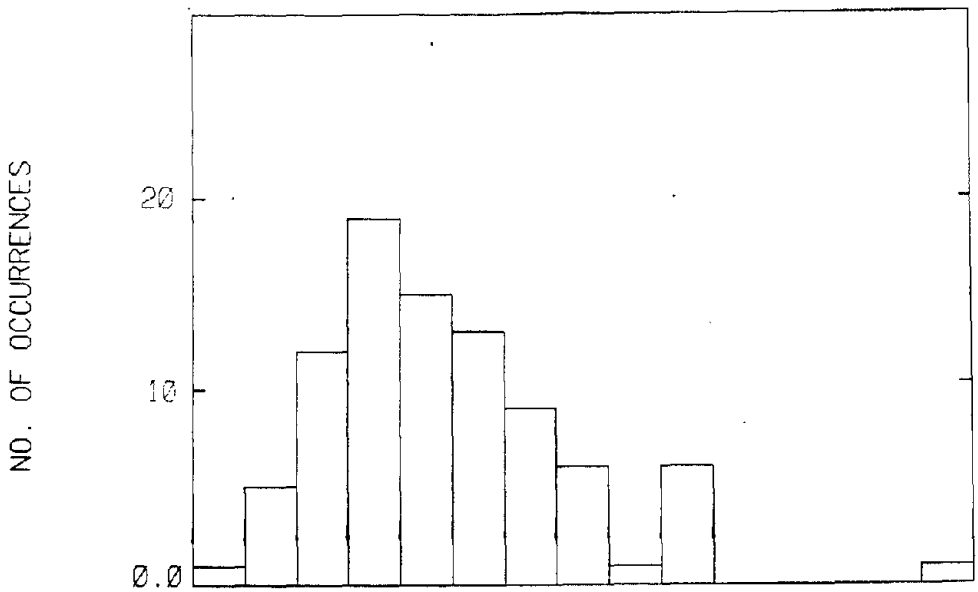

Figure 8.146 - Histogram of residual Louisianal gypsum SPT data (upper strata)

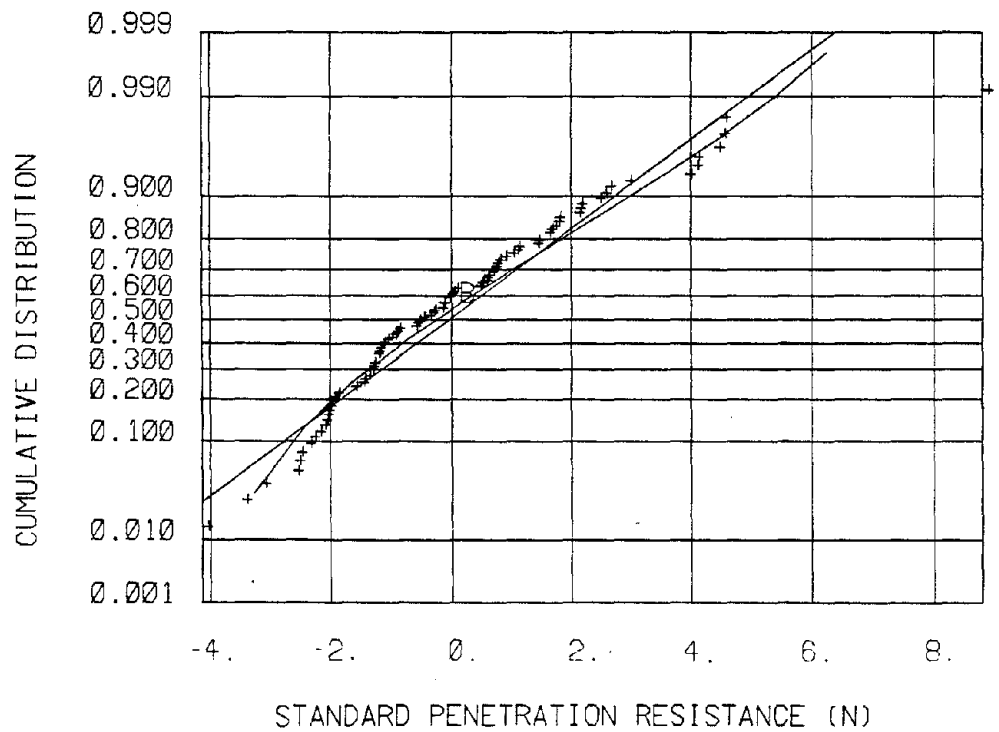

Figure 8.147 - CDF of residual Louisianal gypsum SPT data (upper strata) compared to standard CDF plots

SITE	Florida 1 Data-Gypsum Gypsum Stack	
DATA	Type	4 SPT Borings
	Number	111
	Quality Index	B
TREND WITH DEPTH	N = 10.7 + 0.072z(ft)	

DATA SCATTER

	mean	SD	β_1	β_2
Raw Data	12.7	8.41	1.17	4.23
Residual Data	--	8.31	0.98	4.10

GOODNESS OF FIT STATISTICS

	Raw		Residual	
	χ^2	D_m	χ^2	D_m
normal	96.9	0.13	82.4	0.11
beta	90.8	0.056	138	0.073
exponential	47.1	0.13	--	--
lognormal	22.2	0.11	--	--
gamma	18.4	0.07	--	--
5% confidence limit	23.7	0.129	--	--

INTERPRETED STRENGTH PARAMETERS 34^{o}

Table 8.30 - Table of Floridal gypsum data

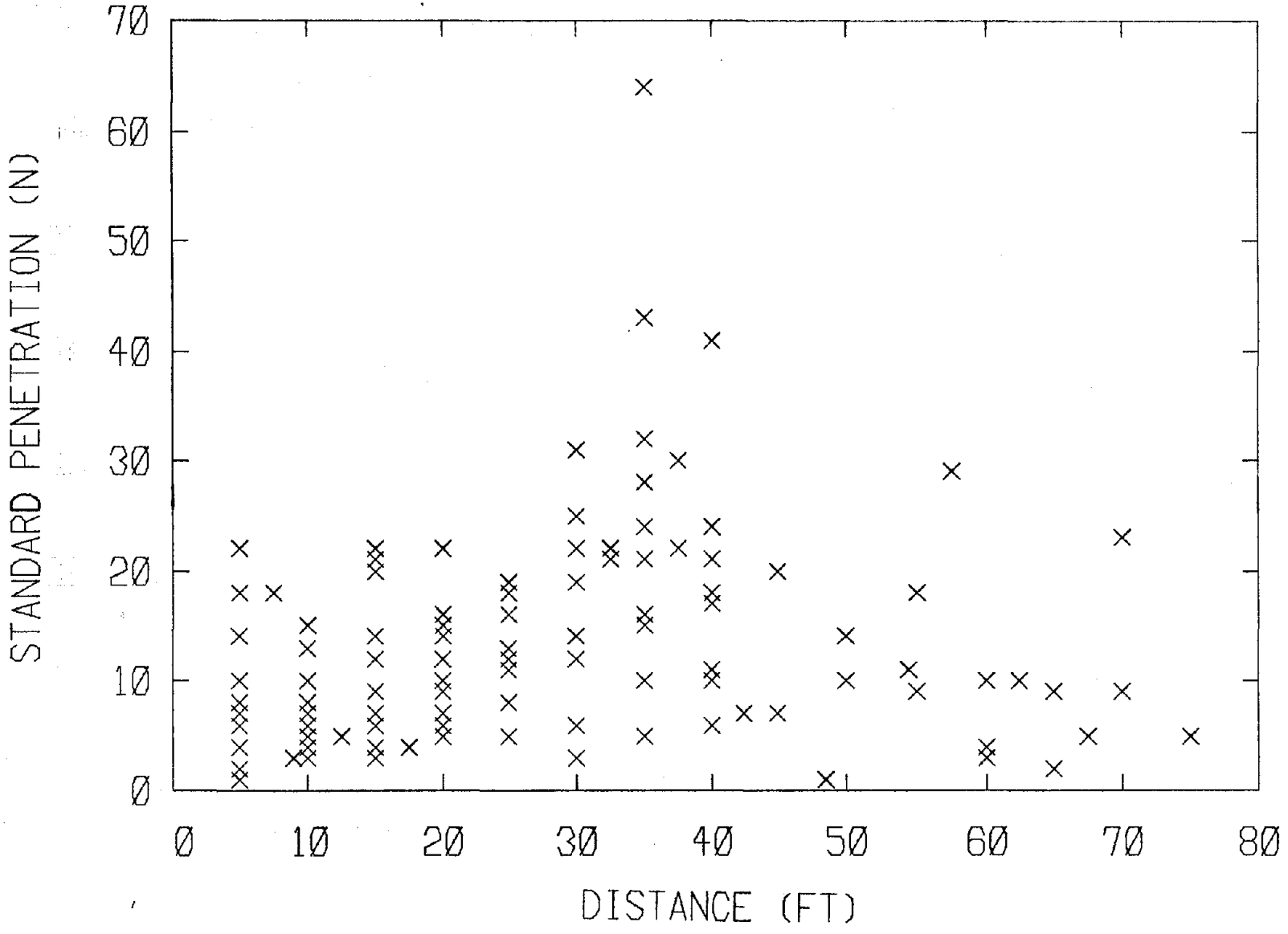

Figure 8.148 - SPT (N) v. depth for Floridal SPT data

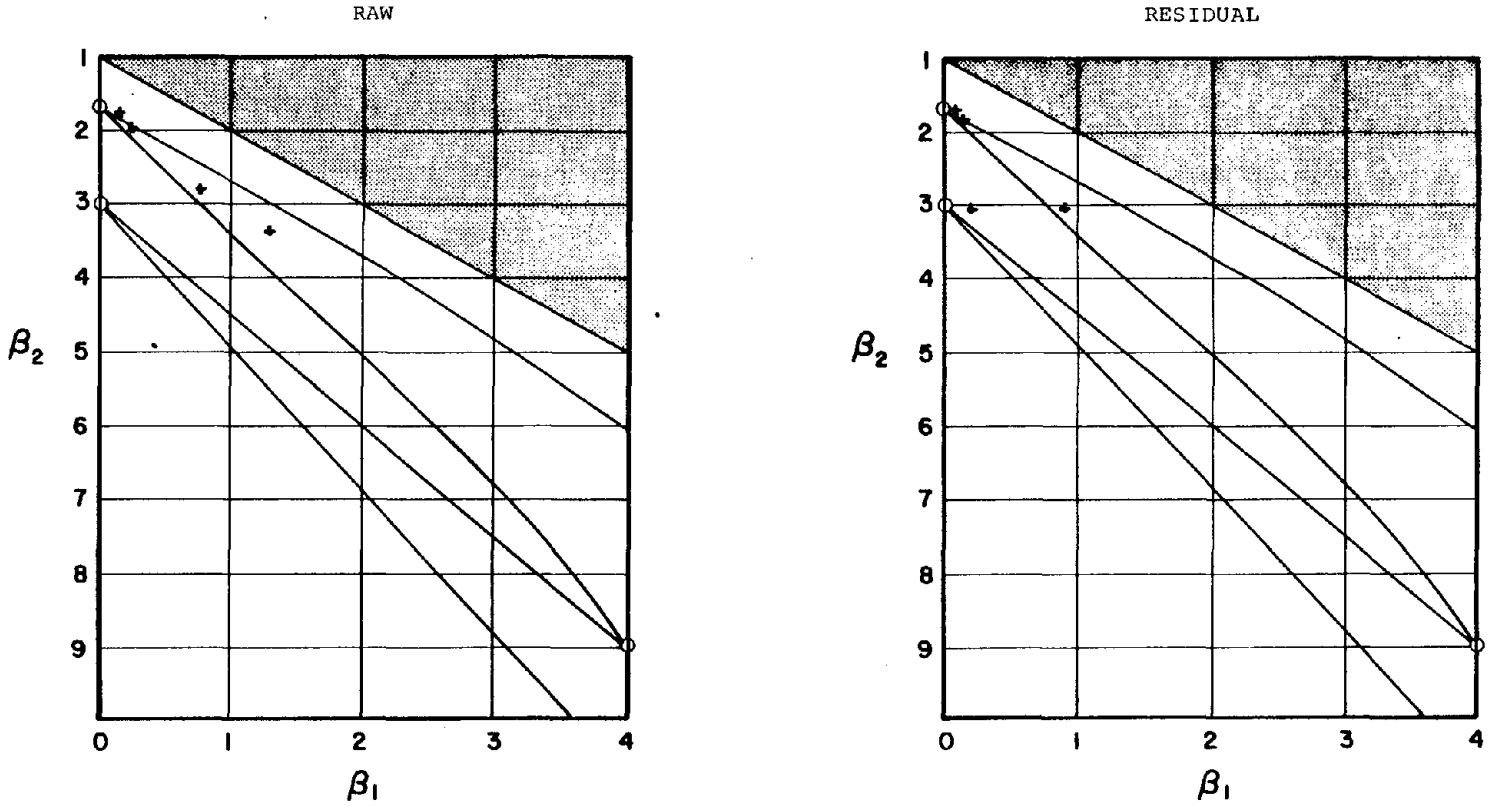

Figure 8.149 - Pearson diagrams of raw and residual SPT data for Floridal gypsum

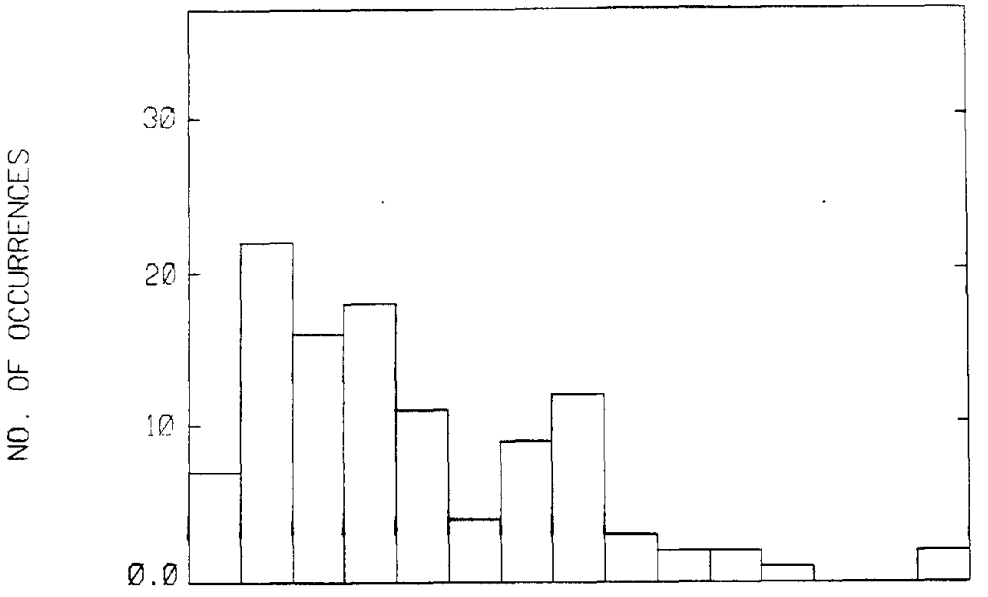

Figure 8.150 - Histogram of raw Floridal gypsum SPT data

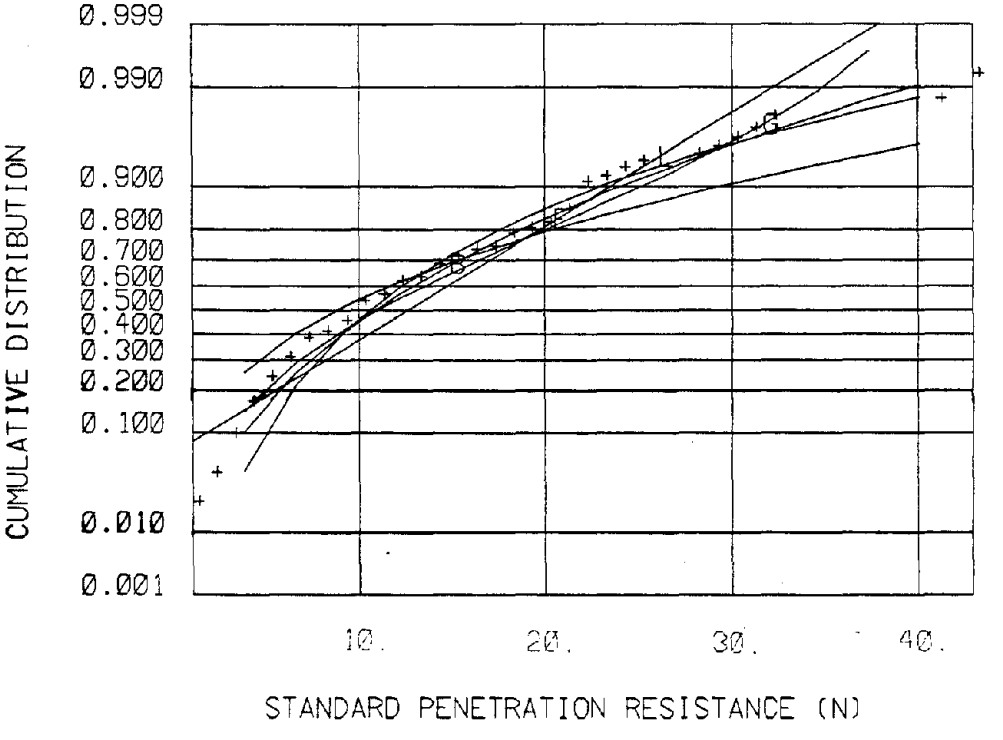

Figure 8.151 - CDF of raw Floridal gypsum SPT data compared to standard CDF plots

SITE	Piney Point (Gypsum) Florida	
DATA	Type	Cone Penetration (Combined in one hole)
	Number	92
	Quality Index	NA
TREND WITH DEPTH	q_c(psi) = 191 - 0.124z(m)	

DATA SCATTER

	mean	SD	β_1	β_2
Raw Data	161	85.6	1.98	5.49
Residual Data	--	83.9	2.65	5.96

GOODNESS OF FIT STATISTICS

	Raw		Residual	
	χ^2	D_m	χ^2	D_m
normal	49.8	0.17	54.3	0.194
beta	64.0	0.13	61.0	0.16
exponential	87.1	0.31	--	--
lognormal	21.2	0.086	--	--
gamma	24.5	0.105	--	--
5% confidence limit	23.7	0.142	--	--

INTERPRETED STRENGTH PARAMETERS NA

Table 8.31 - Table of Piney Point gypsum cone penetration data

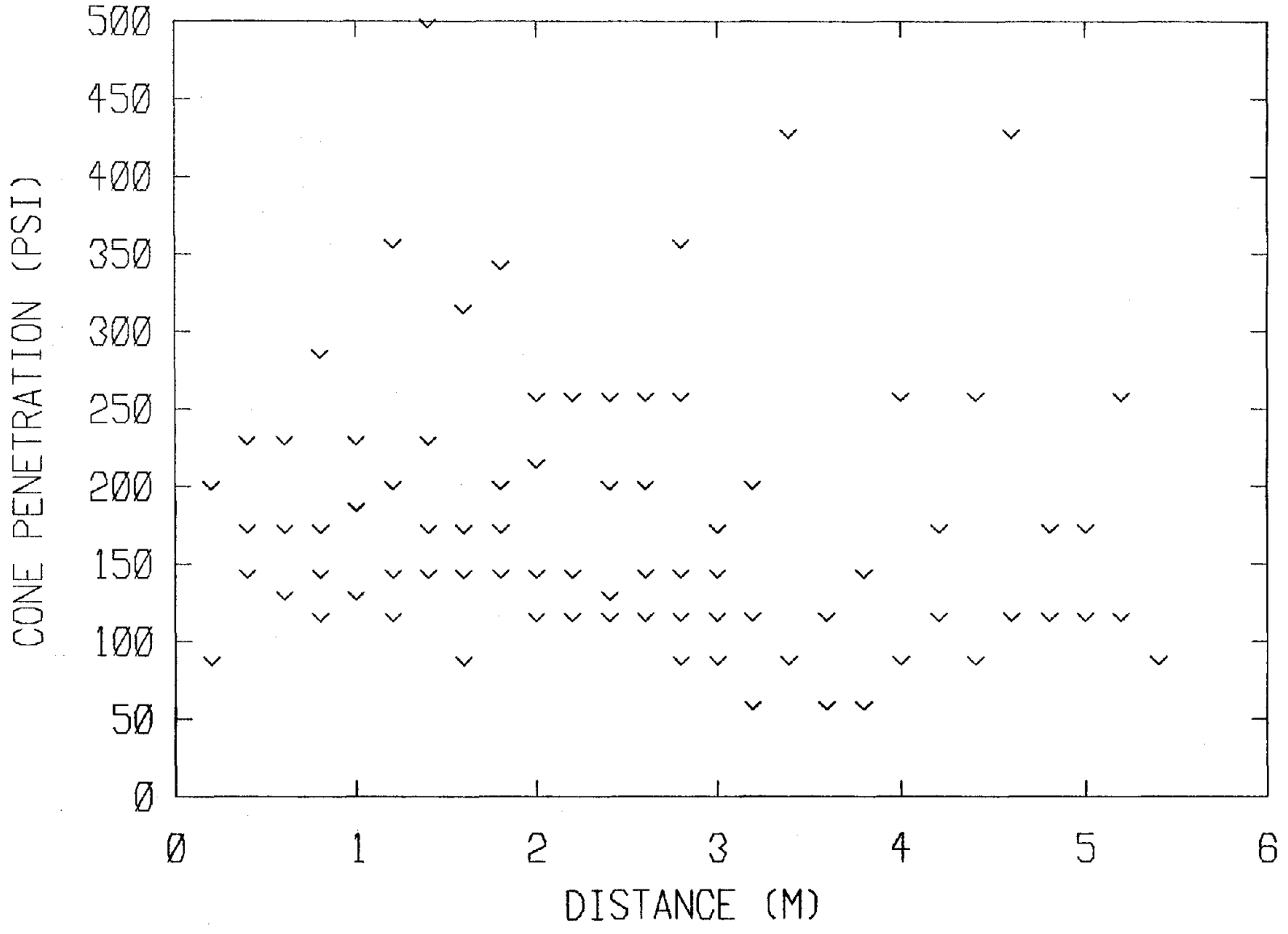

Figure 8.152 - Cone penetration resistance v. depth for Piney Point gypsum

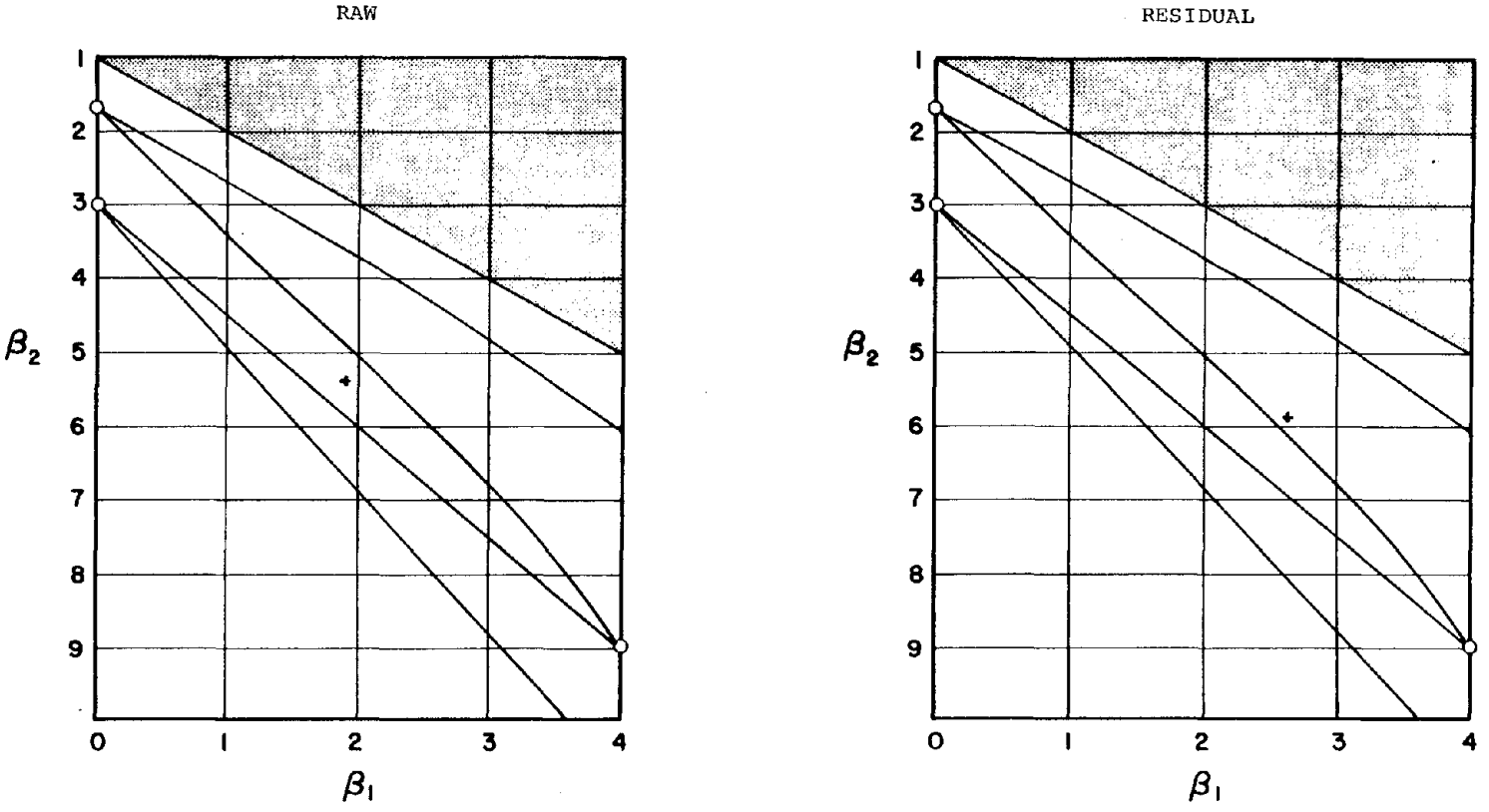

Figure 8.153 - Pearson diagrams of raw and residual cone penetration resistance data for Piney Point gypsum

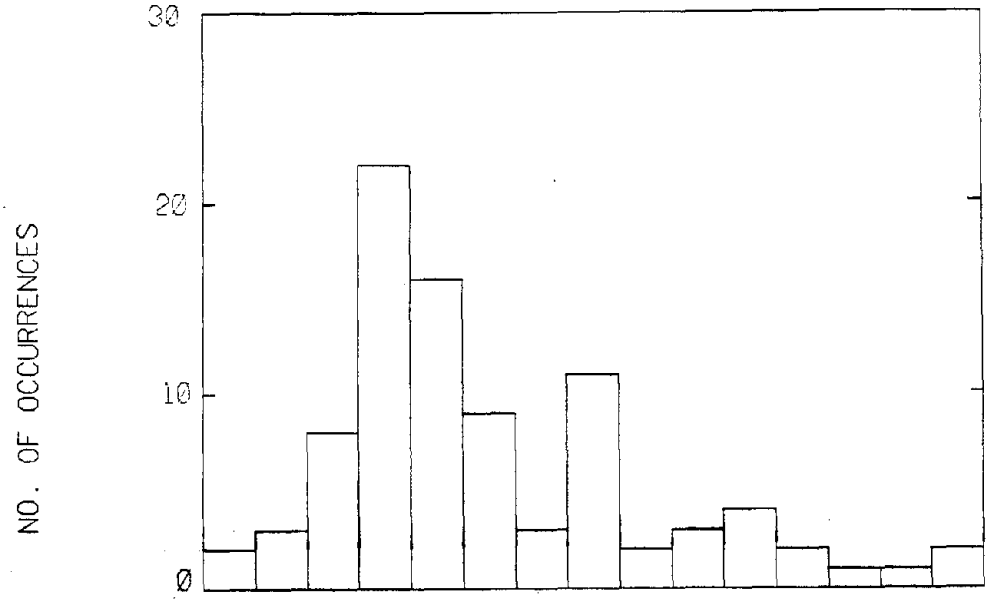

Figure 8.154 - Histogram of residual Piney Point gypsum cone penetration resistance data

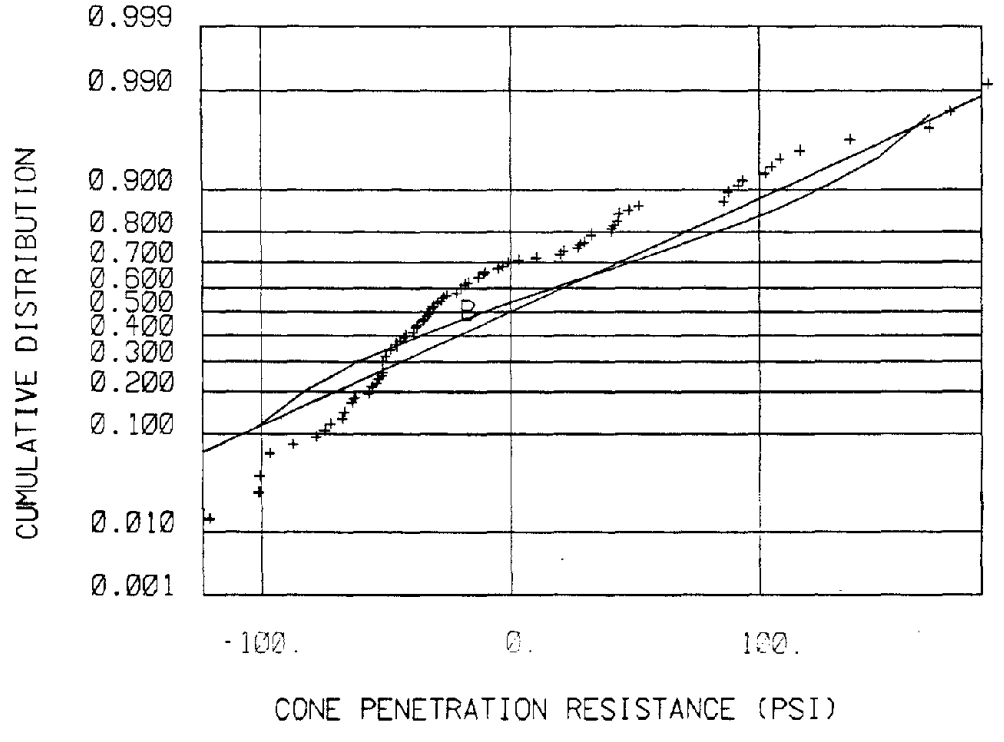

Figure 8.155 - CDF of residual Piney Point gypsum cone penetration resistance data compared to standard CDF plots

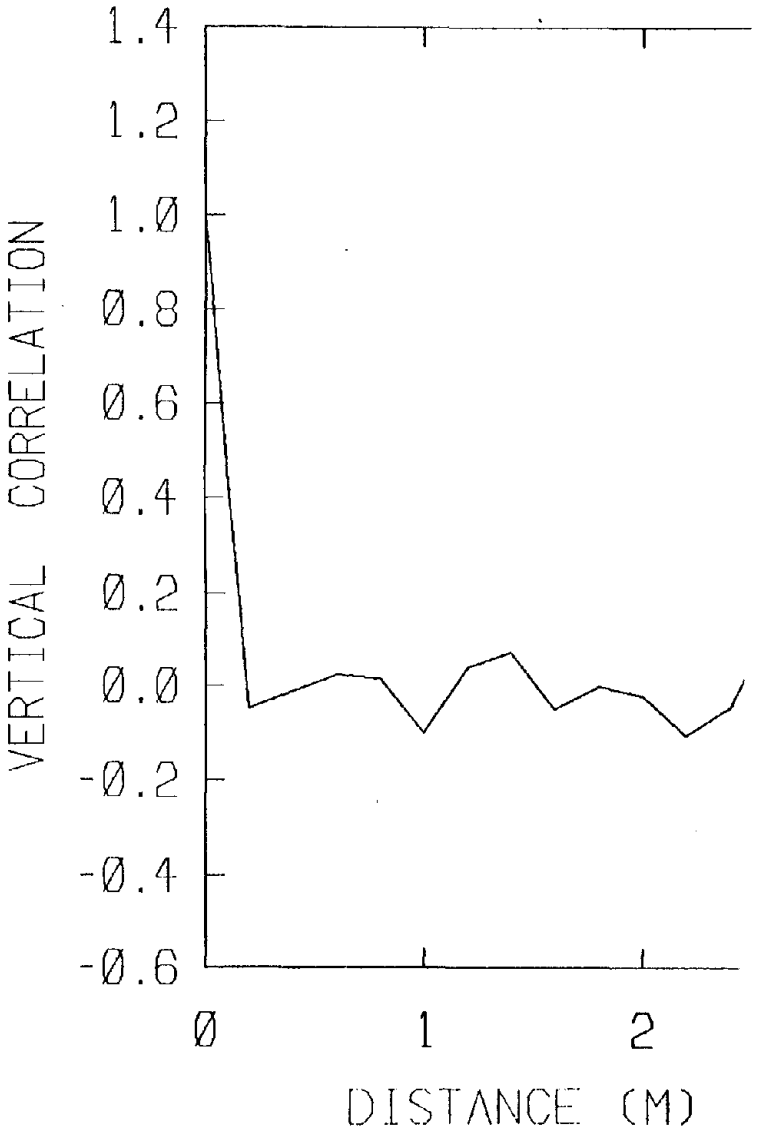

Figure 8.156- Vertical correlation of residual Piney Point cone penentration resistance data

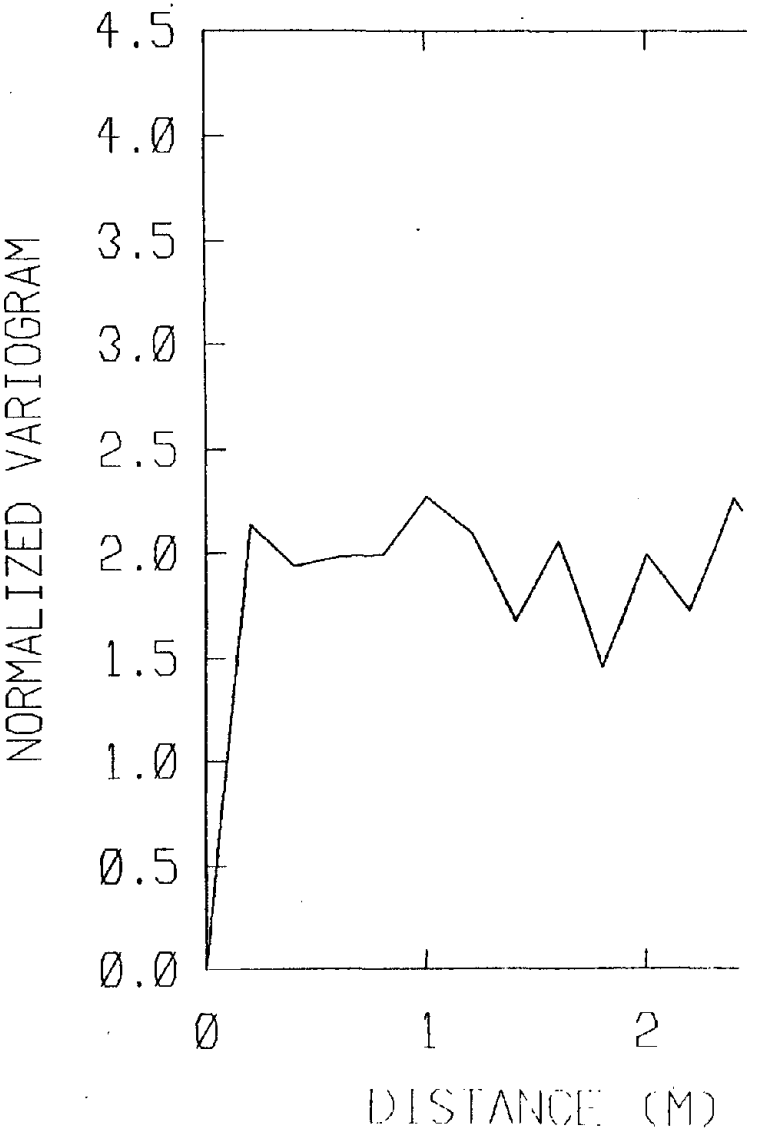

Figure 8.157- Normalized variogram of residual Piney Point cone penetration resistance data

SITE Vick (Gypsum)

DATA Type SPT (combined)

Number 20

Quality Index A

TREND WITH DEPTH $N = 31.95 + 0.72z(m)$

DATA SCATTER

	mean	SD	β_1	β_2
Raw Data	33.9	19.6	0.389	2.309
Residual Data	--	19.6	0.454	2.412

GOODNESS OF FIT STATISTICS

	Raw		Residual	
	χ^2	D_m	χ^2	D_m
normal	11.3	0.143	10.5	0.146
beta	12.7	0.085	9.70	0.068
exponential	20.02	0.240	--	--
lognormal	16.6	0.197	--	--
gamma	12.9	0.152	--	--
5% confidence limit	23.7	0.29	--	--

INTERPRETED STRENGTH PARAMETERS III

Table 8.32 - Table of Vick gypsum SPT data

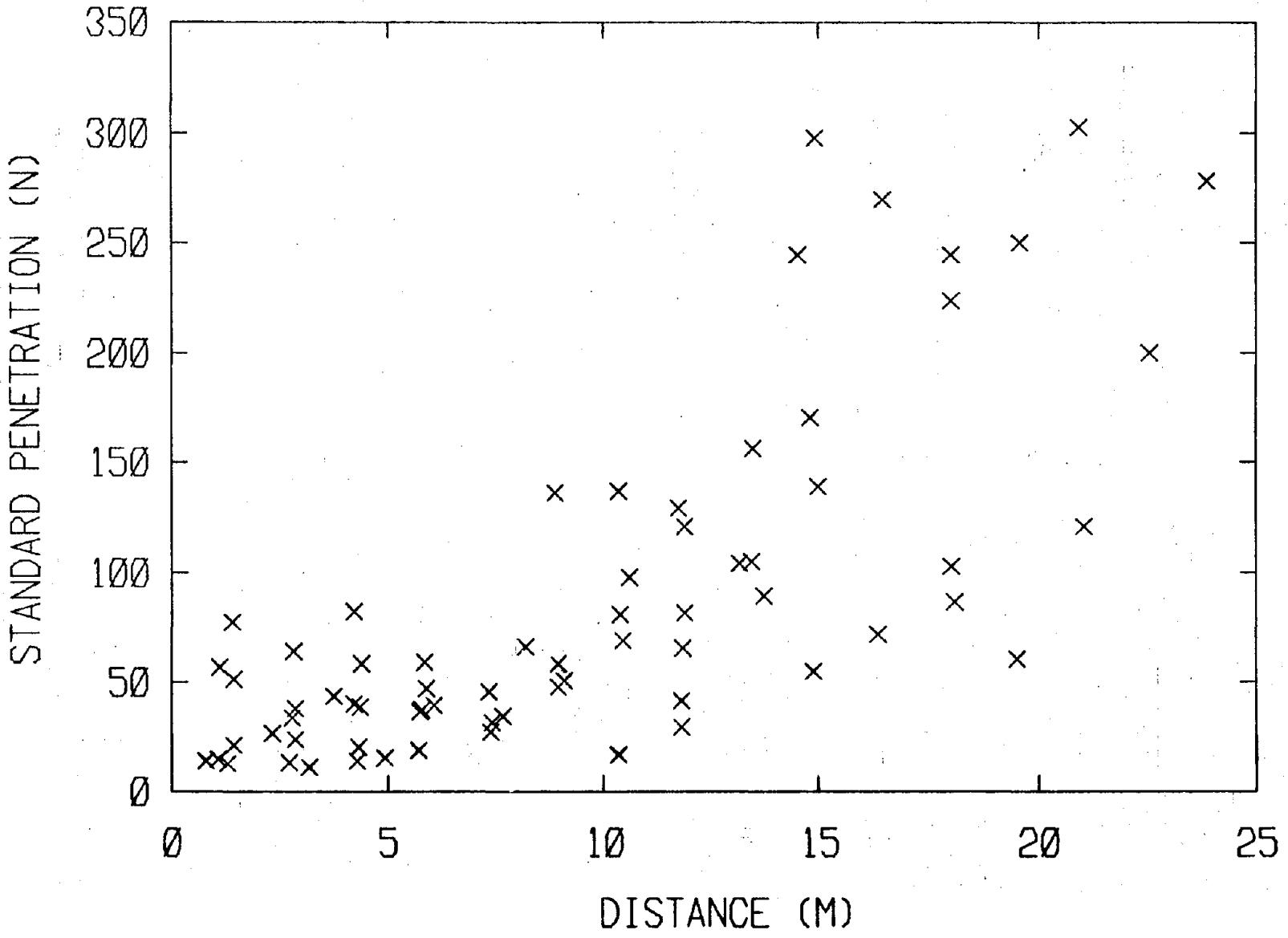

Figure 8.158 - SPT (N) data v. depth for Vick gypsum data

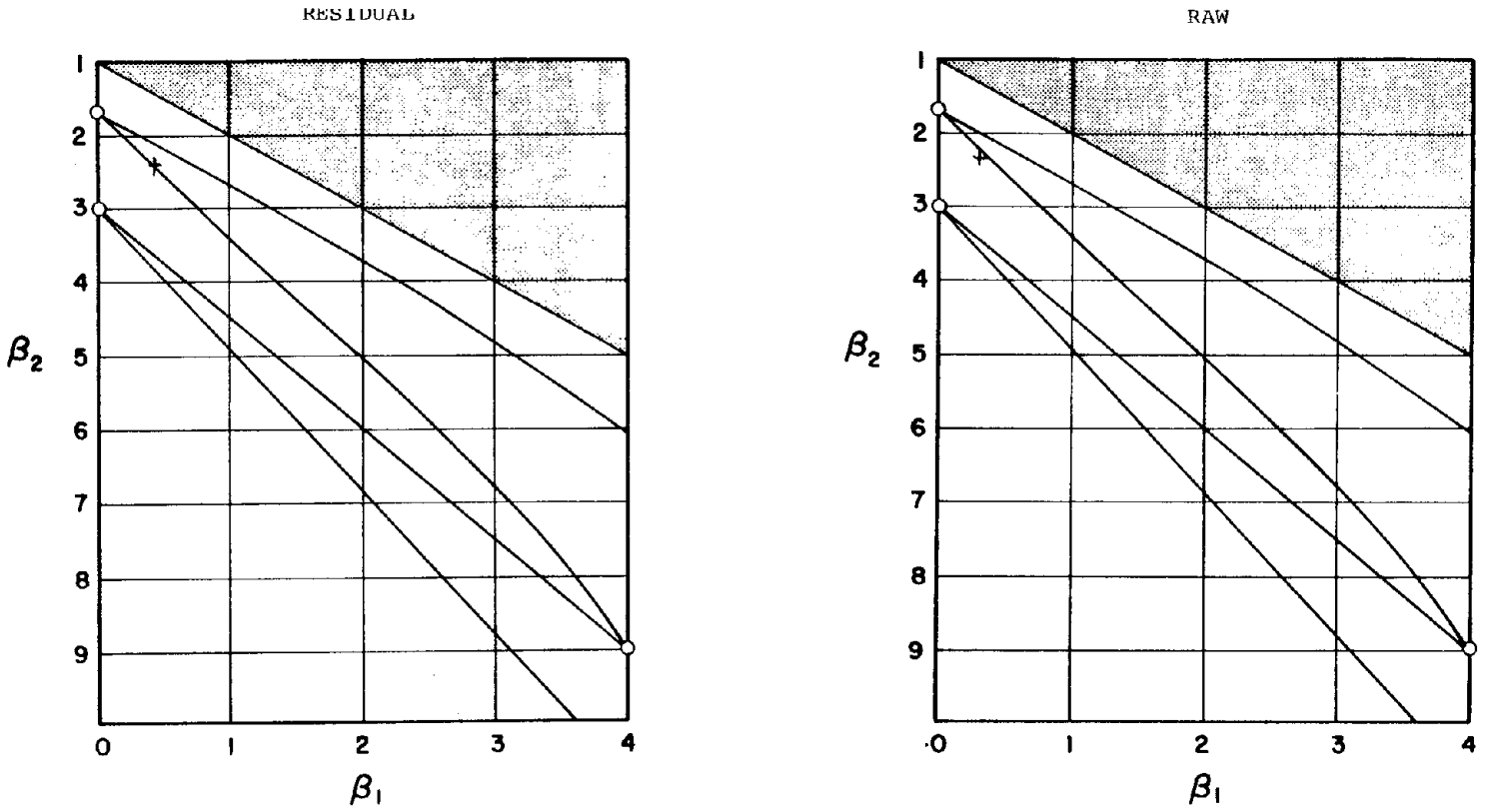

Figure 8.159 - Pearson diagrams of raw and residual SPT data for Vick gypsum

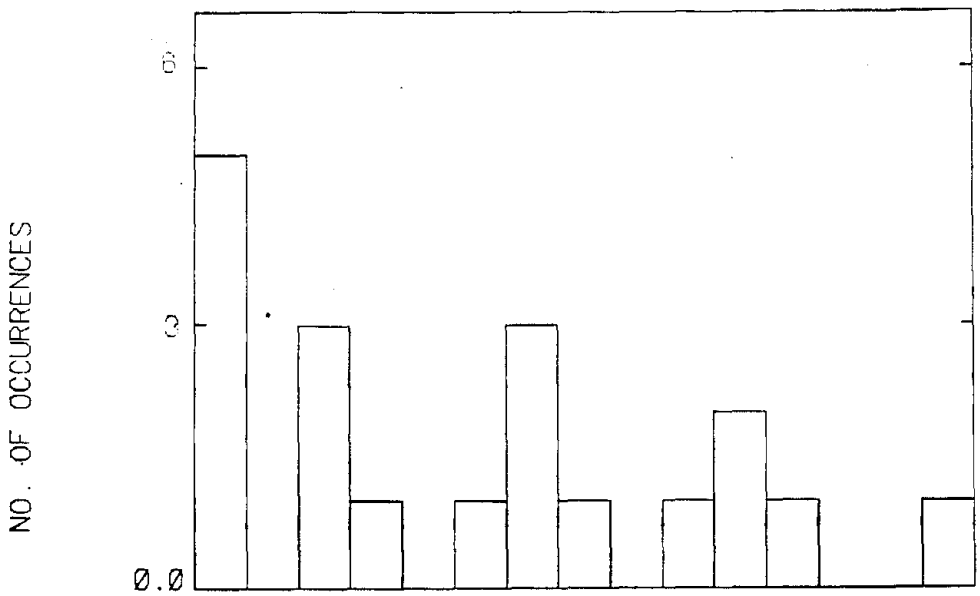

Figure 8.160 - Histogram of raw Vick gypsum SPT data

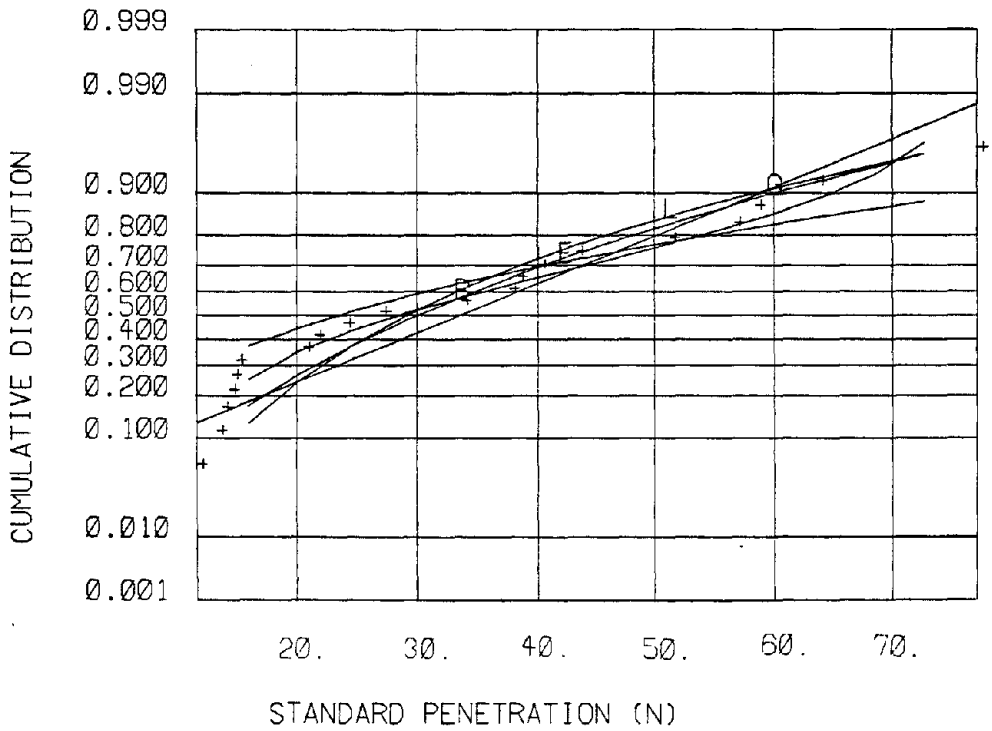

Figure 8.161 - CDF of raw Vick gypsum SPT data compared to standard CDF plots

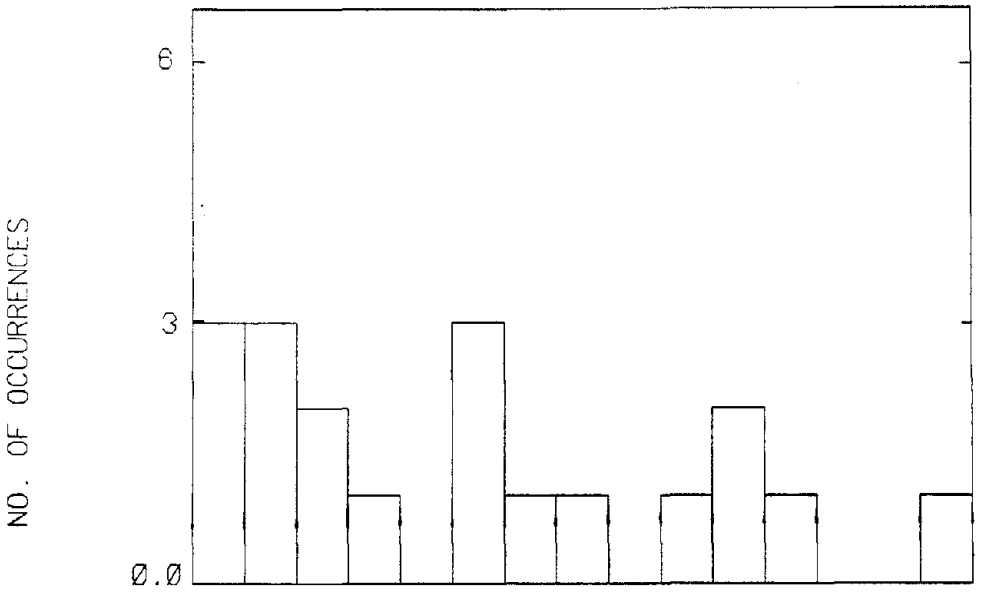

Figure 8.162 - Histogram of residual Vick gypsum SPT data

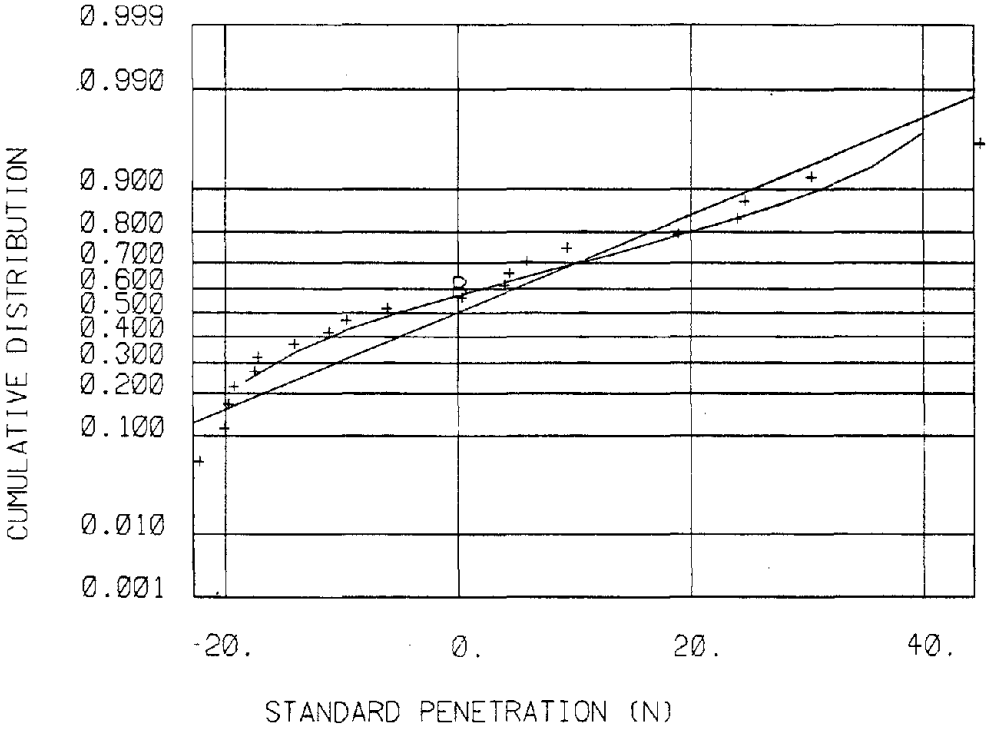

Figure 8.163 - CDF of residual Vick gypsum SPT data compared to standard CDF plots

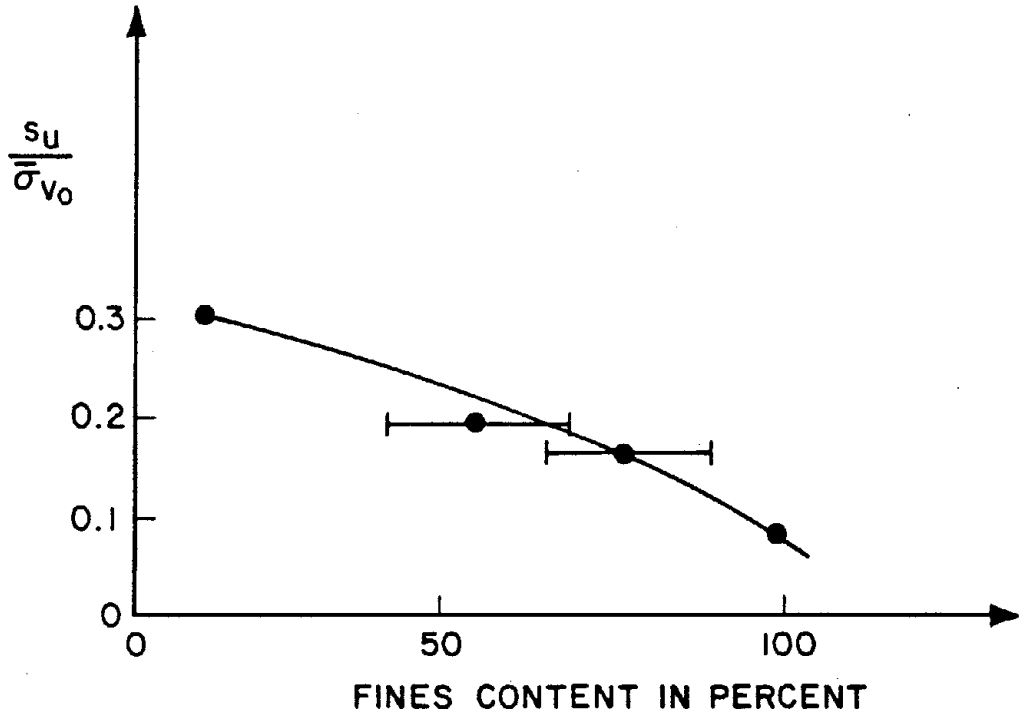

FIGURE 8.164 STRENGTH vs. PERCENT PASSING No. 200 US SIEVE SIZE (FINES CONTENT) FROM JAPANESE COPPER TAILINGS

9. DISCUSSION OF RESULTS

Distribution Functions

As a general rule, both the in situ and laboratory data display well behaved frequency distributions. The distributions are unimodal, often symmetric, and decay more or less uniformly away from the modes. However, from a statistical view about one-quarter of the data sets do not verify any of the common analytical forms tested in the present work. There is some support, as evidenced by Table 9.1, that removing a mean trend from the data increases normality. This seem unsurprising, given that trends are fit by regression which are usually based on a least-squares or similar criterion.

By inspection, many of these latter data sets have frequency distributions which closely approximate analytical forms. However, the numbers of measurements constituting most of the data sets are so large that even apparently minor deviations from the analytical forms are statisticly. significant and thus refute the hypothesis that the data did in fact arise from the theoretical distribution. The K-S goodness-of-fit test, which is somewhat more forgiving of large data sizes than the chi-square, does show more distributions providing adequate fits to the data, particularly for residuals off the mean trend. Secondly, while central frequencies (i.e., those say within two standard deviations of the mean) in many cases appear to closely conform to analytical distributions, the extreme values of the data sets (i.e., the tails) often vary considerably. This has the effect of refuting the overall hypothesis that the analytical form is appropriate to the data, even though for certain purposes it may conveniently be used.

Inspection of Tables 9.1, 9.2, and of the Pearson diagrams for individual borings shows that beta distributions of one form or another often provide reasonable models of data frequencies. The principal reasons for this observation are that (1) the mixing of data from different types of materials (particularly in copper tailings which are known to be extremely heterogeneous and difficult to zone) increases the kurtosis of resulting frequency distributions thus favoring beta shapes, and (2) the Beta is a four-parameter function which as a result is quite flexible. The beta distribution can be specified to take cn a variety of shapes from unimodal to bimodal, from quasi-exponential to "J"

Table 9.1
DISTRIBUTIONS PASSING CHI-SQUARE GOODNESS-OF-FIT TEST AT 5%

COMMODITY	SITE	MEASUREMENT	RAW DATA	RESIDUALS
Copper	Chambishi	cone penetration	none	none
	Chibuluma	cone penetration	beta	none
	Chino	SPT	normal	normal
			beta	
			lognormal	
			gamma	
	Chingola	cone penetration	none	none
	Magna	water contents	normal	none
			beta	
		field ane	gamma	none
		dry density	normal	none
			beta	
	Mindola	cone penetration	none	none
Uranium gamma	Colorado	SPT	none	none
		triaxial phi	normal	
			beta	
			lognormal	
			gamma	

continued on next page

Table 9.1 -- Continued

COMMODITY	SITE	MEASUREMENT	RAW DATA	RESIDUALS
gypsum	Texas	SPT	normal	normal
			beta	
			lognormal	
			gamma	
		unit weight	beta	normal
				beta
	La. 1	SPT(0 to 50ft)	normal	normal
			beta	beta
		SPT(55 to 100ft)	lognormal	none
			gamma	
	Florida 1	SPT	lognormal	none
			gamma	
	Piney Point	cone penetration	lognormal	none

Table 9.2
DISTRIBUTIONS PASSING KOLMOGOROV-SMIRNOV GOODNESS-OF-FIT TEST AT 5%

COMMODITY	SITE	MEASUREMENT	RAW DATA	RESIDUALS
Copper	Chambishi	cone penetration	none	none
	Chibuluma	cone penetration	beta	normal
				beta
	Chino	SPT	all	normal
	Chingola	cone penetration	none	none
	Magna	water contents	normal	normal
			beta	beta
			lognormal	
			gamma	
		field ane	normal	normal
			beta	beta
			lognormal	
			gamma	
		dry density	normal	none
			beta	
			lognormal	
			gamma	
	Mindola	cone penetration	none	none
Uranium	Colorado	SPT	none	none
		triaxial phi	normal	none
			beta	
			lognormal	
			gamma	

continued on next page

Table 9.2 -- Continued

COMMODITY	SITE	MEASUREMENT	RAW DATA	RESIDUALS
gypsum	Texas	SPT	normal	normal
			beta	
			lognormal	
			gamma	
		unit weight	normal	normal
			beta	beta
			lognormal	
			gamma	
	La. 1	SPT(0 to 50ft)	normal	normal
			beta	beta
			lognormal	
			gamma	
		SPT(55 to 100ft)	beta	normal
			lognormal	beta
			gamma	
	Florida 1	SPT	beta	normal
			lognormal	beta
			gamma	
	Piney Point	cone penetration	beta	none
			lognormal	
			gamma	

shaped. For these two reasons, it comes as little surprise that the beta distribution in general appears to fit experimental data more closely that do other pdf's.

The conclusion should not be drawn upon first inspection, however, that the beta distribution should be chosen over other analytical pdf's for the purposes of engineering analysis and reliability modeling. First, because the beta requires that four parameters rather than two be estimated from strength data, the statistical uncertainty of the parameter estimates can be large for limited numbers of data. Second, and more importantly, the beta distribution is defined over a doubly limited domain. That is, a beta distributed random variable, such as strength, has minimum and maximum values which it cannot exceed. Friction angle, for example, might be defined only between 20 and 30 degrees. There is usually no cogent physical reason for this limitation, and in fact the limitation seldom makes physical sense. Adopting "natural" limits, such as 0 and 90 degrees for friction angle, usually leads to distribution functions that do not fit the bulk of the data. Using common statistical criteria to estimate the limits usually leads to unuseful results. For example, the maximum likelihood estimators of the upper and lower bounds, respectively, are the maximum and minimum measurements in the data set. In reliability modeling, beta distributions preclude any possibliity that strengths or other geotechnical properties turn out to be less than the lower bound specified a priori, and thus ignore extreme tail behavior of geotechnical properties.

Given the diversity of distributional forms that appear to model emprical strength data, and the unsuitability of any one distribution across all or even the majority of sites, no one distributional form can be recommended for reliability modeling of tailings embankments. At the present state of practice either (1) distributional forms will have to be verified on a site-by-site basis, or (2) second-moment techniques using only means, variances, and covariances will have to be used. Given the large numbers of data necessary to verify the tail behavior of strength data and the relatively ad anced development of second-moment reliability analysis, the second option appears the better of the two.

Spatial Correlation

Autocovariance functions for geotechical data pertain to that part of the spatial variation which is not included in

the estimation of spatial trends. Thus, the nature of the autocovariance function and its extend cannot be separated from decisions made in modeling spatial trends. If no trends are removed from the data, autocovariances can extend very far. If very intrecate trends are identified and removed, then autocovariances will decay rapidly. In the present work linear trends with depth were estimated by regression analysis and thus the vertical autocovariance functions refer to residuals off this linear trend. As can be seen in Table 9.3, typical autocovariance distances (i.e., the distance at which the autocovariance decays to a factor of 1/e, the based of the natural logarithms) for each of the three commodities studies are in the range of one meter. These are clearly evident in the cone resistance and index property data, but are somewhat masked by measurement error for SPT blow count data. This observation is consistent with others reported in the literature, which show correlation decaying fairly quickly in the vertical direction.

An interesting although problematic discovery was that very few site in estigation programs collect sufficiently many or appropriately arrayed data to allow estimation of horizontal autocorrelation functions. In the present work only one such site was found. While the lack of data with which to estimate horizontal autocorrelations has been recognized for a long time, the extent of the problem was somewhat surprising. The implication is that, if reliability modeling is to be used on tailings embankments then field in estigation programs will have to be modified. These modifications need not entail greatly increased costs, but they will have to include explicit consideration of the placement of borings or penetrations with respect to statistical data analysis.

The horizontal correlation structure estimated at the one site shows a decrease of correlation of cone resistance to about 30% at one meter, and to about 10% at ten meters. As a first approximation, this might mean an autocovariance distance on the order of a few meters, possibly 2 to 5. Spacings among borings in the range 2 to 9 meters were not available at the site. This autocorrelation distance is somewhat lower than those commonly reported in the literature for more uniform soils (e.g., marine clay), which typically are in the 10 to 50m range, once any obvious spatial trends are removed. Given the heterogeneity of copper tailings, this small autocovariance distance seems appropriate.

Using the procedure described in earlier sections to infer measurement error, the noise associated with the cone

Table 9.3
VERTICAL AUTOCOVARIANCE DISTANCES

COMMODITY	SITE	MEASUREMENT	COVARIANCE DISTANCE
Copper	Chambishi	cone resistance	1m
	Chibuluma	cone resistance	2
	Chino	SPT	<1
	Chingola	cone resistance	<1
	Magna	water contents	0+
		field ane	1
		dry density	0+
	Mindola	cone penetration	2
	Morenci	cone penetration	1
Uranium	Colorado	SPT	3
Gypsum	Texas	SPT	0+
		unit weight	1
	La. 1	SPT	0+
	Florida 1	SPT	0+
	Piney Point	cone penetration	0+

penetration measurements analyzed here appears small. The noise associated with field vanes, although only analyzed for one site, appear to be moderate (say, in the range of 30 to 40%). The noise associated with SPT blow counts appears very large. In part, these differences are caused by the differences in spacings among the three types of measurements, for example, blow counts recorded on one meter inter als do not reflect smaller scale correlations. On the other hand, the relative ranking of these measurement errors conforms to common wisdom. As discussed earlier, measurement noise inferred via the autocovariance function does not distinguish between errors introduced by the measurement procedure and those very small scale fluctuations that actually exist in the tailings materials. However, for the purposes of common stability modeling the distinction is unimportant.

Uncertainty in Factor of Safety

Several factors influence uncertainty in the computed factor of safety for a critical sliding mass. For an effective stress analysis uncertainty in slope geometry, soil unit weight, applied body forces and external loads, and pore pressure affect the driving moment. In addition to these, uncertainty in strength parameters affects the resisting moment.

Alonso (1976) illustrated the influence of these factors (excluding applied body forces and external load) on variance in moments used to calculate factor of safety for the Green Creek slide reproduced in Figure 9.1. His results for the critical surface reproduced in Figure 9.2 show that two parameters contribute the primary uncertainty in factor of safety--pore pressure and cohesion. Uncertainty in geometry and unit weight are of secondary importance. Two important qualifications apply to his results. He determined variance in pore pressure by taking the maximum differences in measured pore pressure at several points in the slope and considering these differences as belonging to the same population centered about a constant mean value. This assumption is not very realistic for a tailings deposit where flow and differences in elevation produce a distinct variation in pore pressure. Also he considered strength parameters as two independent variables. Since by definition $\bar{c}$ and $\bar{\phi}$ are dependent, his conclusion on the greater importance of $\bar{c}$ compared to $\bar{\phi}$ is misleading. A simplified way to consider variation in strength is to assume $\bar{c}$ equals zero and represent strength with $\bar{\phi}$ only. This simplification is acceptable when considering a particular value of effective stress and using strengths measured in different tests for that stress level.

To measure the relative importance of uncertainty in strength and pore pressure for tailings deposits, a typical example using Japanese copper data illustrated in Figures 9.3 and 9.4 was evaluated. Considering an important sliding mass (not necessarily the critical one) the variance in FS was calculated from variance in pore pressure and friction angle as

$$V(FS) = \left(\frac{\alpha FS}{\alpha \phi}\right)^2 V(\phi) + \left(\frac{\alpha FS}{\alpha u}\right) V(u) \qquad (9.1)$$

The derivatives $\frac{\alpha FS}{\alpha u}$ and $\frac{\alpha FS}{\alpha \phi}$ were found for this surface by performing stability analyses with different values of $\bar{\phi}$ and u.

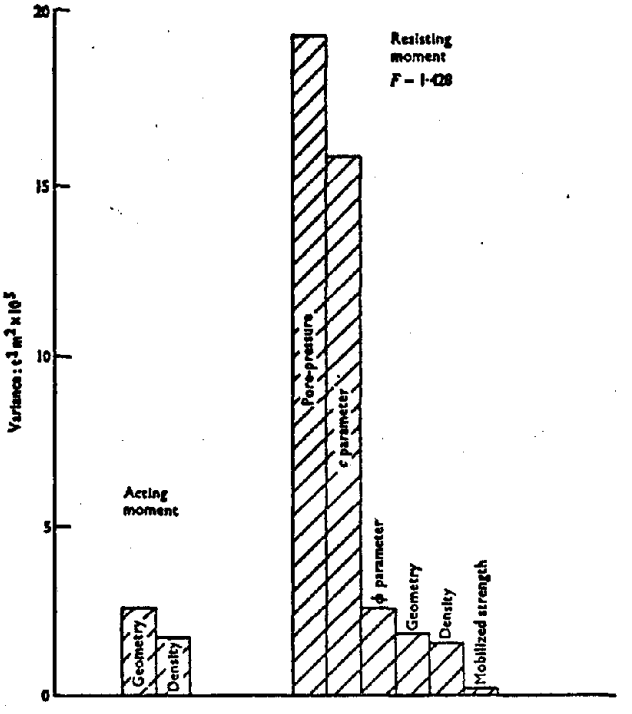

Figure 9.1 Contribution of different factors to variance of moments for critical circle, Green Creek slide (after Alonso, 1976)

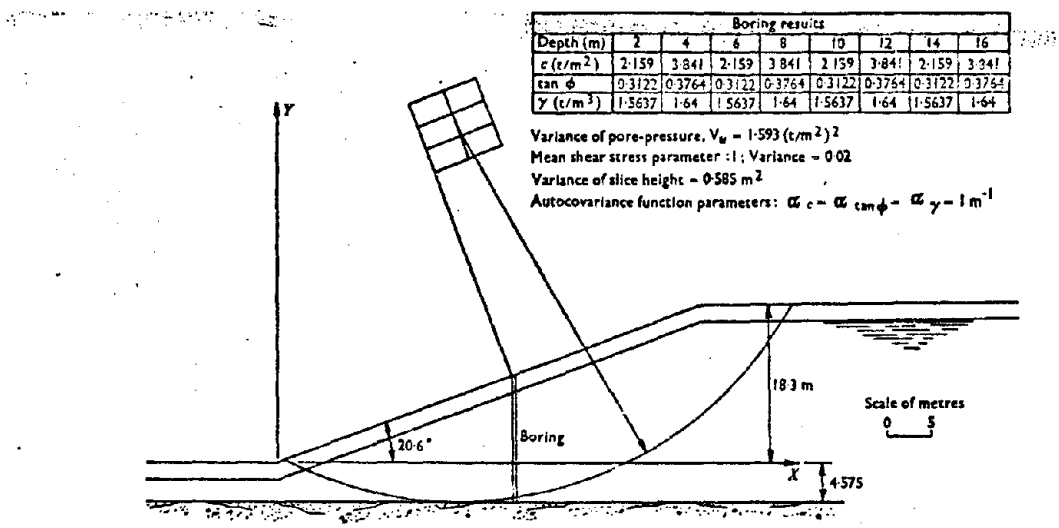

Figure 9.2 - Geometry and Parameters of Green Creek Slide (after Alonso 1976)

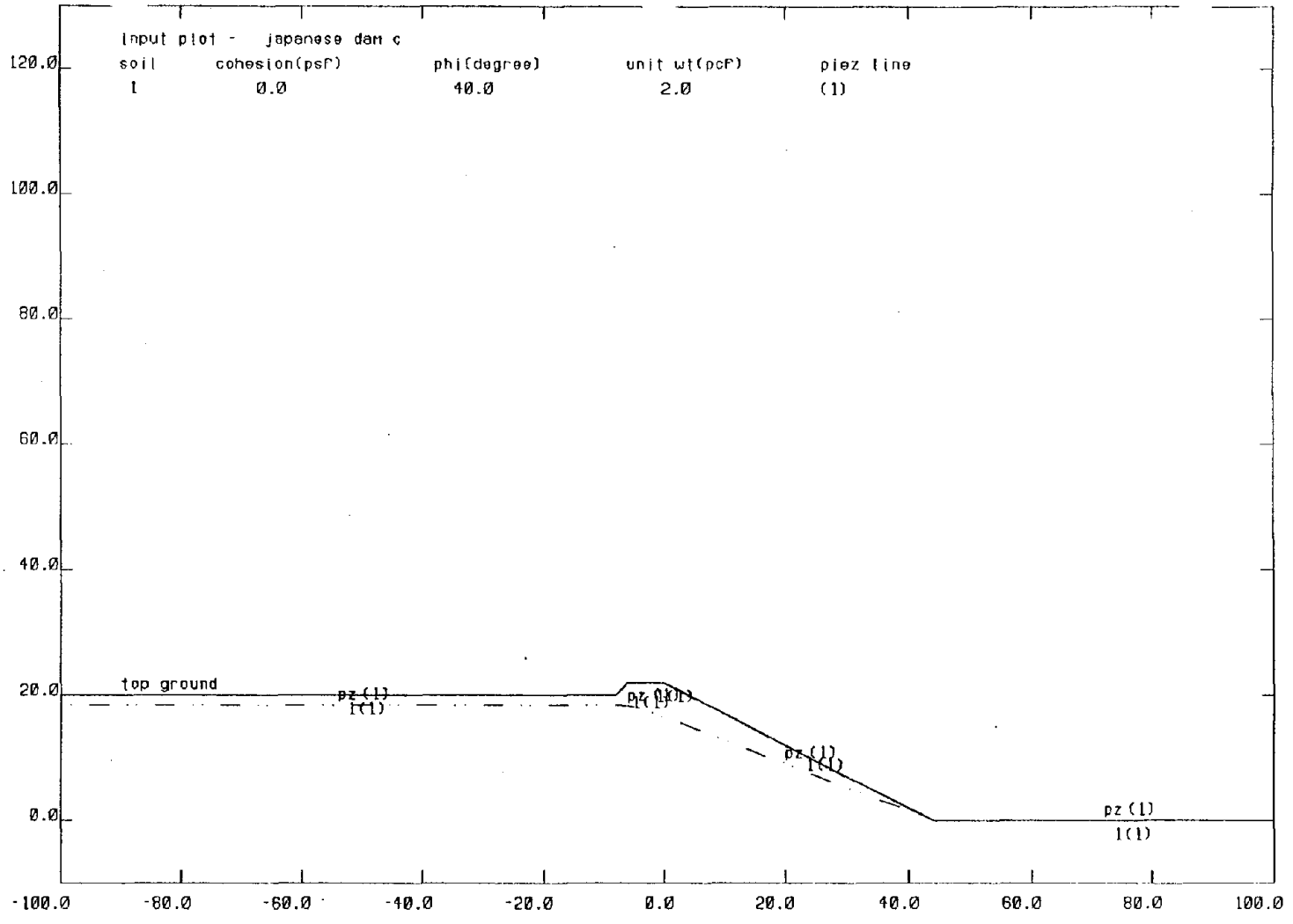

Figure 9.3 - Standard case input (Japanese copper tailings dam "C") with increased pore pressure (u)

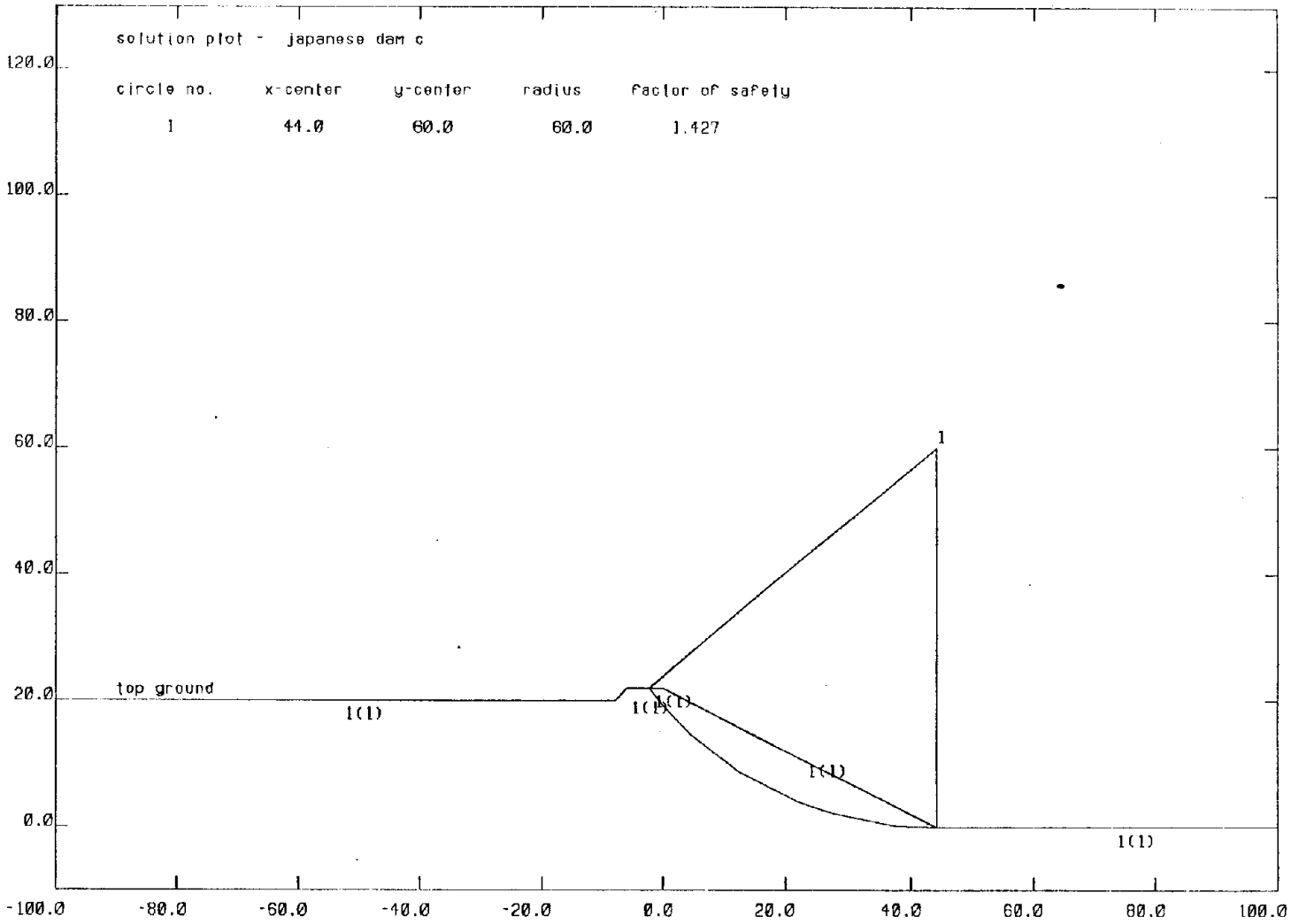

Figure 9.4 - Solution plot, Japanese copper tailings dam "C"

Meaningful descriptions of variations of pore pressure in these analyses are difficult. Here the distribution of pore pressure along the failure surface was determined from a typical flow net fitting the measured pore pressures in the Japanese data. All values of pore pressure along the failure surface were then considered to increase or decrease by the same percentage. This approximation matches the actual, systematic uncertainty faced in predicting field pore pressures for stability analysis. For the surface conditions shown

$$\left(\frac{\Delta FS}{\Delta \Phi}\right)^2 = 2.3 \times 10^{-3}$$

$$\left(\frac{\Delta FS}{\Delta u}\right)^2 = 4.67 \times 10^{-2}\, m^{-2}$$

Field measurements of steady state pore pressure in Japanese copper tailings were used to establish Var(U) as Ø.85 m . Table 9.4 summarizes the measured data leading to this value. Note that the steady state values of pore pressure are about one-half of those obtained by assuming static conditions below the measured ground water surface. V(u) was calculated as the difference between measured pore pressures and those predicted using one-half of hydrostatic values.

The Japanese data include 17 strength tests performed on high quality undisturbed samples. These tests were consolidated to the in situ effective stresses and the resulting strength envelope expressed as a friction angle. Insufficient data exist to establish $V(\overline{\phi})$ for each site. Instead values measured at all sites were used to estimate $V(\overline{\phi})$. This should exceed the variance in $V(\overline{\phi})$ for any individual site. For the eight Japanese sites $V(\overline{\phi})$ equals 14.Ø5 and the variance in FS becomes

$$V(FS) = (2.3 \times 10^{-3})(14.Ø5) + (.Ø467)(Ø.85)$$

$$V(FS) = Ø.Ø72$$

Variance in pore pressure has a slightly larger influence on variance in FS than variance in friction angle obtained from all Japanese sites. It appears that for most tailings deposits, variance in pore pressure is likely to be the largest contributor to variance in factor of safety.

Table 9.4: JAPANESE COPPER DATA: PORE PRESSURE COMPARISONS

MINE	PHI	DEPTH	h_p	u_s	u	u_s-u	MEAN	VAR.
A	30	1.30	.30	3.0	1.0	+0.5	0.183	0.118
A	38	4.45	3.45	3.5	2.0	-0.25		
A	NA	5.05	4.05	4.1	2.2	-0.15		
A	NA	9.61	8.61	8.6	3.8	+0.5		
A	32.5	10.45	9.45	9.5	4.3	+0.45		
A	NA	13.05	12.05	1.21	6.0	+0.05		
B	DR*	7.60	1.60	1.6	1.5	-0.7	-1.325	1.984
B	DR	10.30	4.30	4.3	3.6	-1.45		
B	DR	13.57	7.57	7.6	6.2	-2.4		
B	DR	14.25	8.25	8.3	6.3	-2.15		
D	45.5	4.35	-2.15	-2.2	-1.0	-0.1	0.068	0.724
D	NA	9.00	+2.50	2.5	+1.1	+0.025		
D	42	9.35	2.85	2.9	3.0	-1.55		
D	NA	11.86	5.36	5.4	1.9	+0.80		
D	NA	17.42	10.92	11.0	4.9	0.60		
D	34	18.35	11.85	11.9	5.0	0.95		
D	NA	20.00	13.50	13.5	7.0	-0.25		
E	NA	4.70	1.20	1.2	1.2	-0.60	-0.129	1.911
E	NA	6.75	3.25	3.3	3.2	-1.55		
E	37.5	7.91	4.41	4.4	3.0	-0.80		
E	38	8.39	4.89	4.5	3.0	-0.75		
E	NA	8.59	5.09	5.1	2.9	-0.35		
E	NA	10.23	6.73	6.7	2.9	+0.45		
E	NA	12.48	8.98	9.0	1.8	2.70		
F	NA	6.42	3.92	3.9	0.9	1.05	0.619	0.593
F	NA	7.91	5.41	5.4	2.4	0.30		
F	NA	9.83	7.33	7.3	2.6	1.05		
F	37	12.40	9.90	9.9	3.7	1.25		
F	38.5	12.44	9.94	9.9	3.7	1.25		
F	NA	13.65	11.15	11.2	4.5	1.10		
F	37.3	15.34	12.84	12.8	6.8	-0.40		
F	NA	15.41	12.91	12.9	7.1	-0.65		
G	37.5	14.30	2.80	2.8	0.5	+0.90	1.419	0.217
G	37	16.30	4.80	4.8	0.6	1.80		
G	NA	17.70	6.20	6.2	2.0	1.10		
G	38.5	17.90	6.40	6.4	2.5	0.70		
G	NA	19.25	7.75	7.8	2.0	1.90		
G	NA	23.10	11.60	11.6	4.0	1.80		
G	31	24.30	12.80	12.8	5.0	1.40		
G	NA	27.00	15.50	15.5	6.0	1.75		
I	NA	5.57	4.24	4.2	2.8	-0.70	-0.953	0.398
I	35.5	8.45	7.12	7.1	4.0	-0.45		
I	NA	8.79	7.46	7.5	4.7	-0.95		
I	NA	14.89	13.56	13.6	8.6	-1.80		
I	NA	19.16	18.83	18.8	11.0	-1.60		
I	39	23.90	22.57	22.6	13.5	-0.22		

TOTALS: MEAN OF MEAN=-0.017; MEAN OF VAR.=0.849; VAR. OF VAR.=0.606

*only drained friction angle available

The Japanese data taken on inactive mines consistently show pore pressures less than hydrostatic values. Limited data from active mines (Mittal and Morgenstern, 1975) show pore pressures up to 1ØØ percent greater than those calculated by assuming hydrostatic conditions below the measured ground water level. Without field measurements of pore pressure, the engineer may be faced with large uncertainties in what pore pressures to use in a deterministic or reliability analysis. We believe more study of variability in field pore pressures is essential to improving our ability to assess safety of tailings dams.

10. CONCLUSIONS

This study examined data from 41 tailings dams storing gypsum, uranium and copper tailings. We evaluated data from 64 borings with standard penetration tests, 142 soundings with Dutch cone tests and laboratory samples from 36 sites. The work reported here supports five general conclusions:

(1) The variability of strength data for tailing materials is similar across commodities. Coefficients of variation of average strength parameters from one mine to another are about 10% for copper and gypsum tailings and about 20% for uranium. The uranium number may be influenced by limited data, however.

(2) The variability of strength data within an embankment differs considerably across types of strength measurement. For laboratory measurements coefficients of variation on the order of 10-20% are common. For in situ measurements such as SPT and cone penetration resistance, coefficients of variation from 50 to 100% are common.

(3) No one distributional form appears appropriate as a general model of tailings strength variability; however individual data sets appear to follow fairly regular frequency distributions.

(4) The amount of measurement noise (or microscale variability) in in situ measurements can be large, often on the order of 50% of the data scatter and differs significantly with measurement procedures. SPT data display considerably more noise than do cone penetration data.

(5) The spatial variability of tailings properties is erratic, leading to autocorrelation functions which decay rapidly in both the horizontal and vertical directions. Vertical autocovariance distances on the order of 1 to 3 meters are typical· horizontal autocovariance distances may be about ten times the vertical.

Our results show that at any specific site an appropriate distributional form to serve as input for reliability modeling should be verified against site specific data. However, once spatial trends were removed, most of the data sets studied displayed unimodal distribution functions which were more or less symmetric. Highly skewed distributions were infrequent, but many of the empirical distributions displayed more kurtosis (broader shoulders) than do normal distributions.

Measurement errors and small scale variability mask much of the spatial structure of tailings properties, but correlation functions appear to be identifiable in cone penetration profiles and other high quality data. Due to the heterogeneity of tailings, particularly copper tailings, these correlation distances are small. Less than one or two meters in the vertical direction and perhaps two or three times that in the horizontal direction appear typical. Removing spatial trends reduces correlation distances correspondingly.

Two non-statistical conclusions derive from the present work, dealing respectively with the interpretation of Mohr-Coulomb strength parameters from cone penetration measurements, and the prediction of pore fluid measures in tailings embankments. The short correlation distances require measurement of properties over a close vertical spacing. The Dutch cone with measurements every 10 cm seems ideally suited. However, due to the heterogeneity of tailings particularly those associated with copper mining, drainage conditions during cone penetration differ throughout the profile, and are difficult to interpret without direct measurement. Thus, with cone penetration resistances alone (i.e. when not using a piezocone) the measurements recorded may be associated with drained failure, undrained failure, or something in between. This makes the calculation of appropriate strength parameters difficult. Piezocone measurements which include direct measurements of pore pressures during penetration as well as equilibrium pore pressures circumvent this difficulty.

Secondly, equilibrium pore pressures in the tailings embankments for which direct measurements were available differ significantly from those predicted assuming hydrostatic conditions below the measured ground water surface. Observed pore pressures in older inactive ponds averaged about half those predicted for hydrostatic conditions. Other measurements on active ponds show pore pressures as much as 100% greater than hydrostatic values. These discrepancies result from the complex flow patterns that develop in most tailings dams. Given the sensitivity of stability prediction to pore pressures, this represents a

major source of uncertainty which is often undervalued in deterministic and reliability analyses.

From our work we make the following recommendations for further work which would help meet the USBM objective of improving methods for safety analysis of tailings dams.

(1) Extend the data analysis reported herein to other commodities such as iron, lead, silver and zinc. From our experience this might be most successful if the Bureau of Mines initiated a cooperative arrangement with mining companies where the companies provide data and the Bureau provides the analysis and evaluation. This cooperation would circumvent the problem of confidential data we repeatedly encountered.

(2) Undertake a program to evaluate the use of piezocones to assess in situ tailings strength. Much of the regular cone data gathered for tailings is useless in that unknown drainage conditions make it impossible to interpret the test. Piezocones allow one to measure in situ pore pressures and those generated by the test so that one can better interpret the test. The piezocone may give the industry a reliable tool to economically determine strength and pore pressure in existing dams and measure changes in strength with time.

(3) Undertake a study of the uncertainty in pore pressure in tailings dams and the effects of such uncertainty on safety evaluation. Uncertainty in pore pressure probably provides the largest component to uncertainty in the safety evaluation of a tailings dam. Present practice usually considers hydrostatic pore pressures below the phreatic surface. Theoretically pore pressures may vary from zero to more than twice the hydrostatic values depending on details of the dam. Measured pore pressures reported herein vary from 50 percent less than to 100 percent greater than hydrostatic values. Such uncertainties dominate a reliability analysis. A cooperative effort with industry involving field measurements of pore pressures in several dams, analytical studies to predict such pore pressures, and studies to formulate recommendations for obtaining and using uncertainties in pore pressures in deterministic and reliability analyses would in our opinion provide the largest contribution to improved safety evaluations of tailings dams.

(4) Conduct a comprehensive risk analysis for an existing tailings dam to define the analytical tools necessary for such a study, to isolate the principal uncertainties in the safety of tailings dams and to illustrate the use and benefits of reliability analysis to the mining industry. This analysis should include systematic uncertainties as well as spatial variation, and economic aspects of construction, instrumentation and failures. Earlier work by Anderson et. al., 1982, sponsored by the USBM, could serve as starting point.

REFERENCES

COPPER TAILINGS

Blight, G.E., "Waste Gypsum as an Embankment Material", Proceedings of the Seventh International Conference on Soil Mechanics and Foundation Engineering, Mexico City, 1969.

Ishihara, K. et. al., "Cyclic Strength Characteristics of Tailings Materials", Japanese Society of Soil Mechanics and Foundation Engineering, Soils and Foundations, Vol. 20, No. 4, Dec. 1980.

Jeyapalan, Jey K., "Flow Failures of Some Mine Tailings Dams", Geotechnical Engineering, Vol. 12, 1981.

Klohn, Earle J. and Maartman, C.H., "Construction of Sound Tailing Dams by Cycloning and Spigoting", Tailings Disposal Today, Denver, Colorado, 1979.

Marr, W. Allen, Compilation of Strength Data from Tests on Copper Tailings in the Zambian Copperbelt, USBM-MIT Study, 1981.

McGregor D., and Dopson, G. W., "How Magma Copper Builds Tailings Dams", World Mining, March, 1973.

Mittal, H. K. and Morgenstern, N. R., "Parameters for the Design of Tailings Dams", Canadian Geotechnical Journal, Vol. 12, 1975.

Murthy, Y. K. et. al., "Mine Tailings in India", 12th International Congress on Large Dams, Mexico, 1976.

Sandy, J. D. et. al., "Failure and Subsequent Stabilization of No. 3 Dump at Mufulira Mine", Transactions Section A of the Institute of Mining and Metallurgy, Vol. 85, 1976.

Volpe, Richard L., "Physical Engineering Properties of Copper Tailings", Current Geotechnical Practice in Mine Waste Disposal, ASCE, 1979.

Wahler, W. A., "Evaluation of Mill Tailings Disposal Practices and Potential Dam Stability Problems in the Southwestern United States', Investigation Report, Kennecott Copper Corporation, Magna Tailings Dam, Magna, Utah, Dec. 1974.

Wahler, W. A. and Schlick, D. P., "Mine Refuse Impoundments in the United States", Proceedings, 12th

International Congress on Large Dams, Mexico, Vol. 1, Q44, R14, 1976.

Werno, M. and Osckowicz, J., "Stability of Tailings Dam above Copper Mines", Archiwum Hydrotechniki, Tom. XXVI, Zeszyt 3, 1979.

GYPSUM TAILINGS

Blight, G. E., "Waste Gypsum as an Embankment Material", Proceedings of the 7th International Conference on Soil Mechanics and Foundation Engineering, Mexico. 1969.

Blight, G. E.. "Slopes in Industrial Waste", Ninth International Conference on Soil Mechanics and Foundation Engineering, Tokyo, 1977.

Kleiner, D. E., "Design and Construction of an Embankment Dam to Impound Gypsum Wastes", 12th International Congress on Large Dams, Mexico, 1976.

Scheiner, B. J. et. al., "Large-scale Dewatering of Phosphatic Clay Waste from Central Florida", USBM RI 8611, 1982.

Toland, G. C., "Gypsum Tailings Pond Design. Kimberly, British Columbia", Dames and Moore Inc., Salt Lake City, Utah, 1971.

Vick, Steven G., "Rehabilitation of a Gypsum Tailings Embankment", Proceedings, Conference on Geotechnical Practice for Disposal of Solid Waste Materials, ASCE, 1977.

URANIUM TAILINGS

Berry, John B. and Velarde, Jose, "Stabilization of Existing Uranium Tailings Piles at Uravan Colorado", Symposium on Uranium Mill Tailings Management, Fort Collins, Colorado, Colorado State University, Oct. 26-27, 1981.

Heuze, Francois and Dessenberger, Nancy, "Preliminary Soil Mechanics Studies of Inactive Uranium Mill Tailings", Proceedings, Second Symposium on Uranium Mill Tailings Management, Colorado State University, Fort Colins, Colorado, Nov. 19-20, 1979.

Heuze, Francois and Markos, Gergely et. al., "DOE Progress Report: Pollution of Ground Water Due to Inactive Uranium Mill Tailings Piles", Feb. 6, 1980.

Macbeth, P. J. et. al., "Laboratory Research on Tailings Stabilization Methods and Their Effectiveness in Radiation Containment", USDOE/GJO GJT-21, April, 1978.

Martin, Joseph P. et. al., "Characterization of the Inactive Tailings Sites", Symposium on Uranium Mill Tailings Management, Colorado State University, Nov. 24-25, 1980.

Moghissi, A. A. et. al., Nuclear Power Waste Technology, The American Society of Mechanical Engineers, New York, 1978.

Nelson, John D. and Kane, Joseph D., "Failure of the Church Rock Tailings Dam", Symposium on Uranium Mill Tailings Management, Colorado State University, Fort Collins, Colorado, Nov. 24-25, 1980.

Sharp, Kevan et. al., "A Model for Assessing Slope Reliability Utah State University, Department of Civil and Environmental Engineering, Logan, Utah, 1981.

"Engineering Assessment of Inactive Uranium Mill Tailings", USDOE/GJO, Dec., 1977.

"Uranium Geophysical Technical Symposium Summaries and Visual Presentation", USERDA/GJO and BFEC/GJO, Sept. 14-16, 1976.

"Fourth Annual Uranium Seminar", South Texas Minerals Section, SME of AIME, Corpus Christi, Texas, Sept. 14-17, 1980.

"Materials Tested at Three Inactive Uranium Tailings Sites", Colorado State University, Fort Collins, Colorado, 1982.

OTHER TAILINGS

GENERAL DESIGN MODELS FOR TAILINGS DAMS UNSPECIFIED MINERALOGY

Baecher, Gregory B., "Autocorrelation of Field Vane Strengths Beneath Axis B-6", MIT, Jan. 1982.

Bloomfield, R. A. and Stewart, B. M., "Design Parameters for Oil Shale Waste Disposal Systems", USBM RI 8544, 1981.

Brawner, C. O. et. al., "Stability of Waste Embankments", A Report by the Canadian Advisory Commitee on Rock Mechanics, Oct. 1969.

Brawner, C. O. and Milligan V., "Geotechnical Practice for Stability in Open Pit Mining", Proceedings of 2nd International Conference on Stability in Open Pit Mining, Vancouver, British Columbia, Canada, Nov. 1-2, 1971.

Campbell, David B. and Brawner, C. O., "The Tailings Dam, an Engineered Structure", Western Miner, April, 1971.

Hardy, R. M., "Tailings Dams", EIC Western Regional Tar Sands Conference, Edmonton, Alberta, 1974.

Jones, Gary, Van Zyl, Dirk and Rust, Eben, "Mine Tailings Characterization by Piezometer Cone", in Cone Penetration Testing and Experience, proceedings of a session sponsored by Geotechnical Division of the ASCE, National Convention, St. Louis, 1981.

Kealy, Daniel C. and Busch, Richard A., "Determining Seepage Characteristics of Mill Tailings Dams by the Finite Element Method", USBM RI 7477.

Klohn, Earle J., "Tailings Dams in British Columbia", Symposium on the Stability of Open Pit Mines, 1972.

Klohn, Earle J., "Design and Construction of Tailings Dams", CIM Transactions: Vol. LXXV, 50--66, 1972.

Klohn, Earle et. al., "Simplified Seismic Analysis for Tailings Dams", Earthquake Engineering and Soil GT Specialty Conference, Pasadena, California, June 19-21, 1978.

McKee, Bill et. al., "Upstream Design for Extension of an Abandoned Tailings Pond", Tailings Disposal Today, Tucson, Arizona, 1973.

Mittal, Hari K. and Morgenstern, Norbert R., "Design and Performance of Tailings Dams", Geotechnical Practice for Disposal of Solid Waste Materials, ASCE, 1977.

Monk, Carl D. "Workshop on Research Needs in Relation to Surface Mining in Eastern United States", Georgia University, Department of Botany, Athens, Georgia, Sept. 1974.

Nicholson, David E. and Wayment, William R., "Properties of Hydraulic Backfills and Preliminary Vibratory Compaction Tests", USBM RI 6477, 1964.

Pederson, Gerald R., Bureau of Mines Research 1981, USBM, 1981.

Pettibone, Howard C. and Kealy, Dan C., "Engineering Properties of Mine Tailings", ASCE: Soil Mechanics and Foundations Division, Vol. 97, 1971.

Phukan, A., "Design and Construction of Tailings Dams", Western Miner, Dec. 1971.

Phukan, A., "Geotechnical Engineering Applications to Tailings Dams", Woodward-Lundgren and Associates, undated.

Sazonov, G. T., "Design, Construction and Operation of Tailings Systems", Tailings Disposal Today, Denver, Colorado, 1979.

Sharp, Kevan D. et. al., "A Model for Assessing Slope Reliability", Utah State University, Logan, Utah, January 1981.

Soderberg, Roy L. and Busch, Richard A., "Design Guide for Metal and Non-metal Tailings Disposal", USBM IC 8755, 1977.

Tesarik, D. R., and McWilliams, P. C., "Factor of Safety Charts for Estimating the Stability of Saturated and Unsaturated Tailings Pond Embankments", USBM RI 8564, 1981.

Williams, Roy E., Waste Production and Disposal in Mining, Milling, and Metallurgical Industries, Miller Freeman Publications Inc., 1975.

Yuan, Georgia, "A Blight on the West", The Amicus Journal, Winter 1891.

"Containment Pond Technology: State of the Art", USBM OFR 94-80 Dec. 1979.

"Design of Small Dams", US Department of Interior, Bureau of Reclamation, 1973.

"Mine Waste Disposal Technology", USBM IC 8857, 1981.

STRENGTH

Baligh, M. M., Vivatrat, V. and Ladd, C. C., "Exploration and Evaluation of Engineering Properties for Foundation Design of Offshore Structures", MIT, Department of Civil

Engineering, Constructed Facilities Division, Research Report R78-40, 1978.

Janbu, N. and Senneset, K., "Effective Stress Interpretation ofIn-situ Static Penetration Tests", Proceedings of the European Symposium on Penetration Testing, Stockholm, Vol. 2:2, PP. 181-193.

Lambe, T. W. and Whitman, R. V., Soil Mechanics, Wiley and Sons, New York, 1969.

Lambe, T. W. and Marr, W. A. "Stress Path Method: Second Edition," Proceedings, ASCE: JGED. Vol. 105, No. GT6 June 1969, pp. 727-738.

Sanglerat, G., The Penetrometer and Soil Exploration, Elsevier Publishing Company, Amsterdam, 1972.

Wright, Steven G., "A Study of Slope Stability and the Undrained Shear Strength of Clay Shales," a thesis submitted to the University of California at Berkeley in partial fulfillment of the requirements for the degree of Doctor of Philosophy, 1969.

PROBABLILITY

Anderson, Loren R. et al., "Probability Modeling of Tailings Embankment Designs," Report to the US Bureau of Mines, Contract J0295029, 1982.

Cochran, W. C., Sampling Techniques, John Wiley and Sons, New York, 1963.

Kendall, M. G. H. and Stuart, A., The Advanced Theory of Statistics, v.1, Macmillian Publishing Co., New York, 1977.

Kendall, M. G. H. and Stuart, A., The Advanced Theory of Statistics, v.2, (3d Edition), Hafner Publishing Co., New York, 1973.

Ord, J. K., Families of Frequency Distributions, Griffin, London, 1972.

APPENDIX A: Site Descriptions

Introduction

Tailings dam sites from all over the world were analyzed in this study. Figure A.1 locates these sites on a world map. Figure A.2 locates sites in North America to a larger scale.

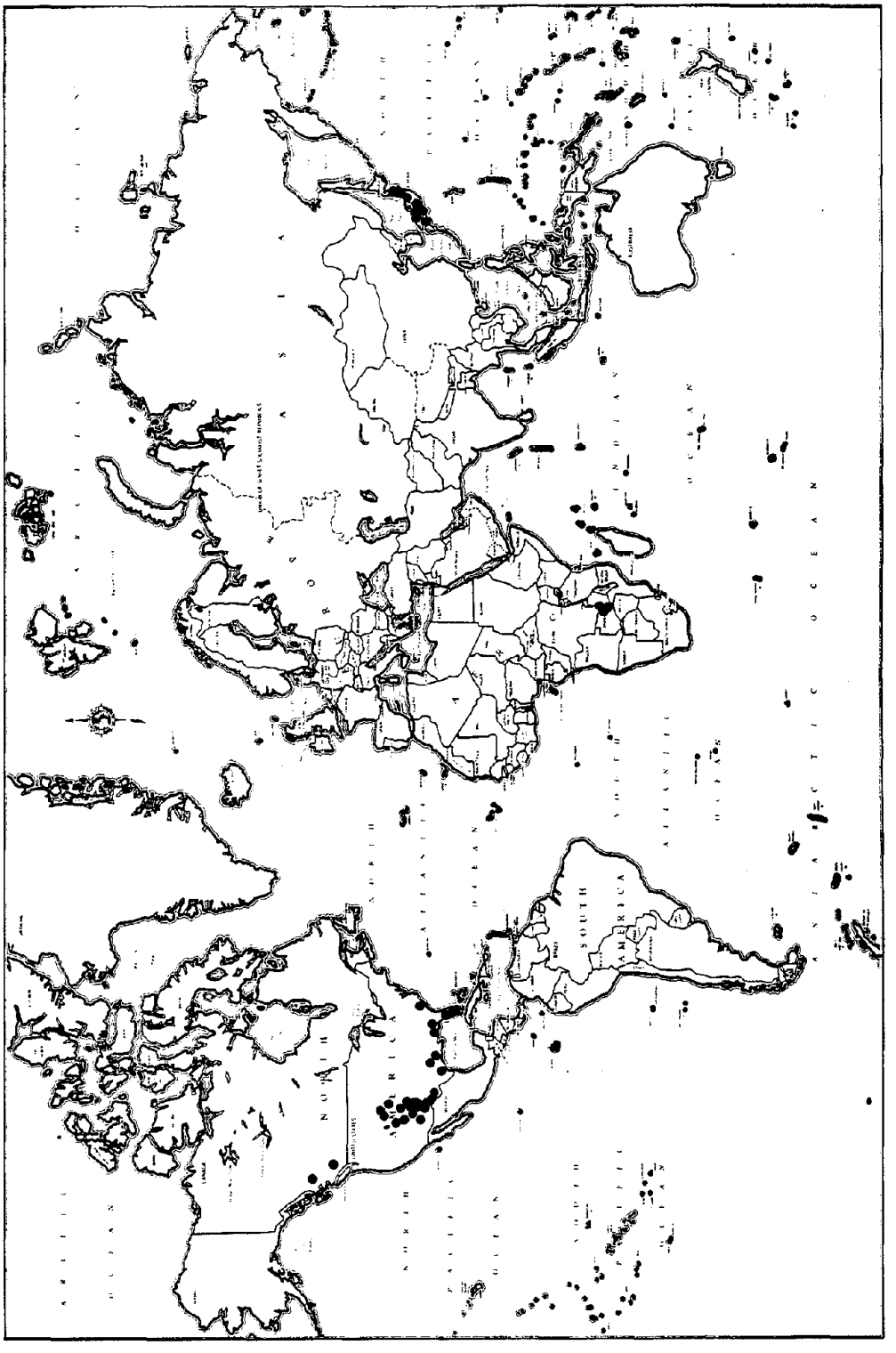

FIGURE A1 TAILINGS SITE LOCATIONS

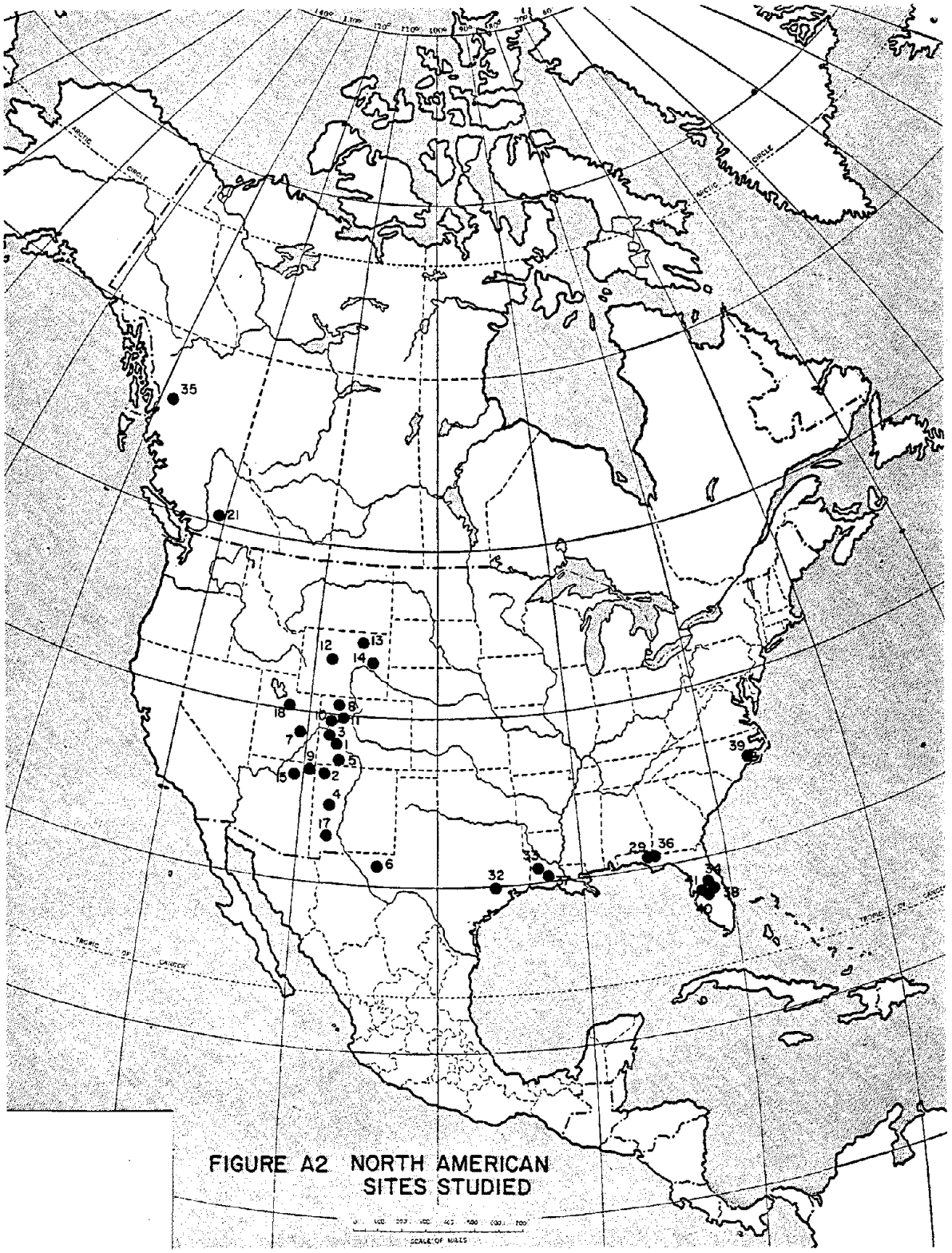

FIGURE A2 NORTH AMERICAN SITES STUDIED

Gypsum Data: Piney Point

A 1969 study by T. William Lambe and Associates for the Borden Chemical Company produced seven cone penetration soundings and CD triaxial results. The Borden tailings ponding system at the time of the study entailed 110 acres of gypsum retained by a 10,000-foot perimeter storage embankment constructed from sands found at the site. The sloping natural ground surface was used where possible as part of the embankment. Between 1500-2000 tons of gypsum were produced each day. When an existing dam was filled at some point in time, its storage capacity was increased by removing gypsum from the pond and then placing, drying and compacting it on the crest and slopes of the existing dike. It was estimated that the dam's height would have to have been increased 5 feet/year to have maintained adequate freeboard.

The Piney Point site is in a highly cultivated region near US highway 41. Subsoils in the dam foundation are: dense sand at the surface underlain by a 10 feet thick layer of sand with gravel and shells; below 10 feet in depth is found a dense slightly plastic silt ending at bedrock at -50 feet.

Prior to the 1969 investigation by Lambe several sections of the dam had experienced local failure due to piping and excessive seepage. As a result of the study several remedial strategies were suggested.

Gypsum Data: Florida2, Florida3, Florida4, Louisiana2 and North Carolina

Strength data from triaxial CIUC with pore pressure measurements and CIDC tests from five separate gypsum sites in Florida, Louisiana and North Carolina formed the basis for two data sets analyzed here: ultimate effective friction angles ($\bar{\phi}_u$) and peak effective friction angles (ϕ_p).

The largest of the five studies, Florida4, was done in 1980 for a power company to determine properties of waste gypsum as a by-product from the power plant's stack scrubbers which daily produce 12-26 tons of gypsum. The waste gypsum is moved from the power plant in a 10-20% solids slurry to a settling pond to sediment out within perimeter dikes. The slurry discharge pipe is moved about the ponding area to uniformly raise the gypsum elevation to an eventual height of fifteen feet. Decant pipes are located in the pond to remove the process water. Gypsum is the only mineral present in the pile, occuring both in sedimented and cast forms in non-plastic, coarse silt-size particles grading out as 100% fines. The pile overlies a foundation of 3-13 feet of clayey sand, which overlies 3-7 feet of soft plastic clay which in turn overlies hundreds of feet of limestone and dolomite.

Two other Florida gypsum studies concerned a gypsum stack at a phosphate complex near Bartow, Florida (Florida3) and a gypsum stack in Polk County, Florida (Florida4). Analysis of the Florida3 stack revealed a mineralogy of gypsum with some quartz and hydrous calcium-aluminum-sulfur, with 80-100% of the non-plastic silt size gypsum particles passing the US No. 200 sieve. At Florida4 the tailings dam is a result of processing Florida phosphate rock. Waste gypsum here contained only 3-5% quartz with 25-50% of the sample retained on a US No. 200 sieve. Lab analyses for Florida4 used one coarse and one fine sample to get a range of material properties.

A study for a chemical plant tailings dam in North Carolina yielded extremely high strength values from CIDC testing: maximum effective friction angles ($\bar{\phi}$) ranging from 53-57 degrees. Gypsum crystals in the pile contained only a trace of quartz. In contrast the gypsum pile at a phosphate company in Louisiana, (Louisiana2) contained only pure gypsum as a by-product from Moroccan phosphate rock. The Louisiana2 gypsum contained predominantly non-plastic, coarse silt-szed particles, 80% finer than the US No. 200 sieve. Strength data for Louisiana2 gypsum was obtained from CU tests with pore pressure measurements.

Gypsum Data: Louisianal

Eleven SPT data sets run on a Louisiana gypsum stack. The gypsum pile at an average height of 48 feet, covers a 13ØØ feet by 23ØØ feet rectangular area. Eventual gypsum storage capacity is expected to be 2,ØØØ,ØØØ cubic yards. The combined settlement rate of the clays and gypsum will average about 12 inches per year providing approximately 5Ø,ØØØ cubic yards of additional storage capacity each year. This stack is composed of a sandy-silty gypsum of firm to stiff consistency. Foundation soils include 4Ø-5Ø feet of silts and silty clays (very soft to firm) including some fibrous materials, overlying a 2-14 foot layer of sand. Strength data came from CU triaxial tests with pore pressure measurements.

Gypsum Data· Floridal

Twelve SPT cases run on by-product gypsum from Floridal were analyzed. No other information is available.

Gypsum Data: Texas

Engineering evaluations of Texas have supplied six SPT data sets, eight holes with dry density determinations and two sets of effective strength parameters from CU tests with pore pressure measurements. The gypsum pile covers an area of fifty-five acres stacked to a height of 90-100 feet. This stack has been used to store waste gypsum from a chemical plant and has been unused for several years. The stack is founded on ten feet of silty-sand, sandy-silt fill overlying five feet of stiff gray clay (with occasional slickensides) which in turn overlies 95 feet of stiff, silty Beaumont clay.

Gypsum Data: Southeastern Idaho Abandoned Site (Vick)

One additional SPT gypsum dataset was made part of this study by referring to an article by Vick (1977). Vick reviewed the properties of an unnamed abandoned gypsum tailings disposal area in southeastern Idaho. The tailings pile was begun in 1955 and was raised using the upstream construction method over the course of nine years until 1964. This dam experienced repeated failures and was noted to have side slopes of about 1:1. The phosphate plant which had used the tailings dump site in question, decided in 1975 to begin a new embankment to be built at the rear of the abandoned dam. At the time of decommission the dam was nearly 80 feet in height with a retaining pond covering about 60 acres.

Thirty foot layers of silts and gravelly silts underlay much of the embankment. In some toe areas the tailings were built upon alluvial sands and gravels. Underlying the natural soils were porphrytic latites and rhyolitic tuffs of the Tertiary Starlight Formation. The tailings themselves consist of non-plastic silt (ML) with quite angular needle-like grains. The abandoned embankment displays severe settlement cracking, polygonal dessication cracking and exposed cavities. As a result Vick noted that careful design was essential if the new embankment was to last.

Copper Data: Brenda

An article published by Klohn and Maartman (1979) reviewed the construction of two large sand dams in British Columbia, and included one set of Dutch Cone data (qc v. z) from Brenda Dam. Brenda Mine is located on a mountain plateau in south central British Columbia near Kelowna, B.C. Owners of the Brenda Coppermine completed a review of dam performance in 1978. This open pit mine produces 24,000-34000 tons/day of tailings from low-grade copper and molybdenum which will eventually total well over 225 million tons of tailings over the twenty years of the mines predicted life. The mine is situated in the Okanagan Valley which is a prime tourist and recreation region in British Columbia. Thus strict requirements for tailings disposal were made from the beginning.

A high dam (450 feet) was required in that the valley is very steep and narrow in the area near the mine pit. The main dike is being built from cycloned sand over a 125 feet high starter dike constructed from rockfill and impervious blanketing. The structure has a free-draining rock toe, as well as under-drainage provided by an upstream blanket drain connecting to finger drains running up under the dam. The dam has been designed with a maximum crest length of 6500 feet and base width of 1800 feet at a height of 450 feet with downstream gradient of 3.5 on 1. Brenda Dam is being raised using the centerline method of construction with an upstream face composed of intermixed cycloned sand and slimes. Total sand required is projected to be about 32.5 million cubic yards.

Brenda Mines utilizes a relatively coarse grind which allows about 50% of the total tailings to be used in embankment construction. The bulk of other material used was basically pit waste rock while natural borrow was obtained for constructing impervious blankets and underdrain filters.

Decanting at Brenda for water reclaim was done by floating pump barge. A reclamation dam downstream catches seepage from the main tailings dam. No pond water is permitted to migrate beyond the reclamation dam.

Tailings are transported 9000 feet to the pond in a 30 inch wood stave pipeline by gravity. Dam building sand from the pipeline discharge is created by two-stage cycloning (single stage cycloning yielded an unsatisfactory construction material) which is then hydraulically moved through an additional pipeline to spigot onto the dam. The spigotting process forms a wide low permeability slimes

beach upstream between the pond and the sand beach. This process resulted in very flat (10 on 1) slopes due to a large amount of excess water in the sands due to water added to facilitate transport to a final pipeline after second stage cycloning. Thus the dam raising rate was extremely slow and was thus judged to be unsatisfactory. As a result later raising utilized conventional hydraulic fill placement. This was done by the construction of cells and the pouring of the diluted sand parallel to the dam axis. The cells are made by bulldozer by pushing sand dike barriers 6-8 feet high covering an area 300 feet by 100 feet. The sand water cyclone discharge is thus spigotted onto the cell forming a 25:1 slope. Excess water is either decanted by syphoning through plastic pipes or exits through seepage to finger drains in the base of the dam. When a cell is full, a bulldozer scrapes off the top 2 feet to form the perimeter dikes for the next cell to be filled thus permitting the next round of hydraulic tailings dam raising. Due to the limited storage capacity of the dam initially, winter construction was a necessity during the early building phases. Also due to local failures in the first cells built, cell filling time for a single cell has been limited to 6-8 hours to avoid over-saturation of the loose perimeter dikes.

Brenda Dam is considered to be in an area of low seismicity. The relatively loose cycloned sand is securely held in place by a large rockfill toe dam.. Here the density of the sand with respect to possible liquefaction is not considered to be critical as long as the sand is kept drained. In addition the design calls for an extra amount of freeboard to accomodate any settlement resulting from a seismic event.

Piezometers on the site monitor internal dam flow and saturation conditions. Observations have shown the saturation and seepage amounts to be low with most observed water resulting from the dam raising operation. Thus it has been predicted (in spite of hydraulic tailings placement) that Brenda Dam will have a low phreatic surface with seepage safely exiting almost entirely from finger drains upstream of the dam toe.

Copper Data: Eight Japanese Sites

An article (March 1981) entitled "Soil Properties of Mine Tailings Deposits in Japan" included geotechnical data summaries for eight Japanese copper mines. The article was based on an original report by OYO Corporation which was prepared for the Subcommittee on the Stability of Mine Tailings Deposits. Thus this report has furnished two data sets for probabilistic analysis: SPT N values versus depth and triaxial test results (phi with respect to depth).

Copper Data: Chino

W.A. Wahler and Associates 1974 investigation of Kennecott Copper Company's Chino Leaching Dump in Santa Rita in north central New Mexico, is the source of 3 SPT data files and one dry density data set. Chino dump reaches a maximum height of up to 300 feet while occupying an area of 28 million square feet. Trucks transport about 70,000 tons daily to the site. Dump material transported consists of coarse waste and low grade ore excavated by blasting from benches in open pits. Host rock here is granodiorite porphyry with chalcocite as the principal copper mineral. This site is located in the physiographic province known as the Mexican Highland of the Basin and Range. Chino leaching dump is generally built directly upon relatively impervious quartz diorite porphyry bedrock, while tailings here are distribute around the dam perimeter by wood stave pipe with spigots. Chino's dump leaching method involves the recovery of copper from waste material or low grade ore by introducing piped sulfuric acid to dissolve the copper into solution in the leaching ponds. Copper is then precipitated out of solution by the introduction of free ferric iron (Fe++) after the solution has been pumped to the precipitation plant. Dump material generally consists of silty to slightly clayey, sandy-gravel with approximately 20% fines, 20% sand and 60% gravel. Texture of this material ranges from angular blocks of hard silicified rocks to highly weathered fine-grained soils grading to a mixture of soils and rocks. Wahler used triaxial testing to obtain strength data for the Chino tailings.

Copper Tailings Data: Four Zambian Sites

A 1981 study of four copper tailings dams in the Zambian copperbelt have yielded Dutch Cone strength data files (qc v. depth). The Dutch Cone penetrometer was hydraulically operated with an automatic recording meter and a capacity of 2000 kg. The study by W.A. Marr for Watermeyer, Legge, Piesold, and Uhlmann was done on Mindola, Chingola, Chambushi and Chibuluma tailings dams.

Mindola East Beach is founded on clay: a slightly sandy clay overlain by lateritic clay and a layer of laterite. Chambishi Dam No. 6 has a wall founded on dark red sandy clayey silt. Chibuluma No.1 is underlain by residual soils and laterites from 3-12 meters thick. In the dam's toe the soft orange brown clayey silt overlies a transition zone to laterite which becomes hard at depths up to two and one-half meters. No water table is encountered at this depth. The soil at the Chingola Tailings Dam No. 2 is notably less lateritic and considerably more free-draining than at the other sites. Beneath a thin upper layer of sandy silt the soil is the decomposition product of the feldspathic gneiss country rock.

Copper Tailings Data: Magna

Several data sets were gained for analysis from the 1974 W.A. Wahler and Associates study of Kennecott Copper Company's Magna Tailings Dam in Magna, Utah: analysis of grain size, of water content with respect to depth, of dry density versus depth and triaxial strength data.

Magna Dam is located west of Salt Lake City and southeast of the Great Salt Lake about fifteen miles north of Kennecott's open pit copper mine in the northern Oquirrh Mountains. This dam covers an area of eight square miles and is situated in the Basin and Range physiographic province. Located on partially indurated lake sediments of the Great Salt Lake (and the former Lake Bonneville) the tailing deposit is thus founded on a 300-1000 feet thickness of bluish clay, sand and gravel. The tailings themselves are byproducts of ore rock crushed to obtain copper. These tailings are generally 89% finer than the US No. 200 sieve. This degree of fineness is necessary to facilitate a copper flotation recovery process. Thus the tailings are found as fine to medium sands with some clayey silts. Steel pipe transports and distributes the tailings under pressure to a diked pond where two steel syphons and vacuum pumps are available for decanting. Strength data was obtained by Wahler from CIU and CKoD tests in which the angularity of the crushed ore particles has influenced intergranular shear strength.

Copper Tailings Data: Morenci

The 1974 W. A. Wahler and Associates' study for the tailings embankments at Morenci, Arizona yielded datasets: five SPT, five Dutch Cone as well as triaxial data. The Morenci mining site consisted of mine, mill, concentrator, smelter, refuse dumps and tailings dams. Morenci is located in eastern Arizona in a geologic setting in transition between the Colorado Plateau and the Basin and Range. Basically this area is a volcanic faulted plateau underlain by sedimentary layers, igneous intrusives and metamorphic rocks. The faulting has controlled the overall surface design and greatly influenced the region's drainage pattern. An old erosion surface of the Gila Conglomerate is the main physiographic feature of the Morenci area. Deep, steep-walled canyons have been carved into this erosion surface. At the tailings dam site the Gila Conglomerate displays a thickness of nearly 700 feet, while depth to volcanic bedrock here is about 1200 feet. The Gila Conglomerate is composed of irregularly bedded conglomerate, continental indurated sandstone and siltstone. Within the sedimentary rocks are basalt layers. At the Morenci site the Gila Conglomerate is seen as alluvial fan deposits consisting of grayish-white boulders, coarse-grained conglomerate sandstone beds with interbedded lenses of sand, silt and clay. The conglomerate also contains fragments of older area rocks which are partially cemented by calcareous material and gypsum. In some regions these cemented rocks are intractable and require blasting to be workable. As a result the conglomerate is a very strong, stable foundation.

The Copper Mountain fault crosses the Morenci site and is noted to have displaced the area some 200 feet in Late Tertiary time. In general the area is considered to one of low seismicity today.

Morenci produces about 60,000 tons/day of tailings which are transported through concrete launders. The launders in turn feed into 30-inch diameter manifold pipelines which connect to 6-inch diameter spigots spaced at 30 feet intervals. The spigotted tailings are deposited on the pond surface in a slurry of 45% water. Dam crests are raised in 10 foot increments by dragline. Free water in the pond is decanted by vertical decant towers. A pumping system moves 11,000 gallons/minute of decanted water back to the Morenci smelter and concentrator sites for reuse.

Uranium Tailings Data: Colorado

Twenty-six boreholes from a Colorado tailings dam have provided SPT data for analysis. The dam near Uravan, Colorado is located in the western part of the state near the Utah border south of Grand Junction. Standard Penetration Testing was done in 1979. Stratigraphy of the area generally includes the tailings as overlying 1ØØ feet of interbedded sandstone and shales (Saltwash Formation); which overlies fifty feet of light green sandstone and siltstones (Summervillle Formation); which overlies 34Ø feet of light brown sandstone (Entrada Formation and Kayenta Formation); finally overlying massive brown sandstone (Winngate Formation).

Here there are three pond areas utilizing a single point discharge which is regularly moved about, being alternately placed in ponds 1, 2 and 3. The major design criteria for the Colorado site has been based on Nuclear Regulatory Guide 3.11. These ponds are routinely raised by the upstream construction method. Stabilization here is chiefly due to the beach sands which are deposited near the surrounding dike. Dikes surrounding the ponds are raised by bulldozer excavation and compaction of coarse tailings when tailings are not being deposited. Height of the dam is currently about 16Ø feet.

In 1978 it was decided that the existing pondings were potentially unstable in the event of a seismic event. As a result it was determined to stabilize the existing piles. In 1979 a program was implemented to stabilize the older dikes. The strategy used was to install a rockfill berm overlaying a drainage layer. Once a minimum amount of berm and drain are installed, a pond can be reactivated.

Uranium Tailings Data: DOE Report--22 Sites

A 1980 Department of Energy (DOE) progress report, "Pollution of Groundwater Due to Inactive Uranium Mill Tailings Piles", by Francois Heuze et. al. was the source of two SPT case studies (Grand Junction, Colorado and Shiprock, New Mexico) as well as effective friction angles from 13 sites obtained from drained direct shear tests. Twenty-two inactive uranium mill tailings sites specified by DOE for remedial treatment and/or stabilization. Of 22 sites surveyed eight of the tailings piles are considered stable, five are targeted for partial stabilization (seeding is often used to stabilize slopes) while eight others are considered to be unstable. The sites generally fall into five geographical areas: (1)scattered sites not yet analyzed (Fairview, Oregon; Lowman, Idaho; and Ray Point, Texas); (2)sites in the northern Utah, northern Colorado and central Wyoming area (Salt Lake City, Utah; Riverton, Wyoming; Maybell, Colorado; and Spook, Wyoming); (3)sites in the "four corners" area; (Shiprock, New Mexico; Durango, Colorado; Mexican Hat, Utah; Ambrosia Lake, New Mexico; Monument Valley, Arizona; Slick Rock/North Continent, Colorado; Slick Rock/Union Carbide, Colorado and Tuba City, Arizona); (4)sites in central Colorado and Utah (Grand Junction, Colorado; Gunnison, Colorado; New Rifle, Colorado; Old Rifle, Colorado and Green River, Utah); and finally (5)other scattered initially visited sites (Canonsburg, Pennsylvania and Falls City, Texas). Preliminary testing of soil properties was done at eighteen of these sites with detailed sampling done at three sites. A 1968 study of the Durango tailings pile by Woodward-Clyde and Associate's Denver office for Foote Mineral Company (Shiprock, New Mexico) is indicative of the uranium piles in the western United States. The Durango pile is approximately 160 feet in height, built of tailings of gradation 30% finer than US No. 200 sieve with side slopes ranging from 2.3:1 to 1.5:1. This pile, considered by Woodward-Clyde to be one of the most stable in the western United States, had not been used since 1963 at the time of their 1968 study. Tailings material at Durango primarily consisted of fine to medium sands built upon natural overburden. When the Durango mill was operative, the pile was raised by pumping tailings from the mill to the ponds and distributing them from a single flexible pipe. Detachable sections of the pipe allow the discharge point to be moved around the ponds' perimeters. Water is removed from the largest pond by a launder, which is then directed to an agitator tank and then to a second launder. The water finally is routed to either a water treatment building or to a small pond where it is allowed to soak into the pond itself or to evaporate without decanting. Tailings sand is

pushed around the perimeter of pile tops with bulldozers. At Durango no drainage provisions were engineered into the construction of the piles. Nor were any initial toe dams or retainer dams considered. Once one of the tailings ponds overtopped sending tailings and water into the mill area. However it was not a major problem. The tailings pile is graded so as not to trap water on the pile top, thus avoiding erosion damage to the pile's sides. Sites other than Durango have been scheduled for more detailed samplings.

APPENDIX B· Computer Codes

Two computer programs, CORL and PROB, were used in the analyses as described in this report. The program CORL was used to read digitized strength data which in turn was used to perform linear regression analyses. It then calculated the estimated means, standard deviations, and betal and beta2 parameters for Pearson Diagrams for both original and residual data. Finally CORL plotted and estimated data correlations and variograms.

The program PROB performed statistical testing: the chi-square test and the Kolmogorov test on the original and residual strength data. In the chi-square test, the data was divided into ten or fifteen equal intervals. In the case of original data, Beta, Normal, Lognormal. Exponential and Gamma probability distributions were tested. While for residual data, testing was done only for Normal and Beta distributions. Two sets of figures were generated for each run, with each set containing two figures: a histogram and a normal probability plot. The normal probability plot, while containing data points, also illustrated all of the probability distributions tested.